Universitat
de les Illes Balears

Instituto de Física Interdisciplinar y Sistemas Complejos

INDIVIDUAL-BASED MODELS OF COLLECTIVE DYNAMICS IN SOCIO-ECONOMIC SYSTEMS

Adrián Carro Patiño

Doctoral Thesis

Universitat de les Illes Balears

2016

Doctoral Program in Physics

Universitat de les Illes Balears

Instituto de Física Interdisciplinar y Sistemas Complejos

INDIVIDUAL-BASED MODELS OF COLLECTIVE DYNAMICS IN SOCIO-ECONOMIC SYSTEMS

Thesis submitted by

Adrián Carro Patiño

to the

Department of Physics

of the

Universitat de les Illes Balears

for the degree of

Doctor of Philosophy

in

Physics

Doctoral advisors:

Prof. Raúl Toral

Prof. Maxi San Miguel

Universitat de les Illes Balears

2016

Individual-based models of collective dynamics in socio-economic systems

Adrián Carro Patiño
Instituto de Física Interdisciplinar y Sistemas Complejos (IFISC)
Universitat de les Illes Balears (UIB)
Consejo Superior de Investigaciones Científicas (CSIC)

PhD Thesis

Doctoral advisors: Prof. Raúl Toral and Prof. Maxi San Miguel

For an updated version of this document, please visit http://ifisc.uib-csic.es/ or contact the author at adrian.carro@ifisc.uib-csic.es or adrian.carro@gmail.com

Document typeset in *Latin Modern* using LaTeX 2ε

WE,

Raúl Toral and Maxi San Miguel,
Professors of the Universitat de les Illes Balears,

DECLARE

that the thesis entitled "*Individual-based models of collective dynamics in socio-economic systems*", submitted by Adrián Carro Patiño to the Department of Physics of the Universitat de les Illes Balears in partial fulfillment of the requirements for the degree of Doctor of Philosophy in Physics, has been completed under our supervision and meets the requirements for the International Mention.

Palma de Mallorca, 8th July 2016.

Prof. Raúl Toral
Advisor

Prof. Maxi San Miguel
Advisor

Adrián Carro Patiño
Candidate

Abstract

Complex systems science addresses the study of systems composed of many interacting units, and whose collective (macroscopic) behavior does not only depend on the individual (microscopic) behaviors of these constituent units, but also on the interplay and connections between them. While the study of these emergent collective properties of complex systems is broadly interdisciplinary, with important contributions from different scientific communities, statistical physics has provided a rich set of fundamental concepts and methods, originally developed to explain the macroscopic properties of physical systems in terms of the microscopic interaction rules among their constituent particles. Significant developments in the study of complex networks have also allowed to deal with the non-trivial topologies characterizing the structure of interactions in real social and economic systems, as opposed to the regular lattices typical in condensed matter physics.

The main purpose of this thesis is to contribute to the understanding of how complex collective behaviors emerge in social and economic systems. To this end, we use a combination of mathematical analysis and computational simulations along the lines of the agent- or individual-based modeling paradigm, i.e., we propose models in which the individual units (agents) and their interactions are explicitly taken into account, and whose design is simple enough to allow for a deep understanding of the mechanisms of emergence while being elaborate enough to display complex collective behaviors. In particular, we focus on three main topics: opinion dynamics, herding behavior in financial markets, and language competition.

Opinion dynamics models focus on the processes of opinion formation within a society consisting of an ensemble of interacting individuals with diverse opinions. One of the main problems addressed by these models is whether these processes of opinion formation will eventually lead to the emergence of a consensus within the society, with a vast majority of the agents adopting the same opinion, or to the fragmentation of its constituent individuals into different opinion groups. We

are interested here in situations where the particular issue under consideration allows for opinions to vary continuously, for example, from "completely against" to "in complete agreement", and thus opinions are modeled as real variables. In particular, we focus on a model consisting of two mechanisms or rules for the evolution of the agents' opinions: a mechanism of social influence, by which two interacting agents reach a compromise at the midpoint opinion, and a mechanism of homophily, by which two agents do only interact if their opinion difference is less than a given threshold value. In this context, we study the influence of the initial distribution of opinions in the asymptotic solution of the model. A modification of this model accounting for random changes of opinion is also studied.

Financial time series are characterized by a number of *stylized facts* or non-Gaussian statistical regularities found across a wide range of markets, assets and time periods, such as volatility clustering or fat-tailed distributions of returns. A growing number of contributions based on heterogeneous interacting agents have interpreted these stylized facts as the macroscopic outcome of the diversity among the economic actors, and the interplay and connections between them. In particular, we focus here on a stochastic model of information transmission in financial markets based on a competition between pairwise copying interactions between market agents (herding behavior) and random changes of state (idiosyncratic behavior). On the one hand, we develop a generalization of this herding model accounting for the arrival of information from external sources, and study the influence of this incoming information on the market. On the other hand, we study a network-embedded version of the herding model and focus on the influence of the underlying topology of interactions on the asymptotic behavior of the system.

Language competition models address the dynamics of language use in multilingual social systems due to social interactions. The main goal of these models is to distinguish between the interaction mechanisms that lead to the coexistence of different languages and those leading to the extinction of all but one of them. While traditionally conceptualized as a property of the speaker, it has been recently proposed that the use of a language can be more clearly described as a feature of the relationship between two speakers —a link state— than as an attribute of the speakers themselves —a node state—. Inspired by this link-state perspective, we first develop a coevolving model that couples a majority rule dynamics of link states with the evolution of the network topology due to random rewiring of links in a local minority. Finally, we develop a model where the coupled dynamics of language use, as a property of the links between speakers, and language preference, as a property of the speakers themselves, are considered in a fixed network topology.

Resumen

La ciencia de los sistemas complejos se ocupa del estudio de sistemas compuestos por muchos elementos en interacción, y cuyo comportamiento colectivo (macoscópico) no solo depende de los comportamientos individuales (microscópicos) de estos elementos constituyentes, sino también de las interacciones y conexiones entre ellos. Aunque el estudio de estas propiedades colectivas y emergentes de los sistemas complejos supone un esfuerzo mayoritariamente interdisciplinar, con importantes contribuciones desde diferentes comunidades científicas, la física estadística ha venido proporcionando un conjunto de conceptos y métodos fundamentales, originalmente desarrollados para ofrecer una explicación de las propiedades macroscópicas de los sistemas físicos en términos de las reglas de interacción microscópicas entre sus partículas constituyentes. Desarrollos significativos en el estudio de redes complejas han sido también fundamentales para el tratamiento de las topologías no triviales que caracterizan la estructura de interacciones en los sistemas sociales y económicos, al contrario de las redes regulares habituales en la física de la materia condensada.

El propósito principal de esta tesis es el de contribuir a la comprensión del modo en el que comportamientos colectivos complejos emergen en sistemas sociales y económicos. Para ello, hacemos uso de una combinación de análisis matemático y simulaciones computacionales en la línea del paradigma de modelado basado en agentes o individuos. De esta manera, proponemos modelos en los que aparecen representados explicitamente tanto los elementos individuales (agentes) como las interacciones entre ellos, y cuyo diseño es lo suficientemente simple como para permitir una comprensión profunda de los mecanismos de emergencia pero también lo suficientemente elaborado como para dar lugar a comportamientos colectivos complejos. En particular, nos centramos en tres temas principales: dinámica de opiniones, comportamiento gregario en mercados financieros y competición lingüística.

Los modelos de dinámica de opiniones se centran en los procesos de formación de opiniones en el seno de una sociedad compuesta por un conjunto de individuos

en interacción y con opiniones diversas. Uno de los principales problemas abordados por estos modelos es el de determinar si estos procesos de formación de opiniones llevan a la emergencia de una situación de consenso en la sociedad correspondiente, con una clara mayoría de agentes adoptando la misma opinión, o si, por el contrario, llevan a la segregación de los individuos en diferentes grupos de opinión. Nos interesamos aquí por situaciones en las que el asunto que se discute permite la existencia de un contínuo de opiniones, desde el "desacuerdo absoluto" hasta el "acuerdo total", y por tanto las opiniones pueden ser modeladas como variables reales. En particular, nos centramos en un modelo consistente en dos mecanismos o reglas para la evolución de las opiniones de los agentes: un mecanismo de influencia social, por el cual dos agentes interaccionantes llegan a un compromiso en el punto medio entre sus opiniones, y un mecanismo de homofilia, por el cual dos agentes interaccionan únicamente si la diferencia entre sus opiniones es inferior a un cierto umbral. En este contexto, estudiamos la influencia de la distribución inicial de opiniones en la solución asintótica del modelo. Además, estudiamos también una modificación de este modelo para tener en cuenta cambios de opinión aleatorios.

Las series temporales financieras están caracterizadas por una serie de *hechos estilizados* o regularidades estadísticas no gaussianas observadas en un amplio rango de mercados, activos y períodos temporales, como el agrupamiento de la volatilidad o las distribuciones de retornos con colas pesadas. Un número creciente de contribuciones basadas en agentes heterogéneos en interacción han venido a ofrecer una interpretación de estos hechos estilizados como el resultado emergente de la diversidad entre actores económicos y de las interacciones y conexiones entre ellos. En particular, nos centramos aquí en un modelo estocástico de transmisión de información en mercados financieros basado en una competición entre interacciones de copia a pares entre agentes de mercado (comportamiento gregario) y cambios de estado aleatorios (comportamiento idiosincrático). Por un lado, desarrollamos una generalización de este modelo de comportamiento gregario para tener en cuenta la llegada de información desde fuentes externas y estudiamos la influencia de esta información entrante en el mercado. Por otro lado, estudiamos una versión en red del modelo de comportamiento gregario y nos centramos en la influencia de la topología de interacciones subyacente en el comportamiento asintótico del sistema.

Los modelos de competición lingüística abordan la dinámica del uso de lenguas en sistemas sociales multilingües debida a interacciones sociales. El principal objetivo de estos modelos es el de diferenciar entre aquellos mecanismos de interacción que llevan a la coexistencia de diferentes lenguas y aquellos que llevan a la extinción de todas menos una de ellas. Aunque tradicionalmente se ha conceptualizado como una propiedad del hablante, recientemente se ha propuesto que el uso de una lengua puede ser más claramente descrito como una propiedad de la

relación entre dos hablantes —un estado del enlace— que como una propiedad de los hablantes mismos —un estado del nodo—. Inspirados por esta perspectiva de estados de los enlaces, desarrollamos primero un modelo de coevolución que acopla una dinámica de estados en los enlaces basada en una regla de mayoría con la evolución de la topología de la red debida al re-enlace aleatorio de enlaces en una minoría local. Finalmente, desarrollamos un modelo en el que las dinámicas acopladas de uso de la lengua, como propiedad de los enlaces entre hablantes, y preferencia lingüística, como propiedad de los hablantes mismos, son consideradas en una topología de red fija.

Resum[1]

La ciència dels sistemes complexos s'ocupa de l'estudi de sistemes compostos per molts elements en interacció, i el comportament col · lectiu (macoscòpic) no només depèn dels comportaments individuals (microscòpics) d'aquests elements constituents, sinó també de les interaccions i connexions entre ells . Encara que l'estudi d'aquestes propietats col · lectives i emergents dels sistemes complexos suposa un esforç majoritàriament interdisciplinar, amb importants contribucions des de diferents comunitats científiques, la física estadística ha vingut proporcionant un conjunt de conceptes i mètodes fonamentals, originalment desenvolupats per oferir una explicació de les propietats macroscòpiques dels sistemes físics en termes de les regles d'interacció microscòpiques entre les seves partícules constituents. Desenvolupaments significatius en l'estudi de xarxes complexes han estat també fonamentals per al tractament de les topologies no trivials que caracteritzen l'estructura d'interaccions en els sistemes socials i econòmics, al contrari de les xarxes regulars habituals en la física de la matèria condensada.

El propòsit principal d'aquesta tesi és el de contribuir a la comprensió de la manera en què comportaments col · lectius complexos emergeixen en sistemes socials i econòmics. Per això, fem ús d'una combinació d'anàlisi matemàtica i simulacions computacionals en la línia del paradigma de modelat basat en agents o individus. D'aquesta manera, proposem models en els quals apareixen representats explícitament tant els elements individuals (agents) com les interaccions entre ells, i el disseny és prou simple com per permetre una comprensió profunda dels mecanismes d'emergència però també prou elaborat com per donar lloc a comportaments col · lectius complexos. En particular, ens centrem en tres temes principals: dinàmica d'opinions, comportament gregari en mercats financers i competició lingüística.

Els models de dinàmica d'opinions se centren en els processos de formació d'opinions en el si d'una societat composta per un conjunt d'individus en interacció i amb opinions diverses. Un dels principals problemes abordats per aquests

[1] Aquest resum ha estat traduït automàticament per Google™

models és el de determinar si aquests processos de formació d'opinions porten a l'emergència d'una situació de consens en la societat corresponent, amb una clara majoria d'agents adoptant la mateixa opinió, o si, pel contrari, porten a la segregació dels individus en diferents grups d'opinió. Ens interessem aquí per situacions en què l'assumpte que es discuteix permet l'existència d'un continu d'opinions, des del "desacord absolut" fins a l'"acord total", i per tant les opinions poden ser modelades com a variables reals . En particular, ens centrem en un model que consisteix en dos mecanismes o regles per a l'evolució de les opinions dels agents: un mecanisme d'influència social, pel qual dos agents interaccionantes arriben a un compromís en el punt mig entre les seves opinions, i un mecanisme de homofilia, pel qual dos agents interaccionen únicament si la diferència entre els seus opinions és inferior a un cert llindar. En aquest context, estudiem la influència de la distribució inicial d'opinions en la solució asimptòtica del model. A més, estudiem també una modificació d'aquest model per tenir en compte canvis d'opinió aleatoris.

Les sèries temporals financeres estan caracteritzades per una sèrie de fets estilitzats o regularitats estadístiques no gaussianes observades en un ampli rang de mercats, actius i períodes temporals, com l'agrupament de la volatilitat o les distribucions de retorns amb cues pesades. Un nombre creixent de contribucions basades en agents heterogenis en interacció han vingut a oferir una interpretació d'aquests fets estilitzats com el resultat emergent de la diversitat entre actors econòmics i de les interaccions i connexions entre ells. En particular, ens centrem aquí en un model estocàstic de transmissió d'informació en mercats financers basat en una competició entre interaccions de còpia a parells entre agents de mercat (comportament gregari) i canvis d'estat aleatoris (comportament idiosincràtic). D'una banda, vam desenvolupar una generalització d'aquest model de comportament gregari per tenir en compte l'arribada d'informació des de fonts externes i estudiem la influència d'aquesta informació entrant en el mercat. D'altra banda, vam estudiar una versió en xarxa del model de comportament gregari i ens centrem en la influència de la topologia d'interaccions subjacent en el comportament asimptòtic del sistema.

Els models de competició lingüística aborden la dinàmica de l'ús de llengües en sistemes socials multilingües deguda a interaccions socials. El principal objectiu d'aquests models és el de diferenciar entre aquells mecanismes d'interacció que porten a la coexistència de diferents llengües i aquells que porten a l'extinció de totes menys una. Encara que tradicionalment s'ha conceptualitzat com una propietat del parlant, recentment s'ha proposat que l'ús d'una llengua pot ser més clarament descrit com una propietat de la relació entre dos parlants —un estat de l'enllaç— que com una propietat de els parlants mateixos —un estat del node—. Inspirats per aquesta perspectiva d'estats dels enllaços, desenvolupem primer un model de coevolució que acobla una dinàmica d'estats en els enllaços basada en

una regla de majoria amb l'evolució de la topologia de la xarxa deguda al re-enllaç aleatori d'enllaços en una minoria local. Finalment, vam desenvolupar un model en què les dinàmiques acoblades d'ús de la llengua, com a propietat dels enllaços entre parlants, i preferència lingüística, com a propietat dels parlants mateixos, són considerades en una topologia de xarxa fixa.

List of publications

Published articles

- Carro, A., Toral, R., and San Miguel, M. (2013). The role of noise and initial conditions in the asymptotic solution of a bounded confidence, continuous-opinion model. *Journal of Statistical Physics*, 151(1):131–149.
- Carro, A., Vazquez, F., Toral, R., and San Miguel, M. (2014). Fragmentation transition in a coevolving network with link-state dynamics. *Physical Review E*, 89(6):62802.
- Carro, A., Toral, R., and San Miguel, M. (2015). Markets, Herding and Response to External Information. *PLoS ONE*, 10(7):e0133287.
- Carro, A., Toral, R., and San Miguel, M. (2016). The noisy voter model on complex networks. *Scientific Reports*, 6:24775.

Manuscripts in preparation

- Carro, A., Toral, R., and San Miguel, M. (2016). Coupled dynamics of node and link states: A model for language competition.

Acknowledgements

Firstly, I would like to express my sincere gratitude to my advisors, Prof. Raúl Toral and Prof. Maxi San Miguel, for their supervision and guidance. In particular, I would like to thank Raúl for his readiness to accept new challenges and help with all sorts of technical details, from mathematical analysis to computer programming. I would also like to emphasize my gratitude to Maxi for sharing with me his ability to step back, look at the bigger picture, and focus on the fundamental questions, and for keeping me on track with his constant "Where is the paper?". I could not possibly imagine any better combination of personalities and skills for advising a PhD candidate!

This work would not have been possible without the advice and feedback from a great number of people. Among them, I would like to personally thank Dr. Luis Fernández Lafuerza, Dr. Juan Fernández Gracia, Dr. Marina Diakonova, Dr. Federico Vázquez, and Dr. Marco Patriarca.

Finally, I would like to thank my family: it is only by knowing that I could always rely on their support and understanding that I found the courage to pursue this adventure.

Contents

Introduction

CHAPTER 1

Introduction

One of the main goals of complex systems science is to understand the complex behavior displayed by systems composed of many interacting units. In particular, the focus is on systems whose collective (macroscopic) behavior cannot be directly derived from the individual (microscopic) behaviors of their constituent units —the whole is more than the sum of its parts—. The collective behavior of these systems is thus said to be an "emergent" phenomenon, dependent not only on the individual units, but also on the interplay and connections between them. Paradigmatic examples of emergent collective phenomena in complex systems are the phase transitions observed in many physical systems, the foraging and nest-building behaviors typical of ant colonies, the flocking behavior of birds, the dynamics of neural networks in the brain, traffic congestion phenomena, price fluctuations in financial markets, and the emergence of institutions in social systems.

The study of complex systems is a broad and intrinsically interdisciplinary field, attracting the attention of different scientific communities, from social science and economy to physics, computer science and biology. In particular, a rich toolbox of concepts and methods has been provided by statistical physics, whose main purpose is largely coincident with that of complex systems science: to explain the macroscopic properties of physical systems in terms of the microscopic interaction rules among their constituent particles. As a consequence of this overlap, there has been a growing interest by physicists in the modeling of emergent phenomena in social (Castellano et al., 2009) and economic systems (Chakraborti et al., 2011a,b). In parallel to this shift, the study of complex networks, the skeleton of complex systems, has also received an increasing level of attention (Boccaletti et al., 2006; Newman, 2010), allowing to deal with the non-trivial topological features characterizing the structure of interactions in real

social and economic systems (Watts and Strogatz, 1998; Barabási, 1999), as opposed to the regular lattices typical in condensed matter physics.

One of the most important conceptual frameworks for the study of emergent collective properties in complex systems is agent- or individual-based modeling, a collection of computational techniques in which the individual units (agents) and their interactions are explicitly simulated (Epstein and Axtell, 1996; Axelrod, 2006; Newman, 2011). A key notion in this context is that simple behavioral rules at the microscopic level can give rise to complex dynamics at the macroscopic level. Thus, the goal is to design models which are simple enough to allow for a deep understanding of the mechanisms of emergence while being elaborate enough to display complex collective behaviors.

In this context, the main purpose of this thesis is to contribute to the understanding of how complex collective behaviors emerge in social and economic systems. To this end, we study the macroscopic consequences of simple individual behavioral mechanisms, by means of a combination of mathematical analysis and computational simulation. In particular, we focus on three main topics: opinion dynamics, herding behavior in financial markets, and language competition.

1.1

Opinion dynamics

Opinion dynamics models focus on the processes of opinion formation within a society consisting of an ensemble of interacting individuals with diverse opinions. Inspired by statistical mechanics and nonlinear physics, a wide variety of models have been developed in order to deal with the different phenomena observed in real societies (Castellano et al., 2009; Battiston et al., 2016): emergence of fads, minority opinion survival and spreading, collective decision making, emergence of extremism, and so forth. One of the main problems addressed by some of these models is whether the opinion formation processes within a society will eventually lead to the emergence of a consensus, with a vast majority of the agents adopting the same opinion, or to the fragmentation of its constituent individuals into different opinion groups (Ben-Naim et al., 2003b; Pluchino et al., 2005; Klimek et al., 2008).

In opinion dynamics, each agent is characterized by an opinion which is coded as a dynamical variable from a certain space, evolving in accordance with some rules. These behavioral laws codify a variety of internal and external factors governing the evolution of an agent's opinion, such as the social influence of its acquaintances, the social pressure of a group or the influence of advertising and

mass media. Regarding the opinion variable, models can be broadly classified as *discrete opinion models*, where opinions can only adopt a finite set of values, and *continuous opinion models*, where opinions are modeled as real numbers in a finite interval and thus two interacting agents can always reach a compromise in an intermediate opinion (Stauffer, 2005).

Discrete models have traditionally been predominant in the physics literature, due to their correspondence with spin systems. They have been applied to analyze situations where individuals are confronted with a limited number of options, such as choosing among a few political parties in an election or between two languages in a language competition situation (Abrams and Strogatz, 2003). On the contrary, continuous models are applied when a single issue is considered and opinions can vary continuously, for example, from "completely against" to "in complete agreement". Typical examples of continuous opinion issues are the degree of agreement regarding the legalization of drugs or abortion, or predictions about macroeconomic variables.

Two models of continuous opinion dynamics were introduced around 2000 and, ever since, have received much attention (Fortunato et al., 2005; Lorenz, 2007a; Török et al., 2013; Iñiguez et al., 2014): the model of Hegselmann and Krause (Hegselmann and Krause, 2002), and that of Deffuant, Weisbuch et al. (Deffuant et al., 2000; Weisbuch et al., 2002, 2003). The former was first introduced in a mathematical context as a nonlinear version of older consensus models (Krause, 2000), while the latter was developed in the context of a European Union project for the improvement of agri-environmental policies. Both models implement basically two mechanisms or rules for the evolution of the agents' opinion variables. On the one hand, there is a mechanism of social influence, by which two interacting agents tend to bring their opinions closer and, eventually, they reach a compromise at the midpoint opinion. On the other hand, both models take into account a mechanism of homophily, in particular a *bounded confidence* rule, in the sense that two agents do only interact if their opinion difference is less than a given threshold value. In other words, an agent will only take into account the opinions of other agents if they differ less than a bound of confidence ϵ from its own current opinion, simply ignoring the rest of them.

The main difference between the model by Hegselmann and Krause and the Deffuant, Weisbuch et al. model is the interaction regime. In the case of Deffuant, Weisbuch et al., the interaction is assumed to be pairwise, i.e., agents meet in random pairwise encounters after which they compromise or not. On the contrary, in the model by Hegselmann-Krause interaction takes place in groups, as each agent moves its own opinion to the average of the opinions of all the agents within a bound of confidence, including its own current opinion.

Contributions of this thesis

In this context, we focus on the Deffuant, Weisbuch et al. dynamics, which leads to final states where either a perfect consensus has been achieved, or the individuals split into a finite number of opinion clusters, depending on a parameter representing the confidence bound of the agents (Fortunato, 2004; Lorenz, 2007a,b). In particular, two different contributions are presented in Chapter 2. On the one hand, we study the influence that the initial distribution of opinions among the agents has upon the configuration of the final states. The fundamental question that we try to answer is: can we, by imposing a given initial condition, force the system to reach a consensus, or, equivalently, prevent a consensus and force it to split in several opinion groups? As a result of this analysis, we prove that the use of different initial distributions does not only have an effect in the average final opinion, but also in the fact that a consensus is found or not for a certain threshold level, i.e., that the consensus can be encouraged or prevented by certain initial conditions. On the other hand, we also study the influence of the initial conditions in the case of a Deffuant, Weisbuch et al. model modified to account for an additional element of randomness in the form of a noise (Pineda et al., 2009, 2011, 2013). This noisy term can be thought of as a certain kind of "free will", since the agents are given the opportunity to change their opinion independently of their acquaintances. Concerning this noisy case, we find that, even if the noise hides most of the importance of the initial distribution, the latter has still some noticeable effects upon the final configuration.

1.2

Herding behavior and financial markets

The analysis of financial data has led to the characterization of some non-Gaussian statistical regularities found in financial time series across a wide range of markets, assets and time periods (Mandelbrot, 1963; Cont, 2001; Di Matteo, 2007; Clementi et al., 2006). These robust empirical properties are known in the economic literature as *stylized facts*. It has been found, for instance, that the unconditional distribution of returns is characterized by a fat-tailed or leptokurtic shape, i.e., it shows a higher concentration of probability in the center and in the tails of the distribution as compared to the Gaussian (Mandelbrot, 1963), leading to a higher probability of large returns. A second example is the intermittent behavior of the volatility, measured as absolute or squared returns. This property, known as volatility clustering, implies a tendency for calm and turbulent market periods to cluster together (De Vries, 1994). This temporal bursting behavior of

the volatility leads to the existence of positive autocorrelations for absolute and squared returns which decay only slowly as a function of the time lag (Ding et al., 1993).

Two competing hypotheses have been proposed to explain the origin and ubiquity of stylized facts in financial data. On the one hand, the traditional efficient market hypothesis states that markets are efficient, in the sense that they correctly aggregate all available information, and therefore price changes (returns) fully and instantaneously reflect any new information (Fama, 1970). Thus, according to this hypothesis, any particular characteristic of the distribution of returns is a direct consequence of the statistical properties of the news arrival process. On the other hand, recent years have witnessed the development of an alternative approach which might be called the interacting agent hypothesis[1], as coined by Alfarano et al. (2005). Indeed, a growing number of contributions based on heterogeneous interacting agents (Kirman, 1992) have interpreted these stylized facts as the macroscopic outcome of the diversity among the economic actors, and the interplay and connections between them (Kirman, 1991, 1993; Brock and Hommes, 1997; Lux and Marchesi, 1999; Cont and Bouchaud, 2000; Thurner et al., 2012). Heterogeneity refers here to the agents' different level of access to available information or to their capability to choose from a set of various market strategies or trading rules. Regarding their interplay, different interaction mechanisms have been studied, whether direct or indirect, global or local. Thus, according to this hypothesis, any statistical regularity found in financial time series is an emergent property endogenously produced by the internal dynamics of the market.

Along the lines of earlier works (Lux, 2006; Alfarano and Milaković, 2009), we can classify the different agent-based financial models into three broad categories. The first one seeks inspiration in well-known critical systems from the statistical physics literature, and it is able to reproduce non-Gaussian statistics by carefully adjusting model parameters near criticality (Stauffer and Sornette, 1999; Cont and Bouchaud, 2000; Bornholdt, 2001; Iori, 2002). The second group of models, inspired by a seminal work by Brock and Hommes (1997), assumes that agents interact globally through the price mechanism and public information about the performance of strategies subject to noise (Hommes, 2006; Chang, 2007). These models are able to reproduce some of the aforementioned stylized facts when their signal-to-noise ratio is adjusted around unity. Finally, the third category is composed by a series of stochastic models of information transmission (Kirman, 1991, 1993) whose main ingredient is their emphasis on the processes of social interaction among agents, based on herding behavior or a tendency to follow the

[1]The "Workshop on the Economic Science with Heterogeneous Interacting Agents (WEHIA)", organized annually since 2003 by the "Society for Economic Science with Interacting Agents (ESHIA)", and the "Econophysics Colloquium", organized annually since 2005, are important expressions of this new school of thought.

crowd (Lux and Marchesi, 1999; Eguíluz and Zimmermann, 2000; Alfarano et al., 2005). These models endogenously give rise to some of the universal statistical properties characterizing financial time series.

A paradigmatic example of this third category of agent-based financial models is the herding mechanism proposed by Kirman (1991, 1993), which is based on a competition between pairwise copying interactions (herding behavior) and random changes of state (idiosyncratic behavior). In its original, extensive formulation, where the intensity of the interaction is proportional to the density of agents in a given state, the main consequence of this competition is the appearance of a noise-induced, finite-size transition between two different behavioral regimes —a mostly ordered regime dominated by pairwise interactions and a mostly disordered regime dominated by noise (Kirman, 1993)—. In a subsequent, non-extensive reformulation of the model (Alfarano et al., 2005, 2008) in terms of an interaction strength proportional to the absolute number of agents in a given state, the transition is not anymore a finite-size effect. Interestingly, the original, extensive formulation of the model is equivalent to a variant of the voter model (Clifford and Sudbury, 1973; Holley and Liggett, 1975) accounting for the effect of noise. This noisy variant of the voter model has been studied by, at least, four mutually independent strands of research, largely unaware of each other and belonging to different fields. Namely, percolation processes in strongly correlated systems (Lebowitz and Saleur, 1986), heterogeneous catalytic chemical reactions (Fichthorn et al., 1989; Considine et al., 1989), herding behavior in financial markets (Kirman, 1993), and probability theory (Granovsky and Madras, 1995). While both the first and the last strands of literature are directly inspired by the voter model, explicitly using terms such as "noisy voter model" or similar, contributions in the contexts of catalytic reactions and financial markets do not refer to the voter model, and use terms such as "catalytic reaction", "herding" or "Kirman model" instead. For coherence with these different strands of literature, we will use hereafter either "noisy voter model", "Kirman model", or "herding model" depending on the context, and we will explicitly state, in each case, if we refer to the extensive or the non-extensive formulation.

Contributions of this thesis

If the efficient market approach neglected the importance of the interplay and connections between different economic actors, agent-based finance literature has traditionally overlooked the influence of external sources of information upon markets, treating them as completely closed entities or subject to a constant level of noise. The research of our first contribution, presented in Chapter 3, is motivated by the observation that, even if markets are complex systems able to endogenously give rise to non-Gaussian statistical properties, they are by no

means closed entities, insensitive to the arrival of external information. Indeed, the recent availability of tools and methods to retrieve and process large corpora of news has allowed empirical financial research to start collecting evidence on how markets react, for instance, to the publication of: news about companies, economic indices, rumors related to the economy, forecasts and recommendations by analysts, news on world events, and financial information by mass media (Hanousek et al., 2009; Kiymaz, 2001; Jegadeesh and Kim, 2006; Arin et al., 2008; Alanyali et al., 2013). A more extensive survey of the literature on the influence of external sources of information has been recently developed by Lillo et al. (2015), while for a more detailed account of the debate about the endogenous and exogenous components of market dynamics we refer to Johansen and Sornette (2002) and Bouchaud (2010). Most of this literature addresses this question from a purely empirical point of view. As a complement to the aforementioned empirical works, the main purpose of the research presented in Chapter 3 is to contribute to the theoretical assessment of the influence of an external source of information upon an agent-based financial market characterized by the existence of a certain herding behavior. In particular, we develop a financial market herding model along the lines of the works by Kirman (1991, 1993) and Alfarano et al. (2008), i.e., with all-to-all interactions, but open to the arrival of external information affecting the traders' behavior (for other approaches, see Harras and Sornette, 2011; Shapira et al., 2014; Golub et al., 2015; Rambaldi et al., 2015). Finally, we introduce a real information input in this model and we compare its output with real financial data. We show that a nonzero but weak intensity or convincing power of the external source of information allows the model to better reproduce the statistical properties of real data. Furthermore, our results suggests the existence of different market regimes regarding the assimilation of incoming information: amplification, precise assimilation and undervaluation of incoming information.

In a second contribution, developed in Chapter 4, we focus on the influence of the topology of the underlying social network of interactions upon the behavior of stochastic, binary-state models, an example of which is the noisy voter model or Kirman model. While most of these models were initially studied in regular lattices, there has recently been a growing interest in more complex and heterogeneous topologies (Albert and Barabási, 2002; Newman and Park, 2003; Barrat et al., 2008; Newman, 2010). An important result of these recent works has been to show that, for a given model, the structure of the underlying network may strongly influence the dynamics of the system and affect its critical behavior, leading, for instance, to different critical values of the model parameters (Lambiotte, 2007; Gleeson, 2011; Vilone et al., 2012; Gleeson, 2013). This has been shown to be the case, for example, for the critical temperature of the Ising model (Dorogovtsev et al., 2002; Leone et al., 2002; Viana Lopes et al., 2004), for the epidemic threshold in spreading phenomena (Boguñá et al., 2003; Durrett, 2010;

Castellano and Pastor-Satorras, 2010; Parshani et al., 2010), for the mean return and first-passage times in random walks (Masuda and Konno, 2004; Sood et al., 2005), and for the critical number of cultural traits in the Axelrod model (Klemm et al., 2003). Thus, the quantification of the effect of the underlying topology on such systems and dynamics is, from a practical point of view, a matter of prime importance. While the effect of different network topologies on the behavior of the voter model has been well established (Suchecki et al., 2005a; Sood and Redner, 2005; Suchecki et al., 2005b; Vazquez and Eguíluz, 2008), the case of the noisy voter model has received much less attention, most of the corresponding literature focusing only on regular lattices (Lebowitz and Saleur, 1986; Granovsky and Madras, 1995) or on a fully-connected network (Kirman, 1993; Alfarano et al., 2008). Finally, the use of a mean-field approach in some recent studies considering more complex topologies (Alfarano and Milaković, 2009; Alfarano et al., 2013; Diakonova et al., 2015) did not allow to find any effect of the network properties —apart from its size and mean degree— on the results of the model.

In this context, we propose in Chapter 4 an alternative analytical approach, based on an annealed approximation for uncorrelated networks and inspired by a recently introduced method to deal with heterogeneity in stochastic interacting particle systems (Lafuerza and Toral, 2013). Moving beyond the usual mean-field approximations (Vazquez et al., 2008; Alfarano and Milaković, 2009; Diakonova et al., 2015), we approximate the network by a complementary, weighted, fully-connected network whose weights are given by the probabilities of the corresponding nodes being connected in uncorrelated networks of the configuration ensemble (Newman, 2003; Boguñá et al., 2004; Bianconi, 2009; Sonnenschein and Schimansky-Geier, 2012). Furthermore, we present a formulation of the problem in terms of a master equation for the probability distribution of the individual states of the nodes. In this way, we are able to find approximate analytical expressions for the critical point of the transition, for a local order parameter and for the temporal correlations, finding that the degree heterogeneity —variance of the underlying degree distribution— has a significant impact on all of these variables. Finally, we show how this influence opens the possibility of inferring the degree heterogeneity of the underlying network by observing only the aggregate behavior of the system as a whole, an issue of interest for systems where only macroscopic, population level variables can be measured.

1.3

Language competition

The study of language competition in processes of language contact addresses the dynamics of language use in multilingual social systems due to social interactions. It belongs to the general class of consensus problems, and its main goal is to distinguish between the mechanisms that lead to the coexistence of different languages and those leading to the extinction of all but one of them. The focus of the field is on language shift in terms of users, rather than changes in the language itself. As a consequence, language is conceptualized as a discrete property of the speakers (Castelló et al., 2013). In recent years, a number of contributions lying outside the realm of traditional sociolinguistics have addressed the problem of language competition from alternative perspectives, using tools and methods from statistical physics, nonlinear dynamics, and complex systems science (Stauffer et al., 2006; Schulze and Stauffer, 2006; Loreto and Steels, 2007; Schulze et al., 2008; Baronchelli et al., 2012; Patriarca et al., 2012; Mufwene, 2016). Much of this research stems from the seminal work by Abrams and Strogatz (2003) about the dynamics of endangered languages. The models proposed in this context focus on the analysis of simple mechanisms of social interaction with the aim of determining their specific macroscopic consequences. The collective behavior of the system is thus interpreted as the macroscopic outcome of simple interaction rules between speakers. Some of these studies adopt a macroscopic, mean-field-based perspective (Abrams and Strogatz, 2003; Patriarca and Leppänen, 2004; Mira and Paredes, 2005; Pinasco and Romanelli, 2006; Isern and Fort, 2014), where only population densities are considered, while others develop a microscopic, agent-based perspective (Castelló et al., 2006; Stauffer et al., 2007; Vazquez et al., 2010; Caridi et al., 2013), where the social network of interactions between individuals is explicitly taken into account.

The model proposed by Abrams and Strogatz (2003) considers a binary-state society, where individuals can be either speakers of language A or speakers of language B. The authors develop a macroscopic description of the system based on nonlinear ordinary differential equations for the population densities of both types of speakers. The corresponding microscopic, agent-based version of this model was first studied by Stauffer et al. (2007). In particular, the probability for a speaker to switch language is assumed to depend on the fraction of speakers of the opposite language (global fraction in the macroscopic version, local fraction in the microscopic one) and on two parameters: the relative social prestige of both languages and the volatility of the speakers' choices. The prestige is a symmetry breaking parameter, favoring one or the other language because of the individual and social advantages derived from its use. The volatility parameter determines

the functional form of the switching probabilities, and it is related to the propensity of the speakers to change their current language. In the case of two socially equivalent languages (equal prestige) and for linear switching probabilities (neutral volatility), the Abrams-Strogatz model becomes the voter model (Clifford and Sudbury, 1973; Holley and Liggett, 1975; Suchecki et al., 2005a). By definition, the Abrams-Strogatz model can only account for societal bilingualism, i.e., for the coexistence of two different monolingual groups (Appel and Muysken, 2006). Subsequent studies, on the contrary, have considered generalizations of the original model accounting for the existence of bilingual individuals (Wang and Minett, 2005; Mira and Paredes, 2005; Castelló et al., 2006; Minett and Wang, 2008; Heinsalu et al., 2014)[2]. In particular, the AB-model was proposed by Castelló et al. (2006) based on the works of Wang and Minett (2005). It develops a modification of the original, binary-state Abrams-Strogatz model to account for the case of two non-excluding options by introducing a third, intermediate state (AB), representing the bilingual speakers. While the focus was initially placed on the case of two socially equivalent languages and neutral volatility, later works have further explored the prestige-volatility parameter space (Vazquez et al., 2010). In general, the AB agents have been found to play a relevant role in the interface dynamics of the system, facilitating the extinction of one of the languages in networks without mesoscale community structure, while allowing for long-lived coexistence of both languages in networks with communities (Castelló et al., 2007; Toivonen et al., 2009; Vazquez et al., 2010). Coexistence, however, is always a metastable state based on the segregation of both languages, with bilingual speakers acting as a bridge between the two groups.

A much more natural way of accounting for bilingual speakers is to consider language as a property of the interactions between individuals. In fact, while traditionally conceptualized as a property of the speaker in the above-mentioned literature, the use of a language as a means of communication can be more clearly described as a feature of the relationship between two speakers —a link state— than as an attribute of the speakers themselves —a node state—. In this manner, bilingualism is not anymore an ad-hoc intermediate state, but the natural consequence of individuals using different languages in different interactions. Furthermore, this approach allows for a more nuanced understanding of bilingualism: speakers are not only characterized by being bilinguals or not, but by a certain degree of bilingualism, depending on the share of conversations in each language.

The study of models and dynamics based on link states has received increasing attention from areas of research other than language competition, such as social balance theory, community detection and network controllability. Social balance

[2]Interestingly, an alternative modeling approach developed by Baggs and Freedman (1990, 1993) had already addressed the problem of individual bilingualism from a macroscopic, mean-field perspective more than a decade before the introduction of the Abrams-Strogatz model.

theory (Heider, 1946) is the first and most established precedent. Assuming that each link or social relationship can be positive (friendship) or negative (enmity), this theory proposes that there is a natural tendency to form balanced triads, defined as those for which the product of the states of the three links is positive. The question of whether a balanced global configuration is asymptotically reached for different network topologies has been addressed by several recent studies (Antal et al., 2005, 2006; Radicchi et al., 2007). Large scale data on link states associated with trust, friendship or enmity has recently become available from on-line games and communities, providing an ideal framework to test the validity of this theory and propose alternative interaction rules (Szell et al., 2010; Leskovec et al., 2010a,b; Marvel et al., 2011). In the context of community detection, the definition of network communities as a partition of the links instead of the nodes has allowed to account for overlapping communities (Traag and Bruggeman, 2009; Evans and Lambiotte, 2009, 2010; Ahn et al., 2010; Liu et al., 2012): a node is naturally assigned to several communities if it has links belonging to them. Finally, an approach based on a link-state dynamics has also proven to be useful in the field of network controllability (Nepusz and Vicsek, 2012), where the aim is to determine the conditions under which the dynamics of a network can be driven from any initial state to any desired final state within finite time. In particular, by introducing a dynamics of link states, one can identify the most influential links for determining the global state of the network. While these models set a precedent in the use of a link-state perspective, they are not suitable for modeling the dynamics of competing languages: the two link states considered by social balance theory are not equivalent, friendship and enmity playing rather different roles; no dynamics of the link states has been considered in the context of community detection; and only continuous link states have been considered in network controllability problems.

More relevant in the context of language competition, a prototypical model of link-state dynamics with binary, equivalent states has been recently introduced by Fernández-Gracia et al. (2012). In particular, a majority rule for link states is implemented, such that at each time step the state of a randomly chosen link is updated to the state of the majority of its neighboring links, i.e., those sharing a node with it (see Häggström, 2002; Castellano et al., 2005; Castellano and Pastor-Satorras, 2006; Baek et al., 2012, for studies on the majority rule for node states). The authors find a broad distribution of non-trivial asymptotic states characterized by the coexistence of both languages, including both frozen and dynamically trapped configurations. Interestingly, these non-trivial asymptotic configurations are found to be significantly more likely than under the traditional majority rule for node states in the same topologies. These results can be qualitatively understood in terms of the implicit topological difference between running a given dynamics on the nodes and on the links of the same network. Indeed, one can define a node-equivalent graph by mapping the links of the original network

to nodes of a new one, known as line-graph (Rooij and Wilf, 1965; Krawczyk et al., 2011), where nodes are connected if the corresponding links share a node in the original network. Line-graphs are characterized by a higher connectivity (Chartrand and Stewart, 1969) and a larger number of cliques (Mańka-Krasoń et al., 2010), which results in more (and more complex) topological traps and, therefore, in a wider range of possible disordered asymptotic configurations where both languages can survive.

Contributions of this thesis

Inspired by the link-state perspective proposed by Fernández-Gracia et al. (2012), we develop in Chapter 5 a coevolution model that couples the aforementioned majority rule dynamics of link states with the evolution of the network topology. The study of coevolving dynamics and network topologies has received an increasing attention (Zimmermann et al., 2001, 2004; Gross and Blasius, 2008; Herrera et al., 2011; Sayama et al., 2013), particularly in the context of social systems and always from a node states perspective. In the most common coupling scheme, node states are updated according to their neighbors' states while links between nodes are rewired taking into account the states of these nodes. This coupled evolution generically leads to the existence of a fragmentation transition: for a certain relation between the time scales of both processes, the network breaks into disconnected components.

While a large number of dynamics and rewiring rules have been studied (Zimmermann et al., 2001, 2004; Holme and Newman, 2006; Vazquez et al., 2007, 2008; Mandrà et al., 2009; Demirel et al., 2014), all of them belong to the class of models based on node states. The goal of our first contribution in this context is, thus, to offer a prototype model for the study of coevolution from a link-state perspective. In addition to the majority rule for link states studied by Fernández-Gracia et al. (2012), according to which links adopt the state of the majority of their neighboring links in the network, we define a rewiring mechanism inspired by the case of competing languages. In particular, this mechanism captures the fact that, when a speaker is uncomfortable with the language used on a given interaction, she can either try to change that language or simply stop this interaction and start a new one in her preferred language. Depending on the ratio between the probability of a majority rule updating and that of a rewiring event, the system evolves towards different absorbing configurations: either a one-component network with all links in the same state —extinction of one of the languages— or a network fragmented in two components with opposite states —survival of both languages in completely segregated communities—. Therefore, we find that the frozen and dynamically trapped coexistence configurations predominant in fixed topologies (Fernández-Gracia et al., 2012) are not robust against the coevolution

of the network: even a very small amount of rewiring is enough to slowly drive the network to a situation where there are no contacts between links in different state. In this way, the described dynamics leads always to the progressive disappearance of the bilingual speakers, whether as a consequence of the extinction of one of the languages or as a result of the complete segregation between users of one or the other language. While for low rewiring rates and finite-size networks there is a domain of bistability between fragmented and non-fragmented final states, a finite-size scaling analysis indicates that fragmentation is the only possible scenario for large systems and any nonzero rate of rewiring. Thus, both the fragmentation transition and the existence of a region of bistability are finite-size effects.

In a second contribution, we turn our attention back to fixed topologies and we focus on the fact that, while the use of a language can be clearly described as a property of the interactions between speakers —link states—, there are certain features intrinsic to these speakers —node states— which have a relevant influence on the language they choose for their communications. In particular, the attitude of a speaker towards a given language —which determines her willingness to use it— is affected by individual attributes such as her level of competence in that language, her degree of cultural attachment and affinity with the social group using that language, and the strength of her sense of identity or belonging to that group. For simplicity, we consider that all individual properties affecting language choice can be subsumed under the concept of "preference". At the same time, the evolution of the speakers' individual preferences is, in turn, affected by the languages used in their respective social neighborhoods. In this manner, the problem of language competition can be studied from the point of view of the intrinsically coupled evolution of language use and language preference. Ultimately, this change of perspective can be regarded as a shift from a paradigm in which language is considered only as a means of communication to one in which its tight entanglement with culture and identity is also taken into account.

In order to address this intertwined dynamics of language use and language preference, we develop in Chapter 6 a model of coevolution of node and link states. As before, the use of two socially equivalent languages is represented by a binary-state variable associated to the links. In addition, nodes are endowed with a discrete real variable representing their level of preference for one or the other language. The dynamics of link states results from the interplay between, on the one hand, the tendency of speakers to reduce the cognitive effort or cost associated with switching between several languages (Meuter and Allport, 1999; Jackson et al., 2001; Abutalebi and Green, 2007; Moritz-Gasser and Duffau, 2009) and, on the other hand, their tendency to use their internally preferred language. Regarding the dynamics of node states, we assume that speakers update their preference towards the language most commonly used in

their respective social neighborhoods, i.e., the one most frequently used by their neighbors to communicate between themselves. Note that we implicitly assume that triangles represent actual group relationships, in which each speaker is aware of the interaction between the other two. Thus, we are led to focus on network topologies where triangles are abundant, a topic that has received a great deal of attention throughout the last decade (Serrano and Boguñá, 2005; Newman, 2009; Bianconi et al., 2014). Interestingly, it has been recently shown that real social networks are characterized by large clustering coefficients and, therefore, contain a large proportion of triangles (Newman and Park, 2003; Dorogovtsev and Mendes, 2003; Newman, 2010; Foster et al., 2011; Colomer-de Simón et al., 2013). Triadic closure (Rapoport, 1953) —the principle that individuals tend to make new acquaintances among friends of friends— has been found to be a successful mechanism in reproducing these structural properties. While a number of different implementations of the triadic closure mechanism have been studied in different contexts (Holme and Kim, 2002; Davidsen et al., 2002; Solé et al., 2002; Vázquez, 2003; Boguñá et al., 2004; Krapivsky and Redner, 2005; Jackson and Rogers, 2007), we focus on a socially inspired network generation algorithm proposed by Klimek and Thurner (2013), whose results have been validated with data from a well-known massive multiplayer online game (Szell et al., 2010; Szell and Thurner, 2010, 2012). Note, nonetheless, that in order to have a well-defined evolution of speakers' preferences, we introduce a small modification to the algorithm so as to ensure that every node belongs to, at least, one triangle.

A broad range of possible asymptotic configurations is found as a result of the coupled dynamics of node and link states described above. Each of these asymptotic configurations belongs to one of these three classes: frozen extinction of one of the languages, frozen coexistence of both languages or dynamically trapped coexistence of both languages. Furthermore, metastable states with non-trivial dynamics and very long survival times are frequently found. The situations of coexistence are characterized by one of the languages becoming a minority but persisting in the form of "ghetto-like" structures, where predominantly bilingual speakers use it for the interactions among themselves —mostly triangular— but switch to the majority language for communications with the rest of the system —generally non-triangular—. A system size scaling shows, on the one hand, that the probability of extinction of one of the languages vanishes exponentially for increasing system sizes and, on the other hand, that the time scale of survival of the non-trivial dynamical metastable states increases linearly with the size of the system. Thus, non-trivial dynamical coexistence is the only possible outcome for large enough systems.

1.4

Outline

The contents of this thesis are divided in three parts, corresponding to the three main topics addressed:

- The first part is devoted to opinion dynamics and it consists of Chapter 2, where we study the influence of the initial distribution of opinions in a model of continuous-opinions under bounded-confidence. A modification of the model accounting for random changes of opinion is also studied (Carro et al., 2013).
- The second part deals with a model of herding behavior in financial markets and is divided in two chapters:
  - In Chapter 3 we address the influence of an external source of information upon the financial market model (Carro et al., 2015).
  - In Chapter 4 we study a network-embedded version of the herding model and focus on the influence of the underlying topology of interactions on the asymptotic behavior of the system (Carro et al., 2016a).
- The third part of the thesis focuses on the dynamics of language competition and consists of two chapters:
  - In Chapter 5 we develop a coevolving model of language competition, where language use is considered as a property of the links between speakers. In particular, the time evolution of the system is based on a majority rule for link states and random rewiring for links in a local minority (Carro et al., 2014).
  - In Chapter 6 we focus on the couple dynamics of language use, as a property of the links between speakers, and language preference, as a property of the speakers themselves (Carro et al., 2016b).

Finally, in Chapter 7, we offer some concluding remarks and point out some possible future developments.

Opinion dynamics

CHAPTER 2

Continuous-opinion dynamics under bounded confidence: the role of noise and initial conditions

We study, in this chapter, the importance of the initial distribution of opinions in determining the asymptotic configuration of a continuous-opinion model under bounded confidence. In particular, we focus on the model developed by Deffuant, Weisbuch et al. (Deffuant et al., 2000; Weisbuch et al., 2002). To this end, we analyze, by means of numerical simulation of the time evolution of the agents density, the effect of introducing a bias in the initial distribution towards the extremes or the center of the opinion space, with a parameter which allows for a continuous change between these two situations. In order to check the impact of the symmetry of the initial distribution, this analysis is performed both in a symmetric and in an asymmetric context. We find that, for a given value of the confidence bound parameter, the initial condition has a strong importance in determining the final state of the system, not only the position of the final opinion groups being affected, but also the total number of these clusters, i.e., that the consensus can be encouraged or prevented by certain initial conditions.

Furthermore, we also consider the case of a modification of the Deffuant, Weisbuch et al. model to take into account a certain element of randomness in the form of a noise (Pineda et al., 2009, 2011, 2013). This noisy term can be thought of as a certain kind of "free will", since the agents are given the opportunity to change their opinion independently of their acquaintances. As a consequence, the importance of the initial condition is partially replaced by that of the statistical distribution of the noise. Nevertheless, we still find evidence of the influence of

the initial state upon the final configuration for a short range of the bound of confidence parameter.

In Section 2.1 we present and in-depth description of the Deffuant, Weisbuch et al. model, as well as a brief review of some results published in recent years regarding this model. The extension of this original model to take into account noisy perturbations in the opinions of the agents is addressed in Section 2.2. A description of the different initial conditions tested is offered in Section 2.3, as well as a description of the measures used to characterize these distributions and to quantify the obtained results. We present also in this section the general features of the simulations performed. Sections 2.4 and 2.5 are devoted to the presentation of the results. In the first one we study the importance of the initial distribution of opinions for the stationary result of the original Deffuant, Weisbuch et al. model, while in the second one we analyze the case in which a noise is added to the system. We draw, in Section 2.6, some general conclusions from the results of this study.

2.1

The original, noiseless model

We review here the model developed by Deffuant et al. (2000) and Weisbuch et al. (2002) in its original agent-based form, i.e., with its dynamics or behavioral rules defined for a finite population of N agents. We present, as well, a redefinition of the system as a density-based model, as introduced by Ben-Naim et al. (2003a) and by Lorenz and Tonella (2005), where the dynamics is defined for the density of agents in the opinion space. We use this second approach for the computation of all the results presented in this chapter.

In order to define the original agent-based version of the model, we begin by considering a group of N agents, where we denote by $x_i(t)$ the real number representing the opinion that individual i has at time step t about a given topic. Without loss of generality we take $x_i(t) \in [0, 1]$. The behavioral rules defined for the agents basically state that, at each time step, a pair of individuals, say i and j, is randomly chosen. Then, if their opinions are close enough, that is, if they satisfy $|x_i(t) - x_j(t)| < \epsilon$, being ϵ the bound of confidence, they are respectively adjusted as

$$\begin{aligned} x_i(t+1) &= x_i(t) + \mu\,[x_j(t) - x_i(t)]\ , \\ x_j(t+1) &= x_j(t) + \mu\,[x_i(t) - x_j(t)]\ , \end{aligned} \tag{2.1}$$

remaining unchanged otherwise. The iteration of this dynamical rule leads the system to a static final configuration which, depending on the parameters μ and

ϵ, can be a state of full consensus or one of fragmentation, where the individuals split in several opinion clusters of different sizes. This definition generates a mean field model, since all the agents have the same probability to be chosen as interaction partners.

The parameter μ, which is restricted to the interval $(0, 1/2]$, can be thought of as the "persuasibility" of the individuals, since it states how far an agent is willing to change its opinion. It basically fixes the speed of convergence and, as a consequence, it has some importance in determining the final number of clusters (Laguna et al., 2004; Porfiri et al., 2007). In particular, for intermediate and large values of μ, the speed of convergence becomes so fast in the extremes of the opinion space that some small amount of agents are left around that region with no possibility of communication with the rest of the individuals. These agents are therefore unable to change and moderate their opinions, forming two minority clusters of extremists. On the contrary, for small values of μ, i.e., for slow convergence speeds, all the agents have the opportunity to meet and interact with others, being influenced by them, and thus slowly converging to the major clusters. Following most studies, and trying to avoid any further complexity, we adopt from now on in this chapter the value $\mu = 1/2$, meaning a perfect compromise between interacting individuals.

In the context of the opinion space introduced above, the confidence parameter is restricted to the interval $\epsilon \in [0, 1]$. It is a measure of the receptiveness of the agents, that is, their willingness or readiness to interact with other individuals whose ideas are different from theirs. It states up to what point the ideas of two individuals must be similar in order for them to be willing to interact with each other. In a typical realization of the agent-based dynamics starting from uniformly distributed random initial opinions, a consensus is obtained for large values of the confidence parameter, $\epsilon \geq 1/2$, while a fragmentation into opinion clusters separated by distances larger than ϵ can be observed for smaller values, $\epsilon < 1/2$, whether these clusters are large or small (Deffuant et al., 2000; Weisbuch et al., 2002, 2003).

The first density-based approach to the Deffuant, Weisbuch et al. model, developed by Ben-Naim et al. (2003a), basically involved changing the scope from a finite number of agents to an idealized infinite number of individuals which are distributed in the opinion interval as defined by a density function. Therefore, the system is described in terms of a master equation for this density function $P(t, x)dx$, defined as the fraction of agents that have opinions in the

range $[x, x+dx]$ at time t,

$$\frac{\partial}{\partial t}P(t,x) = \int_0^1 dx_1 \int_{|x_1-x_2|\leq\epsilon} dx_2 \Bigg[P(t,x_1)P(t,x_2)\Bigg(\underbrace{2\delta\left(x - \frac{x_1+x_2}{2}\right)}_{\text{Fraction joining state } x} - \underbrace{\Big(\delta(x-x_1)+\delta(x-x_2)\Big)}_{\text{Fraction leaving state } x}\Bigg)\Bigg], \tag{2.2}$$

where the persuasibility of the agents is taken as $\mu = 1/2$. According to this dynamical rule, the two first moments of the opinion distribution —the total mass and the mean opinion—, are conserved. In particular, if we define the kth moment as $M_k(t) = \int dx\ x^k P(t,x)$, then it can be easily found that $\dot{M}_0 = 0 = \dot{M}_1$. For large values of the bound of confidence, $\epsilon \geq 1/2$, the stationary solution

$$P_{st}(x) = \delta(x - x_0)\,, \tag{2.3}$$

where x_0 is the mean opinion, is asymptotically found ($t \to \infty$), that is, only one opinion cluster is formed (Ben-Naim et al., 2003a). On the contrary, for low values of the bound of confidence, $\epsilon < 1/2$, it is numerically found that a finite number of opinion groups are formed, leading to the stationary distribution

$$P_{st}(x) = \sum_{i=1}^{r} m_i \delta(x - x_i)\,, \tag{2.4}$$

where r is the number of clusters, and x_i, m_i are, respectively, the position and the mass of cluster i.

We follow here a slightly different approach, along the lines of the works by Lorenz and Tonella (2005) and Lorenz (2007b, 2010), which involves a previous discretization of the opinion space into a finite number of opinion classes. The behavioral rules for the individuals are then translated to dynamical rules for the density of agents in these resulting opinion classes. Concerning the discretization, we divide the opinion space $[0,1]$ into n subintervals or *opinion classes* as $\left[0, \frac{1}{n}\right), \left[\frac{1}{n}, \frac{2}{n}\right), \ldots, \left[\frac{n-1}{n}, 1\right]$, which are labeled as $1, \ldots, n$. The bound of confidence ϵ is also naturally transformed into its opinion classes counterpart $[n\epsilon]$, where the square brackets $[\cdot]$ denote the integer part of a number. Therefore, the state of the system can be represented by a vector $\boldsymbol{p}(t)$, where each component $p_i(t)$ is the fraction of the total population which holds opinions in class i, and the time evolution of the system can be written as a discrete Markov chain. The density-based dynamics can then be defined as

$$\boldsymbol{p}(t+1) = \boldsymbol{p}(t)T[\boldsymbol{p}(t)]\,, \tag{2.5}$$

where $T[\boldsymbol{p}(t)]$ is a transition matrix depending only on the current state of the system $\boldsymbol{p}(t)$. In the case of the Deffuant, Weisbuch et al. model, this transition matrix can be written as

$$T_{ij}[\boldsymbol{p}] = \begin{cases} \dfrac{\pi^i_{2j-i-1}}{2} + \pi^i_{2j-i} + \dfrac{\pi^i_{2j-i+1}}{2}\,, & \text{if } i \neq j\,, \\ \displaystyle\sum_{j\neq i, j=1}^{n} T_{ij}[\boldsymbol{p}]\,, & \text{if } i = j\,, \end{cases} \tag{2.6}$$

where

$$\pi^i_m = \begin{cases} p_m\,, & \text{if } |i-m| \leq [n\epsilon]\,, \\ \displaystyle\sum_{j\neq i, j=1}^{n} T_{ij}[\boldsymbol{p}]\,, & \text{otherwise.} \end{cases} \tag{2.7}$$

This transition matrix states that the probability of an agent to change from opinion i to opinion j depends only on the fractions of agents in the opinion classes $2j-i-1$, $2j-i$ and $2j-i+1$, and only if these classes are not farther than $[n\epsilon]$ from i. Indeed, these are the only opinion classes whose average with i results in j. In the case of $2j-i-1$ and $2j-i+1$ it is only half of the agents who switch to j, the other half switching to $j-1$ and $j+1$ respectively. This discrete time and discrete opinion approach has been shown to lead to the same results as the previously presented continuous density-based model (Lorenz, 2007b).

In this context, the distribution of opinions at any point in time $P(t,x)$ can be directly and unequivocally determined from the initial distribution $P(0,x)$, avoiding the need for different realizations of the process. This is related to the fact that this density-based approach corresponds to the limit of a very large number of agents, $N \to \infty$, and thus to a case without finite-size fluctuations. As a consequence, the differences between the agent and the density-based approaches become larger the smaller the number of agents (Toral and Tessone, 2007). Some examples of disagreement are commented below. Another interesting advantage of the density-based approaches is that the conservation of the symmetry can be directly observed, in the continuous case, in the master equation (2.2) and, in the discrete case, in the definition of the transition matrix. This latter point implies that, if the initial distribution of opinions is symmetric around the central point $x = 1/2$, then we have $\forall t$ that $P(t,x) = P(t,1-x)$.

In order to determine the attractive cluster patterns for each bound of confidence and observe transitions of attractive patterns at critical values of ϵ, bifurcation diagrams are drawn. The asymptotic results of the model are shown in these graphs, where the location of clusters in the opinion space is plotted versus the continuum of values of the bound of confidence ϵ. *Bifurcation* refers here to

the appearance, dominance or splitting of a given cluster. Sometimes it is useful, when studying cluster patterns, to establish a difference between "major" opinion clusters, containing a high fraction of the population, and "minor" opinion clusters, containing a much smaller fraction. The bifurcation diagram for the Deffuant, Weisbuch et al. model with a uniform initial density in the opinion space is shown in panel **(b)** of Fig. 2.4. A detailed analysis shows that there are in these results four basic modes of bifurcation, which are repeated in descendant order of the bound of confidence ϵ and in shorter and shorter ϵ-intervals (Ben-Naim et al., 2003a). Let us describe, as an example, the first sequence. For $\epsilon \geq 1/2$ only one big central cluster evolves, gathering the vast majority of the population. As the bound of confidence decreases from $\epsilon = 1/2$, we can notice the nucleation of two minor clusters from the boundaries of the opinion space. Around $\epsilon \approx 0.266$ there is a bifurcation of the central cluster into two major clusters. Further decreasing ϵ, the central cluster has a rebirth as a minor cluster from $\epsilon \approx 0.222$, before suddenly increasing its mass around $\epsilon \approx 0.182$, pushing the two major clusters outwards.

A topic that has received much less attention in the relevant literature is the dependence of the model on the initial conditions, that is, on the initial distribution of opinions among the agents. As a first argument, we could notice that the model, as has been presented, conserves the mass and the mean opinion of the population, so the position of the final clusters depends on the mean of the initial distribution. However, also different initial conditions with the same mean opinion could give rise to different final configurations. In fact, it can be shown theoretically and confirmed by simulation that any combination of delta-functions is a steady state solution of the master equation describing the model, provided these delta-peaks are separated by a distance larger than ϵ and they conform to the mean opinion conservation (Lorenz, 2007b; Pineda et al., 2009). In fact, as we show in Section 2.4, it is perfectly possible to force or prevent a consensus by varying the initial distribution of opinions.

2.2

The modified, noisy model

A final configuration consisting of one or more delta functions means that all the agents within one of these opinion groups would share exactly the same opinion, which is clearly not very realistic. In order to avoid this perfect consensus within each cluster, Pineda et al. (2009) presented an extension of the original Deffuant, Weisbuch et al. model taking into account some additional randomness. Thus, a noise is introduced into the dynamics as a certain kind of "free will", which

allows for the agents to change their opinion from time to time to a randomly chosen value, independently of the opinions of other agents. Thus, the distribution of the noise is uniform in the opinion space (see Mäs et al., 2010, for a more complex, adaptive noise approach).

In this way, the dynamics is modified by allowing, at each time step, a randomly chosen agent to follow the original Deffuant, Weisbuch et al. interaction rule with probability $(1-m)$ or to choose at random a new opinion with probability m. This new parameter m is therefore a measure of the noise intensity. As a result of this extension, there is a transition between an ordered and a disordered phase at a critical value of the noise intensity. In the disordered state, corresponding to quite high noise rates, there is no cluster formation, as noise is stronger than the nucleation processes; on the contrary, in the ordered state, corresponding to lower noise rates, we can still clearly observe the formation of clusters, even if they broaden with respect to the noiseless case. Another difference between the original and the noisy models is that the position of the clusters in the latter case only vary at the bifurcation points, remaining constant between them. These features are shown in panel **b** of Fig. 2.8, where the asymptotic probability distribution $P_{st}(x)$ is plotted as a function of the bound of confidence ϵ for a small noise intensity, $m = 0.01$.

Starting from the master equation of the original Deffuant, Weisbuch et al. model, Eq. (2.2), the dynamics of the noisy case can be derived as

$$\frac{\partial}{\partial t}P(t,x) = (1-m)\int_0^1 dx_1 \int_{|x_1-x_2|\leq\epsilon} dx_2 \Bigg[P(t,x_1)P(t,x_2)\Bigg(2\delta\left(x-\frac{x_1+x_2}{2}\right) - \Big(\delta(x-x_1)+\delta(x-x_2)\Big)\Bigg)\Bigg] + m\underbrace{(P_a(x)-P(t,x))}_{\text{Noise term}}, \tag{2.8}$$

where $P_a(x)$ is the probability distribution of the noise, which we assume to be uniform in our case. It is clear from Eq. (2.8) that the net effect of the noise is to move the current opinion distribution towards the noise distribution with a velocity or intensity per time step m.

An interesting feature of this extension is that the average opinion of the system is not anymore a constant, but tends to the average of the noise distribution, regardless of the initial condition. Thus, the time evolution of the first moment is

$$\frac{dM_1}{dt} = m[M_1^a - M_1], \tag{2.9}$$

where M_1^a is the first moment of the distribution $P_a(x)$. Note, nevertheless, that even if the importance of the initial condition regarding the average opinion is

replaced by that of the noise distribution, the former has still some influence in determining the bifurcation patterns, as we show in Section 2.5.

2.3

Initial conditions, measures and simulations

We present in this section the two sets of different initial conditions employed in our simulations, as well as the measure used to characterize and differentiate between these distributions. Furthermore, we also present in this section some measures developed in the literature for the analysis of the resulting final configurations. Finally, we also give some details about the simulations performed.

Regarding the initial conditions, we explored two different functional forms as initial distributions of opinions: a symmetric quadratic function and an asymmetric piece-wise linear function. Concerning the quadratic functional form, we chose the distribution to be symmetric around $x = 1/2$. Its general form would then be $P(0,x) = c + b(x - 1/2)^2$ for $x \in (0,1)$. The normalization condition $\int_0^1 dx\, P(0,x) = 1$ implies $c = 1 - b/12$. This yields the final expression

$$P(0,x) = 1 + b\left[\left(x - \frac{1}{2}\right)^2 - \frac{1}{12}\right] . \tag{2.10}$$

Furthermore, the positivity of this quadratic form requires that the parameter b lies in the range $b \in [-6, 12]$. At $b = 0$ the quadratic function smoothly changes from a concave ($b < 0$) to a convex ($b > 0$) shape. By construction, the average value of this distribution is $\langle x \rangle = 1/2$, and its variance $\sigma^2 = b/180 + 1/12$. If $b = 0$, the distribution is uniform in the interval $(0,1)$ and its variance is $\sigma^2 = 1/12$. In order to easily distinguish between convex and concave distributions, we define the *shifted variance* $S_2 := \sigma^2 - 1/12$, or $S_2 = b/180$ in this case. This new measure is such that $S_2 > 0$ corresponds to a convex distribution, $S_2 < 0$ to a concave distribution, and $S_2 = 0$ to the uniform distribution. The minimum and maximum possible values for S_2, respecting the positivity of the distribution, are $-1/30$ and $1/15$, respectively.

In order to test the effect of asymmetries we defined a piece-wise linear distribution with a "triangular" shape, given by

$$P(0,x) = \begin{cases} 1 + a\left(\dfrac{3}{10} - x\right) & \text{if } x \leq \dfrac{3}{4}\,, \\ 1 + \dfrac{27}{5}a\left(x - \dfrac{5}{6}\right) & \text{if } x > \dfrac{3}{4}\,, \end{cases} \tag{2.11}$$

where the parameter a is restricted to the interval $a \in [-10/9,\ 20/9]$ in order to keep the function always positive. Again, the different terms have been tuned so that the average value of the distribution is still $\langle x \rangle = 1/2$. The variance can be easily found to be $\sigma^2 = 3a/160 + 1/12$. The *shifted variance*, which makes the convexity/concavity of the distribution more evident, is thus $S_2 = 3a/160$ in this case. Its minimum and maximum values, regarding the positivity of the distribution, are $-1/48$ and $1/24$, respectively.

Both sets of distributions are exemplified in Fig. 2.1 for the maximum and minimum values of the respective a and b intervals. It is evident in this figure that the *shifted variance* S_2 correctly distinguishes situations where a majority of agents have initially opinions around the center of the opinion interval $(S_2, a, b < 0)$ from other cases where a majority of agents have opinions towards the extremes $(S_2, a, b > 0)$. The former corresponds to an initial condition which would favor consensus while the latter corresponds to facilitating the splitting of the population into, at least, two opinion groups.

Since we are interested on assessing the effect of the initial condition on the final state of the system, we use some measures of consensus already introduced in the literature to quantify this final distribution of opinions. In particular, we use bifurcation diagrams as already described in Section 2.1. For the construction of these diagrams, we need a precise definition of what a cluster is and what its position in the opinion space is (Lorenz, 2007b). We define a *cluster* with a given precision, in our case 10^{-3}, as a set of adjacent opinion classes each of them with a fraction of agents or mass larger than the precision threshold and surrounded by neighboring classes with masses smaller than this precision. Regarding the *position* in the opinion space or the opinion corresponding to a given cluster, we approximate it by the average opinion of the agents within this group. In order to quantify the degree of consensus within the population, the *mass of the largest cluster* has been pointed out as an appropriate measure. We define the mass of the largest cluster as the total fraction of agents within it (Lorenz, 2010).

As explained below, the introduction of a noise in the original Deffuant, Weisbuch et al. model allows the system to undergo certain transitions between states which are forbidden in the original model. One could argue that this effect is related to the fact that the asymptotic states reached with the original model are,

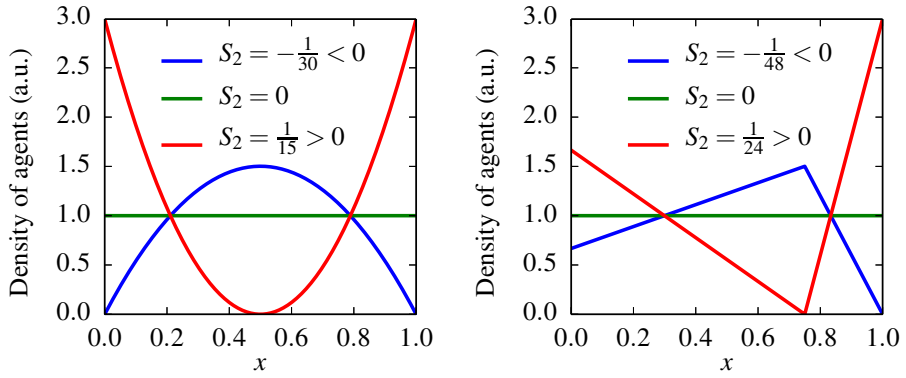

(a) Symmetric initial distributions **(b)** Asymmetric initial distributions

Figure 2.1: Illustration of the symmetric and asymmetric sets of initial distributions of opinions. S_2 is the *shifted variance* of the distributions, defined as $S_2 = \sigma^2 - 1/12$, where $\sigma^2 = \langle x^2 \rangle - \langle x \rangle^2$ is the variance and the value $1/12$ corresponds to the variance of a uniform distribution in the interval $[0, 1]$

in fact, metastable states, and that the presence of noise allows the system to exit from those states and reach a globally stable state. In order to characterize their relative stability we defined a Lyapunov function for the Deffuant, Weisbuch et al. model, that is, a positive-definite function which always decreases in time, given the interaction rules of the model, and whose minimum is zero. Let us write here only the definition of the Lyapunov function, while we leave its proof for Appendix 2.A,

$$\mathcal{L}[\boldsymbol{x}] = \sum_{i>j} (x_i - x_j)^2 \,, \tag{2.12}$$

where $\boldsymbol{x}(t)$ is a vector whose components are the opinions of the agents at time t. In the absence of noise, only transitions from states with a given value of $\mathcal{L}$ to those with a smaller (or equal) value would be permitted,

$$\mathcal{L}[\boldsymbol{x}(t+1)] \leq \mathcal{L}[\boldsymbol{x}(t)] \,. \tag{2.13}$$

For the numerical simulations, we used an algorithmic approach based on a discrete density-based reformulation of the Deffuant, Weisbuch et al. model along the lines of the works by Lorenz and Tonella (2005) and Lorenz (2007b). In particular, we discretized the opinion space $[0, 1]$ into 1001 opinion classes, an odd number being the only option allowing for one-class central opinion clusters. This one-class central opinion group in class 501 is quite important since, in the symmetric case, it is the only class which can have a density greater than

1/2. In order to study the bifurcation patterns, we run the algorithm for 100 evenly distributed values of the bound of confidence parameter, from $\epsilon = 0.1$ to $\epsilon = 0.6$. Furthermore, and with the purpose of analyzing the influence of the initial condition, we performed the simulations for 100 different values of the initial distribution parameters a and b, for each value of the bound of confidence.

Regarding the numerical results for the noisy extension of the model, we set the intensity of the noise at $m = 0.01$, in order for the system to be in the ordered state, as explained in above in Section 2.2 (see also Pineda et al., 2009). The convergence time, that is, the number of time steps needed for the system to reach a state where opinions have converged into opinion clusters separated by more than a bound of confidence, is much longer in the noisy than in the noiseless case. Therefore, the 1000 time steps we used for the original model were more than enough in that case, while we decided to use 50000 for the noisy model in order to ensure a good level of convergence.

2.4

The importance of the initial conditions in the noiseless model

In the noiseless case, when $m = 0$, the asymptotic steady state distribution $P_{st}(x) = \lim_{t\to\infty} P(x,t)$ is basically a sum of delta-functions located at certain points. As we are only interested in the fundamental changes caused by the variation of the initial conditions, we have chosen a relatively high threshold level for the detection of opinion groups, 10^{-3}, in order not to detect the minority clusters but only the major ones.

The mass of the largest cluster is shown in Figs. 2.2 and 2.3, respectively, for the symmetric and the asymmetric initial condition sets. In these plots, the x-axis represents the values of the bound of confidence ϵ, while the y-axis corresponds to the shifted variance S_2. Each point of this plane (ϵ, S_2) is colored according to the values of the mass of the largest cluster after stabilization. Parameter regions with major consensus are therefore colored dark red, while light blue means two equally distributed clusters. In order to give a more exhaustive idea about the bifurcation patterns which give rise to the masses of the largest cluster shown in these figures, we present in Figs. 2.4 and 2.5 the bifurcation diagrams for the four cuts or horizontal lines marked in Figs. 2.2 and 2.3, respectively.

Note that some of the transition lines observed in Figs. 2.2 and 2.3 are sharp and clear, while others appear to be more smooth and gradual changes. Let us

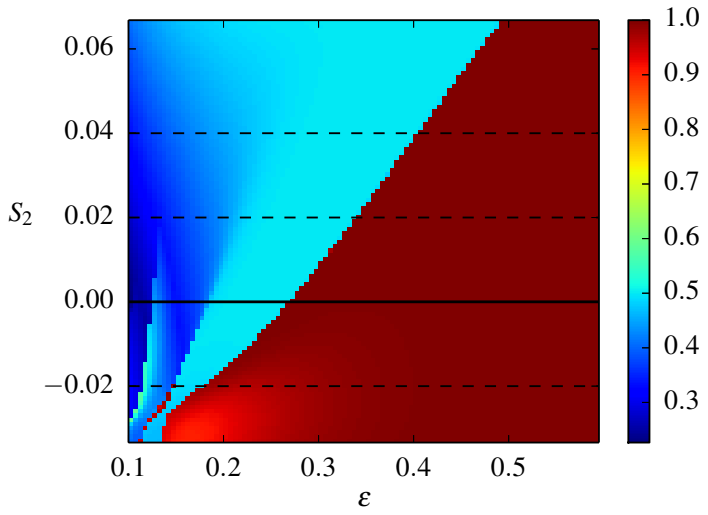

Figure 2.2: Mass of the largest cluster for the set of symmetric initial opinion distributions (quadratic functions) obtained with the noiseless Deffuant, Weisbuch et al. model. The values of the *shifted variance* marked by black horizontal lines (both dashed and solid), are those for which cuts of the opinion distribution are shown in Fig. 2.4.

first focus on the symmetric case, shown in Fig. 2.2, where we observe an oblique line of sudden transition between dark red and light blue, which can be shown to mean (see Fig. 2.4 below) a bifurcation from one central major opinion cluster to two smaller and symmetrical clusters. The smooth transition between light and dark blue represents a gradual decrease of the mass of these symmetrical clusters and the rebirth of the central one. In any case, the point we would like to stress here is the fact that these transition lines or regions, their position and smoothness, are highly dependent on the variance of the initial distribution of opinions, something that is particularly evident for the sharp transition from consensus to more than one opinion cluster.

Focusing now on the asymmetric initial condition case, we notice in Fig. 2.3 a rather different transition pattern. The main difference is the appearance of a new color or state, turquoise blue (between green and blue), meaning a mass of around 0.6 but corresponding to a state with two major opinion clusters, which would be impossible in the previous and symmetrical case. This is due to the fact that the initial distribution is not anymore symmetric around the central opinion 0.5, so a cluster can exist with a mass larger than 0.5 and not being located at the center of the opinion space. Note that the black solid horizontal line is identical

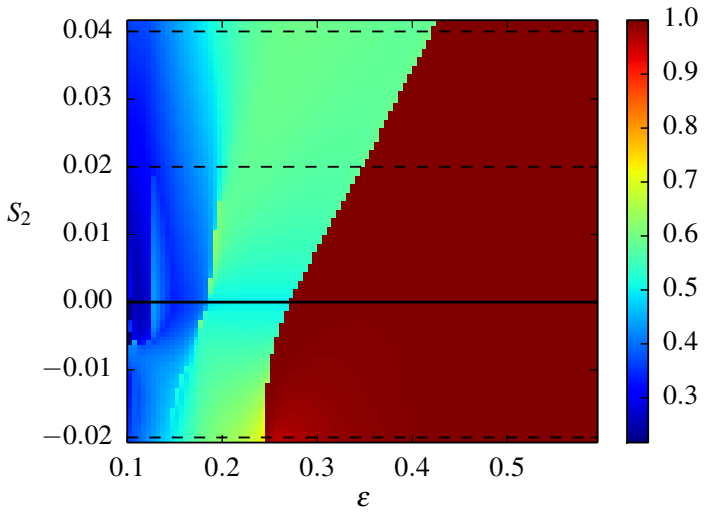

Figure 2.3: Mass of the largest cluster for the set of asymmetric initial distributions of opinions (triangular functions) obtained with the noiseless Deffuant, Weisbuch et al. model. The values of the *shifted variance* marked by black horizontal lines (both dashed and solid), are those for which cuts of the opinion distribution are shown in Fig. 2.5.

in both figures, due to the fact that, when the shifted variance equals zero, both initial conditions are equal and uniform.

Four examples of bifurcation diagrams are presented in Figs. 2.4 and 2.5 for each set of initial conditions, corresponding to the cuts marked, respectively, in Figs. 2.2 and 2.3. By comparing between these bifurcation diagrams and the previous plots of the mass of the largest cluster, we can notice that some of the opinion groups found are actually minority clusters. They are detected in the bifurcation diagram but, being their mass just slightly larger than the precision threshold 10^{-3}, they have no relevant influence in the mass of the largest cluster. The most clear examples of these minority groups are, on the one hand, the two symmetric clusters appearing on the bifurcation diagram for $S_2 = -0.02$ in Fig. 2.4 from $\epsilon \approx 0.3$ to $\epsilon \approx 0.2$ and, on the other hand, the cluster appearing just from the lower end of the opinion interval from $\epsilon \approx 0.35$ to $\epsilon \approx 0.25$ on the bifurcation diagram for $S_2 = -0.02$ in Fig. 2.5.

Both Fig. 2.4 and Fig. 2.5 serve as a confirmation of the strong importance of the initial condition in determining the bifurcation patterns of the steady state solution in the noiseless Deffuant, Weisbuch et al. model. In the symmetric case, even though the pattern of bifurcations is rather similar in each and every

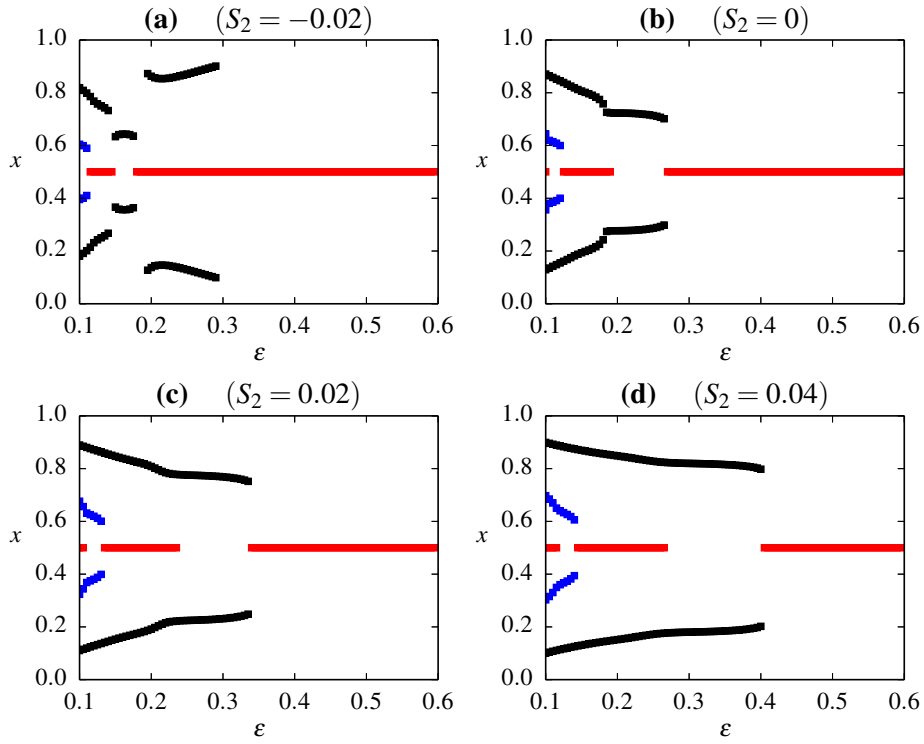

Figure 2.4: Bifurcation diagrams for four different symmetric initial distributions of opinions (quadratic functions) obtained with the noiseless Deffuant, Weisbuch et al. model.

example, the points of the bound of confidence axis where the bifurcations do take place smoothly increase with the variance of the initial distribution of opinions. This change is particularly relevant for the first bifurcation, which takes place at $\epsilon \approx 0.270$ in the uniform case, shown in plot **(b)**, but moves from $\epsilon \approx 0.180$ in plot **(a)** to $\epsilon \approx 0.405$ in plot **(d)**. Regarding the case of asymmetric initial conditions shown in Fig. 2.5, it is not only the bifurcation points, but also the general bifurcation structure which is perturbed by a variation of the initial distribution of opinions. In particular, we observe that the bifurcation patterns shown in plots **(a)**, **(c)** and **(d)** are clearly asymmetric and the first bifurcation point moves from $\epsilon \approx 0.245$ to $\epsilon \approx 0.420$.

In order to check whether the particular shape of the initial condition function has any important influence upon the bifurcation patterns of the model, we also tested a symmetric initial distribution with the shape of a centered triangle,

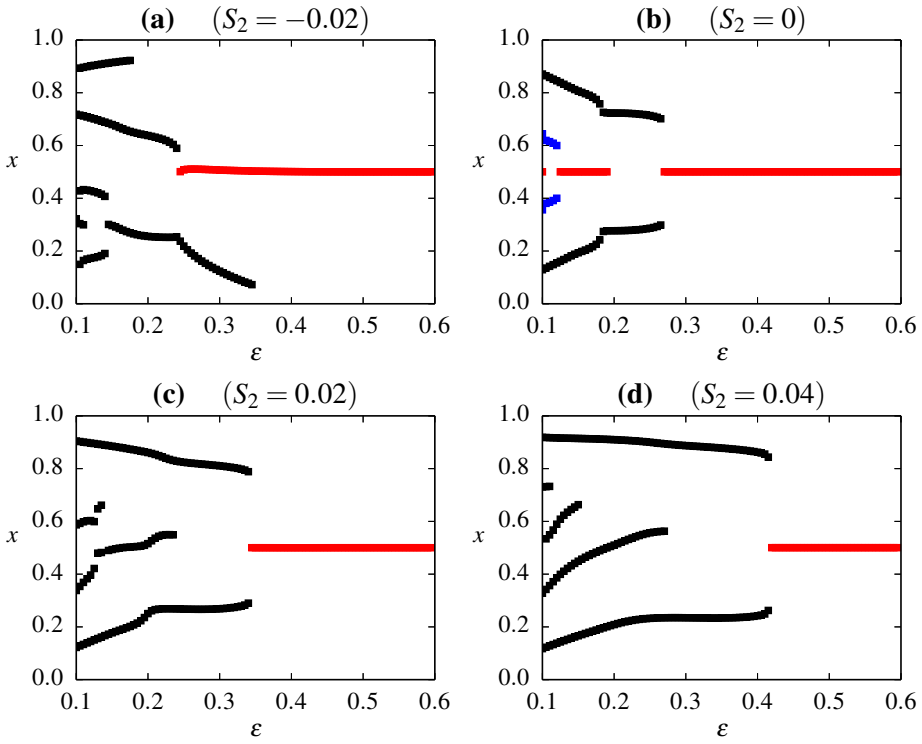

Figure 2.5: Bifurcation diagrams for four different asymmetric initial distributions of opinions (triangular functions) obtained with the noiseless Deffuant, Weisbuch et al. model.

thus different from the quadratic one. The results obtained being remarkably similar to the case of the symmetric quadratic condition, we deduce that the particular shape of the distribution does not play a major role regarding the final asymptotic solution of the model. Therefore, we conclude that the two most important variables for the characterization of the initial condition and its effects upon the Deffuant, Weisbuch et al. model are the symmetry and the variance of the distribution.

2.5

The importance of the initial conditions in the noisy model

If a noise of the type described in Section 2.2 is added to the original system, that is, if $m > 0$, then the asymptotic solution of the model is not anymore a collection of delta-functions, but a smooth distribution of opinions. Furthermore, if this noise m is small enough for the system to be in the ordered state, then the smooth steady state solutions are peaked around some specific values. In particular, we set the noise intensity at $m = 0.01$. Although, as a consequence, the definition of a cluster is not so obvious in this case as it is in the original noiseless model, the cluster detection mechanism presented in Section 2.3 aims to give correct results also in this noisy situation, and so we use it for the mass of the largest cluster plots. However, with regard to the bifurcation diagrams, and following Pineda et al. (2009), we decided to show here the whole probability density distribution and not just the position of the major clusters.

The mass of the largest cluster is shown for the noisy model in Figs. 2.6 and 2.7 for the symmetric and asymmetric initial condition cases respectively. It is interesting to notice, in a first and general view, that the range of mass values taken by the largest cluster is slightly shorter in the noisy case than in the noiseless results. This is mainly due to the fact that the agents no longer gather in just a small number of opinion classes, but they are distributed all along the opinion interval. Therefore, even if the distribution is peaked around some popular opinion classes, a non-negligible fraction of the population is dispersed among the rest of the opinion classes, not taking part in any major opinion cluster. This effect is also clearly observed in Figs. 2.8 and 2.9, which show a logarithmic color map of the density of agents in each opinion class for the four cuts marked, respectively, in Figs. 2.6 and 2.7. These latter plots are, as already pointed out, the equivalent of the bifurcation diagrams in Section 2.4.

As before, we can observe in the mass of the largest cluster plots of Figs. 2.6 and 2.7 some sharp as well as some smooth lines of transition. Comparing with the noiseless case results in Figs. 2.2 and 2.3, we notice that the transition lines are now mostly straight and vertical, unlike the oblique lines observed before. This feature basically means that the initial conditions are, in this case, less important in determining the final configuration of the system. However, we can observe a smaller but still noticeable influence in the oblique transition line from $S_2 = -0.02$ to $S_2 = 0.02$ in Fig. 2.6, and in the small change of the transition line around $S_2 = 0.01$ in Fig. 2.7.

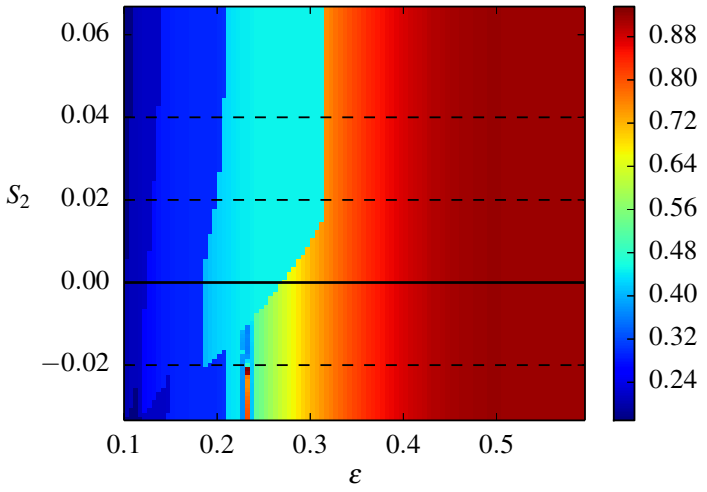

Figure 2.6: Mass of the largest cluster for the set of symmetric initial distributions of opinions (quadratic functions) obtained with the noisy Deffuant, Weisbuch et al. model, with a noise intensity $m = 0.01$. The values of the *shifted variance* marked by black horizontal lines (both dashed and solid), are those for which cuts of the opinion distribution are shown in Fig. 2.8.

By computing the value of the Lyapunov function in Eq. (2.12), we know that the most stable situation —leading, in particular, to $\mathcal{L} = 0$— is that where all the agents share the same opinion, and thus there is only one cluster. This is the most stable configuration, in the sense of the Lyapunov function defined above, even if there is a certain small spread in the opinion of the group participants. A configuration with two clusters corresponds to much higher values of the Lyapunov function, but still it may constitute a metastable state when the bound of confidence does not allow for interactions between the agents of both groups. Therefore, when the system starts from an initial condition very close to the two clusters final state, then it quickly evolves towards that final configuration. However, when introducing a small noise in this last situation, the system is able to overcome the barrier introduced by the bound of confidence and undergo a transition to the globally stable state of one cluster. This is so for large and intermediate values of the bound of confidence, namely for $\epsilon > 0.310$. On the contrary, for small values of this threshold, the time needed to arrive at a consensus becomes so large relative to the noise rate that the system is not able to leave the two clusters state. Regarding those initial conditions imposing a certain consensus from the beginning, even if their initial state is already more stable than a two cluster configuration, the presence of noise is able, for small

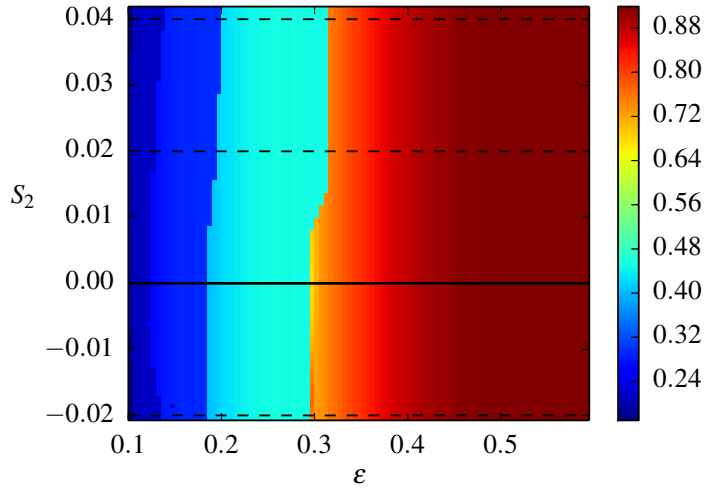

Figure 2.7: Mass of the largest cluster for the set of asymmetric initial distributions of opinions (triangular functions) obtained with the noisy Deffuant, Weisbuch et al. model, with a noise intensity $m = 0.01$. The values of the *shifted variance* marked by black horizontal lines (both dashed and solid), are those for which cuts of the opinion distribution are shown in Fig. 2.9.

values of the bound of confidence, to take the system to the two opinion groups state, which is the metastable state most easily reached from the noise opinion distribution, uniform in our case. Jumps between the stable and the metastable configurations have indeed been reported in the case of a uniform initial condition for the noisy Deffuant, Weisbuch et al. model (Pineda et al., 2009, 2011).

Four examples of bifurcation diagrams are shown in Figs. 2.8 and 2.9, in the form of probability density distributions, for each set of initial conditions. Some clusters and bifurcation patterns that we can observe in these plots are similar to the those in the bifurcation diagrams of the previous, noiseless case. However, we notice two significant differences, apart from the fact that now we have a smooth distribution of opinions in the final state and not anymore a collection of delta-functions. On the one hand, the bifurcation points are now very sharply defined, with no region of progressive transition from one state to the next. On the other hand, the location of the maximum values of the density does not significantly depend on the bound of confidence between bifurcation points, unlike the position of clusters in the noiseless model. This is due to the fact that the noisy perturbation allows the system to always reach the most stable configuration permitted by the bound of confidence, which only changes at the bifurcation points, when this confidence distance allows for more clusters

to appear. On the contrary, the noiseless model freezes on stable configurations even if they are not the most stable.

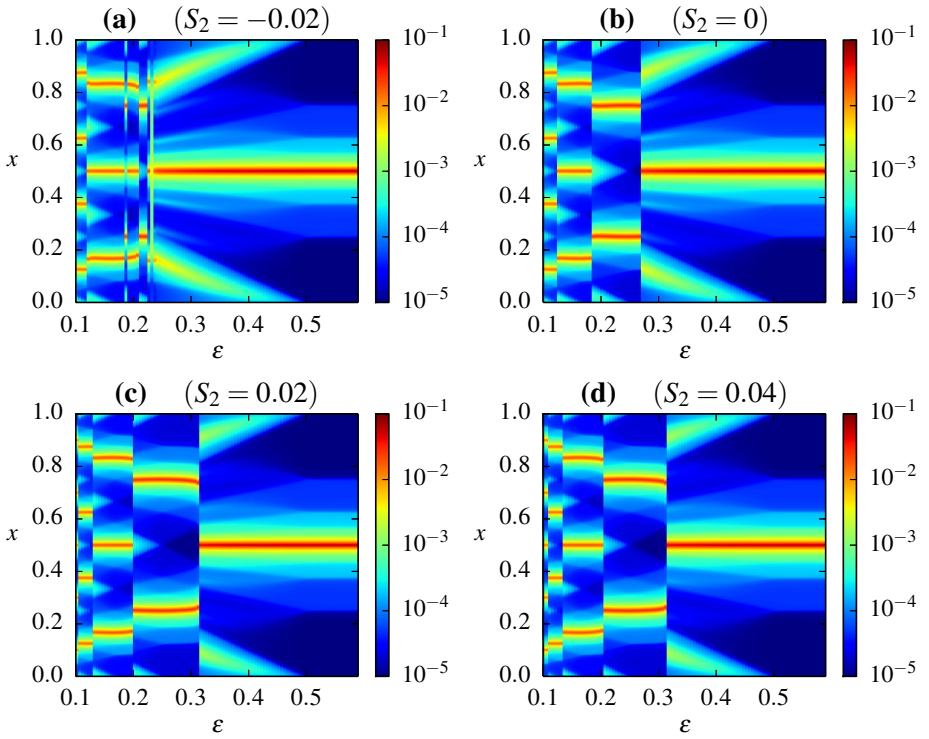

Figure 2.8: Bifurcation diagrams for four different symmetric initial distributions of opinions (quadratic functions) obtained with the noisy Deffuant, Weisbuch et al. model, with a noise intensity $m = 0.01$.

It is important to underline here the considerably long times needed for convergence when the initial conditions strongly force a consensus, as it is the case in panel **(a)** of both Figs. 2.8 and 2.9, where $S_2 = -0.02$. The unclear and short transitions that can be observed on the low ϵ part of these panels are, in fact, a consequence of the system not having totally converged even after 50000 time steps.

Unlike the results of the noiseless case, now the bifurcation patterns shown have generally the same structure for all the initial distributions tested. Nevertheless, there is still a noticeable influence of the initial conditions, as the location of the bifurcation points clearly changes among the different plots of the bifurcation diagrams, confirming what was noted before about the mass of the largest cluster

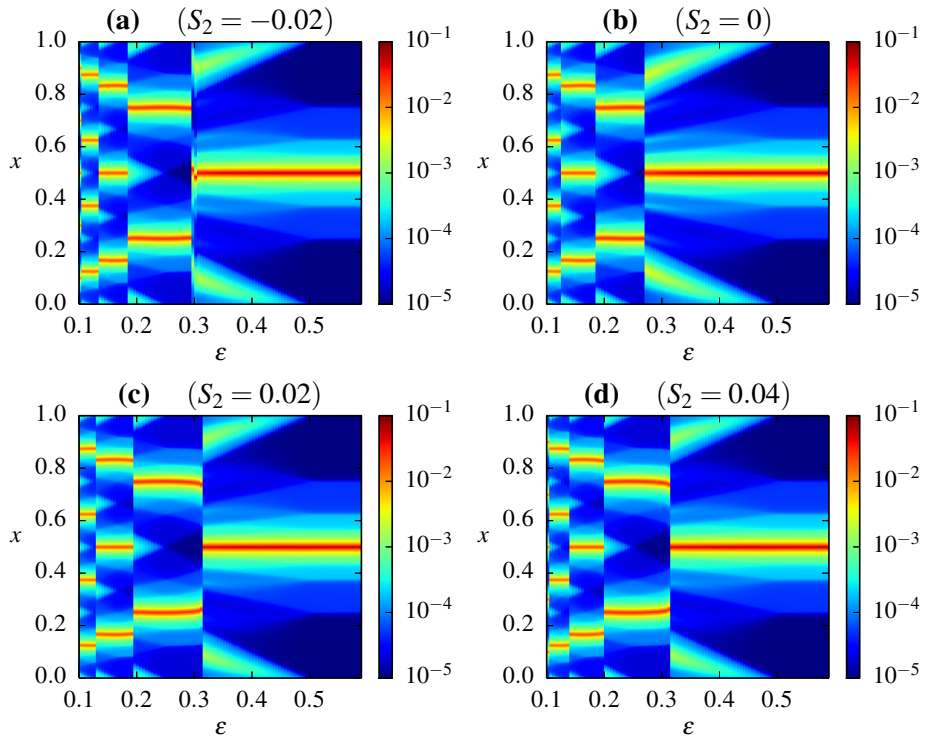

Figure 2.9: Bifurcation diagrams for four different asymmetric initial distributions of opinions (triangular functions) obtained with the noisy Deffuant, Weisbuch et al. model, with a noise intensity $m = 0.01$.

plots. Excluding the first and unconverged plot in panel **(a)**, the first bifurcation point, from consensus to two opinion clusters, moves from a minimum value of $\epsilon \approx 0.270$ in the uniform initial condition plot in panel **(b)** to a maximum of $\epsilon \approx 0.315$ in panel **(d)** for both the symmetric and the asymmetric cases.

Another interesting feature to notice in the bifurcation diagrams is the strong difference between Fig. 2.9, in this section, and Fig. 2.5, in the previous one. They both show the results of the model starting from an asymmetric initial condition. However, only in the noiseless case the resulting bifurcation diagram is asymmetric. The graph obtained with the noisy model for an asymmetric initial distribution is, in fact, equal to the one obtained with a symmetric initial condition. This is a case of symmetry restored by noise, and it is due to the fact that the distribution of the noise we use is always symmetric and uniform. As it was proved by Pineda et al. (2009) and shown in Section 2.2, the prevalent

condition, regarding the moments of the final distribution, is the distribution of the noise. Thus, the mean opinion value to be conserved and the general bifurcation structure to be found is that corresponding to a uniform distribution.

Again, we checked that the particular shape of the initial distribution has no major effect concerning the asymptotic solution of the model by simulating also a symmetric initial distribution with the shape of a centered triangle, thus different from the quadratic one. As in the noiseless case, we found that the results are remarkably similar to the case of the symmetric quadratic condition. Thus, we conclude, again, that the symmetry and the variance of the distribution are still good parameters for the characterization of the initial condition and its effects upon the noisy Deffuant, Weisbuch et al. model.

2.6

Concluding remarks

We have shown, by numerical simulation, that the asymptotic solution of the original Deffuant, Weisbuch et al. model is highly dependent on the initial condition. As a consequence, we have shown that it is indeed possible to promote or prevent a consensus among a group of agents by just varying the initial distribution of opinions in a case where the only dynamical mechanism is a pairwise bounded confidence interaction rule. For instance, systems with an initial distribution of opinions moderately polarized into two different opinion groups will find it much more difficult to arrive at a consensus, even if the individuals are willing to deal with very distant opinions. On the contrary, systems with an initial distribution of opinions moderately consensual will very easily find a globally shared opinion, regardless of how close-minded the agents are. In particular, we have shown that the transition from consensus to more than one opinion group can be moved in the range $\epsilon \in (0.135, 0.495)$ for the symmetric set of initial conditions we used, while the range is $\epsilon \in (0.245, 0.425)$ for the asymmetric initial distributions presented.

However, if the agents have the ability to choose a new random opinion from time to time, then the possibility to initially prevent a consensus is totally removed and that of forcing it is substantially reduced. We have shown, both analytically and numerically, that the importance of the initial condition in determining the asymptotic state of the system is mainly replaced by the distribution of the noise. Nevertheless, there is still a slight but noticeable impact of the initial condition upon the final or steady state, particularly for those initial distributions showing a moderate consensus. Thus, we observe in the noisy sym-

metric case that the transition from consensus to more than one opinion group can be a sharp transition at $\epsilon \approx 0.315$ or a smooth transition taking place in the range $\epsilon \in (0.235, 0.315)$ depending on the variance of the initial condition. In the noisy asymmetric case, we observe a change in the location of this transition in the much shorter range $\epsilon \in (0.295, 0.315)$.

Given the important differences observed in the noiseless model between the mass of the biggest cluster plots of the symmetric and the asymmetric sets of initial conditions, it is clear that the variance of the initial opinion distribution is not the correct or not the only parameter to take into account. As it can also be noticed in the related bifurcation diagrams, the variance is not enough to determine if the system will end up in a consensus or not for a given bound of confidence value. We notice that the symmetry of the initial condition does also play an important role. Therefore, we would probably need to take into account other parameters of the initial distribution as, for example, some higher moments.

Regarding the model with noise, the differences found in the bifurcation diagrams and the mass of the biggest cluster figures between both sets of initial conditions are not as important as in the original model. In fact, the bifurcation patterns observed in the mass of the biggest cluster figures show that the initial condition is irrelevant in determining the final configuration if the variance is strong enough, that is, if we sufficiently encourage the system to initially split into two main opinion groups at the extremes. Nevertheless, for lower values of the initial distribution variance, the final configuration of the system still depends on this initial condition. In particular, the variance is again unable to precisely determine the existence or not of a consensus, even though it gives a much better prediction than in the noiseless case.

APPENDICES TO CHAPTER 2

2.A

Lyapunov function for the Deffuant, Weisbuch et al. model

In order to write a Lyapunov function for the Deffuant, Weisbuch et al. process, we need to find a function $\mathcal{L}[\boldsymbol{x}(t)]$, where $\boldsymbol{x}(t)$ is a vector whose components are the agents' opinions at time t, which satisfies

$$\mathcal{L}[\boldsymbol{x}(t)] \geq 0 \quad \forall t, \tag{2.14}$$

$$\mathcal{L}[\boldsymbol{x}(t+1)] \leq \mathcal{L}[\boldsymbol{x}(t)] \quad \forall t, \tag{2.15}$$

where Eq. (2.14) simply means that it is a positive-definite function and Eq. (2.15) that it cannot increase with time.

Let us first write a positive-definite function and then prove that it is decreasing in time for the model interaction rules. In particular, let us write a function which only depends on the distances between the agents opinions as

$$\mathcal{L}[\boldsymbol{x}] = \sum_{i>j} (x_i - x_j)^2 \,, \tag{2.16}$$

where we only sum over all terms which are different. Let us then focus on one interaction, i.e., on the changes of the positions of only two agents in the opinion space, say agents i_1 and j_1. Thus, we may divide the Lyapunov function into two

terms, one dependent and the other independent of i_1 and j_1, and let us call the independent part A for simplicity:

$$\mathcal{L}[\boldsymbol{x}(t)] = A + \sum_{i \neq i_1, j_1} [x_{i_1}(t) - x_i(t)]^2 + \sum_{i \neq i_1, j_1} [x_{j_1}(t) - x_i(t)]^2 + [x_{i_1}(t) - x_{j_1}(t)]^2 \,. \tag{2.17}$$

Each sum contains $N - 2$ terms, being N the number of agents. Now we use the new opinions $x_{i_1}(t+1)$ and $x_{j_1}(t+1)$ that agents i_1 and j_1 hold after the interaction. It is important to notice that this interaction does only take place in case the opinions of the agents are closer than the bound of confidence ϵ. However, this does not affect our analysis, as we are only interested in effective interactions, those which actually take place. The Lyapunov function after the interaction is

$$\mathcal{L}[\boldsymbol{x}(t+1)] = A + \sum_{i \neq i_1, j_1} [x_{i_1}(t+1) - x_i(t)]^2 + \sum_{i \neq i_1, j_1} [x_{j_1}(t+1) - x_i(t)]^2 + [x_{i_1}(t+1) - x_{j_1}(t+1)]^2 \,. \tag{2.18}$$

Replacing the new values $x_{i_1}(t+1)$ and $x_{j_1}(t+1)$ as given by the application of the rule Eq. (2.1) and subtracting, we get the variation of the Lyapunov as $\Delta\mathcal{L} = \mathcal{L}[\boldsymbol{x}(t+1)] - \mathcal{L}[\boldsymbol{x}(t)]$ which, after some algebra, reads:

$$\Delta\mathcal{L} = -2\mu(1-\mu)N[x_{i_1}(t) - x_{j_1}(t)]^2 \,. \tag{2.19}$$

In this manner, we see that the Lyapunov function $\mathcal{L}$ is strictly decreasing in time when any interaction takes place, and it stays constant when no interaction occurs.

Herding behavior and financial markets

CHAPTER 3

Markets, herding and response to external information

We focus here on the influence of external sources of information upon financial markets. In particular, we develop a stochastic agent-based market model of a financial market along the lines of the works by Kirman (1991, 1993) and Alfarano et al. (2008), but open to the arrival of external information in the form of an dynamic signal affecting the traders' behavior. This signal can be interpreted as a time-varying advertising, public perception or rumor, in favor or against one of two possible trading behaviors, thus breaking the symmetry of the system and acting as a continuously varying exogenous shock. As an illustration of information input, we use a well-known *Indicator of Economic Sentiment* published in Germany by the Center for European Economic Research (ZEW). We first analyze the effect of different intensities of the external information upon the market, as well as compare the corresponding results with Germany's leading stock market index, the DAX, in order to find an appropriate value for this model parameter. Once the intensity has been fixed, we study the market conditions for the ensemble of traders to more accurately follow the information input signal, finding an interesting resonance phenomenon, i.e., a maximum of the accuracy of the market in reflecting the arrival of external information for an intermediate range of values of a market parameter related to the importance of random behavior relative to herding among traders. This result suggests the existence of different market regimes regarding the assimilation of incoming information: amplification, precise assimilation and undervaluation of incoming information.

The original herding model is presented in Section 3.1, as well as a brief description of its main results. In Section 3.2 we present the financial market framework in which the herding mechanism is embedded. A general discussion

about different types of external news affecting financial markets is presented in Section 3.3, where we also develop a herding mechanism open to the arrival of external information. In Section 3.4 we describe some details of the numerical simulations used through the chapter. Sections 3.5 and 3.6 contain the main results of the chapter. In the first we study the effect of varying the intensity of the external information. The conditions for the system to better assimilate the incoming information are addressed in the second. Finally, we draw some conclusions in Section 3.7.

3.1

The original herding model

Inspired by a series of entomological experiments with ant colonies, Kirman (1993) proposed a stochastic herding formalism to model the process of decision making among financial agents. In the experiments with ants, entomologists observed the emergence of asymmetric collective behaviors from an apparently symmetric situation: when ants were faced with a choice between two identical food sources, a majority of the population tended to exploit only one of them at a given time, turning its foraging attention to the other source every once in a while. In order to explain this behavior, Kirman developed a stochastic model where the probability for an ant to change its foraging source results from a combination of two mechanism. On the one hand, he postulated the existence of a herding propensity among the ants, i.e., a tendency to follow the crowd, which implies the existence of some kind of interaction among them with information transmission. On the other hand, he also assumed the ants to randomly explore their neighborhood looking for new food sources, so every one of them has an autonomous switching tendency or idiosyncratic behavior, which plays the role of a free will.

This simple herding model was reinterpreted by Kirman in terms of market behavior, by simply replacing an ant's binary choice between food sources by a market agent's choice between two different trading strategies. These different strategies may be related to some particular rules for the formation of the agents' expectations about the future evolution of prices, or result from differences in their interpretation of present and past information. For instance, foreign exchange market traders can adopt different tactics, such as a fundamentalist or a chartist forecast of future exchange rate movements. A further example would be the choice between an optimistic or a pessimistic tendency among the chartist traders. In these examples, the herding model would be the decision making mechanism among financial agents, who decide whether to buy or sell in a given situation,

thus giving rise to market switches between a dominance of one or the other strategy.

A series of subsequent papers (Lux and Marchesi, 1999; Alfarano et al., 2005, 2008; Alfarano and Milaković, 2009; Alfarano et al., 2013) has focused on explaining some of the stylized facts observed in empirical data from financial markets in terms of herding models of the Kirman type. However, there have been two different implementations of the herding term in the literature. In his seminal paper, Kirman (1993) proposed a herding probability that, for each agent, was proportional to the fraction of agents in the opposite state. One of the main drawbacks of this original formalization has been pointed out to be its lack of robustness with respect to an enlargement of the system size N, or N-dependence, since an increasing number of participants in the market causes the stochasticity to vanish and therefore the stylized facts to fade away. On the contrary, some later authors (Alfarano et al., 2005, 2008; Alfarano and Milaković, 2009; Alfarano et al., 2013) avoided this problem with an alternative modeling of the interaction mechanism based on a herding probability that, for each agent, is proportional to the absolute number of agents in the opposite state, thus allowing each individual to interact with any other regardless of the system size. We will hereafter adopt this second and more recent formalism. This approach has proven to be successful in reproducing, for instance, the fat tails in the distribution of returns, the volatility clustering, and the positive autocorrelation of absolute and squared returns.

Let us now briefly review the formalization of the referred herding model —in its non-extensive, N-independent formulation— and some analytical derivations along the lines of previous works by Alfarano et al. (2008) and Kononovicius and Gontis (2012), which will be useful for subsequent analyses. Let the market be populated by a fixed number of traders N, and let n be the number of those agents choosing one of the two possible strategies, while $N - n$ choose the other one. For the sake of clarity, we will hereafter refer to the case of optimistic vs. pessimistic opinions about the future evolution of prices and, in particular, we will call the first group of n agents optimistic and the second group of $N-n$ agents pessimistic. In this manner, $n \in 0, 1, ..., N$ defines the configuration or state of the system. Its evolution is given by the two aforementioned terms: on the one hand there are pairwise encounters of agents, after which one of them may copy the strategy of the other, and on the other hand there are idiosyncratic random changes of state, playing the role of a free will. An additional assumption of the model is the lack of memory of the agents, so their probability of changing state does not depend on the outcome of previous encounters, neither on previous idiosyncratic switches. Therefore, the stochastic evolution of the system can be formalized as a Markov process depending, at each time step, just on the probability to switch from the present configuration of the system n to some other state n' in a time interval Δt,

denoted by $P(n', t+\Delta t|n, t)$. However, if this time interval Δt is taken to be small enough, then the probability to observe multiple jumps is negligible and we can restrict our analysis to $n' = n \pm 1$. Furthermore, the probabilities would then be related to the transition rates per unit time as $P(n', t + \Delta t|n, t) = \pi(n \to n')\Delta t$. The transition rates for each individual i, $\pi_i^+ = \pi_i(\textit{pessimistic} \to \textit{optimistic})$ and $\pi_i^- = \pi_i(\textit{optimistic} \to \textit{pessimistic})$, can be formally defined as

$$\begin{aligned} \pi_i^+ &= a + h\, n\,, \\ \pi_i^- &= a + h\,(N - n)\,, \end{aligned}$$

where the parameters a and h stand for the idiosyncratic switch and the herding intensity coefficients respectively. The rates for the whole system are, therefore,

$$\begin{aligned} \pi^+(n) = \quad \pi(n \to n+1) = \quad (N-n)\ (a + h\, n)\ , \\ \pi^-(n) = \quad \pi(n \to n-1) = \quad n\ (a + h\,(N-n))\ . \end{aligned} \tag{3.1}$$

There are two parameters in the model, a and h, but one of them can be used as a rescaling of the time variable, so that there is only one relevant parameter, such as $\epsilon = a/h$.

For the sake of subsequent analytical derivations, it is useful to replace the extensive variable n, in the range $n \in [0, N]$, by an intensive one which can be treated as continuous for large system sizes N —note, however, that the limit of an infinite number of agents is never the case in real social and economic systems, where finite-size effects may play a role (Toral and Tessone, 2007)—. In particular, we choose $x = 2n/N - 1$ as our intensive variable, giving an opinion index in the range $x \in [-1, +1]$. We choose this range for our intensive variable, as done by Alfarano et al. (2008), in order to ease the comparisons with the external information signal which will be used later, also in the range $[-1, +1]$. Note that an opinion index $x = 0$ would imply a perfect balance of opinions, while $x = -1$ and $x = +1$ would signal a full agreement on the pessimistic and the optimistic opinions respectively. Note as well that the partial derivation with respect to the new intensive variable becomes, in terms of the previous extensive one, $\partial/\partial x = (N/2)\,\partial/\partial n$ and therefore the relation between their probabilities is $P(x, t) = P(n, t)N/2$.

By means of a systematic and consistent expansion in N, it has been shown that the Markovian stochastic process defined above can be approximated by a continuous diffusion process described by the Fokker-Planck equation (Alfarano

et al., 2008),

$$\begin{aligned}\frac{\partial P(x,t)}{\partial t} &= \frac{\partial}{\partial x}\Big[-\mu(x)P(x,t)\Big] + \frac{1}{2}\frac{\partial^2}{\partial x^2}\Big[D(x)P(x,t)\Big] \\ &= \frac{\partial}{\partial x}\Big[2axP(x,t)\Big] + \frac{1}{2}\frac{\partial^2}{\partial x^2}\left[\left(\frac{4a}{N} + 2h(1-x^2)\right)P(x,t)\right],\end{aligned} \tag{3.2}$$

where $\mu(x)$ plays the role of a drift term and $D(x)$ is the diffusion coefficient. As an alternative way to analyze the dynamics of the model, it is possible to derive a stochastic differential equation for the stochastic process $x(t)$, known as Langevin equation. Using the Fokker-Planck equation (3.2) and applying the usual transformation rule (Van Kampen, 2007), within the Itô convention (Itô, 1951), we find the Langevin equation describing the process,

$$\begin{aligned}\dot{x} &= \mu(x) + \sqrt{D(x)}\cdot\xi(t) \\ &= -2ax + \sqrt{\frac{4a}{N} + 2h(1-x^2)}\cdot\xi(t)\,,\end{aligned} \tag{3.3}$$

where $\xi(t)$ is a Gaussian white noise, i.e., a random variable with a zero mean Gaussian distribution, $\langle\xi(t)\rangle = 0$, and correlations $\langle\xi(t)\xi(t')\rangle = \delta(t-t')$.

Let us first analyze the role played by the noise or diffusion term inside the square root in Eq. (3.3), $D(x) = \frac{4a}{N} + 2h(1-x^2)$. The first term, dependent on a and inversely proportional to the system size N, is related to the "granularity" of the system, and so it vanishes in the continuous limit $N \to \infty$. It basically states that for any finite system there are always finite-size stochastic fluctuations related to the fact that the agents have the ability to randomly change their choice. The second term of the diffusion function is a multiplicative noise term, i.e., a noise whose intensity depends on the state variable itself. Furthermore, it is the only term dependent on the herding coefficient, so we will refer to it hereafter as herding term. As this multiplicative noise is maximum for $x = 0$ and vanishes for $x = \pm 1$, it is clear from Eq. (3.3) that it tends to move the system away from the center and towards those extremes by making any random partial agreement on one or the other possible opinions grow to a complete consensus.

Regarding the deterministic drift term, $\mu(x) = -2ax$, it is evident by observing Eq. (3.3) that it has the role of driving the system back to a balanced position at the center of the opinion index, $x = 0$. Therefore, we have a competition between two opposed driving forces. One of them is of a stochastic nature, it is dominated by the herding term for large N and it tends to favor the formation of a majority of traders sharing the same opinion about the future evolution of prices. Whereas the other is of a deterministic nature, it is related to the idiosyncratic switches and it tends to break these majorities and drive the system back

to a balanced situation, where the traders are equally distributed between both opinions. The magnitude of these two driving forces is related to their respective parameters, a and h. Note that in the extreme case of pure herding, $a = 0$, the consensus states $x = \pm 1$ become absorbing: once all the agents agree in the use of a certain strategy, the system is frozen and there is no further evolution [see Eq. (3.3)]. On the opposite, in the extreme case of pure random changes of opinion, $h = 0$, the system would just be characterized by finite-size Gaussian fluctuations around the mean opinion index $\langle x \rangle = 0$.

For non-zero values of both the idiosyncratic and the herding parameters, there is a competition between the two aforementioned driving forces and, depending on their relative magnitude, one or the other behavior prevails: either the tendency to form a large majority of agents sharing the same opinion or the tendency to reverse any random majority to a balanced situation. Indeed, the particular functional form of the noise in this herding model induces a transition in the dynamics of the system from a monostable to a bistable behavior when increasing the value of h relative to that of a. This transition, as well as the particular implications of mono and bistability, can be explained in terms of the probability distribution $P_{\rm st}(x)$, steady state solution of the Fokker-Planck equation (3.2), which can be written as

$$P_{\rm st}(x) = \mathcal{Z}^{-1} \left[\frac{a}{2Nh} + \frac{(1-x^2)}{4} \right]^{\frac{a}{h}-1} . \tag{3.4}$$

The normalization factor $\mathcal{Z}^{-1}$ is given by

$$\mathcal{Z}^{-1} = \frac{\frac{1}{2}\left(\frac{2\epsilon}{N}+1\right)^{-\epsilon}\sqrt{\frac{2\epsilon}{N}+1}}{B\left[\frac{1}{2}\left(1+\sqrt{\frac{2\epsilon}{N}+1}\right);\,\epsilon,\,\epsilon\right] - B\left[\frac{1}{2}\left(1-\sqrt{\frac{2\epsilon}{N}+1}\right);\,\epsilon,\,\epsilon\right]} , \tag{3.5}$$

where $B[x;a,b]$ is the incomplete beta function, defined as

$$B[x;a,b] = \int_0^x u^{a-1}(1-u)^{b-1} du , \tag{3.6}$$

and $\epsilon = a/h$.

Observing the functional form of the steady state solution (3.4), one can notice that the sign of the exponent will determine whether the probability distribution is unimodal with a peak centered at $x = 0$ or bimodal with peaks at the extreme values $x = -1$ and $x = +1$. Therefore, when the idiosyncratic switching a is larger than the herding intensity h, we find a unimodal distribution, meaning that, at any point in time, the most likely outcome of an observation is to find the community of traders equally split between both options. On the contrary,

when the herding h exceeds the idiosyncratic switching intensity a, a bimodal distribution is found, meaning that, at any point in time, the most likely outcome of a static observation is to find a large majority of agents choosing the same option. Nevertheless, in different observations, the option chosen by the majority may be different. Note as well that when $a = h$ ($\epsilon = 1$) the probability distribution is uniform, meaning that any share of agents between the two options is equally probable. Because of the ergodicity of the model, these probability distributions can also be understood in terms of the fractional time spent by the system in each state.

An alternative way to observe the transition between a monostable and a bistable behavior and to explain it as a noise induced phenomenon consists in introducing the *effective potential* (San Miguel and Toral, 2000): a function combining the effects of both the deterministic driving force and the noise such that its minima are attractive points of the dynamics. We can define the effective potential $U_{\text{eff}}(x)$ by assuming an exponential functional form for the stationary probability distribution $P_{\text{st}}(x)$,

$$P_{\text{st}}(x) \equiv \mathcal{C}^{-1} \exp\left(-\frac{U_{\text{eff}}(x)}{D}\right), \tag{3.7}$$

where D is an effective noise intensity that we take as $D = h$, and the constant $\mathcal{C}^{-1}$ plays the role of a normalization factor. Note that, defined as such, the minima of this effective potential function correspond to maxima of the stationary state probability distribution. Let us directly write here the effective potential for the Fokker-Planck equation (3.2), which takes into account the effect of the multiplicative noise over the deterministic driving force related to the drift term (see Appendix 3.A for a derivation),

$$U_{\text{eff}}(x) = (h - a)\,\ln(1 - x^2)\,. \tag{3.8}$$

The change of sign occurring in Eq. (3.8) for $h = a$ marks the transition from a one well to a double well potential when increasing h. The functional form of the effective potential is shown in Fig. 3.1 for the three possible cases: $a < h$, $a = h$, and $a > h$.

In the $a < h$ case, it is worthy of remark the fact that, although both minima of the effective potential at the extremes of the opinion index space are theoretically infinite wells, in fact, they are not absorbing states and so the system will leave them with a probability proportional to a. This can be understood by reexamining the Langevin equation (3.3), where we notice that precisely at the extreme states $x \pm 1$ the only term acting upon the system is the deterministic force driving it towards the center of the opinion index. To sum up, in the $a < h$ case, the role of the herding (h) is to induce a bistable effective potential with

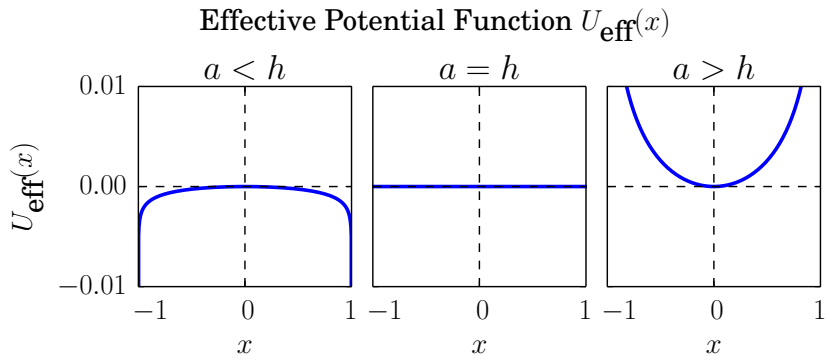

Figure 3.1: Effective potential $U_{\mathrm{eff}}(x)$ for three different values of the idiosyncratic switching tendency, $a = 10^{-4}$, 10^{-3}, 10^{-2}. The rest of the parameter values are $h = 10^{-3}$ and $N = 200$. Note that the values of a shown here correspond to the three main cases $a < h$, $a = h$, and $a > h$.

two wells at the extremes of the opinion index, while that of the idiosyncratic switching (a) is to allow for transitions between these two wells.

Two examples of stochastic realizations of this original herding model are shown in Fig. 3.3 (two panels in the first row, labeled $F = 0$). The first example, with an idiosyncratic switching coefficient smaller than the herding intensity ($a = 5 \cdot 10^{-4}$, $h = 10^{-3}$), corresponds to a bimodal probability distribution of states. We can observe, in this panel, the tendency of the system to be temporarily absorbed in the proximity of the consensus states with random switches between them. Some of those switches are not successful and the system returns to the previous consensus before reaching the opposite one. This type of evolution corresponds to a market where traders strongly tend to agree on their opinion about the future evolution of prices but this forecast agreement switches, from time to time, from optimism to pessimism and vice versa. The case of a unimodal probability distribution of states is displayed in the second panel, corresponding to an idiosyncratic switching coefficient larger than the herding intensity ($a = 5 \cdot 10^{-3}$, $h = 10^{-3}$). Note that, as opposed to the previous example, the opinion index spends most of the time in the central part of the opinion space, between $x = -0.5$ and $x = 0.5$. This corresponds to a market where traders are mostly guided by their own idiosyncratic drives, paying little attention to other traders' attitudes, and thus statistically tending to be equally divided among the two possible opinions.

3.2

The financial market framework

In order to model a financial market, we need to embed the stochastic herding formalism described above into an asset pricing framework. Different implementations of the market have been proposed in the literature (Kirman, 1991; Kirman and Teyssière, 2002; Lux and Marchesi, 1999; Alfarano et al., 2005; Kononovicius and Gontis, 2012), characterized by different degrees of complexity. We will use here a very simple noise trader framework along the lines of previous works by Alfarano et al. (2008). To this end, we need to define the different types of agents acting in the market and relate them to the herding two-state dynamics. In particular, the market is assumed to be populated by two kinds of agents: fundamentalist and noise traders.

Fundamentalist traders assume the existence of a "fundamental" price of the traded asset, towards which the actual market price tends to come back. Therefore, they buy (sell) if the actual market price p is below (above) their perceived fundamental value p_f. Assuming that their reaction depends on the log relative difference between the fundamental value and the current market price, instead of absolute difference, the excess demand by the fundamentalist group is given by

$$ED_f = N_f T_f \ln\left(\frac{p_f}{p}\right) , \tag{3.9}$$

where N_f is the number of fundamentalists in the market and T_f is their average traded volume. The reaction to relative rather than absolute under- and overvaluations not only seems more plausible, but also facilitates subsequent derivations. In any case, the small observed daily changes of price ($\sim 1\%$) assure that results would not diverge much if absolute differences were to be used.

The agents of the second group, noise traders, react according to their particular forecast of the future evolution of prices, which can be optimistic or pessimistic. They are therefore divided into two subgroups: optimistic noise traders expect the price of the traded asset to increase in the future and thus decide to buy at the current market price, while pessimistic noise traders expect the price to decrease and thus choose to sell. It is precisely here where the herding model introduced in the previous section enters into the market framework: it is the decision-making mechanism used by the noise traders to choose whether they are optimistic or pessimistic regarding the future price of the traded asset. In this manner, the excess demand by this group of agents becomes a direct consequence of the dominance of optimism or pessimism among them, quantified by

the opinion index $x = 2n/N - 1$ introduced above, and can be written as

$$ED_c = NT_c x\,, \tag{3.10}$$

where N is the number of noise traders in the market and T_c their average traded volume. Note that only the noise traders N are considered in the herding model described in the previous section.

An equation for the evolution of price can be found by using the Walrasian assumption that relative asset price changes are proportional to the excess demand for the asset (Walras, 1954). Commonly referred to as Walrasian *tâtonnement*, it has become the standard approach in the context of general equilibrium theory (Samuelson, 1965). The dynamics of price adjustment can be expressed in continuous-time as

$$\frac{1}{\beta p}\frac{dp}{dt} = N_f T_f \ln\left(\frac{p_f}{p}\right) + NT_c x\,, \tag{3.11}$$

with β representing a price adjustment speed. We further assume, without loss of generality, an instantaneous market clearing ($\beta \to \infty$) and that the total volume traded by both groups of agents is identical ($N_f T_f = NT_c$). We find, in this manner, an equilibrium price driven by both the fundamental value perceived by the fundamentalists and the opinion index among the noise traders,

$$p(t) = p_f \exp\left(x(t)\right)\,, \tag{3.12}$$

where we have also considered a fundamental value independent of time. This approximation seems plausible in cases where movements of opinion among noise traders occur on a much shorter time scale than changes in the fundamentals of the traded asset, and we are interested in the short time scale behavior. Note that, being the price given by a strictly increasing function of the opinion index among the noise traders, following the majority (herding) is equivalent to following the trends in the price.

For studying the non-stationary properties of returns and volatility, we define the continuously compounded return over an arbitrary time window Δt as the logarithmic change of price,

$$R(t, \Delta t) = \ln p(t + \Delta t) - \ln p(t) = x(t + \Delta t) - x(t)\,, \tag{3.13}$$

and we use absolute returns as a measure of the volatility, $V(t, \Delta t) = |R(t, \Delta t)|$. For clarity, we will refer hereafter to the daily ($\Delta t = 1$ day) returns and volatility as $R(t)$ and $V(t)$ respectively. Furthermore, for comparison with real data in the following sections, we will use the normalized daily returns and volatility, defined as

$$r(t) = \frac{R(t) - \langle R\rangle}{\sigma(R)}, \qquad\qquad v(t) = |r(t)|\,, \tag{3.14}$$

where $\langle R \rangle$ and $\sigma(R)$ are, respectively, the mean and the standard deviation of the time series of daily returns. Finally, the autocorrelation of the normalized daily volatility will also be used for comparison with real data,

$$\mathrm{ACF}(v) = \frac{\Big\langle \Big(v(t) - \langle v \rangle\Big)\Big(v(t+\tau) - \langle v \rangle\Big) \Big\rangle}{\sigma(v)^2}\,, \tag{3.15}$$

where $\langle \cdot \rangle$ denotes an average over time, $\sigma(\cdot)$ stands for the standard deviation, and τ plays the role of a time lag.

The use of this asset pricing framework with the stochastic herding formalism introduced in the previous section gives rise to a market model closed to any external information. The implications of this market model are analyzed below as a particular case of a more general market model open to the arrival of external information (developed in the following section): the case of a zero influence external signal.

3.3

The model with external information

The model described so far represents financial markets as completely closed entities, being the price changes of a given asset determined only by the endogenous evolution of the opinion index among noise traders [see Eq. (3.12)]. Even if we allow for a time-dependent fundamental value p_f, this would only account for the instantaneous arrival of objective information regarding the fundamentals of the asset itself. For instance, the information released in a company's quarterly earnings report directly influences the fundamental value of its stock in the market (Healy and Palepu, 2001). A further example is the instantaneous effect of the devaluation of a given currency on its fundamental value in the exchange market. However, we are not interested here in changes of the perceived fundamental value of an asset resulting from a rational analysis by the fundamentalist traders, and giving rise to direct and linearly proportional movements of the market price [see Eq. (3.12)]. On the contrary, we are interested in the arrival of external information not necessarily related to the traded asset and giving rise to trends of optimism or pessimism among the noise traders —note that, even when dealing with objective information related to the fundamentals of an asset, its disclosure may not only change the value perceived by fundamentalists, but also trigger important speculative movements among noise traders—. Thus, we are concerned with how external news can change the subjective perception or mood of noise traders and generate fads: a prevalence of fear or confidence promoted

from outside the market. Note that we focus our attention on a global and passive reception of external information, rather than an individual and active search for it, as studied by Preis et al. (2010, 2013), Moat et al. (2013) and Curme et al. (2014). As examples of this kind of passively received external information we can mention: the publication of news related to companies by specialized financial media (Joulin et al., 2008; Alanyali et al., 2013; Lillo et al., 2015); the spread of rumors related to the economy (Kiymaz, 2001); the updating of various economic indices, such as those tracking the general performance of the economy (Hanousek et al., 2009; Rangel, 2011); the disclosure of forecasts and recommendations by different analysts (Jegadeesh and Kim, 2006); the announcement of world events, such as terrorist attacks (Arin et al., 2008; Drakos, 2010); and, in general, the molding of public opinion by mass media (Davis, 2006; Tetlock, 2007).

For the sake of illustration, we will use hereafter the *Indicator of Economic Sentiment* developed by the Center for European Economic Research (ZEW)[1] as an example of external information input to the market. This indicator measures the level of confidence that a group of up to 350 financial and economic analysts — experts from the finance, research and economic departments as well as traders, fund managers and investment consultants— has about the current economic situation in Germany and its expected development for the next 6 months. The survey is conducted every month and the corresponding index is constructed as the difference between the percentage share of analysts who are optimistic and the percentage share of analysts who are pessimistic about the development of the economy. We nevertheless underline that the formalism that follows is general and independent of the particular shape of the external information signal used. The only relevant features of this information input having a significant effect on the results are its strength and its frequency or rate of change.

In order to design a financial market model open to the arrival of external information of the aforementioned type, the immediate question becomes how to modify the transition rates (3.1) to take this external input into account. We are here interested in the modification of the social processes of opinion formation and propagation of information among the economic agents. So we are naturally led to introduce the information input signal in the social term of the transition rates, that is, in the herding coefficient h (for a different approach, see Harras et al., 2012). Note that this choice leads to a direct linear dependence of the effect of the external information upon a given agent on the number of agents with the contrary opinion [see Eqs. (3.16) and (3.17)]. In particular, this effect completely vanishes when there is no agent in the opposite state. In this manner, optimist (pessimist) traders in a market with a clear consensus for optimism (pessimism) will be less affected by external information in the opposite sense. Thus, we

[1] Accessible at http://www.zew.de/en/publikationen/

modify the transition rates (3.1) as

$$\begin{aligned} \pi^+(n,t) &= \pi(n \to n+1,t) = (N-n)\,(a + h_+(t)n)\,, \\ \pi^-(n,t) &= \pi(n \to n-1,t) = n\,(a + h_-(t)(N-n))\,, \end{aligned} \tag{3.16}$$

where the herding coefficients are now different in the two possible directions and are both time-dependent functions given by

$$\begin{aligned} h_+(t) &= h_0 + \frac{F}{N} i(t)\,, \\ h_-(t) &= h_0 - \frac{F}{N} i(t)\,, \end{aligned} \tag{3.17}$$

with h_0 playing the role of a constant or background herding coefficient, F acting as the strength or intensity of the external information applied to the whole system, and $i(t)$ being the dynamic information itself. Note that we will refer to a and h_0 as parameters of the market and to F as a parameter of the input signal. As the opinion index x, the information function $i(t)$ takes values in the range $[-1, 1]$, being the negative and positive ones respectively associated with pessimistic and optimistic news. The intensity can be understood as a measure of the resources used by the external source in order to transmit the information and persuade the agents. Note that this information input term is not proportional to the total strength exerted on the system, but to the total strength per agent, F/N. The rationale behind this particular functional form for the external input term is basically a limited resources assumption: the resources spent in transmitting the information and convincing the whole system are divided among its constituents, so that if the system size N increases, the resources available for convincing each of the agents decrease. The reason for adding and subtracting the external input term, respectively in $h_+(t)$ and $h_-(t)$, is just so that positive (negative) values of the information help transitions towards optimism (pessimism) while they hinder transitions towards pessimism (optimism). In order to keep the transition rates always positive, the intensity per agent must satisfy $F/N \leq h_0$.

Proceeding in a similar manner as for the original herding model in Section 3.1, and applying the same approximations, we find the new Fokker-Planck equation,

$$\begin{aligned} \frac{\partial P(x,t)}{\partial t} =& \frac{\partial}{\partial x}\Big[-\mu(x,t)P(x,t)\Big] + \frac{1}{2}\frac{\partial^2}{\partial x^2}\Big[D(x)P(x,t)\Big] \\ =& \frac{\partial}{\partial x}\Big[\Big(2ax - F(1-x^2)i(t)\Big)P(x,t)\Big] \\ &+ \frac{1}{2}\frac{\partial^2}{\partial x^2}\left[\left(\frac{4a}{N} + 2h_0(1-x^2)\right)P(x,t)\right]. \end{aligned} \tag{3.18}$$

Note that, compared to the previous Fokker-Planck equation (3.2), the herding coefficient h has been replaced by its constant part h_0 inside the diffusion coefficient $D(x)$. There is also a new time-dependent term inside the drift function $\mu(x,t)$, which becomes itself dependent on time. Again, the conventional transformation rule leads us, within the Itô form, to the Langevin equation describing the process,

$$\begin{aligned} \dot{x} &= \mu(x,t) + \sqrt{D(x)} \cdot \xi(t) \\ &= -2ax + F(1-x^2)i(t) + \sqrt{\frac{4a}{N} + 2h_0(1-x^2)} \cdot \xi(t)\,, \end{aligned} \tag{3.19}$$

where $\xi(t)$ is, as before, a Gaussian white noise.

The constant part of the herding coefficient h_0 plays exactly the same role as the herding coefficient itself in the original herding model. The new term of the drift function, on the contrary, changes fundamentally the general behavior of the system. In particular, it will force the market to follow the external information signal by favoring or opposing, depending on the sign of this signal, the tendency towards $x = 0$ caused by the first drift term. In other words, the equilibrium point of the drift function is no longer a constant at $x = 0$, but a function dependent on time through $i(t)$ and taking values around this central point. The new parameter F, the strength of the information input, modulates the intensity of this effect. Note also that the factor $(1 - x^2)$ inside the new drift term causes its effects to vanish at the extremes of the opinion index space and its absolute value to be maximal at its center for $i(t) = \pm 1$. Thus, the effect of the external information upon the market vanishes for increasing consensus among the noise traders and becomes strongest when the group is equally divided between the two possible opinions. This behavior seems plausible from the perspective that groups with consensus tend to be confident about their common decision and less prone to pay attention to external sources of information than groups with a division of opinions (Granovetter, 1978). Note as well that the new drift term vanishing at the extremes of the opinion index space, it does not help the system to exit the consensus states, and therefore some idiosyncratic behavior ($a > 0$) is still needed in order to observe transitions between both full agreement states.

Concerning the competition between the deterministic and the stochastic terms of Eq. (3.3), the inclusion of an external information input in Eq. (3.19) has the general effect of counteracting or enhancing the deterministic driving force depending on the sign of this information signal. For a deeper understanding of the transition induced by the multiplicative noise upon the deterministic driving force and the symmetry breaking role of the external information, let us write the effective potential [see Eq. (3.7)] for the Fokker-Planck equation (3.18),

$$U_{\text{eff}}(x,t) = (h_0 - a)\,\ln(1-x^2) - x\,F\,i(t)\,, \tag{3.20}$$

Again, we leave its derivation for Appendix 3.A. Note that the new term, related with the information input signal, is linear in the opinion index variable x, and thereby it breaks the symmetry ($x \leftrightarrow -x$) of the potential for $i(t) \neq 0$.

The dependence of the effective potential on the information input signal is illustrated in Fig. 3.2, where snapshots are presented for five different values of the signal and for three values of the idiosyncratic parameter a. For values of a below h_0, allowing for the creation of a double well effective potential, the role of the external information is to modify the depth of these wells, making one of them relatively more attractive than the other. In this case, large majorities of traders sharing the same opinion tend to emerge in the market, generally including the whole of it, and the external information simply facilitates an optimistic or pessimistic consensus depending on its sign. When a equals h_0 the effective potential becomes a linear function, and the role of the information input is to vary its slope, thus creating a unique minimum at $x = -1$ or $x = 1$. Therefore, in a market where every share of opinions is equally probable, the external information facilitates again the creation of strong majorities, tending to include the whole of the market. Values of a larger than h_0 give rise to a monostable effective potential, where the minimum is moved around the center of the opinion index space by the influence of the information input. Thus, when traders tend to be equally divided between the two possible opinions, the role of the external information is to slightly break this symmetry, giving rise to weak majorities tending to not include the whole of the market.

3.4

Numerical methods

In contrast with the methods presented in the previous literature (Alfarano et al., 2005, 2008; Alfarano and Milaković, 2009; Kononovicius and Gontis, 2012), we have used a Gillespie algorithm for the simulation of the model (Gillespie, 1977, 1992). A single realization of this algorithm represents a random walk with the exact probability distribution of the master equation, therefore generating statistically unbiased trajectories of the stochastic equation. Thereby, we generate an unbiased sequence of times when the transitions of agents between the optimistic and pessimistic states take place. For a stochastic system with time-dependent transition rates $\pi^{\pm}(t) = \pi(n \to n \pm 1, t)$, and assuming that the last transition took place at time t_1, the cumulative probability of observing an event $n \to n \pm 1$

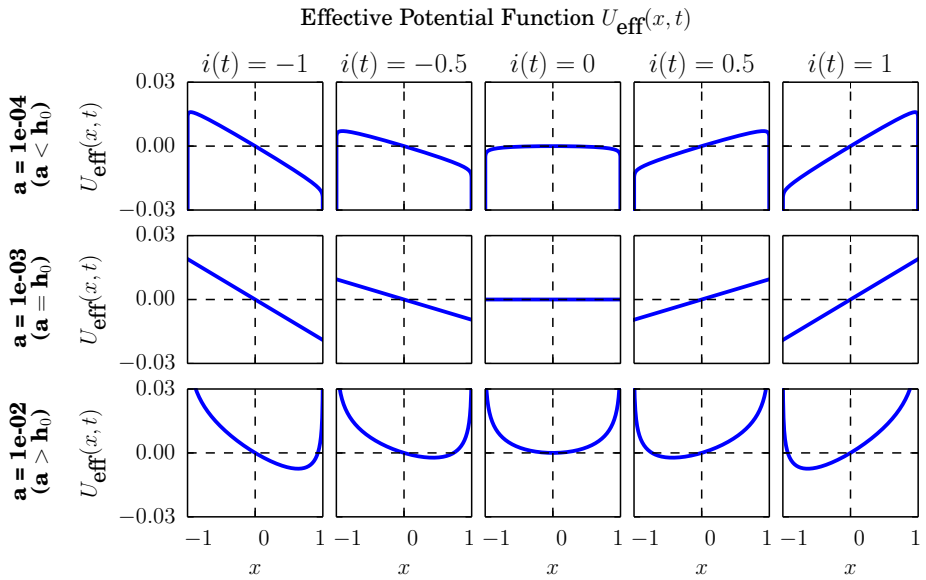

Figure 3.2: Effective potential $U_{\text{eff}}(x,t)$ for various values of the information input signal $i(t)$ and for three different values of the idiosyncratic switching tendency, $a = 10^{-4}$, 10^{-3}, 10^{-2}. The rest of the parameter values are $h_0 = 10^{-3}$, $F = 0.02$, and $N = 200$. Note that the values of a shown here correspond to the three main cases $a < h_0$, $a = h_0$ and $a > h_0$.

at time $t_2^{\pm}$ can be written as

$$F(t_2^{\pm}|\,t_1) = 1 - e^{-\int_{t_1}^{t_2^{\pm}} \pi^{\pm}(t)dt} \,. \tag{3.21}$$

We can equate this expression to a uniformly distributed random number $u^{\pm}$ between 0 and 1 in order to find an equation for the time of the next event, $t_2^{\pm}$,

$$\int_{t_1}^{t_2^{\pm}} \pi^{\pm}(t)dt = -\ln(1-u^{\pm}) \equiv -\ln(u^{\pm})\,, \tag{3.22}$$

where we have used that $u^{\pm}$ and $1-u^{\pm}$ are statistically equivalent. By that means, two different times are found: t_2^{+}, corresponding to the transition rate $\pi^{+}(t)$, and t_2^{-}, related to the transition rate $\pi^{-}(t)$. The event actually taking place is the one related to the shortest time.

For the sake of solving Eq. (3.22), we assume that the information signal $i(t)$ [and thus the transition rates, see Eqs. (3.16) and (3.17)], stays constant between every two releases of information. Moreover, we assume without loss of generality that these announcements or news arrival instants are periodical in time. This is particularly the case when dealing with the publication of some economic surveys such as the ZEW *Indicator of Economic Sentiment* —the input signal we chose for illustration—, which is released monthly. In order to both correctly introduce the external information into the model and compare its results to real data from stock markets, we need to set the relation between the time unit of the model and the real time. For simplicity, we choose the time unit of the model to correspond to a real day of trade. Again, this choice implies no loss of generality, since the time scale of the model —that is, the velocity at which noise traders change their position in the market— can also be varied by modifying the values of the parameters a and h while keeping their relation constant. As a consequence, we update the *Indicator of Economic Sentiment* every 20 time units of the model, corresponding to the 20 trading days of each month (considering, for simplicity, months of four weeks and weeks of five trading days). All simulations start from a random distribution of optimistic/pessimistic opinions among noise traders and evolve for 5280 time units, roughly corresponding to the trading days between December of 1991 and November of 2013: the data period of the ZEW *Indicator of Economic Sentiment* that we use. For comparison with real data we use the daily variations of the German stock exchange index DAX during the same period of time. Note that the monthly variations of these two datasets have a small but positive cross-correlation, showing that there is no direct cause-effect relationship between them, but rather that the ZEW *Indicator of Economic Sentiment* constitutes a relevant input to be fed into the model presented above, whose agents will then filter it in a non-trivial and non-linear way through their idiosyncratic changes and their herding interactions.

3.5

Effect of the external information on the market

The particular modifications of the collective behavior of the market due to the introduction of an external information signal depend on the specific values of the model parameters. We devote this subsection to the analysis of the effect produced by different input signal intensities on the typical simulated patterns of three market variables: the opinion index among noise traders, the normalized daily returns and their bursting behavior, and the autocorrelation function of the daily volatility. For the two latter cases we offer as well a comparison with real

financial data (DAX), allowing us to choose an appropriate value for the intensity of the information signal.

Fig. 3.3 contains two sets of three panels illustrating the effect on the noise traders opinion index of increasing the intensity of the incoming information from the closed market case, $F = 0$, to its maximum allowed value, $F = Nh_0$. The three panels in the first column address the case of market parameters in the bistable regime, $a < h_0$, while the three panels in the second column deal with market parameters in the monostable regime, $a > h_0$. In the first case, $a = 5{\cdot}10^{-4}$ and $h_0 = 10^{-3}$, we observe that the application of an information input reinforces the bistability of the distribution of states. By comparing the closed market case ($F = 0$) with the market subject to a small information strength ($F = 0.02$), we notice that the introduction of a small input intensity is able to modify the behavior of the system by pushing the opinion index towards a fully optimistic or pessimistic extreme. However, the market is not able to follow the mood changes of the external signal: the opinion index may stay around an optimistic extreme while the external information is rather pessimistic (see, for example, the negative peak around $t = 4000$). In the maximum information strength case ($F = 0.2$), we observe an even faster collapse of the opinion index around its extreme values, but we notice now that the changes of mood of the external signal are generally matched by large opinion movements of the market in the same direction.

The effect of increasing the intensity of the incoming information in the case of market parameters (a, h_0) in the monostable regime is shown in the second column of Fig. 3.3, where $a = 5 \cdot 10^{-3}$ and $h_0 = 10^{-3}$. First, we notice that the application of an information input can result in a bistable-like behavior, as the one expected for $a < h_0$ and $F = 0$, especially in the case of a large input intensity (case $F = 0.2$). This is due to the introduction of the external information term as part of the herding coefficient [see Eq. 3.17]. Interestingly, we also notice that for a market with this level of idiosyncrasy even a small input intensity ($F = 0.02$) is able to force the opinion index to follow the shape of the external signal. Similarly to the bistable case ($a < h_0$ column), a large input strength ($F = 0.2$) compels the market to an amplification of the information signal. Nonetheless, the higher level of idiosyncrasy allows now for the collapse of the opinion index around the fully optimistic or pessimistic extremes to take place as soon as the signal becomes, respectively, optimistic [$i(t) > 0$] or pessimistic [$i(t) < 0$]. The convincing power of the external information source being so strong, most of the noise traders are quickly persuaded to align their opinions with the optimism or pessimism of the input signal.

The behavior of the normalized daily returns [see Eq. (3.14)] under different input strengths and for various market parameters is depicted in Fig. 3.4, where the returns of the German DAX index are also displayed in a first panel for visual comparison. Observing the model results for market parameters in the

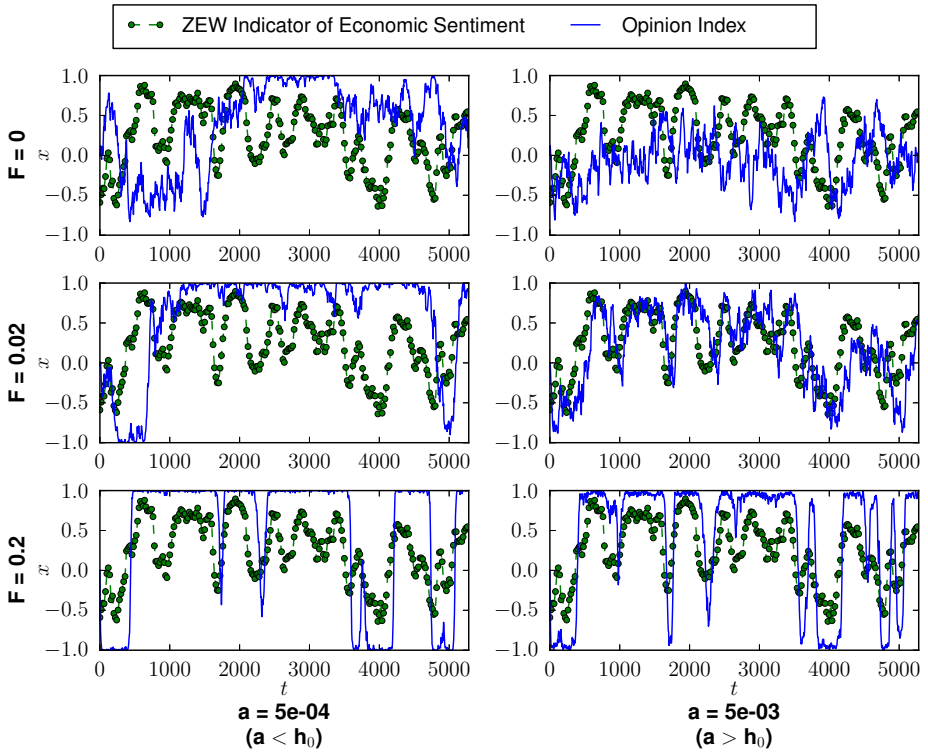

Figure 3.3: Effect of the information intensity on the opinion index. Green points and dashed green line: External information signal, ZEW *Indicator of Economic Sentiment*, data from December 1991 to November 2013. Solid blue line: Time evolution of the opinion index simulated for different values of the external information intensity F and the idiosyncratic switching tendency a. The herding parameter and the system size are fixed as $h_0 = 10^{-3}$ and $N = 200$.

bistable regime (first column, $a = 5 \cdot 10^{-4}$, $h_0 = 10^{-3}$), we notice that an evident effect of an increasing convincing power of the external information source is the strengthening of the volatility clustering phenomenon, i.e., the clustering of periods of large returns and periods of small returns. Even if some volatility clustering is already present —endogenously produced— in the closed market case ($F = 0$), this feature seems to be underrepresented for these market parameters when compared to the DAX data. A clear enhancement of the clustering effect is observed when a low intensity information signal is introduced ($F = 0.02$), bringing the model results closer to the DAX data. A large input strength ($F = 0.2$), however, results in an unrealistic amplification of the clustering: almost all the

returns in the 22 years simulated are realized in less than ten short bursts, when the information input changes sign and the whole market switches from optimism to pessimism or vice versa. A similar but weaker influence of the external information is found for $a = 5 \cdot 10^{-3}$ (second column), a value corresponding to the monostable regime but in the same order of magnitude as h_0. For $a = 5 \cdot 10^{-2}$ (third column), however, the effect of the input signal appears to be negligible regardless of its strength. This can be understood bearing in mind that, being the idiosyncratic switching tendency much larger than the herding propensity, the dynamics is dominated by random changes of opinion of the traders, and therefore the external information is irrelevant in the scale of days, the one used for computing the returns.

The observation of the time series of the normalized daily returns (Fig. 3.4) might lead to think that the parameters used are degenerate, i.e., that different combinations of their values can lead to similar results, as it is the case for the couples $F = 0.02$, $a = 5 \cdot 10^{-4}$ and $F = 0.2$, $a = 5 \cdot 10^{-3}$. However, this degeneracy is only apparent, as it can be shown by simply analyzing other magnitudes, for example: the autocorrelation function of the normalized daily volatility [see Eq. (3.15)], measured as the absolute value of the normalized daily returns, illustrated in Fig. 3.5. The same input intensities and market parameters as in the previous figure are studied, and the corresponding autocorrelation function for the DAX normalized daily volatility is shown for comparison in every panel. If we first focus on the examples for market parameters in the bistable regime (first column, $a = 5 \cdot 10^{-4}$, $h_0 = 10^{-3}$), we find a highly significant autocorrelation of absolute returns which only falls off slowly, in accordance with previous empirical literature (Ding et al., 1993; Mandelbrot, 1997; Cont, 2001, 2005). However, in the closed market case ($F = 0$) this decrease is extremely slow for large time lags, where we still find a significant autocorrelation, as opposed to the DAX data. The introduction of a small input strength signal ($F = 0.02$) is able to modify this behavior, the autocorrelation for large time lags becoming negligible or even slightly negative, as it is found for the DAX index. On the opposite, when the strength of the input is increased up to its maximum value ($F = 0.2$), the outcome of the model becomes strongly driven by the shape of the information signal and, as a result, the autocorrelation function becomes as well a direct consequence of this signal shape and very different from the DAX data. Thus, the expected behavior of the autocorrelation of absolute returns for long time lags is found for markets subject to a low intensity information entrance, while it is not present for closed or completely driven markets. For a market with an idiosyncratic tendency larger but in the same order of magnitude as the herding propensity (second column, $a = 5 \cdot 10^{-3}$), we observe, on the one hand, a complete lack of autocorrelation for both the closed market example ($F = 0$) and the case of a small information influence ($F = 0.02$). On the other hand, the entrance of an information signal with its maximum convincing power ($F = 0.2$) leads again

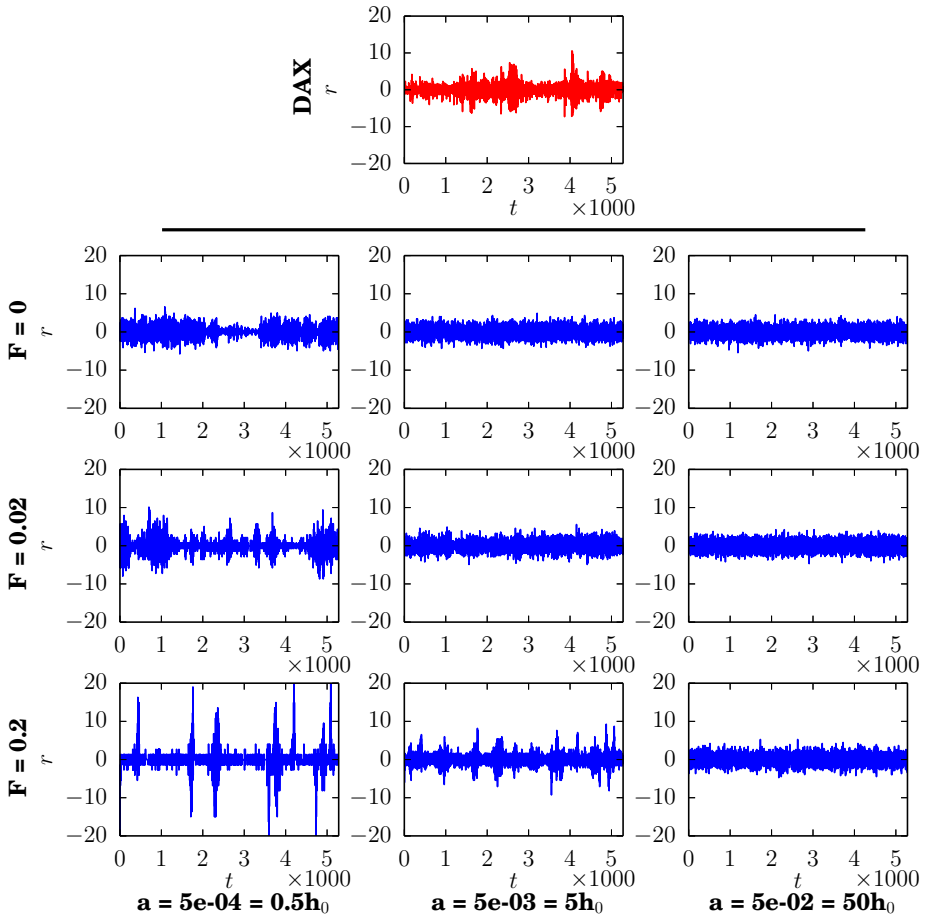

Figure 3.4: Normalized daily returns $r(t)$. First panel, red line: German DAX index from December 1991 to November 2013, shown for comparison. Table of nine panels, blue lines: Model results for three different input intensities of the external information F and three values of the idiosyncratic switching tendency a. The rest of the parameters are fixed as $h_0 = 10^{-3}$ and $N = 200$.

to an unrealistic behavior of the autocorrelation function, which becomes driven by the shape of the incoming information signal. In the case of larger values of the idiosyncratic switching tendency, and being the market dominated by random opinion changes, we find no significant autocorrelation of absolute returns regardless of the information strength applied.

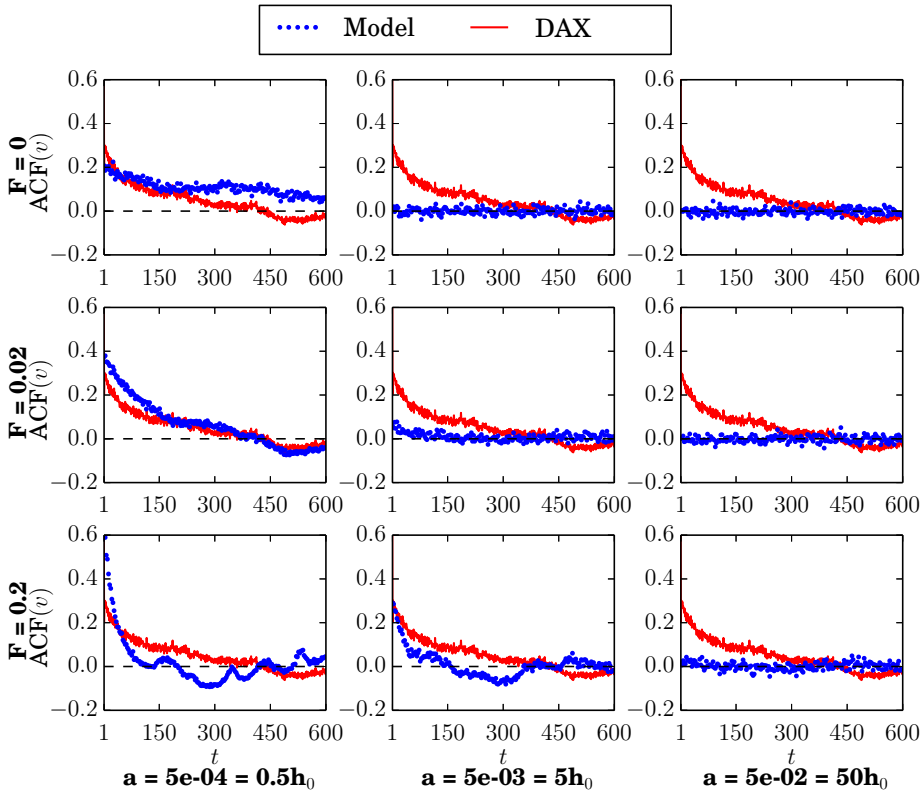

Figure 3.5: Autocorrelation function (ACF) of the normalized daily volatility $v(t)$. Black dots: Model results for three different input intensities of the external information F and three values of the idiosyncratic switching tendency a. The rest of the parameters are fixed as $h_0 = 10^{-3}$ and $N = 200$. Solid blue line: The corresponding ACF of the German DAX index volatility is shown in each case for comparison. The DAX data corresponds again to the period from December 1991 to November 2013.

Note that, with the small value of the information strength, $F = 0.02$, and for some values of the market parameters, the model described here is able to reproduce the main statistical features of the DAX index. On the one hand, the model emulates the behavior of the DAX normalized daily returns (see Fig. 3.4), giving rise to a comparable volatility clustering effect. On the other hand, the model leads to a similar autocorrelation function of the normalized daily volatility (see Fig. 3.5), reproducing both the slow decay of the DAX autocorrelation and its zero and slightly negative values for very long time lags. Note that this last feature, the long time lag behavior of the autocorrelation function, is not captured

by the market model closed to external information. For completeness, we also include the probability distributions of absolute normalized daily returns as a supplementary figure in Appendix Probability distribution of absolute returns, for the same parameter values used in Figs. 3.4 and 3.5: while their lack of temporal structure hides any volatility clustering effect, these distributions seem to support our choice of parameter value. In view of these results, we select the small value of the external information intensity, $F = 0.02$, to be used in the rest of the research presented hereafter.

3.6

Resonance phenomenon

We have analyzed above the effects caused by different information input intensities on the market, finding that a small strength input ($F = 0.02$) produces results consistent with real financial data. Let us now focus on this case, keeping the external information intensity fixed as $F = 0.02$, and search for the values of the model parameters for which the ensemble of agents follows more accurately the shape of this signal. Thus, we are concerned here with the study of the conditions under which the market best reflects the arrival of external information. As mentioned above, although the discussed market model has in principle three parameters (a, h_0, and F), one of them can be used as a rescaling of the time variable, so that there are only two relevant parameters. Given that the effective influence of the external information upon the system is determined by the relative importance of the input strength F and the background herding coefficient h_0 [see Eqs. (3.16) and (3.17)], we choose to keep the latter fixed and therefore use the idiosyncratic switching tendency a as our control parameter. In particular, we choose the values $h_0 = 10^{-3}$, $F = 0.02$ and $N = 200$. The input intensity per agent, F/N, is thus ten times smaller than the herding coefficient, its maximum allowed value. We have also performed simulations with different system sizes ($N = 50$ and $N = 800$), finding a generally equivalent behavior which will be discussed below.

Let us start by considering the influence that varying the idiosyncratic switching tendency a has over the time series of the noise traders opinion index x, illustrated in Fig. 3.6. Note that there is no maximum allowed value for this parameter, as it was the case with the signal intensity F: its only constraint is that it must be $a > 0$ so that the extremes of the opinion index space are not absorbing states. Therefore, we simply choose a reasonable range which includes the different behaviors described in the previous sections and observed in Fig. 3.2: from a fully bimodal case ($a \ll h_0$), with almost two deltas at the extremes of

the probability distribution of states; up to a fully unimodal case ($a \gg h_0$), with an almost perfect Gaussian distribution of states.

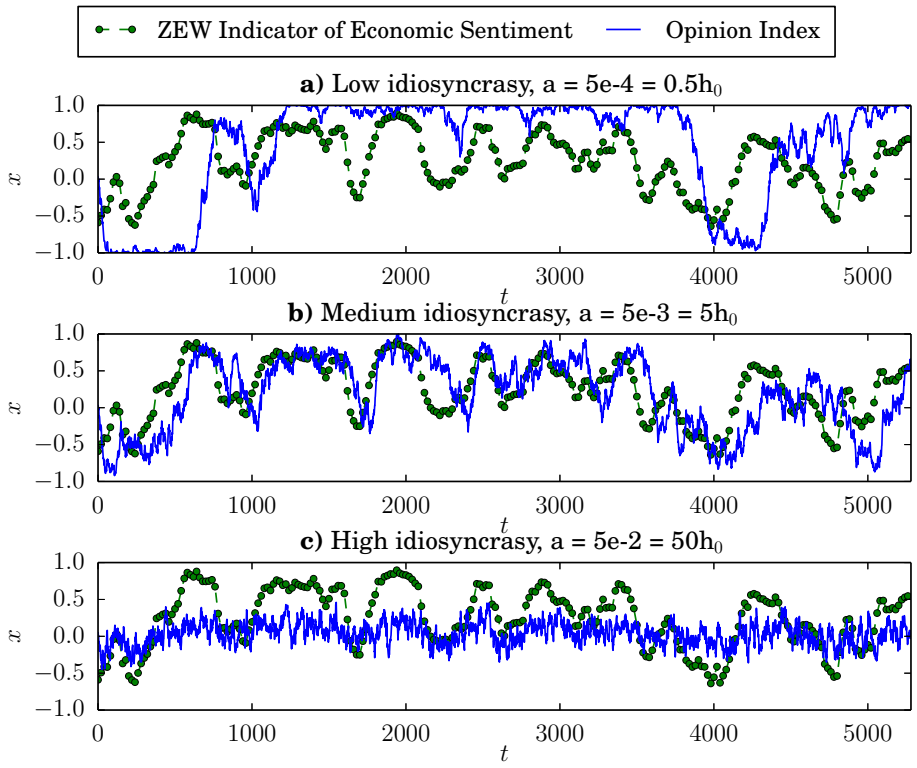

Figure 3.6: Effect of the idiosyncratic switching tendency on the opinion index. Green points and dashed green line: External information signal, ZEW *Indicator of Economic Sentiment*, data from December 1991 to November 2013. Solid blue line: Time evolution of the opinion index simulated for different values of the idiosyncratic switching tendency a and fixed values of the parameters $h_0 = 10^{-3}$, $F = 0.02$, and $N = 200$.

In the first of these cases ($a = 0.5h_0$, panel **a**) the system is clearly unable to follow the shape of the input signal and, in fact, the opinion index stays close to a full agreement state for most of the time. This is due to the extremely low level of idiosyncratic behavior relative to the herding tendency: noise traders tend to form a large consensus group which cannot easily be convinced by the external source. Even if a double well effective potential has been induced, the probability of observing a transition between both wells, proportional to a, is too small to allow for the group to leave the consensus states at a rate large enough for the market to adapt to the updates of the external information. In the intermediate case

($a = 5h_0$, panel **b**), when the idiosyncratic coefficient is slightly larger than the herding tendency, we observe that the system easily follows the shape of the input signal. This can be understood taking into account that intermediate values of a larger than h_0 give rise to a rather wide monostable effective potential where the system can still be largely driven by the external signal. Thus, the market seems to reflect rather precisely the arrival of external information. On the opposite, for very large values of the idiosyncratic coefficient ($a = 50h_0$, panel **c**) the system is again unable to fit the shape of the input signal and the trajectories of the opinion index seem rather noisy. As shown in Section 3.3, very large values of a lead to narrow unimodal effective potentials with minima moving closely around the center of the opinion index space. Thus, the external information input has an almost negligible influence and the market seems to be unaware of it.

In this way, we note that different values of the idiosyncratic coefficient lead to different levels of coincidence between the opinion index resulting from the simulation of the model and the information signal used as an input. In order to quantify this phenomenon —that is, in order to measure the quality of the market response in following the external information driving— we use the input-output correlation (IOC), defined as the maximum of the cross-correlation function between the input signal $i(t)$ and the system output $x(t)$,

$$\mathrm{IOC} = \frac{\max_\tau \left\{ \left\langle \Big(i(t) - \langle i \rangle \Big) \Big(x(t+\tau) - \langle x \rangle \Big) \right\rangle \right\}}{\sigma(i)\sigma(x)} \,, \tag{3.23}$$

where $\langle \cdot \rangle$ denotes an average over time, $\sigma(\cdot)$ stands for the standard deviation, τ plays the role of a time lag, and $\max_\tau\{\cdot\}$ finds the maximum value of a τ-dependent function (Collins et al., 1996). Note that IOC is a scalar measure quantifying the maximum of the input-output cross-correlation function, which depends on the time lag τ. A larger IOC is related with a better entrainment of the market by the external information signal, corresponding its maximum value, $\mathrm{IOC} = 1$, to a perfect fit between the time series $i(t)$ and $x(t)$. Note that an amplification of the input signal is understood here as a worse fit when compared with a perfect input-output correspondence.

The results obtained for the input-output correlation are displayed in Fig. 3.7 for three different system sizes. The same general behavior is observed for all of them: there is a maximum in the response of the system to the weak information input as a function of the idiosyncratic switching parameter a. As said before, this behavior is reminiscent of a well-known phenomenon generally labeled as resonance (Benzi et al., 1981, 1982; Nicolis and Nicolis, 1981; Collins et al., 1995; Gammaitoni et al., 1998). The particular mechanism described here can be classified as an *aperiodic stochastic resonance* (Collins et al., 1996; Heneghan et al., 1996), since the maximum in the response of the system to the external aperiodic

signal is related to the relative importance of the stochastic term as compared to the deterministic one: the ratio between h_0 and a, in our case.

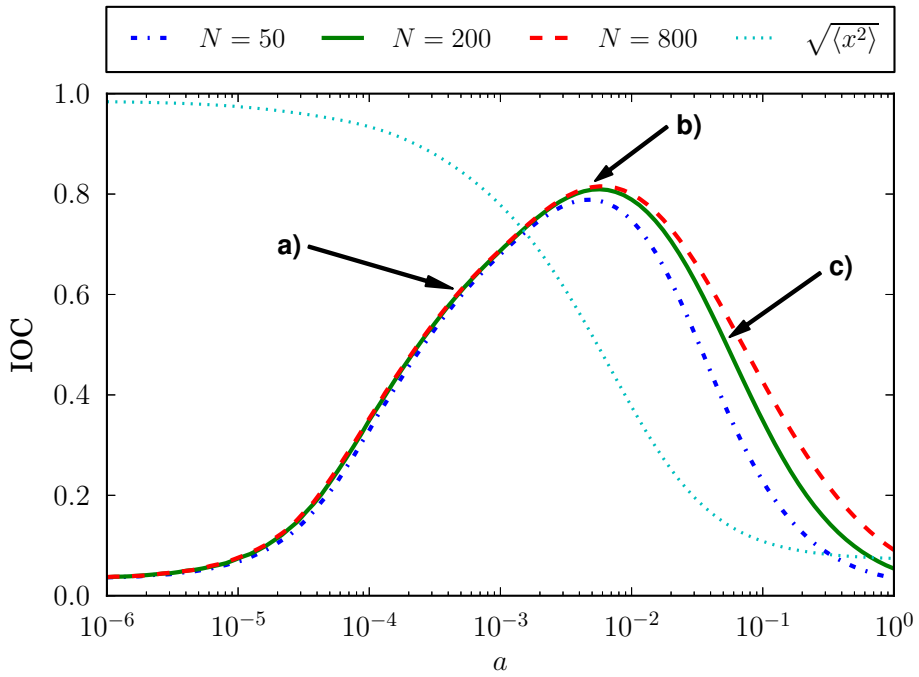

Figure 3.7: Input-output correlation IOC as a function of the idiosyncratic switching tendency a. The correlation is computed according to Eq. (3.23). Parameter values are $h_0 = 10^{-3}$, $F = 0.02$, and three different system sizes, $N = 50,\ 200,\ 800$. A measure of the fraction of time spent by the system near the extremes of the opinion index space, $\sqrt{\langle x^2 \rangle}$, is also shown for the $N = 200$ case. Arrows point at the idiosyncrasy levels whose opinion index time series are shown in Fig. 3.6, marked also by their corresponding letter: a) $a = 5 \cdot 10^{-4}$, b) $a = 5 \cdot 10^{-3}$, c) $a = 5 \cdot 10^{-2}$

Within a financial market framework like the one presented in Section 3.2, a maximum in the response of the system would simply mean that the market optimally reproduces the level of optimism/pessimism contained in the incoming information (see, for example, panel **b** of Fig. 3.6). These results suggest that there is a certain range of idiosyncratic behavior intensity which largely improves the entrainment of the market by the external information. Note that the particular values of the response maxima are quite large, all of them implying a rather good fit of the information input. Note as well that these high levels of entrainment occur for a fairly wide range of values of the control parameter a: the input-output correlation stays above 0.7 for more than a decade (in particular,

for $h_0 \lesssim a \lesssim 20h_0$, with $h_0 = 10^{-3}$). However, there are two regions for which the system seems unable to follow the shape of the input signal: one for values of the idiosyncratic parameter smaller than the herding coefficient, and the other one for values much larger than the herding coefficient. In order to understand the differences between these two low-entrainment regimes, we also show in Fig. 3.7 a measure of the fraction of time spent by the system near the extremes of the opinion index space, $\sqrt{\langle x^2 \rangle}$. By observing this measure, it becomes clear that in the low-idiosyncrasy regime ($a < h_0$) the market cannot follow the input signal because the noise traders group amplifies the incoming information up to a complete consensus ($\sqrt{\langle x^2 \rangle} \simeq 1$) and then this group finds it difficult to leave this consensus and adapt to an updated information in the opposite sense (see also panel **a** of Fig. 3.6). On the contrary, in the high-idiosyncrasy regime ($a > 20h_0$) the problem faced by the market when trying to assimilate the incoming information is that, being the noise traders mostly guided by their own idiosyncratic drives, they pay little attention to external sources or other traders' attitudes, thus statistically tending to be equally divided among the two possible opinions ($\sqrt{\langle x^2 \rangle} \simeq 0$) (see also panel **c** of Fig. 3.6).

Bearing in mind that social and economic systems may have rather reduced sizes, it becomes relevant to assess the importance of size effects (Toral and Tessone, 2007). In our case, the input-output correlation curves for the three different size examples in Fig. 3.7 collapse in the same curve for small values of a, while they are clearly different for intermediate and large values. This behavior can be understood in view of the functional form of the granularity term in the Langevin equation (3.19), the only one dependent on N: directly proportional to the idiosyncratic coefficient a and inversely proportional to the system size N. For small values of the control parameter a, the granularity term is also small and the opinion index x stays most of the time around the consensus states. In the intermediate a region, the granular N dependent term plays a relevant role in taking the system out of the consensus states with a probability uncorrelated with the shape of the input signal. Therefore, a large granularity term —small number of agents N— leads to a worse coincidence of x with the input signal and, thereby, to a smaller input-output correlation. Finally, for large values of the control parameter a, the system does not even reach the extremes of the opinion index space and the behavior is predominantly led by the first term of the drift function and the noise effects produced by the granular term, because of the large value of a appearing in both terms. Note as well that the relative difference between the curves is smaller when comparing the $N = 800$ with the $N = 200$ cases than when comparing this latter with the $N = 50$ example. This is simply a consequence of the granularity term being inversely proportional to the system size N, so for larger and larger N the results become more and more similar.

3.7

Concluding remarks

Our aim in this chapter was to advance towards a quantitative understanding of the influence of an external source of information upon a financial market characterized by a certain herding behavior. The stochastic formalism used as a point of departure for our investigation incorporates individual behavioral heterogeneity as well as a tendency for social interaction, in the tradition of Kirman's seminal ant colony model. As opposed to the previous literature, which considers only the particular case of a closed market, we take into account the arrival of external information in the form of a time-dependent modification of the transition rates defining the individual traders' behavior.

A transition takes place in the original herding model from a monostable to a bistable behavior when increasing the herding propensity of the agents with respect to their idiosyncratic tendency. The monostable case can be understood as a market where each of two possible strategies is used by approximately half of the traders, while the bistable configuration corresponds to a market where there is always a clear majority of traders using one of the strategies, even if the chosen one can change over time. We have reinterpreted this noise-induced transition in terms of the mono- or bistability of an effective potential. In this context, we have demonstrated that the introduction of a dynamic external information input produces a time-dependent modification of this effective potential, whose symmetry is broken. We have used an *Indicator of Economic Sentiment* published in Germany as an example of information input. Extensive simulations of this market model open to the arrival of external information have shown that even a small strength or convincing power of the external source may be enough for the market to follow its information signals. On the contrary, strong intensities lead to an amplification of the input signal: the convincing power of the external source being so strong, most of the traders are quickly persuaded to align their strategies in the sense of the input signal, giving rise to important market movements when the direction of this external information changes. Moreover, we have compared the results of this market model with Germany's leading stock market index, the DAX, showing that the introduction of a small strength information signal is able to reproduce general statistical properties of real financial data. In particular, the introduction of a low intensity signal allows the model to mimic: the volatility clustering effect, the slow decay of the autocorrelation of the normalized daily volatility for short time lags, and its zero and slightly negative values for long time lags.

Furthermore, we have studied the conditions for the market to show an optimal response to the arrival of external news, i.e., for it to optimally reflect the level of optimism/pessimism contained in the information input. The specific range of values for which an optimal response is observed depends on the intensity and the frequency or rate of change of the incoming information. In particular, we have found a certain range of values of the idiosyncratic behavior relative to the herding tendency among noise traders ($h_0 \lesssim a \lesssim 20h_0$) that optimizes their response as a group to a weak information input. We have shown the similarities of this phenomenon with an *aperiodic stochastic resonance*. As a result of this analysis, we have identified three different market regimes regarding the assimilation of incoming information:

1. Amplification of incoming information; any positive (negative) piece of news leads to a rather stable optimistic (pessimistic) consensus and it takes a long time for the market to adapt to updates of the sense of the external information (values of the idiosyncratic switching tendency below the range of the resonance, $a < h_0$).

2. Precise assimilation of incoming information; the market optimally reflects the arrival of external news (values of a within the range of the resonance, $h_0 \lesssim a \lesssim 20h_0$).

3. Undervaluation of incoming information; the arrival of news has an almost negligible influence and the market seems to be unaware of it (values of a above the range of the resonance, $a > 20h_0$).

A possible understanding of the origin of amplification in markets where traders are easily influenced by their peers —markets dominated by collective herding behavior— (regime 1) is that, once the external source of information is able to convince a small number of traders, they quickly spread the information to the rest of the market by influencing the decisions of other traders. On the contrary, in markets where investors behave independently of each other using their own expertise —markets dominated by idiosyncratic behavior— (regime 3), even if the external source is able to convince some of them, the information is not transmitted to the rest of the market: in order to convince the whole of the market, the external source would need to individually persuade each and every one of the traders. A precise assimilation of incoming information occurs when there is a compromise between these two factors (regime 2), i.e., when there is enough communication between traders and collective herding behavior to allow for the spreading of the external information to most of the market but also individual and independent behavior enough to prevent a full consensus in line with the external source of information.

APPENDICES TO CHAPTER 3

3.A

Effective potential derivation

We derive, in this appendix, the effective potential both for the original Kirman dynamics and the model with external information, presented respectively in Eq. (3.8) and Eq. (3.20) in the main text of the chapter. Let us start by restating here the definition of effective potential $U_{\text{eff}}(x)$ given in Eq. (3.7),

$$P_{\text{st}}(x) \equiv \mathcal{C}^{-1} \exp\left(-\frac{U_{\text{eff}}(x)}{D}\right) , \tag{3.24}$$

where $P_{\text{st}}(x)$ is the stationary state probability distribution, D is an effective noise intensity that we take as $D = h$, and the constant $\mathcal{C}^{-1}$ plays the role of a normalization factor. Note that, defined as such, the minima of this effective potential function will be attractive points of the dynamics, corresponding to maxima of the stationary state probability distribution.

For the general Fokker-Planck equation

$$\frac{\partial P_{\text{st}}(x,t)}{\partial t} = -\frac{\partial}{\partial x}\left[q(x)P(x,t)\right] + \frac{\partial^2}{\partial x^2}\left[Dg(x)^2 P(x,t)\right] , \tag{3.25}$$

the stationary distribution is found by assuming $\partial P_{\text{st}}/\partial t = 0$ and solving the resulting equation. By this means, a general effective potential (San Miguel and

Toral, 2000) can be written as

$$U_{\text{eff}}(x) = -\int \frac{q(x)}{g(x)^2} dx + D \int \frac{\partial g(x)}{\partial x} \frac{1}{g(x)} dx \,, \tag{3.26}$$

and, applying this definition to the Fokker-Planck equation (3.2) in the main text, the particular effective potential for the Kirman dynamics is found to be

$$U_{\text{eff}}(x) = (h - a) \ln(1 - x^2) \,. \tag{3.27}$$

Note that this effective potential $U_{\text{eff}}(x)$ is not to be confused with the deterministic potential, which is always monostable and can be found by simply integrating with respect to x the deterministic part of Eq. (3.3).

Even though in the case with an external time varying forcing it is not possible to write a stationary state probability distribution, we assume that, at any point in time, the decay of the system to a quasi-stationary state is faster than the variation of the input signal, i.e., we assume conditions of slow driving. Therefore, we keep the previous definition of the effective potential as an approximation to this time-dependent case,

$$P(x,t) \approx \mathcal{C}^{-1} \exp\left(-\frac{U_{\text{eff}}(x,t)}{D}\right) . \tag{3.28}$$

Applying Eq. (3.26) to the Fokker-Planck equation (3.18) leads to the particular functional form

$$U_{\text{eff}}(x,t) = (h_0 - a) \ln(1 - x^2) - xFi(t) \tag{3.29}$$

for the model with arrival of external information.

3.B

Probability distribution of absolute returns

For completeness, we include in this appendix probability distributions of absolute normalized daily returns, for the same parameter values used in Figs. 3.4 and 3.5. While the lack of any temporal structure hides any volatility clustering effect, these distributions seem to support our choice of parameter value for the external information intensity, $F = 0.02$.

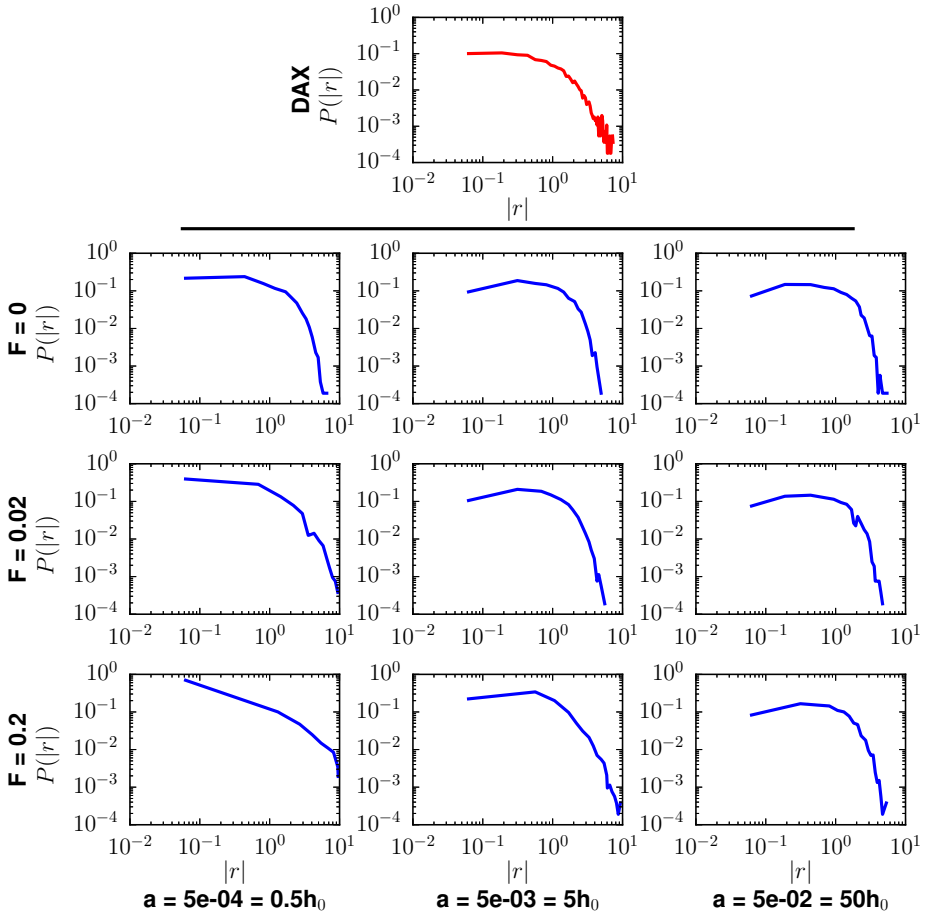

Figure 3.8: Probability distribution of the absolute value of the normalized daily returns, $P(|r|)$. First panel, red line: German DAX index from December 1991 to November 2013, shown for comparison. Table of nine panels, blue lines: Model results for three different input intensities of the external information F and three values of the idiosyncratic switching tendency a. The rest of the parameters are fixed as $h_0 = 10^{-3}$ and $N = 200$.

CHAPTER 4

The role of topology in stochastic, binary-state models: an application to herding behavior

STOCHASTIC, binary-state models have been used to study the emergence of collective phenomena in a wide variety of systems and fields. Examples range from classical problems in statistical physics, such as equilibrium and non-equilibrium phase transitions (Gunton et al., 1983; Marro and Dickman, 1999), to biological and ecological questions, such as neural activity (Hopfield, 1982) and species competition Clifford and Sudbury (1973); Crawley and May (1987), or even to social and epidemiological topics, such as the spreading of diseases in a population (Anderson et al., 1991; Pastor-Satorras and Vespignani, 2001; Watts, 2002; Serrano and Boguñá, 2006; Castellano et al., 2009; Castellano and Pastor-Satorras, 2012). In general, these systems are considered to be embedded in a network structure, where the nodes are endowed with a binary-state variable —spin up or down— and the links between nodes represent the interactions or relations between them. While most of these models were initially studied in regular lattices, there has recently been a growing interest in more complex and heterogeneous topologies (Albert and Barabási, 2002; Newman and Park, 2003; Barrat et al., 2008; Newman, 2010). These studies have shown that, for a given model, the structure of the underlying network may strongly influence the dynamics of the system and affect its critical behavior, i.e., the critical values of the model parameters might depend on certain structural characteristics of the underlying topology (Dorogovtsev et al., 2002; Boguñá et al., 2003; Masuda and Konno, 2004; Lambiotte, 2007; Gleeson, 2011; Vilone et al., 2012; Gleeson, 2013).

Thus, the quantification of the effect of the underlying topology on such systems and dynamics is, from a practical point of view, a matter of prime importance.

A paradigmatic example of this kind of models is the noisy voter model, proposed by different authors in various contexts (Lebowitz and Saleur, 1986; Fichthorn et al., 1989; Considine et al., 1989; Kirman, 1991, 1993; Granovsky and Madras, 1995). As briefly explained in Chapters 1 and 3, for any finite system, the behavior of this noisy variant of the voter model (Clifford and Sudbury, 1973; Holley and Liggett, 1975) is characterized by the competition between two opposing mechanisms, related to two different types of noise. On the one hand, the pairwise interaction mechanism is related to interfacial fluctuations (internal noise) and tends to order the system, driving it towards a homogeneous configuration —all spins in the same state, whether up or down—. Depending on the dimension of the system, this mechanism leads to a coarsening process or to a metastable partially ordered state, both of them perturbed by finite-size fluctuations (one of which eventually drives the system to full order). In the absence of any other mechanism, as it is the case in the original voter model, the homogeneous configurations become absorbing states of the dynamics (Al Hammal et al., 2005). On the other hand, the random change mechanism is related to thermal-like fluctuations (external noise) and tends to disorder the system, pulling it from the homogeneous configurations. Therefore, this second mechanism leads to the disappearance of the typical absorbing states of the voter model and to the restoration of ergodicity (Granovsky and Madras, 1995). The main consequence of this competition is the appearance of a noise-induced, finite-size transition between two different behavioral regimes —a mostly ordered regime dominated by pairwise interactions and a mostly disordered regime dominated by noise (Kirman, 1993; Alfarano et al., 2008). While the effect of different network topologies on the behavior of the voter model has been well established (Suchecki et al., 2005a; Sood and Redner, 2005; Suchecki et al., 2005b; Vazquez and Eguíluz, 2008), the case of the noisy voter model has received much less attention, most of the corresponding literature focusing only on regular lattices (Lebowitz and Saleur, 1986; Granovsky and Madras, 1995) or on a fully-connected network (Kirman, 1993; Alfarano et al., 2008). Finally, the use of a mean-field approach in some recent studies considering more complex topologies (Alfarano and Milaković, 2009; Alfarano et al., 2013; Diakonova et al., 2015) did not allow to find any effect of the network properties —apart from its size and mean degree— on the results of the model.

We propose in this chapter a new analytical method to study stochastic, binary-state models on complex networks. Moving beyond the usual mean-field theories (Vazquez et al., 2008; Alfarano and Milaković, 2009; Diakonova et al., 2015), this alternative approach is based on the introduction of an annealed approximation for uncorrelated networks, allowing to deal with the network struc-

ture as parametric heterogeneity. As an illustration, we study the noisy voter model. The proposed method is able to unfold the dependence of the model not only on the mean degree (the mean-field prediction) but also on more complex averages over the degree distribution. As opposed to previous mean-field approaches, we find that the degree heterogeneity —variance of the underlying degree distribution— has a strong influence on the location of the critical point, on the local ordering of the system, and on the functional form of its temporal correlations. Furthermore, we show how this latter point opens the possibility of inferring the degree heterogeneity of the underlying network by observing only the aggregate behavior of the system as a whole, an issue of interest for systems where only macroscopic, population level variables can be measured. Finally, these results are confirmed by numerical simulations on different types of networks, allowing for a constant mean degree ($\overline{k} = 8$) while leading to different degree distributions. In particular, in order of increasing degree heterogeneity, we focus on Erdös-Rényi random networks (Erdös and Rényi, 1960), Barabási-Albert scale-free networks (Barabási, 1999) and dichotomous networks (Lambiotte, 2007) (whose nodes are assigned one out of two possible degrees, in our case $k_1 = \overline{k}/2$ or $k_2 = \sqrt{N}$).

4.1

Model definition

Consider a system composed of N nodes in a given network of interactions. At any point in time, each node i is considered to be in one of two possible states, and is therefore characterized by a binary variable $s_i = \{0, 1\}$. Moreover, due to the network structure, each node i is also characterized by a certain set of (nearest) neighbors, $nn(i)$, and by its corresponding degree or number of those neighbors, k_i. The evolution of the state of each node, s_i, occurs stochastically with probabilities that depend on the state of the updating node and on the states of its neighbors. In particular, these probabilities consist of two terms: on the one hand, there are random pairwise interactions between node i and one of its neighbors $j \in nn(i)$, after which i copies the state of j; and, on the other hand, there are random changes of state, playing the role of a noise. The transition rates for each node i can be written as

$$\begin{aligned} r_i^+ &\equiv r\left(s_i = 0 \to s_i = 1\right) = a + \frac{h}{k_i} \sum_{j \in nn(i)} s_j \,, \\ r_i^- &\equiv r\left(s_i = 1 \to s_i = 0\right) = a + \frac{h}{k_i} \sum_{j \in nn(i)} \left(1 - s_j\right) , \end{aligned} \tag{4.1}$$

where the noise parameter a regulates the rate at which random changes of state take place, and the interaction parameter h does so with the interaction-driven changes of state. Defined in this way, the noisy voter model becomes the network-embedded equivalent of the herding model introduce by Kirman (1993) in its original, extensive formulation (Alfarano et al., 2008; Alfarano and Milaković, 2009). Furthermore, note that, in the limit case of $a = 0$ and with an appropriate time rescaling, we recover the transition rates of the original voter model (Suchecki et al., 2005a,b).

As explained in Chapter 3, even if the model appears to have two parameters, one of them can always be used as a rescaling of the time variable, so that there is only one relevant parameter: the ratio between the two introduced coefficients, a/h. Indeed, only one parameter is introduced in the previous literature in the context of the noisy voter model (Lebowitz and Saleur, 1986; Granovsky and Madras, 1995; Diakonova et al., 2015). On the contrary, prior works about herding behavior in financial markets usually keep both parameters (Kirman, 1993; Alfarano et al., 2008; Alfarano and Milaković, 2009). For consistency with one and the other strands of literature, we are going to consider both parameters explicitly in our analytical approach, while we keep the interaction parameter fixed as $h = 1$ for our numerical results —allowing the noise parameter a to vary.

In order to characterize the global state of the system, we introduce the global variable n, defined as the total number of nodes in state $s_i = 1$,

$$n = \sum_{i=1}^{N} s_i \,, \tag{4.2}$$

and taking values $n \in 0, 1, ..., N$. Note that this variable does not take into account any aspect of the network structure.

It should be observed that, for $a \neq 0$, there are no absorbing states in the model —the probability to move from one state to any other is strictly positive— and therefore the Markov chain is said to be ergodic: in the steady state, averages over time are equivalent to ensemble averages. In practice, the smaller a is, the longer the time needed for both statistics to be actually equivalent. Thus, in the limit case of $a = 0$ the time needed becomes infinite, and we recover the voter model behavior: non-ergodicity with two absorbing states, at $n = 0$ and $n = N$. Moreover, we are going to use the notation $\langle x \rangle$ for ensemble averages with random initial conditions, while we leave $\overline{f(k)}$ for averages over the degree distribution, i.e.,

$$\overline{f(k)} = \frac{1}{N} \sum_{i=1}^{N} f(k_i) \,. \tag{4.3}$$

Similarly, we will differentiate between the variance of a variable x over realizations, noted as $\sigma^2[x]$, and the variance of the degree distribution, labeled as σ_k^2.

Note, nonetheless, that for the numerical steady state values to be presented in the following sections, averages are performed both over time and over an ensemble of realizations with random initial conditions, assuming an initial transient of N time units.

4.2

General formulation

As in Chapter 3, the stochastic evolution of the system can be formalized as a Markov process. In particular, we can write a general master equation for the N-node probability distribution $P(s_1, \ldots, s_N)$ (see Appendix 4.A for further details) and use it to derive general equations for the time evolution of the first-order moments and the second-order cross-moments of the individual nodes' state variables s_i,

$$\frac{d\langle s_i \rangle}{dt} = \langle r_i^+ \rangle - \langle (r_i^+ + r_i^-) s_i \rangle \,, \tag{4.4}$$

$$\frac{d\langle s_i s_j \rangle}{dt} = \langle r_i^+ s_j \rangle + \langle r_j^+ s_i \rangle - \langle q_{ij} s_i s_j \rangle + \delta_{ij} \left[\langle s_i r_i^- \rangle + \langle (1 - s_i) r_i^+ \rangle \right] , \tag{4.5}$$

where $q_{ij} = r_i^+ + r_i^- + r_j^+ + r_j^-$ and δ stands for the Kronecker delta (see Appendices 4.B and 4.C for details). In general, if the transition rates depend on the individual state variables s_i, these equations involve higher order moments and they cannot be solved without a suitable approximation (Lafuerza and Toral, 2013). However, for the transition rates of the noisy voter model, due to their particular functional form, both equations become independent of higher order moments.

Regarding the first-order moments, introducing the transition rates (4.1) into Eq. (4.4), we obtain

$$\frac{d\langle s_i \rangle}{dt} = a - (2a + h)\langle s_i \rangle + \frac{h}{k_i} \sum_{m \in nn(i)} \langle s_m \rangle \,, \tag{4.6}$$

an equation directly solvable in the steady state, when the influence of the initial conditions has completely vanished and thus $\langle s_i \rangle_{st}$ is independent of i. In this way, we find, for the steady state average individual variables s_i and, by definition, for the steady state average global variable n, respectively,

$$\langle s_i \rangle_{st} = \frac{1}{2} \,, \qquad \langle n \rangle_{st} = \frac{N}{2} \,, \tag{4.7}$$

the expected results given the symmetry of the system.

In the case of the second-order cross-moments, when we introduce the transition rates (4.1) into Eq. (4.5), we obtain

$$\begin{aligned}\frac{d\langle s_i s_j\rangle}{dt} =& a(\langle s_i\rangle + \langle s_j\rangle) - 2(2a+h)\langle s_i s_j\rangle \\ &+ \frac{h}{k_i}\sum_{m\in nn(i)}\langle s_m s_j\rangle + \frac{h}{k_j}\sum_{m\in nn(j)}\langle s_m s_i\rangle \\ &+ \delta_{ij}\left[a + h\langle s_i\rangle + \frac{h}{k_i}\sum_{m\in nn(i)}\langle s_m\rangle - \frac{2h}{k_i}\sum_{m\in nn(i)}\langle s_m s_i\rangle\right],\end{aligned} \tag{4.8}$$

which, even if independent of higher order moments, cannot be solved in the absence of an explicit knowledge of the network connections —the adjacency matrix—. This is due to the presence of sums over neighbors $\sum_{m\in nn(i)}$ where the terms are not independent of the particular pair of nodes m, i. In order to find the corresponding steady state solution, we introduce in the next section an approximation of the network allowing us to write the previous equation in terms of sums over the whole system.

4.3

Annealed approximation for uncorrelated networks

Given a complex network with adjacency matrix A_{ij} and degree sequence $\{k_i\}$, we can use an annealed graph approach (Vilone and Castellano, 2004; Dorogovtsev et al., 2008; Guerra and Gómez-Gardeñes, 2010) to define a complementary, weighted, fully-connected network with a new adjacency matrix $\tilde{A}_{ij}$ and whose structural properties resemble those of the initial network (Sonnenschein and Schimansky-Geier, 2012). In particular, we assume that the weights of this new adjacency matrix are given by the probabilities of the corresponding nodes being connected, that is, $\tilde{A}_{ij} = p_{ij}$, where p_{ij} is the probability of node i, with degree k_i, being connected to node j, with degree k_j.

For uncorrelated networks of the configuration ensemble, i.e., random networks with a given degree sequence $\{k_i\}$ and with a structural cutoff at $k_i < \sqrt{N\bar{k}}$, we can approximate the probability of two nodes i, j being connected (Newman,

2003; Boguñá et al., 2004; Sood et al., 2008; Bianconi, 2009) by

$$p_{ij} \approx \frac{k_i k_j}{N\bar{k}} \,. \tag{4.9}$$

In this way, we can approximate the sums over the neighbors of a given node i as sums over the whole network,

$$\sum_{j \in nn(i)} f_j = \sum_{j=1}^{N} A_{ij} f_j \approx \sum_{j=1}^{N} \frac{k_i k_j}{N\bar{k}} f_j \,, \tag{4.10}$$

where f_j is a function which can depend on the characteristics of node j (k_j and/or s_j). Note that this approximation preserves the initial degree sequence, as it is obvious from

$$k_i = \sum_{j=1}^{N} \tilde{A}_{ij} = k_i \frac{1}{\bar{k}} \left(\frac{1}{N} \sum_{j=1}^{N} k_j \right) \,, \tag{4.11}$$

and, therefore, the total number of links is also conserved.

4.4

Noise-induced, finite-size transition

As shown in the previous literature about the Kirman model (Kirman, 1993; Alfarano et al., 2008), in the fully-connected case, the system is characterized by the existence of a finite-size transition between a bimodal and a unimodal behavior, depending on the relative magnitude of the noise and the interaction parameters. For $a < h/N$ the steady state probability distribution of n is found to be bimodal with maxima at the extremes or fully ordered configurations, $n = 0$ and $n = N$, meaning that, at any point in time, the most likely outcome of a static observation is to find a large majority of nodes in the same state, whether 0 or 1, with different observations leading to different predominant options (see Chapter 3 for an explanation in terms of an effective potential). On the contrary, for $a > h/N$ the distribution of n becomes unimodal with a peak at $n = N/2$, meaning that, at any point in time, the most likely outcome of an observation is to find the system equally split between both options. Given the ergodicity of the model for $a \neq 0$, these probability distributions can also be understood in terms of the fractional time spent by the system with each value of n. In this manner, in the bimodal regime, stochastic realizations of the process will tend to be temporarily absorbed in the proximity of the fully ordered configurations

with random switches between them, while realizations in the unimodal regime will spend most of the time with the system more or less equally divided among the two possible individual states, 0 and 1. At the critical point marking the transition between these two behaviors, $a_c = h/N$, the distribution of n becomes uniform, meaning that any share of nodes between the two options is equally likely. Note that, in this extensive formulation of the model, the transition is a finite-size effect, since the value of the critical point decreases for increasing system size and vanishes in the thermodynamic limit ($N \to \infty$).

The existence of the referred transition when the system is embedded in a network topology has also been reported in the literature both for the Kirman model (Alfarano and Milaković, 2009; Alfarano et al., 2013) and in the context of the noisy voter model (Diakonova et al., 2015). The above described phenomenology can thus also be observed in different network topologies. As an example, we show in Fig. 4.1 two realizations of the dynamics for a Barabási-Albert scale-free network corresponding, respectively, to the bimodal [panel **(a)**] and the unimodal regime [panel **(b)**]. A mean-field approach has been proposed in the literature (Alfarano and Milaković, 2009; Diakonova et al., 2015), leading to an analytical solution for the critical point which does not depend on any property of the network other than its size, $a_c = h/N$, the transition still being a finite-size effect.

Both the analytical and numerical results to be presented here suggest, on the contrary, that the critical point does depend on the network, while they confirm the finite-size character of the transition. As a quantitative description of the transition we are going to use the variance of n: bearing in mind that the variance of a discrete uniform distribution between 0 and N is $N(N+2)/12$, we can identify the critical point of the transition as the relationship between the model parameters which leads the steady state variance of n to take the value $\sigma^2_{st}[n] = N(N+2)/12$. Although it is not necessarily the case, numerical results confirm that the distributions obtained in this manner are indeed uniform.

Variance of n

Introducing the annealed approximation for uncorrelated networks into the equation for the second-order cross-moments of the individual variables s_i, Eq. (4.8), we can replace the sums over sets of neighbors by sums over the whole system. If we then rewrite this equation in terms of the covariance matrix σ_{ij}, defined as

$$\sigma_{ij} = \langle s_i s_j \rangle - \langle s_i \rangle \langle s_j \rangle \,, \tag{4.12}$$

we can use the relation

$$\sigma^2[n] = \langle n^2 \rangle - \langle n \rangle^2 = \sum_{ij} \langle s_i s_j \rangle - \sum_i \langle s_i \rangle \sum_j \langle s_j \rangle = \sum_{ij} \sigma_{ij} \tag{4.13}$$

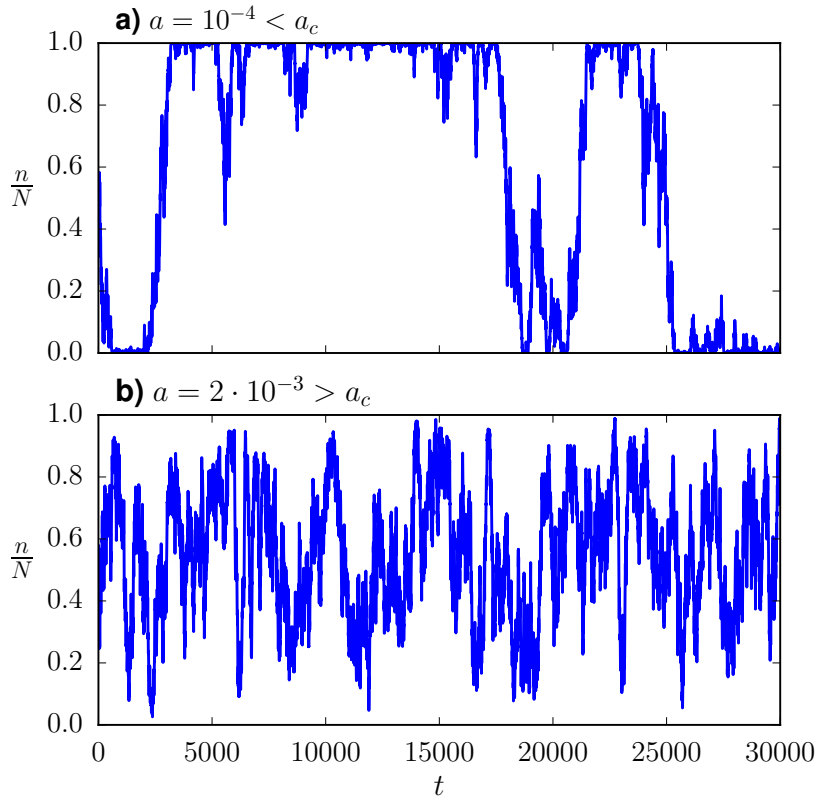

Figure 4.1: Fraction of nodes in state 1 on a Barabási-Albert scale-free network. Single realizations. The interaction parameter is fixed as $h = 1$, the system size as $N = 2500$ and the mean degree as $\overline{k} = 8$.

to find an equation for the variance of n, by simply summing over i and j. Finally, after some algebra (see Appendix 4.D for details), we find, in the steady state,

$$\sigma^2_{st}[n] = \frac{N}{4}\left[1 + \frac{2h\left(1-\frac{1}{N}\right)}{4a+h} + \frac{\left(N-3+\frac{2}{N}\right)\left(\frac{h^2}{\overline{k}}\right)\overline{\left(\frac{k^2}{(4a+h)N\overline{k}+2hk}\right)}}{2a+\left(\frac{h^2}{\overline{k}}\right)\overline{\left(\frac{k^2}{(4a+h)N\overline{k}+2hk}\right)}}\right], \tag{4.14}$$

under the necessary and sufficient condition that

$$\forall i : k_i < \frac{(4a+h)N\overline{k}}{2h}, \tag{4.15}$$

which is generally true and always true for $h > 0$ and $\overline{k} \geq 2$. Note that the only approximation used in the derivation of Eq. (4.14) is the estimation of the adjacency matrix involved in the annealed approximation for uncorrelated networks.

The behavior of the variance $\sigma^2_{st}[n]$ as a function of the noise parameter a is shown in Fig. 4.2 for the three types of networks studied. As we can observe, despite a small but systematic overestimation for intermediate values of the noise parameter —attributable only to the annealed approximation for uncorrelated networks, the only one involved in its derivation—, the main features of the numerical steady state variance are correctly captured by the analytical expression in Eq. (4.14). In particular, both its dependence on a and the impact of the underlying network structure are well described by our approach. On the contrary, the mean-field solution proposed in the previous literature (Alfarano and Milaković, 2009), and included in Fig. 4.2 for comparison, fails to reproduce the behavior of the variance of n for large a and is, by definition, unable to explain its dependence on the network topology. It is, nonetheless, a good approximation for the Erdös-Rényi random network and for values of the noise parameter $a \lesssim 10^{-1}$.

Regarding the limiting behavior of the system when $a \to 0$ and when $a \to \infty$, we can observe, for both the numerical and the analytical results presented in Fig. 4.2, that the influence of the network on the steady state variance of n vanishes in both limits, where we recover the expected behaviors. Notably, in the limit of $a \to 0$ the variance tends to $N^2/4$ for all networks, and we progressively recover the voter model behavior; while in the limit of $a \to \infty$ the variance tends to $N/4$ regardless of the topology, as it corresponds to a purely noisy system composed by N independent units adopting, randomly, values 0 or 1 (equivalent, as well, to a one dimensional random walk confined to the segment $[0, N]$).

Concerning the impact of the network structure, we can observe in Fig. 4.2 that for any finite value of the noise parameter, $0 < a < \infty$, a larger degree heterogeneity of the underlying topology, measured as the variance of the corresponding degree distribution, leads to a larger steady state variance of n. This behavior is further confirmed by the results to be presented in the next subsection, where we show the steady state variance of n as a function of the variance of the underlying degree distribution σ^2_k, respectively, for two different values of the noise parameter a. As we can observe, even if the numerical results are systematically overestimated, our analytical approach [Eq. (4.14)] is able to capture the general features of this dependence and represents a significant improvement from the mean-field prediction of no network impact.

In order to study the bimodal-unimodal transition by using the behavior of the variance of n illustrated in Fig. 4.2, the variance value corresponding to a uniform distribution is included as a horizontal line, so that the critical a value for each network can be easily identified at the corresponding intersection (marked

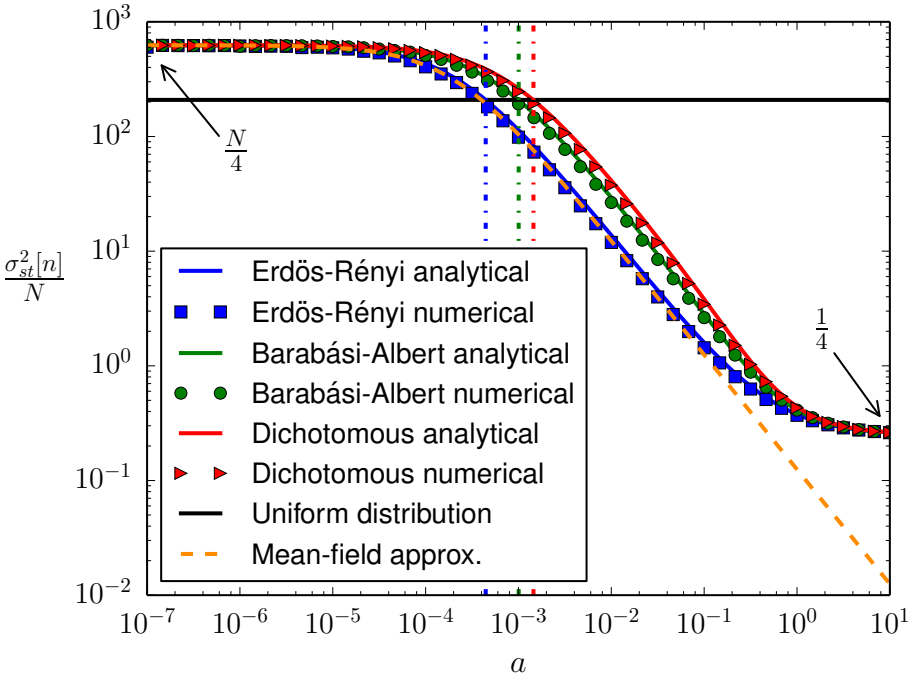

Figure 4.2: Steady state variance of n as a function of the noise parameter a, for three different types of networks: Erdös-Rényi random network, Barabási-Albert scale-free network and dichotomous network. Symbols: Numerical results (averages over 20 networks, 10 realizations per network and 50000 time steps per realization). Solid lines: Analytical results [see Eq. 4.14]. Dash-dotted lines: Analytical results for the critical points [see Eq. 4.18]. Dashed line: Mean-field approximation (see Alfarano and Milaković, 2009). The interaction parameter is fixed as $h = 1$, the system size as $N = 2500$ and the mean degree as $\overline{k} = 8$.

by vertical dashed lines). Note that values of the variance of n above (below) the uniform distribution line correspond to the system being in the bimodal (unimodal) phase. A first observation is that the referred transition still occurs when the noisy voter model is embedded in a network topology, thus confirming the results reported in the previous literature (Alfarano and Milaković, 2009; Diakonova et al., 2015). However, as opposed to these previous studies, we can observe in Fig. 4.2 a clear dependence of the critical point on the underlying topology, an effect which seems to be correctly captured by our approach while it goes completely unnoticed, by definition, from a mean-field perspective. The particular features of this dependence will become clear by means of a first-order approximation of the steady state variance $\sigma^2_{st}[n]$ with respect to the system size

N, allowing us to characterize the asymptotic behavior of the system for both small and large a as well as to find an explicit expression for the critical point a_c.

Asymptotic behavior of the variance of n

Given that Eq. (4.14) does not allow for an intuitive analytical understanding of the network influence on the steady state variance of n, nor does it allow for an explicit analytical solution for the critical point a_c, we develop here a first-order approximation with respect to the system size N, which will also give a relevant insight regarding the asymptotic behavior of the system for both small and large a. In fact, the result of this approximation strongly depends on the relationship between the system size N and the noise parameter a, and we are thus led to consider two different approximation regimes.

In particular, when the noise parameter a is of order $\mathcal{O}(N^{-1})$ or smaller, then the product aN is, at most, of order $\mathcal{O}(N^0)$, and a first-order approximation of Eq. (4.14) with respect to the system size N leads to

$$\sigma_{st}^2[n] = \frac{N^2}{4}\left[\frac{h\left(\frac{\sigma_k^2}{\overline{k}^2}+1\right)}{2aN+h\left(\frac{\sigma_k^2}{\overline{k}^2}+1\right)}\right] + \mathcal{O}(N^{3/2})\,, \tag{4.16}$$

corresponding to the asymptotic behavior of the variance of n for small a and large N. On the contrary, when a is of order $\mathcal{O}(N^0)$ or larger, the product aN is, at least, of order $\mathcal{O}(N)$, and the first-order approximation of Eq. (4.14) becomes

$$\sigma_{st}^2[n] = \frac{N}{4}\left[1+\frac{h}{2a}+\frac{h^2\frac{\sigma_k^2}{\overline{k}^2}}{2a(4a+h)}\right] + \mathcal{O}(N^{1/2})\,, \tag{4.17}$$

corresponding to the asymptotic behavior of the variance of n for large a and large N (see Appendix 4.E for details).

For a more precise characterization of the ranges of validity of these two asymptotic approximations with respect to the noise parameter a, we present in Fig. 4.3 the variance of n as a function of a for the numerical results and the three corresponding analytical expressions presented so far: the analytical result in Eq. (4.14), the asymptotic expression for small a in Eq. (4.16) and the asymptotic expression for large a in Eq. (4.17). Note the use a Barabási-Albert scale-free network as an example. Furthermore, we also show in this figure the crossover point a^* between both approximations, that we define as the

value of a that minimizes the distance between the logarithmic values of both functions (4.17) and (4.16).

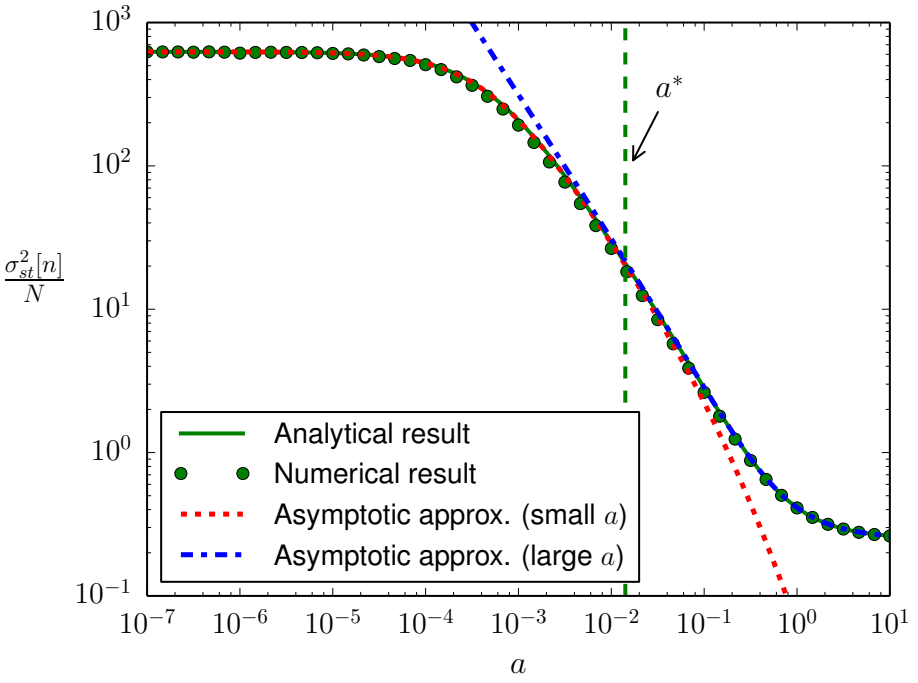

Figure 4.3: Steady state variance of n as a function of the noise parameter a for a Barabási-Albert scale-free network. Symbols: Numerical results (averages over 20 networks, 10 realizations per network and 50000 time steps per realization). Solid line: Analytical results [see Eq. (4.14)]. Dotted line: asymptotic approximation for small a [see Eq. (4.16)]. Dash-dotted line: asymptotic approximation for large a [see Eq. (4.17)]. Dashed line: Crossover point between both asymptotic approximations ($a^* = 0.014157$). The interaction parameter is fixed as $h = 1$, the system size as $N = 2500$ and the mean degree as $\overline{k} = 8$.

Noticing that, for both asymptotic approximations, the variance $\sigma^2_{st}[n]$ becomes an explicit function of the variance of the underlying degree distribution σ^2_k, we present in Fig. 4.4 a comparison between these analytical functional relationships and the corresponding numerical results for two different values of the noise parameter a. In particular, taking into account the ranges of validity of the asymptotic approximations characterized above (see Fig. 4.3), we chose values of the noise parameter respectively before [panel **(a)**] and after [panel **(b)**] the crossover point a^*, and both of them in the region of a leading to significant differences between network types (see Fig. 4.2).

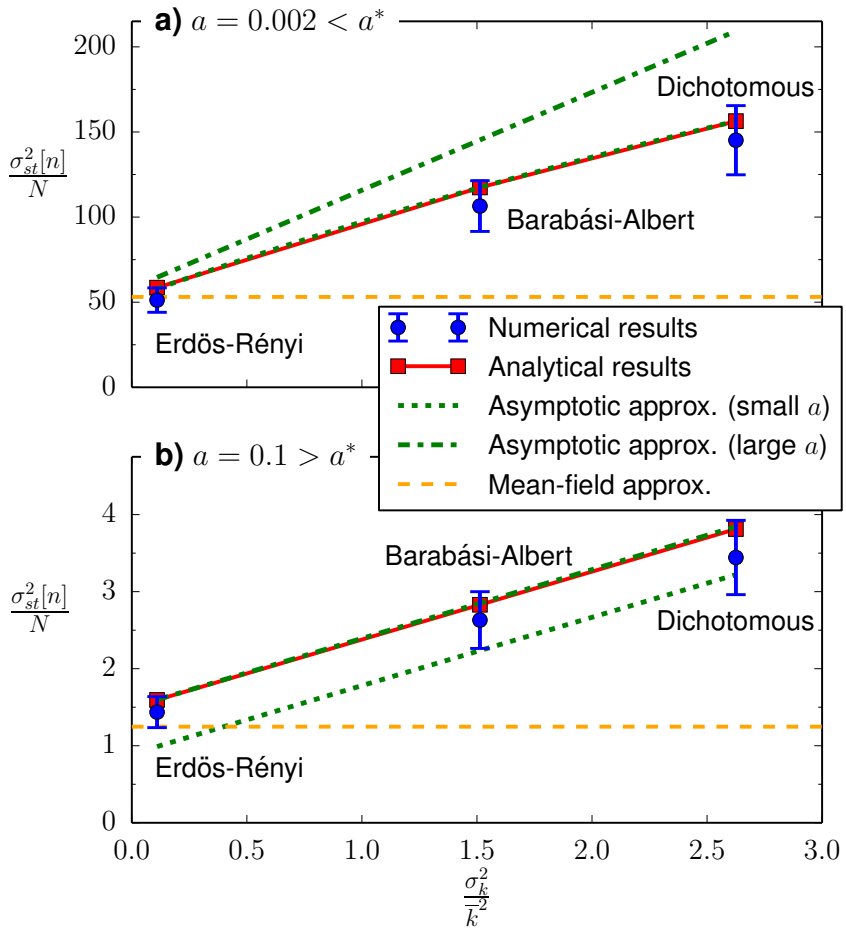

Figure 4.4: Steady state variance of n as a function of the variance of the degree distribution σ_k^2 for two values of the noise parameter a. In order to keep all parameters constant except the variance of the degree distribution, a different network type is used for each point (in order of increasing σ_k^2: Erdös-Rényi random network, Barabási-Albert scale-free network and dichotomous network). Circles with error bars: Numerical results (averages over 20 networks, 10 realizations per network and 50000 time steps per realization). Solid line and squares: Analytical results [see Eq. (4.14)]. Dotted line: asymptotic approximation for small a [see Eq. (4.16)]. Dash-dotted line: asymptotic approximation for large a [see Eq. (4.17)]. Dashed line: Mean-field approximation (see Alfarano and Milaković, 2009). The interaction parameter is fixed as $h = 1$, the system size as $N = 2500$ and the mean degree as $\overline{k} = 8$.

As we can observe, each asymptotic approximation accurately fits the analytical result in Eq. (4.14) within its respective range of validity, while it becomes clearly inaccurate out of this range. Therefore, we can use these approximations instead of Eq. (4.14) to better understand the behavior of the system. In this way, we can conclude that, regarding its impact on the results of the model, the most relevant property of the underlying network is not its mean degree, but the variance of its degree distribution relative to the square of its mean degree, $\sigma_k^2/\overline{k}^2$, a normalized measure of its degree heterogeneity. The results presented in Fig. 4.4 show that this analysis significantly outperforms the mean-field prediction of no network impact, particularly for networks with large levels of degree heterogeneity. Note, nonetheless, that both asymptotic approximations are subject to the same inaccuracies in reproducing the numerical results as the original analytical expression, i.e., the inaccuracies caused by the annealed approximation for uncorrelated networks: a systematic overestimation of the numerical results and an inability to explain the results for topologies with large structural correlations.

Critical point

As described above, the critical point of the bimodal-unimodal transition can be defined as the relationship between the model parameters a and h leading the steady state variance of n to take the value $\sigma_{st}^2[n] = N(N+2)/12$, which corresponds to a uniform distribution between 0 and N. A numerical solution for the critical point a_c can thus be found by applying this definition to the analytical expression for the variance of n given in Eq. (4.14). However, for a fully analytical description of the critical point, we have to use one of the asymptotic approximations presented above, algebraically solvable for a_c. In particular, bearing in mind that the value of the critical point of a fully-connected system is of order $\mathcal{O}(N^{-1})$ and that the change due to the network structure appears to be of order $\mathcal{O}(N^0)$ (see Fig. 4.2), then we can expect the value of the critical point to be still of order $\mathcal{O}(N^{-1})$ and we can therefore use the small a asymptotic approximation in Eq. (4.16) to find

$$a_c = \frac{h}{N}\left(\frac{\sigma_k^2}{\overline{k}^2} + 1\right) + \mathcal{O}(N^{-3/2})\,, \tag{4.18}$$

to the first-order in N (see Appendix 4.F for details). Both this expression and the mean-field approximation previously proposed in the literature (Alfarano and Milaković, 2009; Diakonova et al., 2015) are contrasted with numerical results in Fig. 4.5, where we present the values of the critical point a_c for different types of networks as a function of the variance of the corresponding degree distributions σ_k^2.

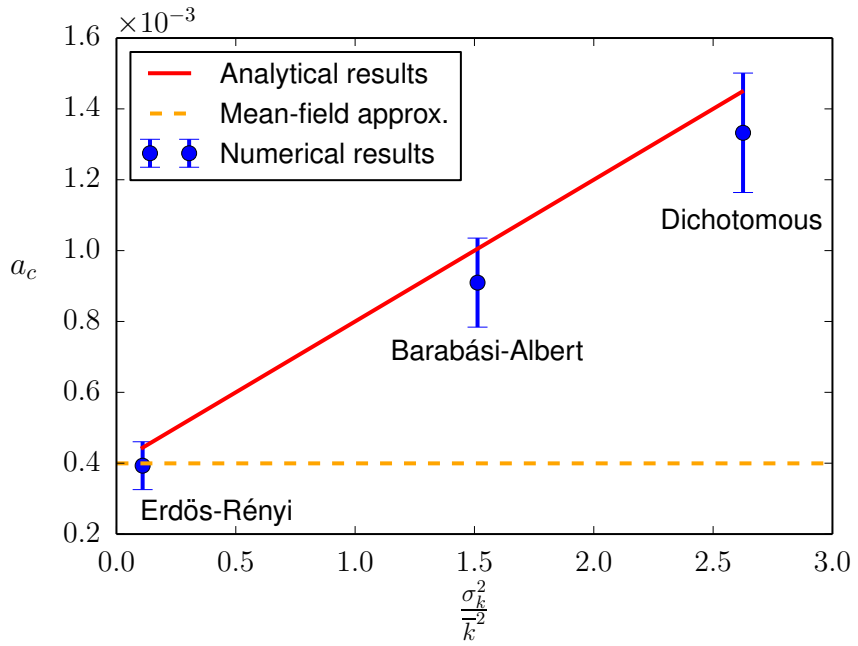

Figure 4.5: Critical value of the noise parameter a as a function of the variance of the degree distribution of the underlying network, σ_k^2. In order to keep all parameters constant except the variance of the degree distribution, a different network type is used for each point (in order of increasing σ_k^2: Erdös-Rényi random network, Barabási-Albert scale-free network and dichotomous network). Symbols: Numerical results (averages over 20 networks, 10 realizations per network and 50000 time steps per realization). Solid line: Analytical results [see Eq. (4.18)]. Dashed line: Mean-field approximation (see Alfarano and Milaković, 2009; Diakonova et al., 2015). The interaction parameter is fixed as $h = 1$, the system size as $N = 2500$ and the mean degree as $\overline{k} = 8$.

As before, we notice in Fig. 4.5 a systematic overestimation of the numerical results by our analytical approach, whose origin lies, again, in the annealed approximation for uncorrelated networks. While both Eq. (4.18) and the mean-field approximation are able to capture the finite-size character of the transition —the fact that $a_c \to 0$ when $N \to \infty$—, only our approach is able to reproduce the influence of the underlying network structure on the critical point. In particular, we observe a numerical behavior approximately consistent with a linear relationship between the value of the critical point and the variance of the underlying degree distribution, as predicted by Eq. (4.18). A quantitative assessment of the significance of this dependence can be obtained by observing the shift between the critical points corresponding to the Erdös-Rényi random network and the di-

chotomous network, the latter being almost a factor of 3 larger than the former. While the persistence of the bimodal-unimodal, finite-size transition in different network topologies had already been reported (Alfarano and Milaković, 2009; Diakonova et al., 2015), to the best of our knowledge, no dependence of the critical point on the characteristics of the underlying network has been documented so far for the noisy voter model nor in the context of the Kirman model (see Lambiotte, 2007, for a similar effect in a different model).

4.5

Local order

We can characterize the local order of the system with an order parameter ρ defined as the interface density or density of active links, that is, the fraction of links connecting nodes in different states,

$$\rho = \frac{\frac{1}{2}\sum_{i=1}^{N} A_{ij}[s_i(1-s_j)+(1-s_i)s_j]}{\frac{1}{2}\sum_{i=1}^{N} A_{ij}}, \tag{4.19}$$

where A_{ij} are the elements of the adjacency matrix. Larger values of ρ imply a larger disorder, corresponding $\rho = 1/2$ to a random distribution of states, while $\rho = 0$ corresponds to full order. Furthermore, note that, as opposed to n, the order parameter does take into account the structure of connections between nodes.

While it has not been studied before in the context of the Kirman model, the interface density ρ is commonly used to describe the time evolution of the voter model (Suchecki et al., 2005b). In the absence of noise, the voter model is characterized by the existence of two absorbing states ($n = 0$ and $n = N$), both of them corresponding to full order ($\rho = 0$). Therefore, the focus is on how the system approaches these absorbing ordered states. In the presence of noise, on the contrary, the system has no absorbing states, i.e., it is always active. Thus, the focus is not anymore on how it reaches any final configuration, but rather on characterizing its behavior once the influence of the initial condition has vanished, that is, in the steady state. In the context of the noisy voter model, it has been recently shown that, after a short initial transient, the average interface density reaches a plateau at a certain value $\langle\rho\rangle_{st}$, with $\langle\rho\rangle_{st} > 0$ for any non-zero value of the noise and $\langle\rho\rangle_{st} = 1/2$ in the infinite noise limit (Diakonova et al., 2015).

Moreover, a mean-field pair-approximation has been used to find an analytical solution for $\langle\rho\rangle_{st}$ as a function of the level of noise and the mean degree of the underlying network. This analytical solution has been shown to be a good approximation for large values of the noise parameter, the small noise region not having been considered.

Let us start the description of our results by emphasizing that individual realizations of the interface density ρ remain always active for any non-zero value of the noise, as it was also the case for the variable n (see Fig. 4.1). As an example, we show in Fig. 4.6 two realizations of the dynamics for a Barabási-Albert scale-free network corresponding, respectively, to the bimodal [panel **(a)**] and the unimodal regime [panel **(b)**]. While in the first of them ($a < a_c$) the system fluctuates near full order, with sporadic excursions of different duration and amplitude towards disorder; in the second ($a > a_c$), the system fluctuates around a high level of disorder, with some large excursions towards full order.

Introducing the annealed approximation for uncorrelated networks described above into the definition of the order parameter given in Eq. (4.19), and focusing on the steady state average value, we obtain

$$\langle\rho\rangle_{st} = \sum_{ij} \frac{k_i k_j}{(N\bar{k})^2} \Big(\langle s_i \rangle_{st} + \langle s_j \rangle_{st} - 2\langle s_j s_j \rangle_{st} \Big) \,. \tag{4.20}$$

In this way, an explicit solution for the steady state average interface density can be found by expressing it in terms of the analytical results presented so far, namely, in terms of the variance $\sigma^2_{st}[n]$ (see Appendix 4.G for details),

$$\langle\rho\rangle_{st} = \frac{1}{2} - \frac{2}{(hN)^2} \left[\frac{(4a+h)(2a+h)}{\left(1-\frac{1}{N}\right)\left(1-\frac{2}{N}\right)} \left(\sigma^2[n] - \frac{N}{4} \right) - \frac{\left(a+\frac{h}{2}\right)}{\left(1-\frac{2}{N}\right)} hN \right] . \tag{4.21}$$

This expression can be contrasted with numerical results in Fig. 4.7, where we present the steady state average interface density $\langle\rho\rangle_{st}$ as a function of the noise parameter a for different types of networks. The mean-field pair-approximation result derived by Diakonova et al. (2015) is also included for comparison.

As we can observe in Fig. 4.7, our approach correctly captures the behavior of the system for both small ($a \lesssim 10^{-3}$) and very large values ($a \gtrsim 3$) of the noise parameter: both the asymptotic convergence towards $\langle\rho\rangle_{st} = 0$ for small a (voter model result for finite systems) and the convergence towards $\langle\rho\rangle_{st} = 1/2$ for large a (full disorder) are well reproduced. On the contrary, our analytical approach fails to reproduce the numerical results for intermediate values of the noise parameter ($10^{-3} \lesssim a \lesssim 3$). The origin of this discrepancy lies in the annealed network approximation: when replacing the original network by a weighted fully-connected topology, all track of local effects is lost —precisely those measured by

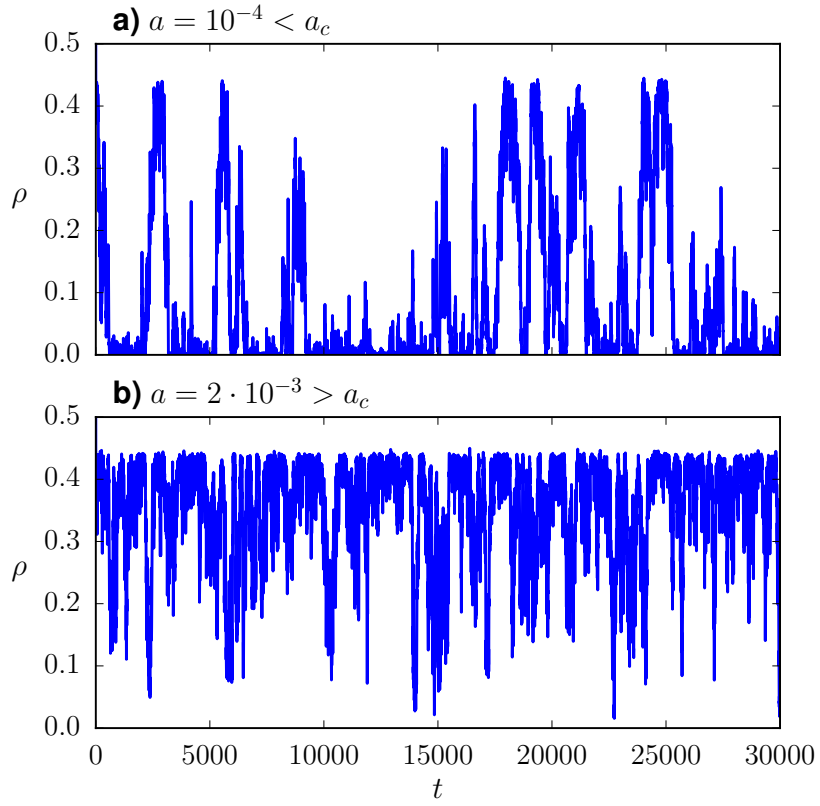

Figure 4.6: Interface density on a Barabási-Albert scale-free network. Single realizations (the same realizations shown in Fig. 4.1). The interaction parameter is fixed as $h = 1$, the system size as $N = 2500$ and the mean degree as $\overline{k} = 8$.

the order parameter—. The fact that this discrepancy is only present for intermediate values of a can be explained, on the one hand, by the lack of locally ordered structures in the fully disordered, large a regime and, on the other hand, by the development of a global order —more and more independent of local effects— for decreasing values of a. Thus, an accurate fit of the numerical results for any value of a can only be expected for topologies where local effects are absent or negligible. In Fig. 4.9, presented in Appendix 4.I, we show, for instance, that our approximation successfully fits the results in a fully-connected network. The good accuracy of the results presented above for the variance of n suggests that the discrepancy between analytical and numerical results appears only when the annealed network approximation is used to derive a relationship between $\langle\rho\rangle_{st}$

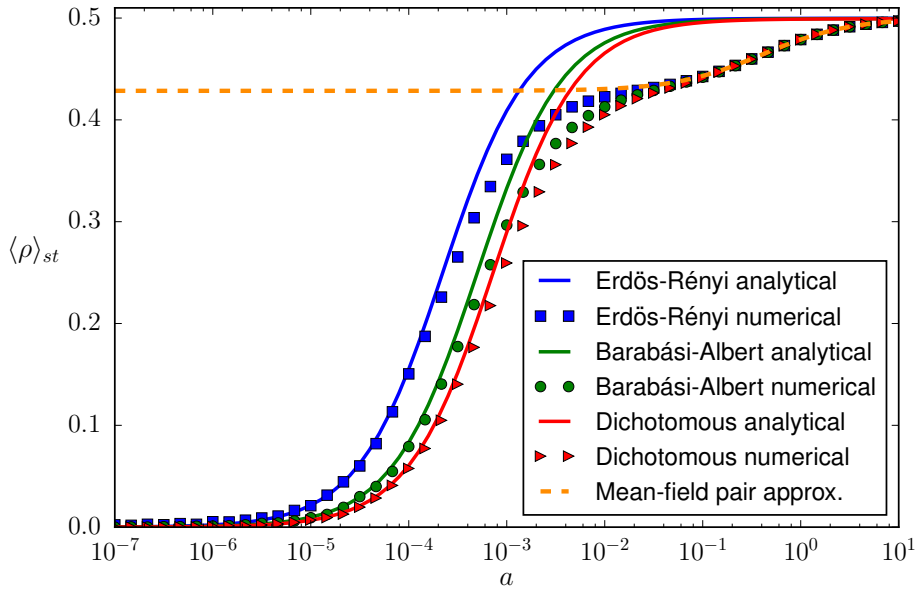

Figure 4.7: Steady state of the average interface density as a function of the noise parameter a in a linear-logarithmic scale and for three different types of networks: Erdös-Rényi random network, Barabási-Albert scale-free network and dichotomous network. Symbols: Numerical results (averages over 20 networks, 10 realizations per network and 50000 time steps per realization). Solid lines: Analytical results [see Eq. (4.21)]. Dashed line: Mean-field pair-approximation (see Diakonova et al., 2015). The interaction parameter is fixed as $h = 1$, the system size as $N = 2500$ and the mean degree as $\overline{k} = 8$.

and $\sigma^2_{st}[n]$, and not in the derivation of the latter, for which only global correlations are relevant. Apart from the functional dependence of the interface density on the noise parameter, our approach is also able to capture the influence of the network, which becomes significant for $a \lesssim 10^{-2}$. In particular, we find that a larger variance of the degree distribution of the corresponding network leads to a smaller interface density, i. e., to a higher level of order.

Even if the mean-field pair-approximation fits the numerical results remarkably well for large and intermediate values of the noise parameter ($a \gtrsim 10^{-2}$), it is completely unable to reproduce the behavior of the system for small a, and it fails to explain the influence of any network property other than the mean degree. While the pair-approximation allows to capture the short-range order characteristic of intermediate values of a, the assumptions implicit in the derivation of the mean-field result (Vazquez et al., 2008) do not allow to reproduce the long-range

order characteristic of the small a region. Note that the limiting case of $a = 0$ (voter model) is a singular point of the mean-field pair-approximation (Diakonova et al., 2015), leading to the existence of two different solutions: a non-zero solution linked to the result displayed in Fig. 4.7 —correct in the infinite size limit—, and a zero solution —correct for finite systems.

4.6

Inference of network properties from the autocorrelation function

As explained above, from any initial condition, the system quickly reaches a dynamic steady state, whose active character can be clearly observed in Fig. 4.1. In order to characterize the dynamic nature of this steady state, let us now focus on the steady state autocorrelation function of n, defined as

$$K_{st}[n](\tau) = \langle n(t+\tau)n(t)\rangle_{st} - \langle n\rangle_{st}^2 \,, \tag{4.22}$$

where τ plays the role of a time-lag. In the fully-connected case, it has been shown in the previous literature (Alfarano et al., 2008) that the autocorrelation decays exponentially, with an exponent proportional to the noise parameter, $K_{st}[n](\tau) = \sigma_{st}^2[n]e^{-2a\tau}$. In the case of different network topologies, the mean-field prediction is that no influence of the network is to be expected and, therefore, the same exponential decay as in the fully-connected case is to be found. In contrast with this prediction, both the analytical and numerical results to be presented here show that the network does have a significant impact on the functional form of the steady state autocorrelation of n.

Introducing the annealed approximation for uncorrelated networks described above into the equation for the time evolution of the first-order moments (4.6), integrating it with carefully chosen initial conditions, and making use of the above reported analytical results (see Appendix 4.H for details), we can find

$$K_{st}[n](\tau) = \left(\sigma_{st}^2[n] - S_1\right) e^{-(2a+h)\tau} + S_1 e^{-2a\tau} \,, \tag{4.23}$$

where S_1 is defined as

$$S_1 = \frac{2a+h}{h\left(1-\frac{1}{N}\right)}\left(\sigma_{st}^2[n] - \frac{N}{4}\right) . \tag{4.24}$$

This expression can be contrasted with numerical results in Fig. 4.8, where we present the autocorrelation function, normalized by the variance, for the two

extreme cases of a network with no degree heterogeneity (regular 2D lattice) and a highly heterogeneous degree distribution (dichotomous network). Note the logarithmic scale in the y-axis.

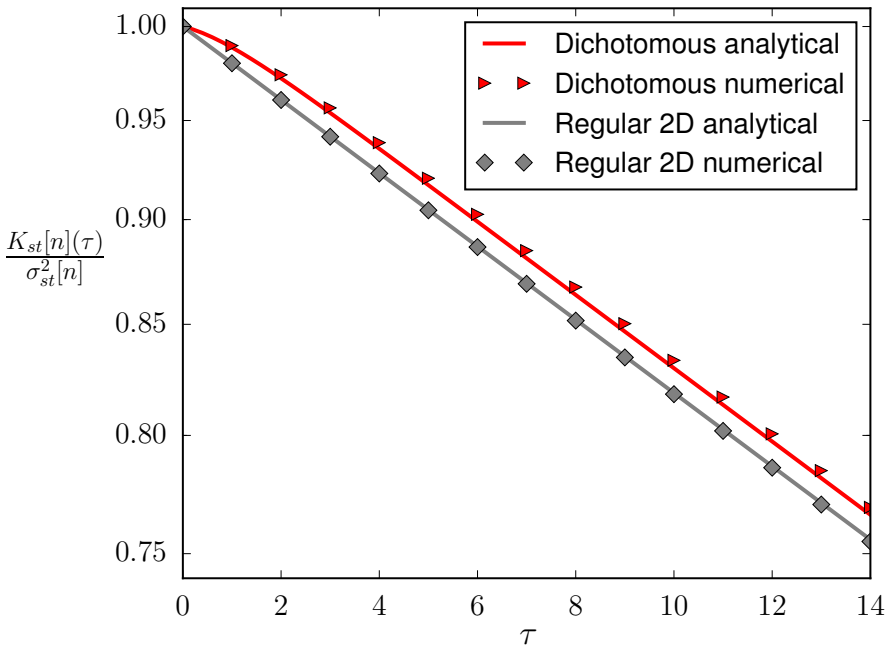

Figure 4.8: Autocorrelation function of n in log-linear scale for a dichotomous network and a regular 2D lattice. Symbols: Numerical results (averages over 10 networks, 2 realizations per network and 200000 time steps per realization). Solid lines: Analytical results [see Eq. (4.23)]. Parameter values are fixed as $a = 0.01$, $h = 1$, the system size as $N = 2500$ and the mean degree as $\overline{k} = 8$.

It is important to note that, in the case of no degree heterogeneity, the new variable S_1 becomes $S_1 = \sigma^2_{st}[n]$. This can be understood by applying, $\forall i$, $k_i = \overline{k}$ in the averages over the degree distribution in Eq. (4.14),

$$\sigma^2_{st}[n] = \frac{N}{4}\frac{(2a+h)}{\left(2a+\frac{h}{N}\right)}, \tag{4.25}$$

and introducing this result into the definition of S_1, Eq. (4.24). Thus, for networks with no degree heterogeneity, the steady state autocorrelation function behaves as in the fully-connected case, and as predicted by the mean-field approximation, $K_{st}[n](\tau) = \sigma^2_{st}[n]e^{-2a\tau}$. This single exponential decay is confirmed by the numerical results presented in Fig. 4.8 for the regular 2D lattice.

On the contrary, for networks with non-zero degree heterogeneity, in general, $S_1 \neq \sigma^2_{st}[n]$, and thus the autocorrelation function consists of two different exponential decay components [see Eq. (4.23)]. When $h > 0$, the exponential $e^{-(2a+h)\tau}$ decays faster than $e^{-2a\tau}$. Therefore, for long time-lags, we expect the normalized autocorrelation function of any network to be parallel to $e^{-2a\tau}$ in log-linear scale, with a vertical shift proportional to its degree heterogeneity and due to the initial deviation from the single exponential behavior. This description is confirmed by the numerical results presented in Fig. 4.8 for the dichotomous network.

Neither Eq. (4.14) nor the asymptotic approximate expressions in Eqs. (4.16) and (4.17) allow to infer, for a given system, the values of the two model parameters, a and h, and the normalized variance of the underlying degree distribution, $\sigma^2_k/\overline{k}^2$, by measuring only the steady state variance of n, $\sigma^2_{st}[n]$. Thus, it is impossible, by using only these relationships, to conclude if the fluctuations observed in a given system have a contribution due to the degree heterogeneity of the network, without a prior knowledge of the model parameters a and h. On the contrary, the particular functional form of the autocorrelation function $K_{st}[n](\tau)$ —with two exponential decay components whose exponents are different functions of a and h— does allow for the values of a, h and $\sigma^2_k/\overline{k}^2$ to be inferred from Eq. (4.23), in combination with Eq. (4.16) or Eq. (4.17), by measuring only the temporal correlations of the aggregated variable n, and assuming we can also know the system size N. Note that the use of Eq. (4.16) or Eq. (4.17) can be determined by self-consistency, depending on the value obtained for a. As an example, a simple fit of Eq. (4.23) to the numerical results presented in Fig. 4.8 for the dichotomous network leads, in combination with Eq. (4.16), to the fitted parameter values $a = 0.0099$, $h = 0.94$ and $\sigma^2_k/\overline{k}^2 = 2.539$, remarkably close to the actual values used for computing the numerical results, $a = 0.01$, $h = 1$ and $\sigma^2_k/\overline{k}^2 = 2.625$. In this way, we are able to infer some information about the underlying network —its normalized level of degree heterogeneity— by studying only the aggregate behavior of the system as a whole.

4.7

Concluding remarks

In this chapter, we have proposed a new analytical method to study stochastic, binary-state models of interacting units on complex networks. Moving beyond the usual mean-field theories (Vazquez et al., 2008; Alfarano and Milaković, 2009; Diakonova et al., 2015), this alternative approach builds on a recent study considering heterogeneity in stochastic interacting particle systems (Lafuerza and

Toral, 2013) and proposes an annealed approximation for uncorrelated networks accounting for the network structure as parametric heterogeneity.

Using the noisy voter model as an example, we have been able to unfold the dependence of the model not only on the mean degree of the underlying topology (the mean-field prediction) but also on more complex averages over the degree distribution. In particular, we have shown that the degree heterogeneity —i.e., the variance of the underlying degree distribution— has a substantial influence on the location of the critical point of the noise-induced, finite-size transition characterizing the model. This shift of the transition might have important practical implications in real systems, since it suggests that different behavioral regimes can be achieved by introducing changes in the underlying network of interactions. Furthermore, we have studied the influence of the network on the local ordering of the system, finding that a larger degree heterogeneity leads to a higher average level of order in the steady state. Interestingly, we have also found the heterogeneity of the underlying degree distribution to play a relevant role in determining the functional form of the temporal correlations of the system. Finally, we have shown how this latter effect can be used to infer some information about the underlying network —its normalized level of degree heterogeneity— by studying only the aggregate behavior of the system as a whole, an issue of interest for systems where macroscopic, population level variables are easier to measure than their microscopic, individual level counterparts.

Numerical simulations on different types of networks have been used to validate our analytical results, finding a remarkably good agreement for all the properties studied except for the local order, for which a significant discrepancy is found for intermediate levels of noise. The origin of this discrepancy has been shown to lie in the annealed network approximation, whose validity is restricted to global properties or situations where local effects are negligible. The generally good agreement found is all the more remarkable considering that, while the uncorrelated network assumption is essential for the proposed analytical method, we did not impose any particular structural constraint to avoid correlations in the networks used for the numerical simulations (Boguñá et al., 2004; Catanzaro et al., 2005).

APPENDICES TO CHAPTER 4

4.A

Master equation

We derive here a general master equation for the N-node probability distribution $P(s_1, \ldots, s_N)$, where the individual node variables are binary and take the values $s_i = \{0, 1\}$. Recalling that r_i^+ is the rate at which node i changes its state from $s_i = 0$ to $s_i = 1$ and r_i^- the rate at which it does so in the opposite direction, we can directly write differential equations for the probability of node i to be in state $s_i = 0$ and for its probability to be in state $s_i = 1$, respectively,

$$\begin{aligned} \frac{dP(s_i = 0)}{dt} &= -r_i^+ P(s_i = 0) + r_i^- P(s_i = 1)\,, \\ \frac{dP(s_i = 1)}{dt} &= -r_i^- P(s_i = 1) + r_i^+ P(s_i = 0)\,. \end{aligned} \tag{4.26}$$

Introducing here the individual-node step operators E_i^{+1} and E_i^{-1}, whose effect over an arbitrary function of the state of node i, $f(s_i)$, is defined as

$$\begin{aligned} E_i^{+1}\big[f(s_i = 0)\big] &= f(s_i = 1)\,, \\ E_i^{+1}\big[f(s_i = 1)\big] &= 0\,, \\ E_i^{-1}\big[f(s_i = 0)\big] &= 0\,, \\ E_i^{-1}\big[f(s_i = 1)\big] &= f(s_i = 0)\,, \end{aligned} \tag{4.27}$$

we can rewrite Eqs. (4.26) as

$$\begin{aligned}\frac{dP(s_i=0)}{dt} &= -r_i^+ P(s_i=0) + r_i^- E_i^{+1} P(s_i=0)\,,\\ \frac{dP(s_i=1)}{dt} &= -r_i^- P(s_i=1) + r_i^+ E_i^{-1} P(s_i=1)\,.\end{aligned} \tag{4.28}$$

Multiplying these two equations, respectively, by $(1-s_i)$ and s_i, we can gather them in a single differential equation,

$$\begin{aligned}\frac{dP(s_i)}{dt} =&(1-s_i)\left[-r_i^+ P(s_i) + r_i^- E_i^{+1} P(s_i)\right]\\ &+ s_i\left[-r_i^- P(s_i) + r_i^+ E_i^{-1} P(s_i)\right]\,,\end{aligned} \tag{4.29}$$

and noticing that $(1-s_i) = E_i^{+1}[s_i]$ and $s_i = E_i^{+1}[(1-s_i)]$, we can rearrange terms as

$$\frac{dP(s_i)}{dt} = \left(E_i^{+1}-1\right)\left[s_i r_i^- P(s_i)\right] + \left(E_i^{-1}-1\right)\left[(1-s_i) r_i^+ P(s_i)\right]\,. \tag{4.30}$$

Finally, we find the master equation for the N-node probability distribution $P(s_1,\ldots,s_N)$ by simply adding up the contribution of every single node $i \in [1,N]$,

$$\begin{aligned}\frac{dP(s_1,\ldots,s_N)}{dt} =&\sum_{i=1}^{N}\left(E_i^{+1}-1\right)\left[s_i r_i^- P(s_1,\ldots,s_N)\right]\\ &+\sum_{i=1}^{N}\left(E_i^{-1}-1\right)\left[(1-s_i) r_i^+ P(s_1,\ldots,s_N)\right]\,.\end{aligned} \tag{4.31}$$

4.B

Equation for the time evolution of the first-order moments

We show, in this section, how to obtain a general equation for the time evolution of the first-order moments $\langle s_i\rangle$ [Eq. (4.4) in the main text of the chapter]. Let us start by using the definition of the step operators in Eq. (4.27) and the binary character of each individual node state variable, $s_i = \{0,1\}$, to derive, for a given function of the state of node i, $f(s_i)$, four relations which will

ease later calculations. While the function f might also depend on the other variables, $f = f(s_1, ..., s_i, ..., s_N)$, we restrict our attention, without loss of generality, to the case $f(s_i)$. For the first two relations, we have that

$$\begin{aligned}\sum_{s_i} \left(E_i^{+1} - 1\right) [s_i f(s_i)] &= \sum_{s_i} \left(E_i^{+1} [s_i f(s_i)] - s_i f(s_i)\right) \\ &= 1 \cdot f(1) - 0 \cdot f(0) + 0 - 1 \cdot f(1) = 0\,,\end{aligned} \tag{4.32}$$

and

$$\begin{aligned}\sum_{s_i} \left(E_i^{-1} - 1\right) [(1 - s_i) f(s_i)] &= \sum_{s_i} \left(E_i^{+1} [(1 - s_i) f(s_i)] - (1 - s_i) f(s_i)\right) \\ &= 0 - 1 \cdot f(0) + 1 \cdot f(0) - 0 \cdot f(1) = 0\,,\end{aligned} \tag{4.33}$$

where the sums are over the two possible values of s_i. Looking at the master equation (4.31), one can understand that these two relations translate the fact that any increase in the probability of a given node being in a given state must be accompanied by a corresponding decrease in the probability of the complementary state. Regarding the other two relations, we can write

$$\begin{aligned}\sum_{s_i} s_i \left(E_i^{+1} - 1\right) [s_i f(s_i)] &= \sum_{s_i} s_i \left(E_i^{+1} [s_i f(s_i)] - s_i f(s_i)\right) \\ &= 0 \cdot (1 \cdot f(1) - 0 \cdot f(0)) + 1 \cdot (0 - 1 \cdot f(1)) \\ &= -1 \cdot f(1) \\ &= -\sum_{s_i} s_i f(s_i)\,,\end{aligned} \tag{4.34}$$

and

$$\begin{aligned}\sum_{s_i} s_i \left(E_i^{-1} - 1\right) [(1 - s_i) f(s_i)] &= \sum_{s_i} s_i \left(E_i^{+1} [(1 - s_i) f(s_i)] - (1 - s_i) f(s_i)\right) \\ &= 0 \cdot (0 - 1 \cdot f(0)) + 1 \cdot (1 \cdot f(0) - 0 \cdot f(1)) \\ &= 1 \cdot f(0) \\ &= \sum_{s_i} (1 - s_i) f(s_i)\,.\end{aligned} \tag{4.35}$$

Let us also introduce, for clarity, the notation $\sum_{\{s\}}$ to refer to the sum over all the possible combinations of states of all the individual nodes' variables,

$$\sum_{\{s\}} \equiv \sum_{s_1} \sum_{s_2} \cdots \sum_{s_N}\,, \tag{4.36}$$

and $\sum_{\{s\}_j}$ to indicate the sum over all the possible combinations of states of all the variables except s_j,

$$\sum_{\{s\}_j} \equiv \sum_{s_1} \cdots \sum_{s_{j-1}} \sum_{s_{j+1}} \cdots \sum_{s_N} . \tag{4.37}$$

Note that these two definitions are related by

$$\sum_{\{s\}} = \sum_{\{s\}_j} \sum_{s_j}, \tag{4.38}$$

which allows us to split the sum over all possible configurations of the system into a sum over the values of one of the variables and a sum over the configurations of the rest of the system. By using the notation in (4.36), the average of a given function of the states of the nodes, $f(s_1, \ldots, s_N)$, can be written as

$$\Big\langle f(s_1, \ldots, s_N) \Big\rangle = \sum_{\{s\}} f(s_1, \ldots, s_N) P(s_1, \ldots, s_N) . \tag{4.39}$$

Using this expression and the master equation in (4.31) we derive an equation for the time evolution of the average value of the state of node i,

$$\begin{aligned} \frac{d\langle s_i \rangle}{dt} =& \sum_{\{s\}} s_i \frac{dP(s_1, \ldots, s_N)}{dt} \\ =& \sum_{\{s\}} \sum_{j=1}^{N} s_i \left(E_j^{+1} - 1\right) \left[s_j r_j^- P(s_1, \ldots, s_N)\right] \\ &+ \sum_{\{s\}} \sum_{j=1}^{N} s_i \left(E_j^{-1} - 1\right) \left[(1 - s_j) r_j^+ P(s_1, \ldots, s_N)\right] . \end{aligned} \tag{4.40}$$

Separating the terms with $j = i$ and those with $j \neq i$, we find

$$\begin{aligned} \frac{d\langle s_i \rangle}{dt} =& \sum_{\{s\}} s_i \left(E_i^{+1} - 1\right) \left[s_i r_i^- P(s_1, \ldots, s_N)\right] \\ &+ \sum_{\{s\}} s_i \left(E_i^{-1} - 1\right) \left[(1 - s_i) r_i^+ P(s_1, \ldots, s_N)\right] \\ &+ \sum_{\{s\}} \sum_{j \neq i}^{N} s_i \left(E_j^{+1} - 1\right) \left[s_j r_j^- P(s_1, \ldots, s_N)\right] \\ &+ \sum_{\{s\}} \sum_{j \neq i}^{N} s_i \left(E_j^{-1} - 1\right) \left[(1 - s_j) r_j^+ P(s_1, \ldots, s_N)\right] . \end{aligned} \tag{4.41}$$

If we now use the relation (4.38) to extract, from the general sum over $\{s\}$, the sum over the values of s_i for the terms with $j = i$, while we extract the sum over the values of s_j for the terms with $j \neq i$, we obtain

$$\begin{aligned}\frac{d\langle s_i\rangle}{dt} = &\sum_{\{s\}_i}\Bigg[\left(\sum_{s_i} s_i\left(E_i^{+1}-1\right)\left[s_i r_i^- P(s_1,\dots,s_N)\right]\right)\\ &+\left(\sum_{s_i} s_i\left(E_i^{-1}-1\right)\left[(1-s_i) r_i^+ P(s_1,\dots,s_N)\right]\right)\Bigg]\\ &+\sum_{j\neq i}^{N}\sum_{\{s\}_j} s_i\Bigg[\left(\sum_{s_j}\left(E_j^{+1}-1\right)\left[s_j r_j^- P(s_1,\dots,s_N)\right]\right)\\ &+\left(\sum_{s_j}\left(E_j^{-1}-1\right)\left[(1-s_j) r_j^+ P(s_1,\dots,s_N)\right]\right)\Bigg],\end{aligned} \tag{4.42}$$

where we can easily identify relations (4.32) and (4.33) for the terms with $j \neq i$, and relations (4.34) and (4.35) for the terms with $j = i$. In this way, we can write

$$\begin{aligned}\frac{d\langle s_i\rangle}{dt} = &\sum_{\{s\}_i}\left(-\sum_{s_i} s_i r_i^- P(s_1,\dots,s_N)\right)\\ &+\sum_{\{s\}_i}\left(\sum_{s_i}(1-s_i) r_i^+ P(s_1,\dots,s_N)\right),\end{aligned} \tag{4.43}$$

which, after combining the sums together again, becomes

$$\frac{d\langle s_i\rangle}{dt} = \sum_{\{s\}}\left[r_i^+ - (r_i^+ + r_i^-)s_i\right] P(s_1,\dots,s_N), \tag{4.44}$$

and we finally find the equation for the time evolution of the first-order moments presented in the main text of the chapter,

$$\frac{d\langle s_i\rangle}{dt} = \langle r_i^+\rangle - \langle (r_i^+ + r_i^-)s_i\rangle. \tag{4.45}$$

4.C

Equation for the time evolution of the second-order cross-moments

In order to find a general equation for the time evolution of the second-order cross-moments $\langle s_i s_j \rangle$ [Eq. (4.5) in the main text of the chapter] we proceed in a similar way as we did in the previous section for the first-order moments. Taking into account the master equation (4.31) and using the definition of the average value in (4.39), we can write for the second-order cross-moments,

$$\begin{aligned}\frac{d\langle s_i s_j\rangle}{dt} &= \sum_{\{s\}} s_i s_j \frac{dP(s_1,\ldots,s_N)}{dt} \\ &= \sum_{\{s\}}\sum_{k=1}^{N} s_i s_j \left(E_k^{+1}-1\right)\left[s_k r_k^- P(s_1,\ldots,s_N)\right] \\ &\quad + \sum_{\{s\}}\sum_{k=1}^{N} s_i s_j \left(E_k^{-1}-1\right)\left[(1-s_k) r_k^+ P(s_1,\ldots,s_N)\right] .\end{aligned} \tag{4.46}$$

For the terms of the sum with $k \neq i, j$, we can use relation (4.38) to write

$$\begin{aligned}\sum_{k\neq i,j}^{N}\sum_{\{s\}_k} s_i s_j \Bigg[&\left(\sum_{s_k}\left(E_k^{+1}-1\right)\left[s_k r_k^- P(s_1,\ldots,s_N)\right]\right) \\ &+ \left(\sum_{s_k}\left(E_k^{-1}-1\right)\left[(1-s_k) r_k^+ P(s_1,\ldots,s_N)\right]\right)\Bigg] = 0\,,\end{aligned} \tag{4.47}$$

where the equality follows from an application of relations (4.32) and (4.33). Similarly, we can use relations (4.34) and (4.35) to transform, in Eq. (4.46), the

terms with $k = i \neq j$ as

$$\begin{aligned}
&\sum_{\{s\}_i} s_j \left[\left(\sum_{s_i} s_i \left(E_i^{+1} - 1 \right) \left[s_i r_i^- P(s_1, \ldots, s_N) \right] \right) \right. \\
&\qquad \left. + \left(\sum_{s_i} s_i \left(E_i^{-1} - 1 \right) \left[(1 - s_i) r_i^+ P(s_1, \ldots, s_N) \right] \right) \right] \\
&= \sum_{\{s\}_i} s_j \left[- \sum_{s_i} s_i r_i^- P(s_1, \ldots, s_N) + \sum_{s_i} (1 - s_i) r_i^+ P(s_1, \ldots, s_N) \right] \\
&= - \sum_{\{s\}} s_i s_j r_i^- P(s_1, \ldots, s_N) + \sum_{\{s\}} (1 - s_i) s_j r_i^+ P(s_1, \ldots, s_N) \\
&= \langle r_i^+ s_j \rangle - \langle (r_i^+ + r_i^-) s_i s_j \rangle \,,
\end{aligned} \tag{4.48}$$

and, equivalently, the terms with $k = j \neq i$ as

$$\begin{aligned}
&\sum_{\{s\}_j} s_i \left[\left(\sum_{s_j} s_j \left(E_j^{+1} - 1 \right) \left[s_j r_j^- P(s_1, \ldots, s_N) \right] \right) \right. \\
&\qquad \left. + \left(\sum_{s_j} s_j \left(E_j^{-1} - 1 \right) \left[(1 - s_j) r_j^+ P(s_1, \ldots, s_N) \right] \right) \right] \\
&= \langle r_j^+ s_i \rangle - \langle (r_j^+ + r_j^-) s_i s_j \rangle \,.
\end{aligned} \tag{4.49}$$

Note that, for both expressions (4.48) and (4.49), we have assumed that $i \neq j$. In order to study the other case, when $i = j$, we simply need to notice that, being the possible values of the variables $s_i = \{0, 1\}$, then $s_i^2 = s_i$, and therefore

$$\frac{d\langle s_i s_i \rangle}{dt} = \frac{d\langle s_i \rangle}{dt} = \langle r_i^+ \rangle - \langle (r_i^+ + r_i^-) s_i \rangle \,, \tag{4.50}$$

where we have used the result (4.45) for the first-order moments derived in the previous section.

Thus, we can write an equation for the second-order cross-moments as

$$\frac{d\langle s_i s_j \rangle}{dt} = \begin{cases} \langle r_i^+ s_j \rangle + \langle r_j^+ s_i \rangle - \langle q_{ij} s_i s_j \rangle & \text{if } i \neq j \\ \langle r_i^+ \rangle - \langle (r_i^+ + r_i^-) s_i \rangle & \text{if } i = j \end{cases} , \tag{4.51}$$

where $q_{ij} = r_i^+ + r_i^- + r_j^+ + r_j^-$. Finally, using the Kronecker delta, we obtain the expression presented in the main text of the chapter,

$$\frac{d\langle s_i s_j\rangle}{dt} = \langle r_i^+ s_j\rangle + \langle r_j^+ s_i\rangle - \langle q_{ij} s_i s_j\rangle + \delta_{ij}\left[\langle s_i r_i^-\rangle + \langle (1-s_i) r_i^+\rangle\right] . \tag{4.52}$$

4.D

Variance of n

We derive in this appendix an analytical expression for the steady state variance of n [Eq. (4.14) in the main text of the chapter]. Let us start by introducing the transition rates of the noisy voter model [Eq. (4.1) in the main text of the chapter] into the equation for the time evolution of the second-order cross-moments obtained in the previous section, Eq. (4.52),

$$\begin{aligned}\frac{d\langle s_i s_j\rangle}{dt} =& a(\langle s_i\rangle + \langle s_j\rangle) + \frac{h}{k_i}\sum_{m\in nn(i)}\langle s_m s_j\rangle + \frac{h}{k_j}\sum_{m\in nn(j)}\langle s_m s_i\rangle \\ & - 2(2a+h)\langle s_i s_j\rangle \\ & + \delta_{ij}\left[a + h\langle s_i\rangle + \frac{h}{k_i}\sum_{m\in nn(i)}\langle s_m\rangle - \frac{2h}{k_i}\sum_{m\in nn(i)}\langle s_m s_i\rangle\right] .\end{aligned} \tag{4.53}$$

Applying now the annealed approximation for uncorrelated networks described in the main text of the chapter [see Eq. (4.10)], we can replace the sums over sets of neighbors by sums over the whole system, finding

$$\begin{aligned}\frac{d\langle s_i s_j\rangle}{dt} =& a(\langle s_i\rangle + \langle s_j\rangle) + \frac{h}{N\bar{k}}\sum_m k_m\left(\langle s_m s_i\rangle + \langle s_m s_j\rangle\right) - 2(2a+h)\langle s_i s_j\rangle \\ & + \delta_{ij}\left[a + h\langle s_i\rangle + \frac{h}{N\bar{k}}\sum_m k_m\langle s_m\rangle - \frac{2h}{N\bar{k}}\sum_m k_m\langle s_m s_i\rangle\right] .\end{aligned} \tag{4.54}$$

Bearing in mind the definition of the covariance matrix in terms of the first-order moments and the second-order cross-moments, $\sigma_{ij} = \langle s_i s_j\rangle - \langle s_i\rangle\langle s_j\rangle$, we can find an equation for its time evolution from Eq. (4.6) in the main text of the

chapter and Eq. (4.54),

$$\begin{aligned}\frac{d\sigma_{ij}}{dt} =& \frac{d\langle s_i s_j\rangle}{dt} - \frac{d\langle s_i\rangle}{dt}\langle s_j\rangle - \langle s_i\rangle\frac{d\langle s_j\rangle}{dt} \\ =& -2(2a+h)(\langle s_i s_j\rangle - \langle s_i\rangle\langle s_j\rangle) \\ &+ \frac{h}{N\bar{k}}\sum_m k_m\Big[(\langle s_m s_i\rangle - \langle s_m\rangle\langle s_i\rangle) + (\langle s_m s_j\rangle - \langle s_m\rangle\langle s_j\rangle)\Big] \\ &+ \delta_{ij}\left[a + h\langle s_i\rangle + \frac{h}{N\bar{k}}\sum_m k_m\langle s_m\rangle - \frac{2h}{N\bar{k}}\sum_m k_m\langle s_m s_i\rangle\right],\end{aligned} \tag{4.55}$$

which can be written in terms of only the covariance matrix and the first moments,

$$\begin{aligned}\frac{d\sigma_{ij}}{dt} =& -2(2a+h)\sigma_{ij} + \frac{h}{N\bar{k}}\sum_m k_m\left(\sigma_{mi}+\sigma_{mj}\right) \\ &+ \delta_{ij}\left[a + \frac{h}{N\bar{k}}\sum_m k_m\langle s_m\rangle + \left(h - \frac{2h}{N\bar{k}}\sum_m k_m\langle s_m\rangle\right)\langle s_i\rangle\right. \\ &\left. - \frac{2h}{N\bar{k}}\sum_m k_m\sigma_{mi}\right].\end{aligned} \tag{4.56}$$

In the steady state, and using also the steady state solution of the first order moments $\langle s_i\rangle_{st} = 1/2$ [Eq. (4.7) in the main text of the chapter], we find

$$\sigma_{ij} = \frac{\frac{h}{N\bar{k}}\sum_m k_m\left(\sigma_{mi}+\sigma_{mj}\right) + \delta_{ij}\left[a + \frac{h}{2} - \frac{2h}{N\bar{k}}\sum_m k_m\sigma_{mi}\right]}{2(2a+h)}. \tag{4.57}$$

Note that, for the sake of notational simplicity, we have dropped the subindex st for the steady state solution of the covariance matrix. Recalling now the relation between the variance of n and the covariance matrix [Eq. (4.13) in the main text of the chapter], we can find an equation for the steady state variance of n by

simply summing Eq. (4.57) over i and j,

$$\begin{aligned}\sigma^2_{st}[n] = \sum_{ij}\sigma_{ij} &= \frac{\frac{h}{N\overline{k}}\sum_{ijm}k_m\left(\sigma_{mi}+\sigma_{mj}\right)+\sum_i\left[a+\frac{h}{2}-\frac{2h}{N\overline{k}}\sum_m k_m\sigma_{mi}\right]}{2(2a+h)}\\ &= \frac{\frac{h}{\overline{k}}\left(\sum_{im}k_m\sigma_{mi}+\sum_{jm}k_m\sigma_{mj}\right)+N\left(a+\frac{h}{2}\right)-\frac{2h}{N\overline{k}}\sum_{im}k_m\sigma_{mi}}{2(2a+h)}\\ &= \frac{N\left(a+\frac{h}{2}\right)+\frac{2h}{\overline{k}}\left(1-\frac{1}{N}\right)\sum_{im}k_m\sigma_{mi}}{2(2a+h)}\,.\end{aligned} \tag{4.58}$$

Let us introduce now the set of variables S_x, with $x\in\{0,1,2,\ldots\}$, and defined as

$$S_x = \sum_{im}k_i^x k_m\sigma_{mi}\,. \tag{4.59}$$

In this way, we can rewrite the steady state variance of n in terms of one of these new variables, S_0,

$$\sigma^2_{st}[n] = \frac{N\left(a+\frac{h}{2}\right)+\frac{2h}{\overline{k}}\left(1-\frac{1}{N}\right)S_0}{2(2a+h)}\,. \tag{4.60}$$

In order to find an equation for this new variable S_0, we could use again the equation for the covariance matrix in (4.57), multiplying it by k_j and summing over i and j, obtaining a solution in terms of the variable S_1. We could then proceed similarly and find an equation for S_1 as a function of S_2, for S_3 as a function of S_4, and so forth. In general, for any x, we have

$$\begin{aligned}S_x &= \sum_{ij}k_i^x k_j\sigma_{ij}\\ &= \frac{\frac{h}{N\overline{k}}\sum_{ijm}k_i^x k_j k_m\left(\sigma_{mi}+\sigma_{mj}\right)+\sum_i k_i^{x+1}\left[a+\frac{h}{2}-\frac{2h}{N\overline{k}}\sum_m k_m\sigma_{mi}\right]}{2(2a+h)}\,,\end{aligned} \tag{4.61}$$

which can be written as

$$\begin{aligned} S_x =& \frac{\dfrac{h}{N\overline{k}}\sum_j k_j \sum_{im} k_i^x k_m \sigma_{mi} + \dfrac{h}{N\overline{k}}\sum_i k_i^x \sum_{jm} k_j k_m \sigma_{mj}}{2(2a+h)} \\ &+ \frac{\sum_i k_i^{x+1}\left(a+\dfrac{h}{2}\right) - \dfrac{2h}{N\overline{k}}\sum_{im} k_i^{x+1} k_m \sigma_{mi}}{2(2a+h)} \\ =& \frac{hS_x + \dfrac{h}{\overline{k}}\overline{k^x} S_1 + N\overline{k^{x+1}}\left(a+\dfrac{h}{2}\right) - \dfrac{2h}{N\overline{k}} S_{x+1}}{2(2a+h)}\,, \end{aligned} \tag{4.62}$$

where the overbar notation is used for averages over the degree distribution [see Eq. (4.3) in the main text of the chapter]. From Eq. (4.62) we can obtain an expression for the variable S_x in terms of only S_1 and S_{x+1},

$$S_x = \frac{\dfrac{h}{\overline{k}}\overline{k^x} S_1 + N\overline{k^{x+1}}\left(a+\dfrac{h}{2}\right) - \dfrac{2h}{N\overline{k}} S_{x+1}}{4a+h}\,. \tag{4.63}$$

By inverting Eq. (4.63), we can write all variables S_{x+1} in terms of the preceding ones,

$$S_{x+1} = \left[-\frac{(4a+h)N\overline{k}}{2h}\right] S_x + \frac{N}{2}\left[\overline{k^x} S_1 + \frac{N\overline{k}}{h}\left(a+\frac{h}{2}\right)\overline{k^{x+1}}\right]\,, \tag{4.64}$$

which has the general form

$$S_{x+1} = AS_x + B_x\,. \tag{4.65}$$

It is easy to see that this recurrence relation has the solution

$$S_{x+1} = A^x S_1 + \sum_{m=1}^{x} A^{x-m} B_x\,, \tag{4.66}$$

where the choice of S_1 instead of S_0 in the first term allows us to write all the variables S_{x+1} in terms of only one of them, S_1. Note that this choice is required by the presence of a term with S_1 inside B_x. Thus, we can write the solution for our original recurrence relation in (4.64) as

$$\begin{aligned} S_{x+1} =& \left[-\frac{(4a+h)N\overline{k}}{2h}\right]^x S_1 \\ &+ \sum_{m=1}^{x}\left[-\frac{(4a+h)N\overline{k}}{2h}\right]^{x-m} \frac{N}{2}\left[\overline{k^m} S_1 + \frac{N\overline{k}}{h}\left(a+\frac{h}{2}\right)\overline{k^{m+1}}\right]\,. \end{aligned} \tag{4.67}$$

If we now rewrite Eq. (4.67) as

$$\frac{S_{x+1}}{\left[-\dfrac{(4a+h)N\overline{k}}{2h}\right]^{x}} = S_1 + \sum_{m=1}^{x}\left[-\frac{(4a+h)N\overline{k}}{2h}\right]^{-m}\frac{N}{2}\left[\overline{k^m}S_1 + \frac{N\overline{k}}{h}\left(a+\frac{h}{2}\right)\overline{k^{m+1}}\right], \tag{4.68}$$

we find that the left hand side of this equation vanishes in the limit of $x \to \infty$,

$$\begin{aligned}\lim_{x\to\infty}\frac{S_{x+1}}{\left[-\dfrac{(4a+h)N\overline{k}}{2h}\right]^{x}} &= \lim_{x\to\infty}\frac{\sum_{ij}k_i^{x+1}k_j\sigma_{ij}}{\left[-\dfrac{(4a+h)N\overline{k}}{2h}\right]^{x}} \\ &= \left[-\frac{(4a+h)N\overline{k}}{2h}\right]\lim_{x\to\infty}\sum_{ij}\left[-\frac{2hk_i}{(4a+h)N\overline{k}}\right]^{x+1}k_j\sigma_{ij} \\ &= 0\,,\end{aligned} \tag{4.69}$$

where we have used the definition of the variables S_x given in Eq. (4.59). A necessary and sufficient condition for the last equality in Eq. (4.69) to hold is that

$$\forall i : \left|-\frac{2hk_i}{(4a+h)N\overline{k}}\right| < 1 \implies \forall i : k_i < \frac{(4a+h)N\overline{k}}{2h}\,, \tag{4.70}$$

which is generally true and always true for $h > 0$ and $\overline{k} \geq 2$. Thus, in the $x \to \infty$ limit, we can equate the right hand side of Eq. (4.68) to zero,

$$\begin{aligned}&S_1 + \left(\sum_{m=1}^{\infty}\left[-\frac{(4a+h)N\overline{k}}{2h}\right]^{-m}\frac{N}{2}\overline{k^m}\right)S_1 \\ &+ \left(\sum_{m=1}^{\infty}\left[-\frac{(4a+h)N\overline{k}}{2h}\right]^{-m}\frac{N^2\overline{k}}{2h}\left(a+\frac{h}{2}\right)\overline{k^{m+1}}\right) = 0\,,\end{aligned} \tag{4.71}$$

and find, in this way, a solution for S_1,

$$S_1 = \frac{-\dfrac{N^2\overline{k}}{2h}\left(a+\dfrac{h}{2}\right)\displaystyle\sum_{m=1}^{\infty}\left[\frac{-2h}{(4a+h)N\overline{k}}\right]^{m}\overline{k^{m+1}}}{1+\dfrac{N}{2}\displaystyle\sum_{m=1}^{\infty}\left[\frac{-2h}{(4a+h)N\overline{k}}\right]^{m}\overline{k^m}}\,. \tag{4.72}$$

Regarding the sums in Eq. (4.72), we can use the sum of the geometric series

$$\sum_{m=1}^{\infty} A^m \overline{k^{m+z}} = \overline{k^z \sum_{m=1}^{\infty} A^m k^m} = \overline{\frac{Ak^{z+1}}{1-Ak}}\,, \quad \text{if} \quad |Ak| < 1\,, \tag{4.73}$$

where the condition of convergence is exactly the same as presented before in Eq. (4.70), and thus generally true and always true for $h > 0$ and $\overline{k} \geq 2$. In this way, applying the result (4.73) to Eq. (4.72) we have

$$\begin{aligned} S_1 &= \frac{N^2\overline{k}\left(a+\frac{h}{2}\right)\overline{\left(\frac{k^2}{1+\frac{2hk}{(4a+h)N\overline{k}}}\right)}}{(4a+h)N\overline{k} - hN\overline{\left(\frac{k}{1+\frac{2hk}{(4a+h)N\overline{k}}}\right)}} \\ &= \frac{N^2\overline{k}\left(a+\frac{h}{2}\right)(4a+h)\overline{\left(\frac{k^2}{(4a+h)N\overline{k}+2hk}\right)}}{4a+h-\frac{h}{\overline{k}}\overline{\left(\frac{(4a+h)N\overline{k}k}{(4a+h)N\overline{k}+2hk}\right)}}\,, \end{aligned} \tag{4.74}$$

where the denominator can be rewritten as

$$\begin{aligned} 4a+h-\frac{h}{\overline{k}}\overline{\left(\frac{(4a+h)N\overline{k}k}{(4a+h)N\overline{k}+2hk}\right)} &= \\ &= 4a+\frac{h}{\overline{k}}\overline{\frac{[(4a+h)N\overline{k}+2hk]\overline{k}-(4a+h)N\overline{k}k}{(4a+h)N\overline{k}+2hk}} \\ &= 4a+\frac{h}{\overline{k}}\overline{\frac{[(4a+h)N\overline{k}+2hk](\overline{k}-k)+2hk^2}{(4a+h)N\overline{k}+2hk}} \\ &= 4a+\frac{h}{\overline{k}}\overline{(\overline{k}-k)}+\frac{2h^2}{\overline{k}}\overline{\left(\frac{k^2}{(4a+h)N\overline{k}+2hk}\right)} \\ &= 4a+\frac{2h^2}{\overline{k}}\overline{\left(\frac{k^2}{(4a+h)N\overline{k}+2hk}\right)}\,, \end{aligned} \tag{4.75}$$

thereby finding a final expression for S_1,

$$S_1 = \frac{N^2\overline{k}\left(a+\frac{h}{2}\right)(4a+h)\overline{\left(\frac{k^2}{(4a+h)N\overline{k}+2hk}\right)}}{4a+\frac{2h^2}{\overline{k}}\overline{\left(\frac{k^2}{(4a+h)N\overline{k}+2hk}\right)}}\,. \tag{4.76}$$

If we now go back to the equation for the steady state variance $\sigma^2_{st}[n]$ as a function of S_0, Eq. (4.60), and we use Eq. (4.63) to find an expression for S_0 as a function of S_1,

$$S_0 = \frac{N\overline{k}\left(a+\frac{h}{2}\right)+\frac{h}{\overline{k}}\left(1-\frac{2}{N}\right)S_1}{4a+h}, \tag{4.77}$$

then we can write an equation for the steady state variance as a function of S_1,

$$\sigma^2_{st}[n] = \frac{N}{4}\left[1+\frac{2h\left(1-\frac{1}{N}\right)}{4a+h}+\left(N-3+\frac{2}{N}\right)\left(\frac{h}{\overline{k}}\right)^2\frac{2S_1}{N^2\left(a+\frac{h}{2}\right)(4a+h)}\right]. \tag{4.78}$$

Finally, introducing here what we found for S_1 in Eq. (4.76), we arrive to the final expression for the steady state variance of the global variable n as presented in the main text of the chapter,

$$\sigma^2_{st}[n] = \frac{N}{4}\left[1+\frac{2h\left(1-\frac{1}{N}\right)}{4a+h}+\frac{\left(N-3+\frac{2}{N}\right)\left(\frac{h^2}{\overline{k}}\right)\overline{\left(\frac{k^2}{(4a+h)N\overline{k}+2hk}\right)}}{2a+\left(\frac{h^2}{\overline{k}}\right)\overline{\left(\frac{k^2}{(4a+h)N\overline{k}+2hk}\right)}}\right]. \tag{4.79}$$

4.E

Asymptotic approximations for the variance of n

We develop here a first-order approximation for the steady state variance of n with respect to the system size N. Given the dependence of the result of this approximation on the relationship between the system size N and the noise parameter a, we are forced to consider two different asymptotic approximation regimes: one for small a [corresponding to Eq. (4.16) in the main text of the chapter] and the other for large a [corresponding to Eq. (4.17) in the main text of the chapter].

Let us start by noticing that the structural constraint imposed by the annealed approximation for uncorrelated networks on the degrees of the network,

$k_i < \sqrt{N\overline{k}}$, allows us to write Eq. (4.79) as

$$\sigma_{st}^2[n] =$$

$$= \frac{N}{4}\left[1 + \frac{2h\left(1-\frac{1}{N}\right)}{4a+h} + \left(N-3+\frac{2}{N}\right)\frac{\left(\frac{h^2}{\overline{k}}\right)\overline{\left(\frac{k^2}{(4a+h)N\overline{k}\left(1+\mathcal{O}\left(N^{-1/2}\right)\right)}\right)}}{2a+\left(\frac{h^2}{\overline{k}}\right)\overline{\left(\frac{k^2}{(4a+h)N\overline{k}\left(1+\mathcal{O}\left(N^{-1/2}\right)\right)}\right)}}\right]. \tag{4.80}$$

In this way, we notice that, depending on the order of the product aN, the approximation of the third term in Eq. (4.80) will lead to different results. In particular, when the noise parameter a is of order $\mathcal{O}(N^{-1})$ or smaller, then the product aN is, at most, of order $\mathcal{O}(N^0)$, and we can continue with the approximation as

$$\sigma_{st}^2[n] =$$

$$= \frac{N}{4}\left[1 + \frac{2h\left(1-\frac{1}{N}\right)}{4a+h} + \left(N-3+\frac{2}{N}\right)\left(\frac{\left(\frac{h^2}{\overline{k}}\right)\left(\frac{\overline{k^2}}{(4a+h)N\overline{k}}\right)}{2a+\left(\frac{h^2}{\overline{k}}\right)\left(\frac{\overline{k^2}}{(4a+h)N\overline{k}}\right)} + \mathcal{O}(N^{-1/2})\right)\right]$$

$$= \frac{N}{4}\left[1 + 2\left(1-\frac{1}{N}\right) + \left(N-3+\frac{2}{N}\right)\left(\frac{h\left(\frac{\overline{k^2}}{\overline{k}^2}\right)}{2aN+h\left(\frac{\overline{k^2}}{\overline{k}^2}\right)} + \mathcal{O}(N^{-1/2})\right)\right], \tag{4.81}$$

which, to the first order in N, becomes

$$\sigma_{st}^2[n] = \frac{N}{4}\left[N\left(\frac{h\left(\frac{\overline{k^2}}{\overline{k}^2}\right)}{2aN+h\left(\frac{\overline{k^2}}{\overline{k}^2}\right)} + \mathcal{O}(N^{-1/2})\right)\right]. \tag{4.82}$$

Using now the definition of the variance of the degree distribution, $\sigma_k^2 = \overline{k^2} - \overline{k}^2$, we find the approximation presented in the main text of the chapter for the steady state variance of n for small a and to the first order in N,

$$\sigma_{st}^2[n] = \frac{N^2}{4}\left[\frac{h\left(\frac{\sigma_k^2}{\overline{k}^2}+1\right)}{2aN+h\left(\frac{\sigma_k^2}{\overline{k}^2}+1\right)}\right] + \mathcal{O}(N^{3/2})\,. \tag{4.83}$$

Note that the remaining terms are *at most* of order $\mathcal{O}(N^{3/2})$.

On the contrary, when a is of order $\mathcal{O}(N^0)$ or larger, then the product aN is, at least, of order $\mathcal{O}(N)$, and we can approximate Eq. (4.80) as

$$\begin{aligned}
&\sigma_{st}^2[n] = \\
&= \frac{N}{4}\left[1+\frac{2h\left(1-\frac{1}{N}\right)}{4a+h}+\left(N-3+\frac{2}{N}\right)\left(\frac{\left(\frac{h^2}{\overline{k}}\right)\left(\frac{\overline{k^2}}{(4a+h)N\overline{k}}\right)}{2a+\left(\frac{h^2}{\overline{k}}\right)\left(\frac{\overline{k^2}}{(4a+h)N\overline{k}}\right)}+\mathcal{O}(N^{-3/2})\right)\right] \\
&= \frac{N}{4}\left[1+\frac{2h\left(1-\frac{1}{N}\right)}{4a+h}+\left(N-3+\frac{2}{N}\right)\left(\frac{h^2\left(\frac{\overline{k^2}}{\overline{k}^2}\right)}{2a(4a+h)N+h^2\left(\frac{\overline{k^2}}{\overline{k}^2}\right)}+\mathcal{O}(N^{-3/2})\right)\right] \\
&= \frac{N}{4}\left[1+\frac{2h\left(1-\frac{1}{N}\right)}{4a+h}+\left(N-3+\frac{2}{N}\right)\left(\frac{h^2\left(\frac{\overline{k^2}}{\overline{k}^2}\right)}{2a(4a+h)N}+\mathcal{O}(N^{-3/2})\right)\right].
\end{aligned} \tag{4.84}$$

Note that the remaining terms are now one order of N smaller than in the previous approximation [Eq. (4.81)]. To the first order in N we have

$$\begin{aligned}
\sigma_{st}^2[n] =& \frac{N}{4}\left[1+\frac{2h}{4a+h}+\frac{h^2\left(\frac{\overline{k^2}}{\overline{k}^2}\right)}{2a(4a+h)}+\mathcal{O}(N^{-1/2})\right] \\
=& \frac{N}{4}\left[1+\frac{4ah+h^2\left(\frac{\overline{k^2}-\overline{k}^2+\overline{k}^2}{\overline{k}^2}\right)}{2a(4a+h)}+\mathcal{O}(N^{-1/2})\right],
\end{aligned} \tag{4.85}$$

and, finally, we find the approximation presented in the main text of the chapter for the steady state variance of n for large a and to the first order in N,

$$\sigma_{st}^2[n] = \frac{N}{4}\left[1 + \frac{h}{2a} + \frac{h^2\frac{\sigma_k^2}{\overline{k}^2}}{2a(4a+h)}\right] + \mathcal{O}(N^{1/2})\,, \tag{4.86}$$

where the remaining terms are *at most* of order $\mathcal{O}(N^{1/2})$.

4.F

Critical point approximation

In this appendix, we derive an analytical approximation for the critical point of the bimodal-unimodal transition [Eq. (4.18) in the main text of the chapter], which can be defined as the relationship between the model parameters a and h leading the steady state variance of n to take the value $\sigma_{st}^2[n] = N(N+2)/12$, corresponding to a uniform distribution between 0 and N. In particular, bearing in mind that the critical value a_c of a fully-connected system is of order $\mathcal{O}(N^{-1})$ and that the change due to the network structure appears to be of order $\mathcal{O}(N^0)$ (see Fig. 4.2 in the main text of the chapter), then we can expect the value of the critical point to be still of order $\mathcal{O}(N^{-1})$, and we can therefore use the small a asymptotic approximation in Eq. (4.83),

$$\sigma_{st}^2[n] = \frac{N^2}{4}\left[\frac{h\left(\frac{\sigma_k^2}{\overline{k}^2}+1\right)}{2a_cN + h\left(\frac{\sigma_k^2}{\overline{k}^2}+1\right)}\right] + \mathcal{O}(N^{3/2}) = \frac{N(N+2)}{12}\,. \tag{4.87}$$

The solution of this equation leads, for large N, to the value of the critical point discussed in the main text of the chapter,

$$a_c = \frac{h}{N}\left(\frac{\sigma_k^2}{\overline{k}^2}+1\right) + \mathcal{O}(N^{-3/2})\,, \tag{4.88}$$

consistent with the assumption of a critical value of order $\mathcal{O}(N^{-1})$. Note that assuming, instead, the critical value to be of order $\mathcal{O}(N^0)$, and using therefore the large a asymptotic approximation in Eq. (4.86), leads again to an a_c of order $\mathcal{O}(N^{-1})$, inconsistent with the initial assumption.

4.G

Order parameter: the interface density ρ

We obtain, in this appendix, an analytical expression for the order parameter ρ [Eq. (4.21) in the main text of the chapter]. ρ is defined as the interface density or density of active links, that is, the fraction of links connecting nodes in different states. In terms of the connectivity matrix A_{ij},

$$\rho = \frac{\frac{1}{2}\sum_{ij} A_{ij}[s_i(1-s_j)+(1-s_i)s_j]}{\frac{1}{2}\sum_{ij} A_{ij}} = \frac{\sum_{ij} A_{ij}(s_i+s_j-s_is_j)}{\sum_{ij} A_{ij}}\,, \tag{4.89}$$

and introducing the annealed approximation for uncorrelated networks described in the main text of the chapter [see Eq. (4.10)], we find

$$\rho = \frac{\sum_{ij} \frac{k_ik_j}{N\bar{k}}(s_i+s_j-s_is_j)}{\sum_{ij} \frac{k_ik_j}{N\bar{k}}} = \sum_{ij} \frac{k_ik_j}{\left(N\bar{k}\right)^2}(s_i+s_j-s_is_j)\,. \tag{4.90}$$

Restricting our attention to the steady state average value of Eq. (4.90),

$$\langle\rho\rangle_{st} = \sum_{ij} \frac{k_ik_j}{\left(N\bar{k}\right)^2}\left(\langle s_i\rangle_{st}+\langle s_j\rangle_{st}-\langle s_is_j\rangle_{st}\right), \tag{4.91}$$

we can use the steady state mean solution found before for the individual node variables s_i, $\langle s_i\rangle_{st}=1/2$, and the definition of the covariance matrix in the steady state, $\sigma_{ij}=\langle s_is_j\rangle_{st}-1/4$, in order to write

$$\langle\rho\rangle_{st} = \frac{1}{2} - \frac{2}{\left(N\bar{k}\right)^2}\sum_{ij} k_ik_j\sigma_{ij}\,, \tag{4.92}$$

where we can identify the variable S_1 [see Eq. (4.59)],

$$\langle\rho\rangle_{st} = \frac{1}{2} - \frac{2S_1}{\left(N\bar{k}\right)^2}. \tag{4.93}$$

Finally, reversing the relation (4.78) between the variance of n and the variable S_1, we can write the steady state average interface density ρ in terms of the

variance of n,

$$\langle\rho\rangle_{st} = \frac{1}{2} - \frac{2}{(hN)^2}\left[\frac{(4a+h)(2a+h)}{\left(1-\frac{1}{N}\right)\left(1-\frac{2}{N}\right)}\left(\sigma^2[n]-\frac{N}{4}\right) - \frac{\left(a+\frac{h}{2}\right)}{\left(1-\frac{2}{N}\right)}hN\right], \quad (4.94)$$

as it appears in the main text of the chapter.

4.H

Autocorrelation function of n

We derive here an analytical expression for the steady state autocorrelation function of n [Eqs. (4.23) and (4.24) in the main text of the chapter], defined as

$$K_{st}[n](\tau) = \langle n(t+\tau)n(t)\rangle_{st} - \langle n\rangle_{st}^2\,, \quad (4.95)$$

where τ plays the role of a time-lag. As far as the second point in time, $t+\tau$, is concerned, we assume that the system was at $n(t)$ at time t, and hence we can treat $n(t)$ as an initial condition,

$$K_{st}[n](\tau) = \langle\langle n(t+\tau)|n(t)\rangle n(t)\rangle_{st} - \langle n\rangle_{st}^2\,, \quad (4.96)$$

which, in terms of the individual variables $\{s_i\}$ and taking into account that $\langle n\rangle_{st} = N/2$, can be written as

$$K_{st}[n](\tau) = \sum_{ij}\langle\langle s_i(t+\tau)|\{s_l(t)\}\rangle s_j(t)\rangle_{st} - \frac{N^2}{4}\,. \quad (4.97)$$

We need, therefore, an expression for $\langle s_i(t+\tau)|\{s_l(t)\}\rangle$, which we find by integration of the equation for the temporal evolution of the first-order moments $\langle s_i\rangle$ —obtained by introducing the transition rates of the noisy voter model into Eq. (4.45)—,

$$\frac{d\langle s_i(t+\tau)|\{s_l(t)\}\rangle}{d\tau} = a-(2a+h)\langle s_i(t+\tau)|\{s_l(t)\}\rangle+\frac{h}{N\bar{k}}\sum_m k_m\langle s_m(t+\tau)|\{s_l(t)\}\rangle\,. \quad (4.98)$$

In order to integrate Eq. (4.98), we must first obtain an expression for

$$b(t+\tau) \equiv \frac{h}{N\bar{k}}\sum_m k_m\langle s_m(t+\tau)|\{s_l(t)\}\rangle\,, \quad (4.99)$$

which we can find by multiplying Eq. (4.98) by $hk_i/N\overline{k}$ and summing over i,

$$\frac{d}{d\tau}\left(\frac{h}{N\overline{k}}\sum_i k_i\langle s_i(t+\tau)|\{s_l(t)\}\rangle\right) = \frac{ah}{N\overline{k}}\sum_i k_i - \frac{(2a+h)h}{N\overline{k}}\sum_i k_i\langle s_i(t+\tau)|\{s_l(t)\}\rangle + \left(\frac{h}{N\overline{k}}\right)^2\sum_i k_i\sum_m k_m\langle s_m(t+\tau)|\{s_l(t)\}\rangle\,. \tag{4.100}$$

In this way, we arrive to the differential equation

$$\frac{db(t+\tau)}{d\tau} = ah - (2a+h)b(t+\tau) + hb(t+\tau) = ah - 2ab(t+\tau)\,, \tag{4.101}$$

which has the solution

$$b(t+\tau) = \frac{h}{2}\left(1-e^{-2a\tau}\right) + b(t)e^{-2a\tau}\,, \tag{4.102}$$

depending on the initial condition $b(t)$. Using this expression, we can now integrate Eq. (4.98) for the first-order moments,

$$\frac{d\langle s_i(t+\tau)|\{s_l(t)\}\rangle}{d\tau} = a - (2a+h)\langle s_i(t+\tau)|\{s_l(t)\}\rangle + b(t+\tau)\,, \tag{4.103}$$

which has the general solution

$$\begin{aligned}\langle s_i(t+\tau)|\{s_l(t)\}\rangle &= \frac{\int_0^\tau e^{(2a+h)\tau'}\left[a+b(t+\tau')\right]d\tau' + c_1}{e^{(2a+h)\tau}}\\ &= \frac{\int_0^\tau e^{(2a+h)\tau'}\left[a+\frac{h}{2}\left(1-e^{-2a\tau'}\right)+b(t)e^{-2a\tau'}\right]d\tau' + c_1}{e^{(2a+h)\tau}}\\ &= \frac{\left(a+\frac{h}{2}\right)\int_0^\tau e^{(2a+h)\tau'}d\tau' + \left(b(t)-\frac{h}{2}\right)\int_0^\tau e^{h\tau'}d\tau' + c_1}{e^{(2a+h)\tau}}\\ &= \frac{1}{2}\left(1-e^{-(2a+h)\tau}\right) + \frac{b(t)-\frac{h}{2}}{h}\left(e^{-2a\tau}-e^{-(2a+h)\tau}\right) + c_1e^{-(2a+h)\tau}\,.\end{aligned} \tag{4.104}$$

Applying now the initial condition $\langle s_i(t)|\{s_l(t)\}\rangle = s_i(t)$, we find

$$\langle s_i(t+\tau)|\{s_l(t)\}\rangle = \tfrac{1}{2}\left(1-e^{-(2a+h)\tau}\right) + \tfrac{b(t)-\frac{h}{2}}{h}\left(e^{-2a\tau}-e^{-(2a+h)\tau}\right) + s_i(t)e^{-(2a+h)\tau}\,. \tag{4.105}$$

We are now ready to go back to the autocorrelation function (4.97) and write, in the steady state,

$$\begin{aligned} K_{st}[n](\tau) =& \sum_{ij} \left\langle \frac{1}{2}\left(1-e^{-(2a+h)\tau}\right) s_j(t) \right\rangle_{st} \\ &+ \sum_{ij} \left\langle \frac{b(t)-\frac{h}{2}}{h}\left(e^{-2a\tau}-e^{-(2a+h)\tau}\right) s_j(t) \right\rangle_{st} \\ &+ \sum_{ij} \left\langle s_i(t)s_j(t)e^{-(2a+h)\tau} \right\rangle_{st} - \frac{N^2}{4}\,. \end{aligned} \tag{4.106}$$

Given that we assume the state of the system at t to be our initial condition, $b(t)$ can be written as

$$b(t) = \frac{h}{N\bar{k}} \sum_i k_i \langle s_i(t) | \{s_l(t)\} \rangle = \frac{h}{N\bar{k}} \sum_i k_i s_i(t)\,, \tag{4.107}$$

and thus we have, for the autocorrelation function,

$$\begin{aligned} K_{st}[n](\tau) =& \frac{1}{2}\left(1-e^{-(2a+h)\tau}\right) \sum_{ij} \langle s_j(t)\rangle_{st} \\ &+ \frac{1}{N\bar{k}}\left(e^{-2a\tau}-e^{-(2a+h)\tau}\right) \sum_{ijm} k_m \langle s_m(t)s_j(t)\rangle_{st} \\ &- \frac{1}{2}\left(e^{-2a\tau}-e^{-(2a+h)\tau}\right) \sum_{ij} \langle s_j(t)\rangle_{st} + e^{-(2a+h)\tau} \sum_{ij} \langle s_i(t)s_j(t)\rangle_{st} \\ &- \frac{N^2}{4}\,. \end{aligned} \tag{4.108}$$

Using now the value found before for the steady state solution of the first-order moments, $\langle s_i \rangle_{st} = 1/2$, and the definition of the covariance matrix in the steady state, $\sigma_{ij} = \langle s_i s_j \rangle_{st} - \langle s_i \rangle_{st}^2 = \langle s_i s_j \rangle_{st} - 1/4$, we find

$$\begin{aligned} K_{st}[n](\tau) =& -e^{-2a\tau}\frac{N^2}{4} + \frac{1}{\bar{k}}\left(e^{-2a\tau}-e^{-(2a+h)\tau}\right) \sum_{jm} k_m \left(\sigma_{mj}+\frac{1}{4}\right) \\ &+ e^{-(2a+h)\tau} \sum_{ij} \left(\sigma_{ij}+\frac{1}{4}\right)\,. \end{aligned} \tag{4.109}$$

Finally, identifying in the previous equation the variance of n and the variable S_1 [see Eq. (4.59)], and reordering terms according to their exponential decay, we

find the expression for the autocorrelation function of n discussed in the main text of the chapter,

$$K_{st}[n](\tau) = \left(\sigma^2[n] - \frac{S_1}{\overline{k}}\right) e^{-(2a+h)\tau} + \frac{S_1}{\overline{k}} e^{-2a\tau} \,. \tag{4.110}$$

The definition of the variable S_1 given in the main text of the chapter, as a function of the variance of n, can be directly obtained by reversing Eq. (4.78).

4.I

Order parameter for a fully connected network

As an example of topology where local effects are absent, we show in Fig. 4.9 both numerical and analytical results for the case of a fully-connected network. As we can observe, our approximation successfully fits the results in this case, suggesting that the origin of the discrepancy observed for intermediate values of a in Fig. 4.7 lies in the annealed network approximation, when we replace the original network by a weighted fully-connected topology, and thus we lose track of all local effects.

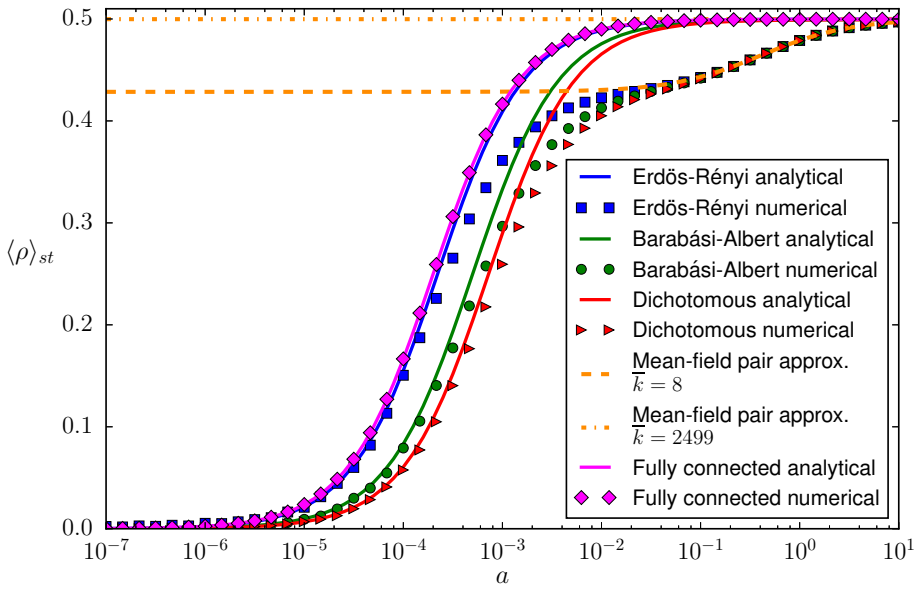

Figure 4.9: Steady state of the average interface density as a function of the noise parameter a in a linear-logarithmic scale and for three different types of networks with mean degree $\overline{k} = 8$: Erdös-Rényi random network, Barabási-Albert scale-free network and dichotomous network. A fully connected topology is also included for comparison. Symbols: Numerical results (averages over 20 networks, 10 realizations per network and 50000 time steps per realization). Solid lines: Analytical results [see Eq. (4.94)]. Dashed line: Mean-field pair-approximation (see Diakonova et al., 2015) for a mean degree $\overline{k} = 8$. Dash-dotted line: Mean-field pair-approximation for a mean degree $\overline{k} = 2499$. The interaction parameter is fixed as $h = 1$ and the system size as $N = 2500$.

Language competition

CHAPTER 5

Link-state dynamics in a coevolving network

Inspired by language competition processes where both the language used in the interactions between speakers and the topological structure of those interactions can evolve in time and affect each other, we propose in this chapter a coevolving network model with link-state dynamics. Along the lines of the model studied by Fernández-Gracia et al. (2012), we consider links with binary, equivalent states —representing the use of two socially equivalent languages— updated according to the majority rule: links adopt the state of the majority of their neighboring links in the network. Additionally, we define a rewiring mechanism capturing the fact that, when a speaker is uncomfortable with the language used on a given interaction, she can either try to change that language or simply stop this interaction and start a new one in her preferred language. In other words, a link that is in a local minority can be rewired to a randomly chosen node while changing its state to conform to the local majority of the rewiring node.

While large systems evolving under the majority rule alone always fall into disordered topological traps composed by frustrated links (whose state conforms to the local but not to the global majority), any amount of rewiring is able to drive the network to complete order, by relinking frustrated links and so releasing the system from traps. However, depending on the ratio between the probability of a majority rule updating and that of a rewiring event, the system evolves towards different absorbing configurations: either a one-component network with all links in the same state —extinction of one of the languages— or a network fragmented in two components with opposite states —survival of both languages in completely segregated communities—. In both cases, the described dynamics leads always to the disappearance of the bilingual speakers. While for finite sys-

tems and small rewiring rates we find a region of bistability between fragmented and non-fragmented absorbing states, larger rewiring rates lead always to the fragmentation of the network into two similar size components with different link states. By means of a scaling analysis we show that the bistability region vanishes as the system size is increased, and thus fragmentation is the only possible scenario for large coevolving systems. We also show that a mean-field approach is able to describe the ordering of the system and its average time of convergence to the final ordered state for large rewiring values.

In Section 5.1 we define the rewiring mechanism which, coupled with the majority rule for link states, leads to a coevolving model. We also present in this section a schematic review of the main results obtained with the majority rule for link states in static topologies and some quantities introduced for its characterization. In Section 5.2 we describe the final states obtained with the coevolving model and we characterize the observed fragmentation transition. A study of the time evolution of the system is presented in Section 5.3, including a description of the trajectories in phase space, a mean-field approximation for the order parameter, and an analysis of the times of convergence to the final ordered state. Finally, Section 5.4 contains a discussion summary.

5.1

The Model

We consider an initially connected Erdös-Rényi random network composed by a fixed number of nodes N and with a fixed mean degree $\mu \equiv \langle k \rangle$. The state of each link ℓ is characterized by a binary variable S_l which can take two equivalent or symmetrical values, for example, A and B. Link states are initially distributed with uniform probability. At each time step, a link ℓ between nodes i and j is chosen at random. Then, with probability p a rewiring event is attempted (see Fig. 5.1 for a schematic illustration of the dynamics): one of the two nodes at the ends of ℓ, for example i, is chosen at random and

1. if S_l is different from the state of the majority of links attached to i, then the link ℓ is disconnected from the opposite end, j, and reconnected to another node, k, chosen at random, and also its state S_l is switched to comply with the local majority around node i;

2. otherwise, nothing happens.

   With the complementary probability, $1-p$, the majority rule is applied: the chosen link, ℓ, adopts the state of the majority of its neighboring links, i.e.,

those links connected to the ends of ℓ (nodes i and j). In case of a tie, ℓ switches state with probability 1/2. Finally, time is increased by $1/N$, so that for each node, on average, the state of one of its relationships is updated per unit time. In this manner, the time scale of the process for each agent becomes independent of system size for constant degree distribution.

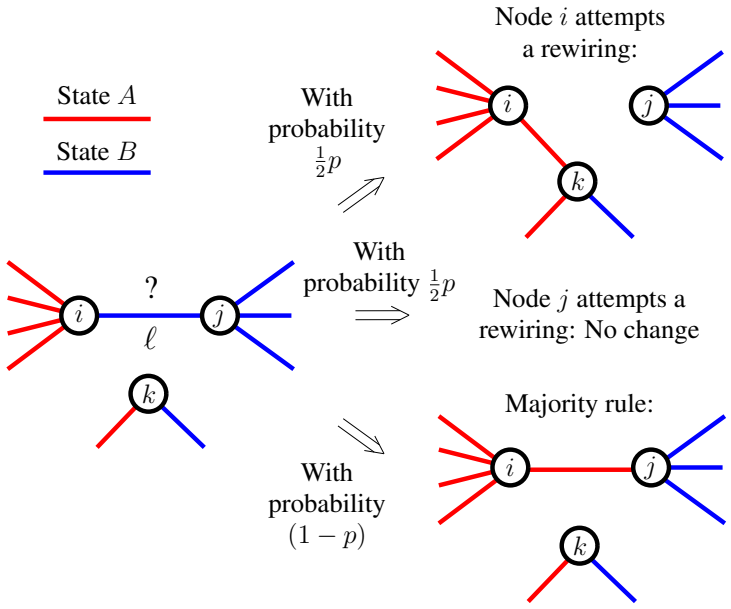

Figure 5.1: Schematic illustration of the dynamics for both a successful and a failed rewiring attempt and the application of the majority rule.

The rewiring mechanism mimics the fact that, when a speaker is uncomfortable with the language used in her interaction with other speaker, one of her possibilities is to stop this relationship and start a new one in her preferred language with any other individual. The majority rule mechanism captures the fact that the language spoken in a given interaction tends to be the one most predominantly used by the interacting individuals, that is, the one they use more frequently in their conversations with other people. In this way, agents tend to avoid the cognitive cost or effort associated with switching between several languages (Meuter and Allport, 1999; Jackson et al., 2001; Abutalebi and Green, 2007; Moritz-Gasser and Duffau, 2009). The rewiring probability p measures the speed at which the network evolves, compared to the propagation of link states. It is, therefore, a measure of the plasticity of the topology. When p is zero the network is static and only the majority rule dynamics takes place (as studied by

Fernández-Gracia et al., 2012), while in the opposite situation, $p = 1$, there is only rewiring.

The implementation of the majority rule that we use here is equivalent to the zero-temperature Glauber dynamics [1], which has been extensively studied in the context of spin systems in fixed networks and from a node states perspective. These studies show that, in Erdös-Rény random networks, most realizations of the dynamics arrive to a fully ordered, consensual state in a characteristic time which scales logarithmically with system size (Castellano et al., 2005; Baek et al., 2012). However, a very small number of runs (around a 0.02% for $N = 10^3$ and $\langle k \rangle = 10$) end up in a disordered absorbing state, which can be frozen or dynamically trapped (Castellano et al., 2005). The same disordered absorbing configurations have also been found by Fernández-Gracia et al. (2012) with a prototype model of link-state majority rule dynamics. Nevertheless, the probabilities are reversed: the frozen and dynamically trapped configurations (see Fig. 5.2 for schematic examples) are the predominant ones in a link-based dynamics, while full order is only reached in very small and highly connected networks.

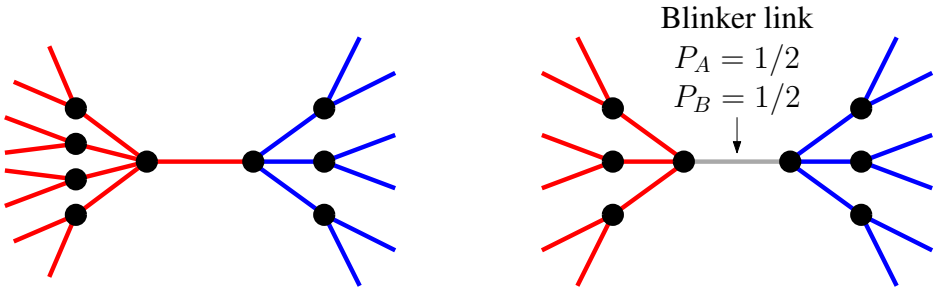

(a) Frozen disordered configuration.

(b) Dynamical trap based on a blinker link which keeps changing state forever with probability 1/2.

Figure 5.2: Schematic illustration of the disordered configurations found with a majority rule dynamics on link states with no rewiring ($p = 0$).

In order to characterize the system at different times it is useful to consider the *density of nodal interfaces* ρ as an order parameter (Fernández-Gracia et al., 2012), defined as the fraction of pairs of connected links that are in different states. If k_i is the degree of node i, and $k_i^{A/B}$ is the number of A/B-links connected to

[1] Different implementations are possible, for example, by varying the probability to switch states in case of tie.

node i (with obviously $k_i = k_i^A + k_i^B$), then ρ is calculated as:

$$\rho = \frac{\sum_{i=1}^{N} k_i^A \, k_i^B}{\sum_{i=1}^{N} k_i(k_i - 1)/2} \, . \tag{5.1}$$

The density ρ is zero only when all connected links share the same state and it takes the value $\rho = 1/2$ for a random distribution of states (as it is the case in our initial condition), thus it is a measure of the local order in the system. Note that complete order, $\rho = 0$, is achieved for both connected consensual configurations, where all links are in the same state, and configurations where the network is fragmented in a set of disconnected components, each formed by links with the same state. In both cases complete order is identified with absorbing configurations, where the system can no longer evolve. In terms of the node-equivalent graph, the line-graph, the order parameter ρ becomes the *density of active links*, i.e., the fraction of links of the line-graph connecting nodes with different states.

5.2

Final states

In order to explore how the coevolution of link states and network topology affects the final state of the system we run numerical simulations of the dynamics described above. The system evolves until the network reaches a final configuration that strongly depends on the system size N and the rewiring probability p. The case $p = 0$ corresponds to a static network situation, analyzed by Fernández-Gracia et al. (2012). In this case, system sizes larger than $N = 500$ lead to disordered final states represented by network configurations composed by several interconnected clusters of type A and B links. A link that connects two clusters is either frozen, because it is in the local majority, or switching *ad infinitum* between states A and B ("blinking"), because it has the same number of neighboring links in each state. Therefore, we refer to these as disordered configurations ($\rho > 0$) that are either frozen or dynamically trapped, respectively (see Fig. 5.2). For $p > 0$ the network always reaches an absorbing ordered configuration that can be, either a one-component network with all links sharing the same state, or a fragmented network consisting of two large disconnected components of size similar to $N/2$ and in different states [2]. We remark that all links inside each component are in the same state, thus the order parameter ρ equals zero, as in the non-fragmented case. The behavior of ρ for different values of p is shown in

[2] A few disconnected nodes can also be occasionally found.

Fig. 5.3, both as an average over different realizations [Fig. 5.3(b)] and as single trajectories [Fig. 5.3(a)]. For $p = 0$ almost every realization reaches a plateau or stationary value of $\rho > 0$ [see upper panel in Fig. 5.3(a)]. For any $p > 0$ every run reaches an ordered absorbing state with $\rho = 0$ [see middle and lower panels in Fig. 5.3(a)]. However, for small values of p we observe a distinction between two groups of realizations, one ordering much faster than the other [see middle panel in Fig. 5.3(a)]. These different time scales will be discussed in Section 5.3.

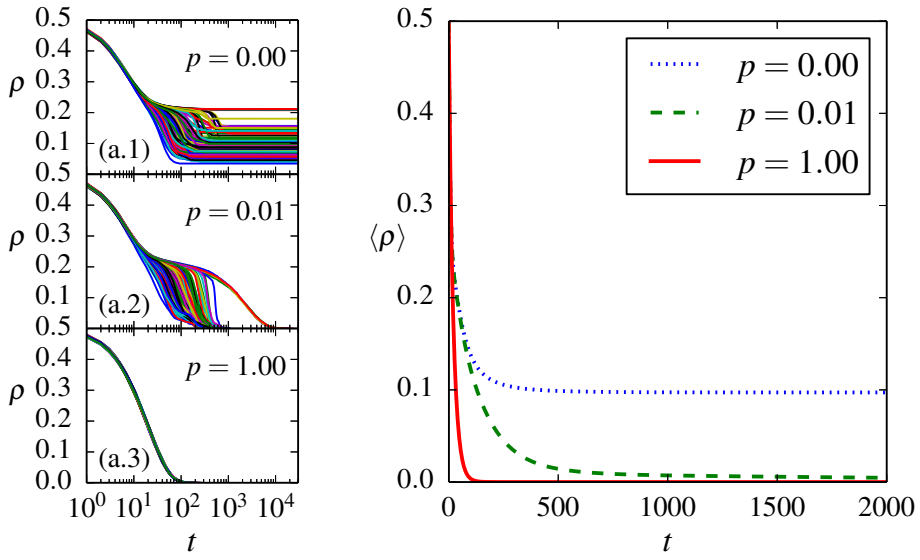

(a) Density of nodal interfaces ρ for 100 individual realizations in a semilogarithmic scale.

(b) Average density of nodal interfaces $\langle\rho\rangle$ over 10000 realizations.

Figure 5.3: Behavior of the order parameter for a system with $N = 2000$ and $\langle k\rangle = 10$. The time interval shown has been chosen for the sake of clarity; actually, the runs for $p = 0.01$ do not reach zero until $t \approx 30000$ while the ones for $p = 1.00$ are zero from $t \approx 350$.

Fragmentation transition in finite systems

We study here three relevant quantities characterizing how the network evolution affects the likelihood and the properties of the two possible outcomes described above, one component or fragmentation in two components. These

quantities are the probability P_1 that the final network is not fragmented, i.e, that it settles in one component, the relative size s_L of the largest network component and the magnitude σ_{s_L} of its associated fluctuations across different realizations.

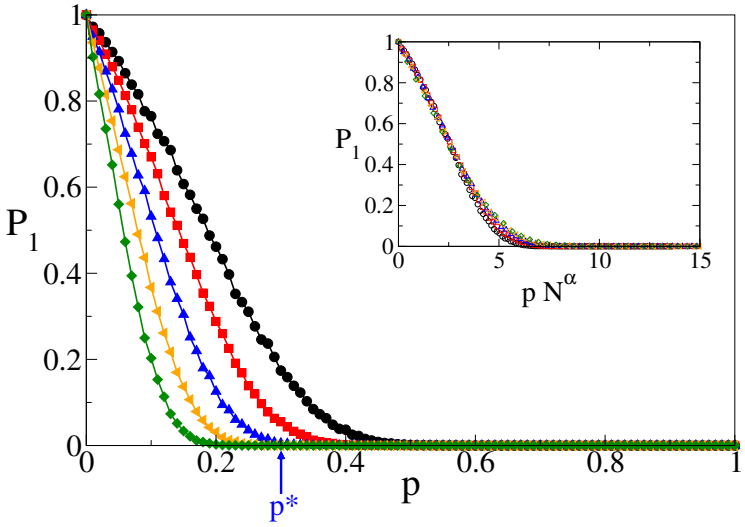

Figure 5.4: Probability P_1 that the system ends in a single network component as a function of the rewiring probability p, for networks of mean degree $\mu = 10$ and size $N = 500$ (circles), $N = 1000$ (squares), $N = 2000$ (triangles up), $N = 4000$ (triangles left) and $N = 8000$ (diamonds). 10000 runs were used to estimate P_1, starting from an Erdös-Rényi network with random initial conditions. The limit of the region of bistability, p^*, is shown for the size $N = 2000$. Note that $\forall p \geq p^*$, $P_1(p) < 1/N$. Inset: Curves collapse when p is rescaled by N^α, with $\alpha = 0.42$.

In Fig. 5.4 we show P_1 as a function of p, calculated as the fraction of simulation runs that ended up in a single component. We observe that $P_1 = 1$ only for $p = 0$, then it decreases continuously between $p = 0$ and a certain value $p = p^*$ and it remains always smaller than $1/N$ for $p \geq p^*$. This defines three regimes regarding p: one point at $p = 0$ where the system is always connected, a region of bistability in $0 < p < p^*$ where the system can both stay connected in one piece or break into disconnected components, and a fragmented region for $p \geq p^*$ where the network always splits apart.

This result is consistent with the behavior of the average value of s_L over many realizations (see Fig. 5.5), which decreases from $\langle s_L \rangle = 1$ for $p = 0$ to $\langle s_L \rangle \simeq 0.5$ for large p. As shown in Fig. 5.6, the standard deviation of s_L (σ_{s_L}) has its maximum at a value $p_{\max}$ for which P_1 is approximately 0.5, that is, where fragmented and non-fragmented realizations are equally likely. The peak in σ_{s_L} indicates a broad distribution of possible largest component sizes in that region

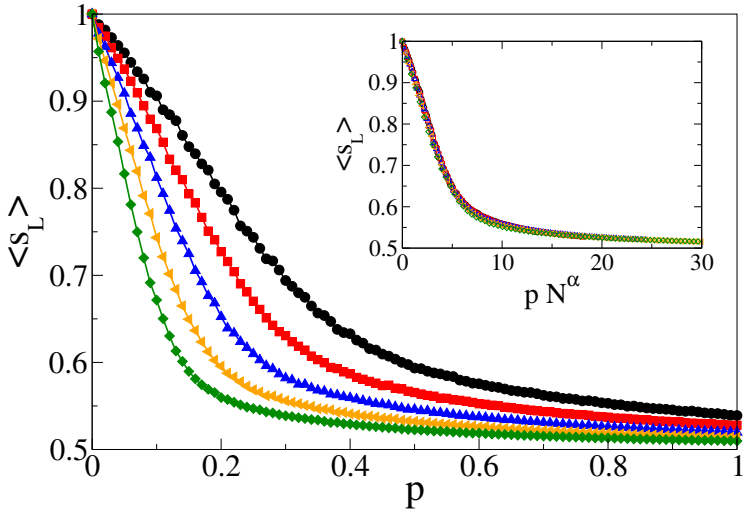

Figure 5.5: Average relative size $\langle s_L \rangle$ of the largest network component as a function of p, and for the same network sizes as in Fig. 5.4. s_L is defined as the fraction of nodes included in the largest connected component. Inset: As in Fig. 5.4, p is rescaled by N^{α}, making the curves collapse to one.

and thus $p_{\max}$ can be used as a footprint of the transition point. This broad distribution can also be seen in Fig. 5.7, where we present a color-map of the fraction of runs that ended up in a given relative size s_L of the largest network component for a network of $N = 2000$ nodes. For the sake of clarity we also present in Fig. 5.8 histograms of network relative sizes s (not only the largest) for four different values of p. We note that the maximum of σ_{s_L} occurs around $p \approx 0.1$ (see Fig. 5.6), which corresponds in the color-map to a distribution of s_L that has a peak at $s_L = 1$ (one component) and a broad distribution corresponding to fragmented cases with $0.5 \leq s_L \leq 0.875$. This division into fragmented and non-fragmented runs can also be clearly observed in the histogram corresponding to $p = 0.1$ [see upper right panel in Fig. 5.8].

Interestingly, a common feature of $P_1(p)$, $s_L(p)$ and $\sigma_s(p)$ curves is that they are shifted to smaller values of p as the system size N increases, and thus the range of p for which there is bistability of fragmented and non-fragmented outcomes seems to vanish in the thermodynamic limit, i.e., $p*$ tends to zero as size is increased. This shifting behavior also points at the fact that the transition point $p_{\max}$ appears to tend to zero in the infinite size limit. A dependence of the transition point with the system size, in a way that it tends to zero in the infinite size limit, has been shown to be the case in several opinion dynamics models (Toral and Tessone, 2007). Such systems, as it is the case here, do not display a

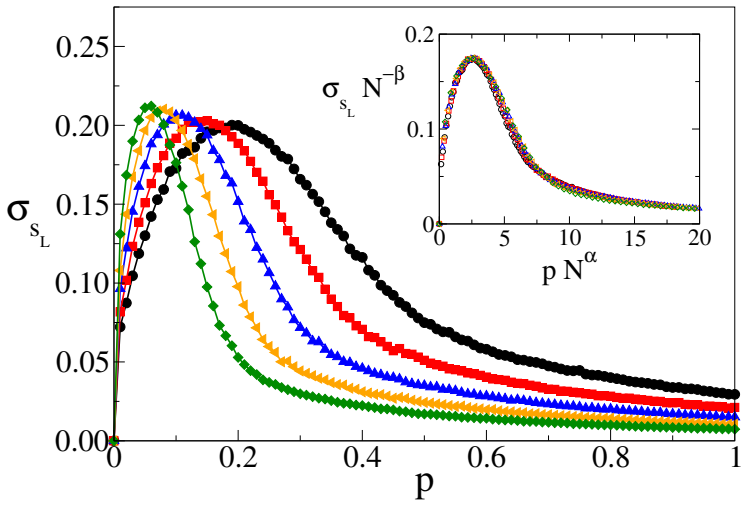

Figure 5.6: Standard deviation σ_{s_L} of the relative size s_L of the largest network component for the same system sizes N as in Fig. 5.4. σ_{s_L} is a measure of the magnitude of the fluctuations in the final size of the largest network component across different realizations of the dynamics. Inset: Collapse of all curves by rescaling p by N^{α} and σ_{s_L} by $N^{-\beta}$, with $\alpha = 0.42$ and $\beta = 0.022$.

typical phase transition in the thermodynamic limit with a well defined critical point and its associated critical exponents, divergences (in case of a continuous, second order phase transition) or discontinuities (in case of a first order phase transition). However, for any finite system a transition point can be clearly defined as separating two different behavioral regimes.

To gain an insight about the $N \to \infty$ behavior, we perform a finite-size scaling analysis by assuming that P_1, s_L and σ_{s_L} are functions of the variable $x \equiv p\,N^{\alpha}$:

$$\begin{aligned} P_1(p,N) &= P_1(p\,N^{\alpha})\,, \\ s_L(p,N) &= s_L(p\,N^{\alpha})\,, \\ \sigma_{s_L}(p,N) &= N^{\beta}\sigma_{s_L}(p\,N^{\alpha})\,. \end{aligned} \tag{5.2}$$

The values of the exponents α and β should be such that the curves for different sizes collapse into a single curve. Therefore, the location of the peak in all $\sigma_{s_L}(p)$ curves of Fig. 5.6 should scale as $p_{\max} \sim N^{-\alpha}$. By fitting a power-law function to the plot $p_{\max}$ as a function of N we found $\alpha \simeq 0.42$. In the insets of Figs. 5.4, 5.5 and 5.6 we observe the collapse for different network sizes when magnitudes are plotted versus the rescaled variable x (rescaling also the y-axis by $N^{-\beta}$ in the case of σ_{s_L}). This scaling analysis shows that, in the thermodynamic limit, the

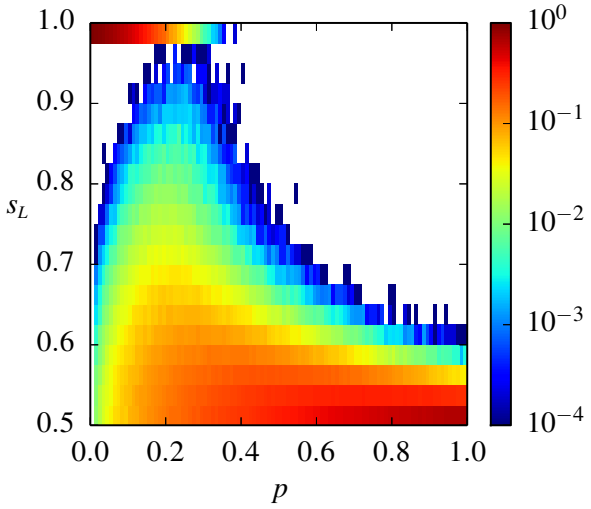

Figure 5.7: Color-map of the fraction of runs ending in a given relative size of the largest network component s_L for $N = 2000$, $\langle k \rangle = 10$ and 10000 runs starting from random initial conditions. Note the logarithmic color scale, with white corresponding to no run ending in that relative size.

network would break apart for any finite value of $p > 0$. This might be related to the fact that when the system evolves under the majority rule alone, it always gets trapped in disordered configurations (in the $N \to \infty$ limit). Then, it seems that even a very small rewiring rate is enough to remove the system from traps, but at the cost of breaking the network apart. However, as we will show in the next section, the time needed for the fragmentation to occur diverges with system size. A deeper understanding of this phenomenon can be achieved by studying stochastic trajectories of single realizations.

5.3

Time evolution

We are interested in quantifying the evolution of the system towards the final states described above. In Fig. 5.9 we plot the survival probability $P_s(t)$, i.e, the probability that a realization did not reach the ordered state ($\rho = 0$) up to time t.

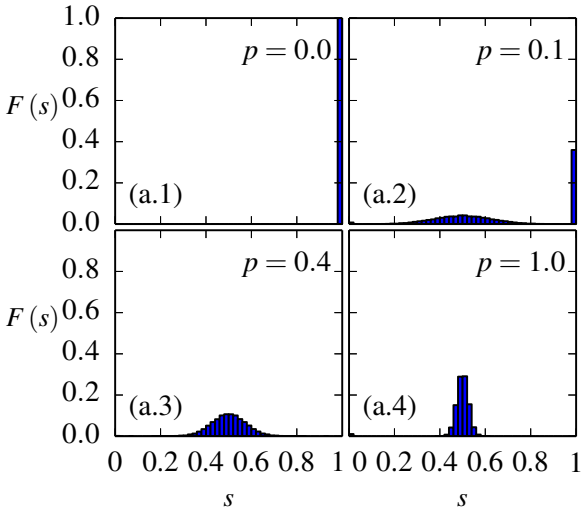

Figure 5.8: Histogram of network relative sizes for four different probabilities of rewiring p, for $N = 2000$, $\langle k \rangle = 10$ and 10000 runs starting from random initial conditions.

When $p = 0$ we have $P_s = 1$ for all times, meaning that all realizations (except for a few runs with the smallest size $N = 500$, as reported by Fernández-Gracia et al., 2012) fall into a disordered configuration characterized by a constant value of $\rho > 0$, as we shall discussed in detail in the next section. For $p = 0.01$, $p = 0.05$ and $p = 0.10$ [panels **(a)**, **(b)** and **(c)**, respectively] we observe that P_s experiences two decays at very different time scales, revealing the existence of two different ordering mechanisms. As we will explain, the first decay from $P_s = 1$ to a plateau corresponds to the ordering of non-fragmented realizations, while the second decay from the plateau to zero is due to the ordering of fragmented runs. Take, for instance, $p = 0.01$ and $N = 8000$. We observe in Fig. 5.4 that the fraction of runs ending in one component is $P_1 \simeq 0.9$. We interpret that it is the arrival of this 90% of runs to a one-component absorbing state with $\rho = 0$ which produces the first decay of the survival probability to $P_s \simeq 0.1$ around a time $t \simeq 10^3$, as can be observed in panel **(a)** of Fig. 5.9. The remaining fraction $P_s \simeq 0.1$ that survive lead to the plateau that lasts up to the second decay around $t \simeq 10^4$, when they arrive to a fragmented absorbing state, again with $\rho = 0$. Note also that both decay times decrease for increasing p, while the height of the plateau rises (P_1 increases). In the $p = 0.30$ case [panel **(d)** of Fig. 5.9] the first decay of P_s is only observed for small systems, since for larger ones most

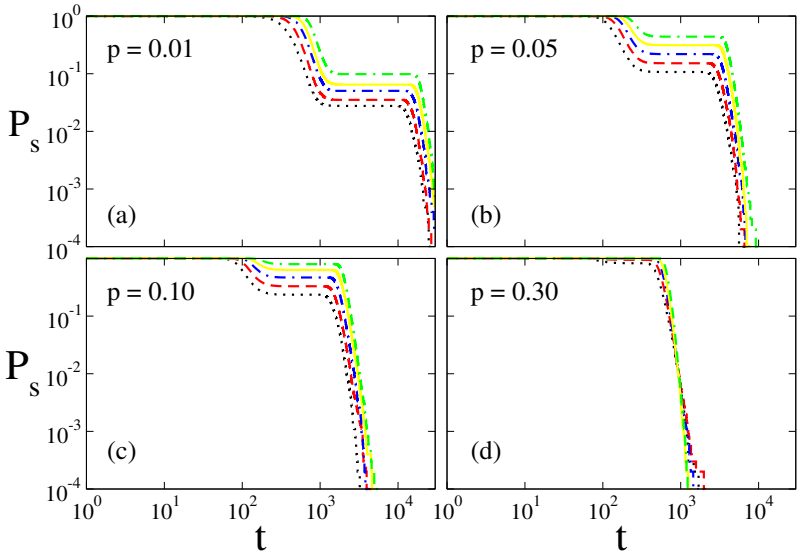

Figure 5.9: Time evolution of the survival probability P_s for different values of p and networks of size $N = 500$, 1000, 2000, 4000 and 8000 (curves from bottom to top and, respectively, dotted, dashed, dash-dotted, solid and dash-dash-dotted). Averages are over 10^4 independent runs.

realizations end up with a fragmented network (see Fig.5.4). This picture also holds for larger values of p.

Description of trajectories in phase space

In order to gain an insight about the fragmentation phenomenon, we investigate in this subsection individual trajectories of the system on the $m - \rho$ plane, where m is the link magnetization (Vazquez and Eguíluz, 2008; Vazquez et al., 2008), the difference between the fractions of A and B links,

$$m = \frac{\sum_{i=1}^{N} \left(k_i^A - k_i^B\right)}{\sum_{i=1}^{N} k_i} \,. \tag{5.3}$$

In Fig. 5.10 we display typical trajectories of the system for a network of $N = 2000$ nodes and values of the rewiring probability $p = 0$, 0.01, 0.1 and 0.5. Trajectories start at $(m, \rho) \simeq (0, 0.5)$, corresponding to random initial conditions. Points $(1, 0)$ and $(-1, 0)$ represent A and B one-component consensual configurations, while the absorbing line $\rho = 0$ with $|m| < 1$ corresponds to a fragmented network.

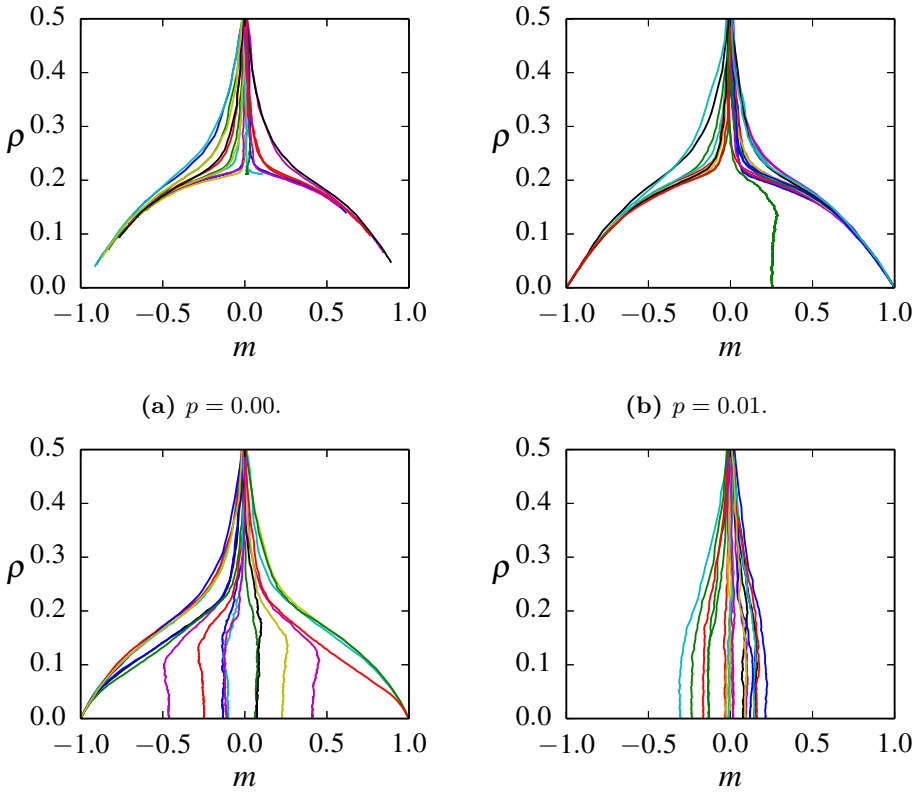

(a) $p = 0.00$. **(b)** $p = 0.01$.

(c) $p = 0.10$. **(d)** $p = 0.50$.

Figure 5.10: Typical trajectories of the system on the (m, ρ) space for a network of $N = 2000$ nodes and different values of the rewiring probability p.

In the $p = 0$ case [Fig. 5.10(a)], we observe that realizations undergo a fast initial ordering in which associated trajectories go from $\rho \simeq 0.5$ to $\rho \simeq 0.2$ (with some small changes in m) in approximately 25 Monte Carlo steps. This corresponds to the fast formation of two giant (connected) domains of opposite states due to the majority rule dynamics, as has been reported in previous works (Castellano and Pastor-Satorras, 2006). Afterwards trajectories enter in a common curve which, as in other cases (Vazquez et al., 2008), can be fit by a parabola, and where the ordering process is accompanied by a change in magnetization. In our case the parabola takes the approximate form $\rho \simeq 0.2(1 - m^2)$ and the system evolves following a direct path towards $|m| = 1$, due to the fact that ρ cannot increase in a majority rule update. This corresponds to the largest domain progressively

invading the other. However, the ordering stops abruptly when the system falls to a topologically trapped state with $\rho > 0$, preventing it from arriving to the one-component ordered A or B states, $(1, 0)$ or $(-1, 0)$ points, respectively.

For $p = 0.01$ [Fig. 5.10(b)], most runs finally arrive to the one-component ordered state, by means of the rewiring mechanism that helps the system escape from frozen or dynamical traps. As mentioned before, even a small rewiring rate is able to unlock frustrated links, allowing the system to keep evolving towards one-component order ($|m| = 1$, $\rho = 0$). Nevertheless, there are some runs that escape from the parabola and follow a nearly vertical downward trajectory (line ending at $\rho = 0$ and $m \simeq 0.25$), even if they are initially attracted towards $|m| = 1$. These runs are trapped around a given value of m and experience a relaxation that decreases ρ very slowly while keeping m almost constant. It seems that in these realizations some rewiring events trigger only a few successful majority rule updates that are not enough to completely order the system in a one-component network. This corresponds to the process of fragmentation of the network in two components with different states. For larger rewiring rates more runs end up fragmenting in two components [see Fig. 5.10(c)], until for large enough p no run is able to follow the parabola [see Fig. 5.10(d)], leading to only fragmented final states.

Mean-field approach

As explained in the last subsection and shown in Fig. 5.3, $\langle\rho\rangle$ undergoes a first fast decay in a short time scale corresponding to the contribution of non-fragmented realizations, and then a second much slower decay that corresponds to fragmented realizations. Therefore, bearing in mind that much of the time evolution of $\langle\rho\rangle$ is controlled by the second very slow dynamics of fragmenting realizations, we develop in this section an analytical approach for this second regime. We assume that the system starts at $t = 0$ from a trapped configuration (see Fig. 5.2), which consists of two network components of similar size $N/2$ interconnected by frustrated links. These are links with the same state as the majority of their neighboring links, thus they cannot change state [see Fig. 5.2(a)], or links with equal number of neighbors in each state, thus they keep flipping state from A to B and vice versa [blinkers, see Fig. 5.2(b)]. To estimate how the density of frustrated links β varies with time, we now describe the events and their associated probabilities that lead to a change in β. In a single time step of interval $dt = 1/N$, a frustrated link is chosen with probability β. Then, with probability $p/2$ the end of the link connected to the minority is randomly chosen and rewired to another random node in the network. Finally, this end lands on the component that holds the link's state with probability $1/2$. After the rewiring, this link does no longer connect both components, thus the number

of frustrated links is reduced by 1, leading to a change $\Delta\beta = -2/\mu N$ (with $\mu \equiv \langle k \rangle$, as above). Gathering all these factors, the average density of frustrated links evolves according to

$$\frac{d\beta(t)}{dt} = -\frac{p}{2\mu}\beta(t)\,, \tag{5.4}$$

with solution

$$\beta(t) = \beta_0\, e^{-\frac{p}{2\mu}t}\,, \tag{5.5}$$

where β_0 is the initial density of frustrated links. Given that, on average, each frustrated link accounts for the existence of $\mu-1$ nodal interfaces, ρ is proportional to β, and therefore we expect the average density of interfaces to decay as

$$\rho(t) \sim e^{-\frac{p}{2\mu}t}\,. \tag{5.6}$$

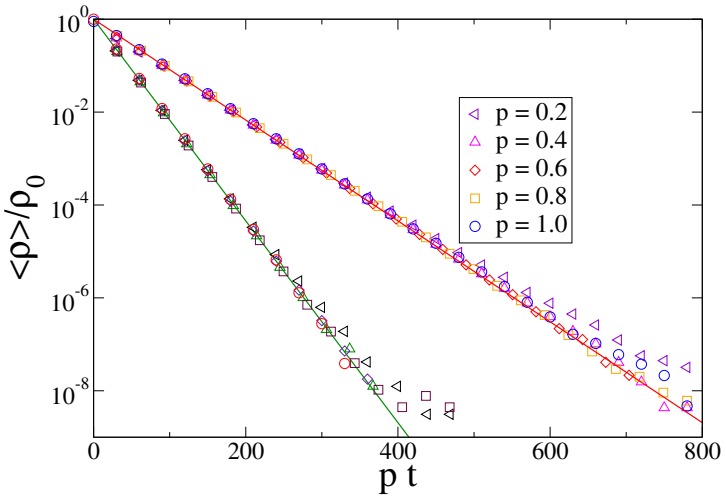

Figure 5.11: Time evolution of the average density of nodal interfaces $\langle\rho\rangle$ on a semilogarithmic scale, for different values of the rewiring probability p. Symbols at the top correspond to simulations on a network of $N = 4000$ nodes and mean degree $\mu = 20$, while bottom symbols are for a network of size $N = 8000$ and mean degree $\mu = 10$. Time is rescaled by p and $\langle\rho\rangle$ is normalized by its initial value to make the data collapse. Solid lines are the analytical approximations from Eq. (5.6).

In Fig. 5.11 we show $\langle\rho\rangle$ as a function of time obtained from numerical simulations for various values of p (symbols) and two different networks, one of size $N = 8000$ and $\mu = 10$ and the other with $N = 4000$ nodes and $\mu = 20$. We observe that the expression (5.6) (solid lines) captures the behavior of $\langle\rho\rangle$ for

most values of p and has the correct scaling with μ. The data for $p = 0.2$ deviates from the pure exponential decay at long times, probably because the analytical approximation works better for large p, where the rewiring process seems to dominate the dynamics.

Convergence times

Another quantity that is worth studying in this system is the time to reach the final state, or convergence time, given that it complements our previous analysis of the two ordering dynamics, majority rule and rewiring. In Fig. 5.12 we show the mean time of convergence to the final ordered state for non-fragmented and fragmented runs, respectively T_1 and T_2, versus the rewiring probability p [3]. Results are shown for three different system sizes. We observe that T_2 is about ten times larger than T_1 for all values of p. This confirms the dynamical picture that we discussed in the previous subsections. There is a first fraction of runs in which the majority rule dynamics plays a leading role, constantly ordering the system until it reaches one-component full order in a short time scale T_1. But there is also a second fraction of runs which fall into particular topological traps that prevent the system from further ordering, and then the rewiring process slowly leads to the fragmentation of the network in a much longer time scale T_2. Interestingly, rewiring always works as a perturbation that frees the system whenever it gets trapped, but it seems that in the first type of runs perturbations trigger cascades of ordering updates which are large enough to completely order the network before it breaks apart.

An approximate expression for T_2 can be obtained by considering the relaxation to the fragmented state given by Eq. (5.6), where the mean number of nodal interfaces decreases to zero. The network breaks into two components when the fraction of frustrated links holding both components together becomes smaller than $2/\mu N$, or $\rho \sim 1/N$, since ρ is proportional to β, as we mentioned before. Then, we can write $1/N \sim \exp(-pT_2/2\mu)$, from where

$$T_2 \sim \frac{\mu}{p} \ln N \,. \tag{5.7}$$

The inset of Fig. 5.12 shows that the approximate expression (5.7) captures the right scaling of T_2 with p and N. In Fig. 5.13 we check the dependence of T_1 and T_2 with the system size N. The y-axis of the main plot showing T_2 has been rescaled according to Eq. (5.7). The inset shows that T_1 also scales as $\ln N$.

As Fig. 5.12 shows, both T_1 and T_2 decay as $1/p$ in the low p limit. This is due to the fact that, when p is very small, we can picture the typical evolution of the

[3] The subindices 1 and 2 refer here to one and two components, even though fragmented runs may also have a few disconnected nodes

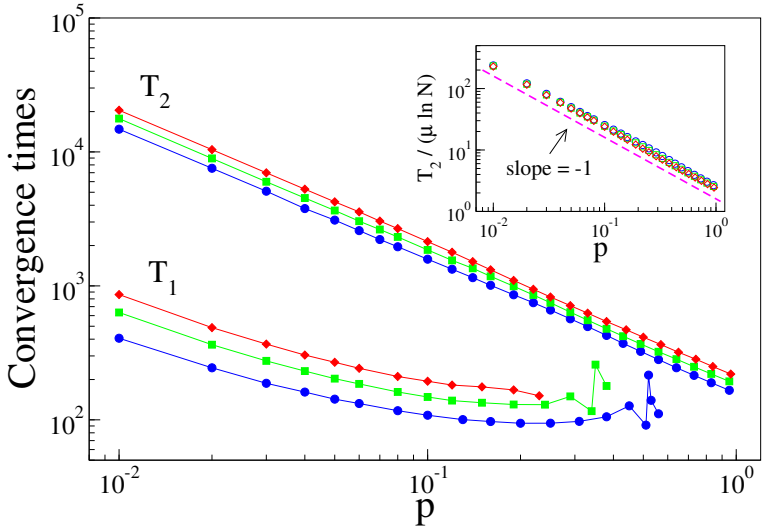

Figure 5.12: Mean time to reach the fragmented and non-fragmented final states, respectively T_1 and T_2, as a function of the rewiring probability p, for networks of size $N = 500$ (circles), $N = 2000$ (squares) and $N = 8000$ (diamonds), and mean degree $\mu = 10$. The inset shows the scaling of T_2 as described by Eq. (5.7).

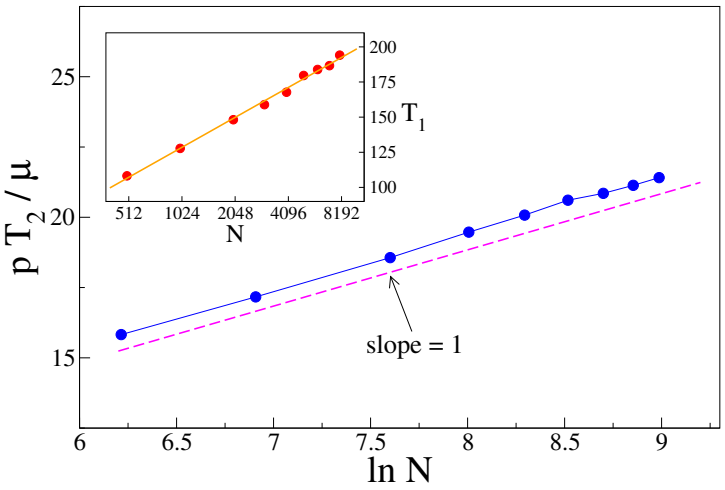

Figure 5.13: Convergence times T_1 and T_2 as a function of the system size N for $p = 0.1$ and $\mu = 10$. Main: y and x-axis have been rescaled according to Eq. (5.7). Inset: Data is shown on a semilogarithmic scale. The solid line is the best fit $T_1 = 30.7 \ln N - 84.5$.

system as a series of alternating pinning and depinning processes. That is, initially a series of majority rule updates take place, which partially order the system until it reaches a frustrated configuration. Then the system stays trapped there for a time of order $1/p$ until a successful rewiring event unlocks it. This is followed by another avalanche of majority rule updates that ends on the next trapped state. This process is repeated until a final absorbing ordered configuration is reached. Given that the mean time interval between two avalanches scales as $1/p$, the convergence time to any final state should scale as $1/p$ (see Fig. 5.12). This implies that T_1 and T_2 diverge as $p \to 0$. However, when p is strictly zero the system is absorbed in a disordered configuration, which can be frozen or dynamically trapped, and so the convergence time is finite. The $p = 0$ case also differs from the $p > 0$ case in the fact that convergence times to the absorbing disordered configurations seem to scale as $T \sim N^{0.375}$ (see Fig. 5.14), instead of $\ln N$.

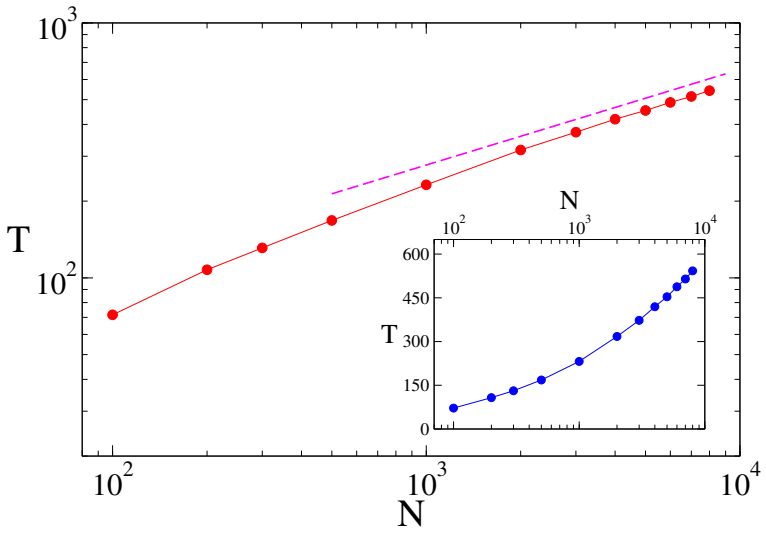

Figure 5.14: Average time to reach an absorbing disordered state T as a function of the systems size N on a logarithmic scale, for a static network ($p = 0$). The dashed line has slope 0.375. The semilogarithmic scale in the inset shows that T grows faster than $\ln N$.

5.4

Concluding remarks

We have studied a model that explores the majority rule link dynamics on a coevolving network, where links in the local minority are rewired at random. On topologically static ($p = 0$) large networks, the ordering process induced by the majority rule stops before a completely ordered state is reached with all links in the same state (the only possibility with no rewiring), because the system falls into trapped disordered configurations. When the rewiring is switched on ($p > 0$), the system is able to escape from these trapped configurations and reach an ordered absorbing state that can be either a one-component network with all links in the same state or a fragmented network with two opposed states disconnected components. The former output is more likely when the rewiring rate is low or networks are small, while the latter output becomes more and more common as the rewiring rate increases or networks get larger, and it is the only possible result for large rewiring rates or in the limit of very large networks. For any finite-size network, a range of values of the rewiring probability p can be found for which there is bistability between both possible outcomes. In the very large size limit, however, the bistability region progressively vanishes and thus even very small amounts of rewiring make the network break apart.

By studying the trajectories of the system in the $m - \rho$ space, we were able to identify two types of evolutions, which provides an insight about the mechanism of fragmentation. For no rewiring, all trajectories fall into an attractive path with a parabolic envelope that ends in a point corresponding to a one-component ordered configuration. However, these trajectories stop before reaching that point, indicating that the system is trapped in a disordered configuration. For low rewiring, most trajectories quickly move along the parabola until they hit the one-component ordered absorbing point. This complete ordering process is mainly driven by majority rule updates, and happens in a quite short time scale. For high rewiring a new scenario appears. Most trajectories quickly stop at some point in the parabola, and then slowly follow a nearly vertical path that ends in the absorbing line $\rho = 0$ with $|m| < 1$, corresponding to a fragmented network. This second fragmentation process takes a much longer time than the initial ordering process, and controls the total convergence time to the final state. Our results show that the frozen and dynamically trapped disordered configurations promoted by the link-based majority rule dynamics are not robust against topological perturbations in the form of a rewiring, since the continuous relinking updates are able to remove the system from the topological traps.

CHAPTER 6

Coupled dynamics of node and link states

In order to address the intertwined dynamics of language use as a means of communication —a property of the links or interactions between speakers— and language preference as an attitude towards it —a property of the nodes or speakers themselves—, we develop in this chapter a model of coupled evolution of node and link states. As in the previous chapter, the use of two socially equivalent languages is represented by a binary-state variable associated to the links. In addition, nodes are endowed with a discrete variable representing their level of preference for one or the other language. We assume the evolution of the language used in the interaction between two speakers to result from the interplay between their tendency to use their internally preferred language and their tendency to reduce the cognitive cost associated with the use of several languages (Meuter and Allport, 1999; Jackson et al., 2001). Finally, we also assume that the use of a certain language among the social contacts of a speaker leads to an increase of her preference for that language. In this way, node states influence the evolution of link states and vice versa.

A broad range of possible asymptotic configurations is found, which can be divided into three categories: frozen extinction of one of the languages, frozen coexistence of both languages or dynamically trapped coexistence of both languages. The probability of reaching a configuration where one of the languages becomes extinct is found to vanish exponentially for increasing system sizes. The coexistence of both languages is based on "ghetto-like" structures, where predominantly bilingual speakers use one of the languages for the interactions among themselves while they switch to the other language for communications with the rest of the population. Furthermore, metastable states with non-trivial dynamics and very

long survival times are frequently found. A system size scaling shows that the time scale of survival of these metastable states increases linearly with the size of the system. Thus, non-trivial dynamical coexistence is the only possible outcome for large enough systems.

A detailed presentation of the model is given in Section 6.1, with a particular emphasis on the coupling between the dynamics of link states and the dynamics of node states. The structural constraints imposed by the definition of the model are also described in this section, as well as the particularities of the networks used for the numerical simulations. The different asymptotic configurations of the model, as well as their respective likelihoods, are presented in Section 6.2, while in Section 6.3 we study two different time scales characterizing the transient dynamics of the model before reaching these asymptotic configurations. In Section 6.4 we investigate the kind of speakers that sustain the coexistence of both languages. A comparison with a previously proposed model which takes into account the existence of bilingual speakers is addressed in Section 6.5. Finally, some conclusions are drawn in Section 6.6. A further exploration of the influence of one of the model parameters is addressed in Appendix 6.A.

6.1

The model

Inspired by the aforementioned language competition processes, we consider a population of N speakers and the linguistic interactions between them —any social interaction mediated through language—, represented, respectively, by the nodes and the links of a network. We focus on the competition between two socially equivalent languages, that we label as A and B. On the one hand, each speaker i, with k_i neighbors in the network of interactions, is characterized by a certain preference x_i for language A (node state), being $(1 - x_i)$ its preference for language B. In particular, we model the preference x_i as a discrete variable taking values $x_i \in \{0, 1/k_i, 2/k_i, \ldots, 1\}$, where $x_i = 1$ indicates an absolute or extreme preference for language A and $x_i = 0$ an absolute or extreme preference for language B. On the other hand, each interaction between speakers can take place in one of the two possible languages, being thus each link i–j characterized by a binary variable S_{ij} (link state) taking the value $S_{ij} = 1$ if the language spoken is A and $S_{ij} = 0$ if language B is used.

Finally, the states of nodes and links evolve asynchronously, i.e., a single node or link is updated at each time step: with probability p a randomly chosen node is updated, and with the complementary probability $(1 - p)$ a randomly chosen

link is updated. Therefore, the probability p sets the relationship between the time scale of evolution of the speakers' preferences and the time scale at which the language used in conversations changes. Note that time is measured in the usual Monte Carlo steps, with N updating events per unit time —whether node or link updates. While the parameter p does have an effect on how fast the system reaches its asymptotic behavior, the main features of this asymptotic regime seem to be unaffected by it (see Appendix 6.A). Thus, we focus here on the particular case of equal probability of node and link updates, i.e., $p = 0.5$.

Evolution of link states

The dynamics of link states —the language used in the interactions between speakers— results from the interplay between two mechanisms. On the one hand, we assume that there is a cognitive effort or cost associated with the use of several languages (Meuter and Allport, 1999; Jackson et al., 2001), which leads speakers to try to use the same language in all their conversations. As a consequence, the interaction between two given speakers tends to take place in the language most often used by both of them in their conversations with other speakers. In particular, we can define for each link i–j the *majority pressure* for language A as the fraction of the total number $(k_i - 1) + (k_j - 1)$ of interactions with other speakers in which language A is used,

$$F_{ij}^A = \frac{k_i^A + k_j^A - 2S_{ij}}{k_i + k_j - 2}\,, \tag{6.1}$$

where k_i^A stands for the number of interactions in which speaker i uses language A, and k_i for its total number of interactions. On the other hand, speakers tend to use their internally preferred language: the higher their preference for a given language, the more willing they are to enforce its use in their conversations with other speakers. Combining the preferences of both participants in each interaction i–j, we can define the *link preference* for language A as

$$P_{ij}^A = \begin{cases} \dfrac{x_i x_j}{x_i x_j + (1-x_i)(1-x_j)}\,, & \text{if} \quad x_i x_j + (1-x_i)(1-x_j) > 0\,, \\ \dfrac{1}{2}\,, & \text{otherwise}\,, \end{cases} \tag{6.2}$$

where the second case ensures that P_{ij} is well-defined when there is a tie between two speakers with extreme preferences for different languages ($x_i = 0$ and $x_j = 1$, or $x_i = 1$ and $x_j = 0$). This expression for P_{ij}^A takes into account the preferences of both nodes, x_i and x_j, in such a way that it yields the value 1 if both nodes have complete preference for language A, $x_i = x_j = 1$, and it yields 0 if both

nodes have null preference for it, $x_i = x_j = 0$. If one of the nodes is neutral with respect to language A, say $x_i = 1/2$, then the link preference is equal to the other node's preference, x_j. Finally, the definition is such that it satisfies the requirement $P_{ij}^A(x_i, x_j) = 1 - P_{ij}^A(1 - x_i, 1 - x_j)$ or $P_{ij}^A(x_i, x_j) = 1 - P_{ij}^B(x_i, x_j)$ reflecting the symmetry between the two languages. A schematic example of the calculation of these two quantities is shown in Fig. 6.1. Note that the majority pressure and link preference for language B are, respectively, $F_{ij}^B = 1 - F_{ij}^A$ and $P_{ij}^B = 1 - P_{ij}^A$.

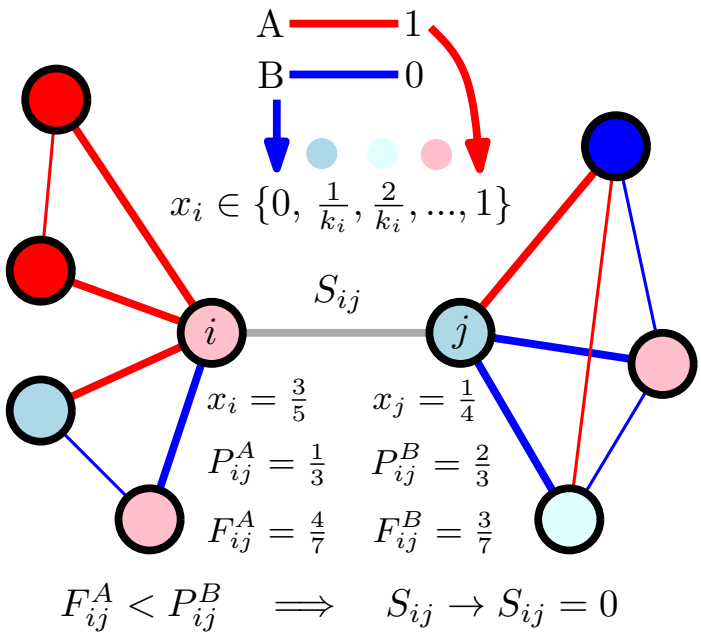

Figure 6.1: Schematic illustration of the evolution of link states. The use of the two competing languages is represented, respectively, by red links and blue links, while the preferences of the speakers are represented by node colors ranging from red to blue through white. The interaction being updated is represented by a gray link. Only bold links are relevant for the particular link update illustrated here.

When a link i–j is picked for updating, its new state is chosen according to the following rules: (*i*) if the sum of the majority pressure and the link preference for language A is larger than the corresponding sum for language B, then language A is chosen; (*ii*) if, on the contrary, the sum is larger for language B than it is for language A, then language B is chosen; (*iii*) if there is a tie between both languages, then one of them is chosen at random. Given the symmetry between

both languages, these rules can be formally written as

$$S_{ij} = \begin{cases} 1 \text{ (language } A)\,, & \text{if} \quad F_{ij}^{A} > P_{ij}^{B}\,, \\ 0 \text{ (language } B)\,, & \text{if} \quad F_{ij}^{A} < P_{ij}^{B}\,, \\ 0 \text{ or } 1 \text{ randomly}\,, & \text{if} \quad F_{ij}^{A} = P_{ij}^{B}\,, \end{cases} \tag{6.3}$$

(see Fig. 6.1 for a schematic example of a link update). Note that, if the preferences of all the speakers are fixed as $1/2$, then all link preferences are also fixed as $1/2$ and we recover the majority rule for link states studied by Fernández-Gracia et al. (2012): the state of a link is updated to the state of the majority of its neighboring links. With freely evolving preferences of the speakers, on the contrary, the threshold for a state to be considered a majority is not anymore universal and fixed at $1/2$, but becomes local and dynamic: the fraction of neighbors in state B needs to be larger than P_{ij}^{A} for link i–j to change its state to B, while the fraction of neighbors in state A needs to be larger than $P_{ij}^{B} = (1 - P_{ij}^{A})$ for it to change its state to A. Finally, note that speakers with extreme preferences ($x_i = 0$ or $x_i = 1$) impose their preferred language in all their conversations, except when they are faced by a speaker with an extreme preference for the other language, when there is an equilibrium between them and the language for their interaction is chosen at random.

Evolution of node states

Regarding the dynamics of node states, we assume that speakers update their preferences according to the language that they observe their neighbors using between them —obviously, only those who are also neighbors of each other. Thus, we implicitly assume that triangles represent actual group relationships, in which each speaker is aware of the interaction between the other two (see Serrour et al., 2011, for a study on the relationship between communities and triangles). In these terms, the more often the participants of the closer social group of a speaker —her triangular relationships— use a given language to communicate between themselves, the more likely it is that the speaker will update her preference towards that language. In particular, when a node i is picked for updating,

its state x_i evolves according to the following probabilities

$$P\left(x_i \to x_i + \frac{1}{k_i}\right) = \begin{cases} \frac{T_i^A}{T_i}\,, & \text{if} \quad x_i \neq 1\,, \\ 0\,, & \text{otherwise}\,, \end{cases}$$
$$P\left(x_i \to x_i - \frac{1}{k_i}\right) = \begin{cases} \left(1 - \frac{T_i^A}{T_i}\right)\,, & \text{if} \quad x_i \neq 0\,, \\ 0\,, & \text{otherwise}\,, \end{cases} \tag{6.4}$$

where T_i is the total number of links between neighbors of node i and T_i^A is the number of those links in state 1, i.e., those in which language A is used (see Fig. 6.2 for a schematic example of a node update). Note that this evolution is equivalent to a one-dimensional random walk in the discrete-state space $x_i \in \{0, 1/k_i, 2/k_i, \ldots, 1\}$ with a bias towards 0 or 1 given by the probabilities in Eq. (6.4). The fact that the modification of the preference ($\Delta x = 1/k_i$) is larger in nodes with fewer links can be motivated by noting that they tend to have fewer triangles and, therefore, each of them has a stronger influence on the node.

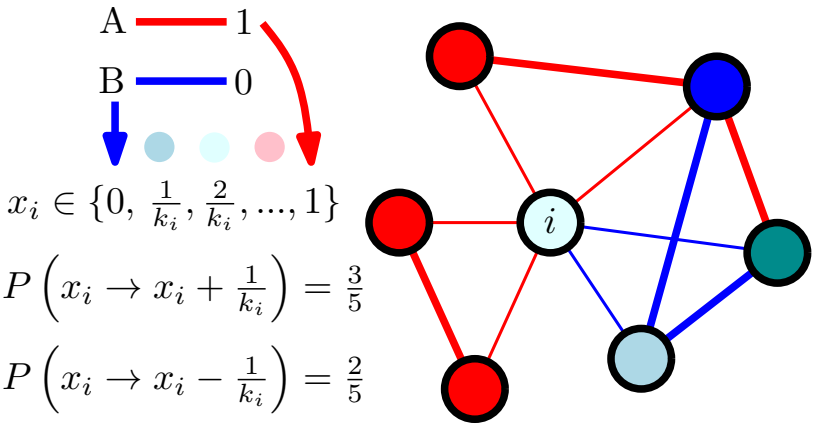

Figure 6.2: Schematic illustration of the evolution of node states. The use of the two competing languages is represented, respectively, by red links and blue links, while the preferences of the speakers are represented by node colors ranging from red to blue through white. Only bold links are relevant for the particular node update illustrated here.

Network structure

The model presented above imposes a structural constraint on the underlying network topology: in order for the evolution of the speakers' preferences to be well-defined, each of them must be part of, at least, one triangle. In fact, it has been recently shown that real social networks are characterized by an abundance of triangles, related to high values of the clustering coefficient (Newman and Park, 2003; Dorogovtsev and Mendes, 2003; Newman, 2010; Foster et al., 2011; Colomer-de Simón et al., 2013). Thus, we are interested in networks with a large proportion of triangles (Serrano and Boguñá, 2005; Newman, 2009; Bianconi et al., 2014). In particular, we focus here on a socially inspired network generation algorithm proposed by Klimek and Thurner (2013) and based on triadic closure, i.e., on the principle that individuals tend to make new acquaintances among friends of friends. Validated with data from a well-studied massive multiplayer online game (Szell et al., 2010; Szell and Thurner, 2010, 2012), this network generation model involves three different mechanisms: random link formation, triadic closure —link formation between nodes with a common neighbor—, and node replacement —removal of a node with all its links and introduction of a new node with a certain number of links.

Bearing in mind the structural constraint imposed by our model, and noticing that the node replacement mechanism might lead to some nodes losing all their triangles, we introduce a modification of the algorithm so as to avoid removing all the triangles from any node. Namely, when the removal of a node would lead to some of its neighbors losing all their triangles, these neighbors are arranged in triangles between themselves, or with randomly chosen nodes when necessary. Furthermore, the new node is introduced as a triangle by initially linking it with a random node and one of its neighbors. Finally, we use the same parameter values found by Klimek and Thurner (2013) when calibrating their algorithm to the friendship network of the above-mentioned online game: a probability of triadic closure $c = 0.58$ [being $(1 - c)$ the probability of random link formation] and a probability of node replacement $r = 0.12$. The degree distribution and the scaling of the average clustering coefficient as a function of the degree are shown in Fig. 6.3 for the networks obtained in this manner. A fit of the degree distribution to a q-exponential function, $e_q(x) = (1 + (1 - q)x)^{(1/(1-q))}$, leads to a value of q compatible with a purely exponential decay [$q = 1.0096$, see panel **(a)**]. Regarding the average clustering coefficient as a function of the degree, a fit to a power-law decay leads to an exponent slightly smaller than one [$\beta = 0.9548$, see panel **(b)**]. Comparing these results with those presented by Klimek and Thurner (2013) (with fitting parameters $q = 1.1162$ and $\beta = 0.693$), we conclude that the described modification does not affect the general characteristics of the networks created, but it does have an effect on the specific values of the different scaling exponents.

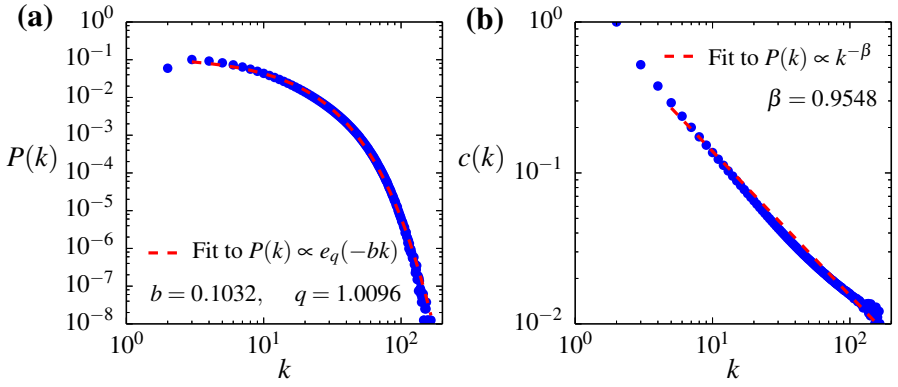

Figure 6.3: Panel **(a)**: Degree distribution and fit to a q-exponential function (for $k \geq 3$). Panel **(b)**: Average clustering coefficient as a function of the degree and fit to a power-law function (for $k \geq 5$). 10000 realizations of the network generation algorithm were used.

6.2

Transient dynamics and asymptotic configurations

By means of numerical simulations, we study the coupled dynamics of node and link states described above. Let us start by introducing three different measures characterizing the state of the system at any given time. Firstly, bearing in mind that we are interested here in the survival of languages regarding their actual use in the interactions between speakers, we can define an *order parameter* ρ in terms of link states. In particular, we define ρ as the density of nodal interfaces (Fernández-Gracia et al., 2012; Carro et al., 2014), i.e., the fraction of pairs of connected links —links sharing a node— that are in different states,

$$\rho = \frac{\sum_{i=1}^{N} k_i^A \, k_i^B}{\sum_{i=1}^{N} k_i(k_i - 1)/2}, \tag{6.5}$$

where k_i is the degree of node i, and $k_i^{A/B}$ is the number of A/B-links connected to node i. The order parameter ρ, by definition $\rho \in [0, 1]$, is thus a measure of

the local order in the system, becoming $\rho = 0$ when all connected links share the same state and $\rho = 1/2$ for a random distribution of link states. Note that, defined as such, the order parameter ρ can also be understood as the usual density of active links —fraction of links connecting nodes with different states— in the line-graph of the original network (Rooij and Wilf, 1965; Krawczyk et al., 2011; Fernández-Gracia et al., 2012; Carro et al., 2014).

Secondly, we introduce the *fraction of links in the minority language*, m, as an alternative, non-local measure characterizing the system in terms of link states,

$$m = \begin{cases} \dfrac{\sum_i k_i^A}{\sum_i k_i}\,, & \text{if} \quad \sum_i k_i^A \leq \sum_i k_i^B\,, \\ \dfrac{\sum_i k_i^B}{\sum_i k_i}\,, & \text{otherwise}\,. \end{cases} \tag{6.6}$$

Note that the minority language is thereby defined as that which is less used in interactions between speakers —fewer links in the corresponding state—, regardless of the total number of those speakers. In this way, even if a majority of the population uses a certain language in some of their interactions, we will still consider it to be the minority language if only a minority of the total number of interactions actually take place in that language. By definition, $m \in [0, 1/2]$.

Finally, we can characterize the system in terms of node states by introducing the *average preference of the speakers for the minority language*, x^M,

$$x^M = \begin{cases} \dfrac{1}{N}\sum_i x_i\,, & \text{if} \quad \sum_i k_i^A \leq \sum_i k_i^B\,, \\ \dfrac{1}{N}\sum_i (1 - x_i)\,, & \text{otherwise}\,, \end{cases} \tag{6.7}$$

where, as before, the minority language is identified according to the fraction of interactions in which it is used. By definition, $x^M \in [0, 1]$.

The time evolution of these three measures is presented in Fig. 6.4 for individual realizations of the model: the order parameter in panel *(a)*, the fraction of links in the minority language in panel *(b)*, and the average preference of the speakers for the minority language in panel *(c)*. All realizations start from a random initial distribution of states for both nodes and links, leading to all three measures starting from 1/2, and they all experience a substantial ordering

process in which one of the languages becomes predominant, leading to a large decrease of all three measures. Nevertheless, a variety of asymptotic behaviors can be observed. These behaviors are a direct consequence of the different types of asymptotic configurations reached by the system, which can be classified as:

(*i*) *Frozen extinction states*: Absorbing configurations where one of the languages has completely disappeared, all links and nodes sharing the same state, and thus no further change of state is possible in the system. As a result, all the three introduced measures become zero (see black lines in Fig. 6.4).

(*ii*) *Frozen coexistence states*: Absorbing configurations where both language still exist but no further change of state is possible in the system. As a result, all our three measures remain constant with non-zero values (see blue lines in Fig. 6.4). Note that these situations of coexistence are characterized by one of the languages becoming a minority but persisting in the form of "ghetto-like" structures, defined as subsets of nodes such that all of them belong to triangles completely included in the subset. A schematic illustration of a simple "ghetto-like" motif composed of a single triangle can be found in Fig. 6.5(a).

(*iii*) *Dynamically trapped coexistence states*: Configurations where both languages still exist and the system is forever dynamic, but only a restricted (and usually small) number of changes of state are possible. In particular, only changes that do not modify the density of nodal interfaces are accessible. Bearing in mind that, by definition of the model, these changes are reversible, the system can move back and forth *ad infinitum* (Olejarz et al., 2011a,b). Depending on the kind of dynamical trap involved, we can identify three types of configurations:

- Configurations based on *Blinker links*: Both the order parameter and the average preference of the speakers for the minority language remain constant while the fraction of links in the minority language fluctuates around a certain value (see orange lines in Fig. 6.4). A schematic illustration of the most simple blinker link motif is presented in Fig. 6.5(b).

- Configurations based on *Blinker nodes*: Both the order parameter and the fraction of links in the minority language remain constant while the average preference of the speakers for the minority language fluctuates around a certain value (see green lines in Fig. 6.4). A schematic illustration of a single blinker node motif can be observed in Fig. 6.5(c).

- Configurations based on both *blinker links* and *blinker nodes*: More or less complex combinations of the two previous types, leading to

a constant order parameter and a fluctuating fraction of links in the minority language and average preference of the speakers for it.

Note that dynamical traps can only appear at the interface between the frozen, "ghetto-like" structures described above and the rest of the network.

Apart from these asymptotic configurations, we can also observe the presence of long-lived *metastable coexistence states*. These non-trivial dynamical states are characterized by fluctuating, non-zero values of all the three introduced measures (see red lines in Fig. 6.4). The metastability of these states is based on a variation or weaker version of the "ghetto-like" structures described above, which would now consist of a subset of nodes such that a significantly large fraction of the triangles they belong to are completely included in the subset, i.e., they have a significantly larger number of triangles towards the inside of the subset than towards the outside. Due to finite-size fluctuations, however, the system always ends up falling to one of the previously described asymptotic states.

Once the different types of asymptotic states of the system have been presented, let us now focus on their relative likelihood. In particular, we show in Fig. 6.6 the fraction of realizations having reached each of the possible asymptotic configurations before the end of the studied time period ($t = 10^5$), as well as the fraction of those still in a metastable state, for different system sizes. While the (frozen) extinction of the minority language is the most likely outcome for small systems ($N < 2000$), its probability decreases exponentially with system size, thus becoming negligible for large enough systems. Frozen coexistence is clearly predominant for large system sizes inside the studied range ($2000 < N \leq 8000$). However, given the linear growth observed in the fraction of dynamically trapped coexistence configurations, the numerical results presented in this figure for limited system sizes are inconclusive regarding the prevalence of frozen or dynamically trapped coexistence in the infinite size limit. Regarding the metastable coexistence states, it should be noted that they are not asymptotic states, and thus the system will eventually end up falling to any of the other frozen or dynamically trapped configurations. The fact that the fraction of metastable realizations at a given time grows linearly with the system size, suggests that the time scale in which the system is able to leave those metastable states also grows linearly with N, a point that will be discussed further in the next section.

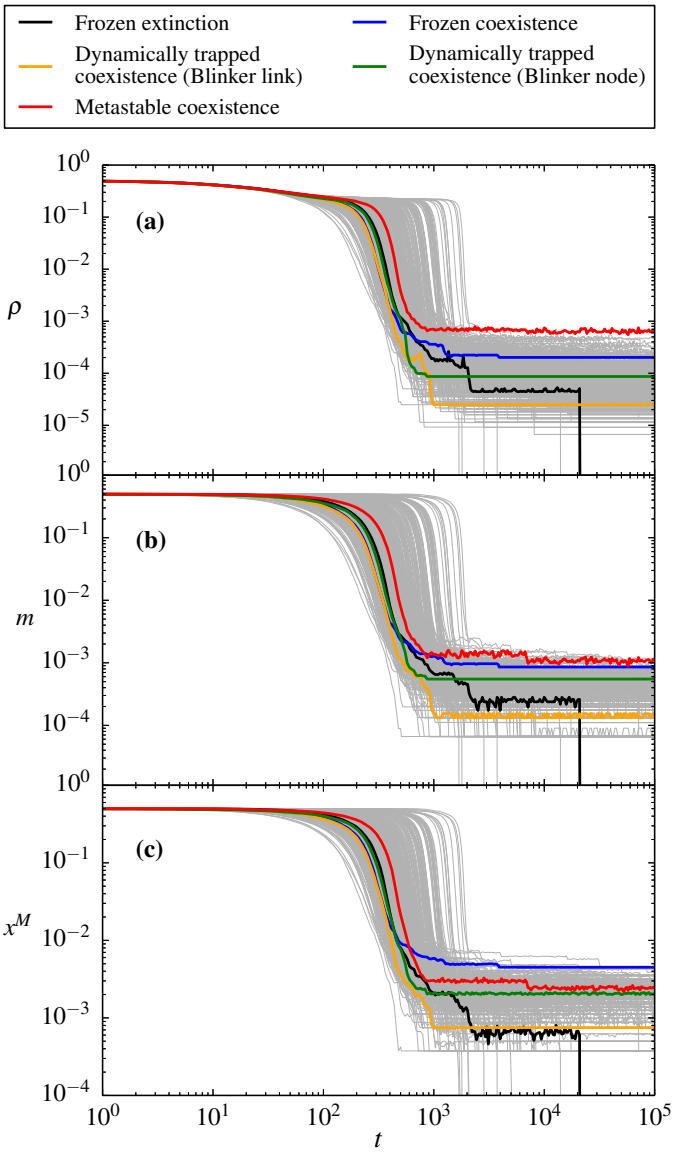

Figure 6.4: Time evolution of **(a)** the order parameter, **(b)** the fraction of links in the minority language, and **(c)** the average preference of the speakers for the minority language. 200 individual realizations of the process are shown, among which 5 realizations are highlighted as representative of the different types of possible trajectories. The system size used is $N = 8000$.

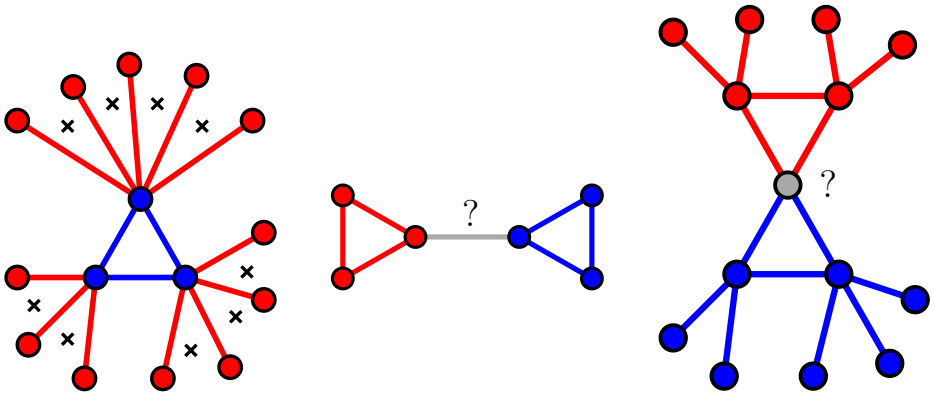

(a) Frozen coexistence

(b) Dynamically trapped coexistence (blinker link)

(c) Dynamically trapped coexistence (blinker node)

Figure 6.5: Schematic illustration of the kind of structural motifs characterizing the different asymptotic configurations. The use of the two competing languages is represented, respectively, by solid red links and dashed blue links, while the preferences of the speakers are represented by node colors ranging from red to blue through white. Gray color is used to represent blinking or undecided situations. Crosses indicate the non-existence of a link.

6.3

Time scales of extinction and metastable coexistence

Due to the diversity of possible asymptotic configurations described in the previous section, different time scales can be defined to characterize the dynamics of the system. In particular, we focus here on two time scales: the characteristic time of extinction of one of the languages and the characteristic duration or survival time of the metastable states. While in the first case we focus on realizations reaching the frozen extinction state over the time period under study, in the second case we consider all realizations leaving the metastable coexistence state over that time period, regardless of the particular asymptotic state they reach.

Let us start by considering the time evolution of the probability of coexistence of both languages $P_c(t)$, i.e., the fraction of realizations not having reached a frozen extinction configuration by time t, depicted in Fig. 6.7 for different system

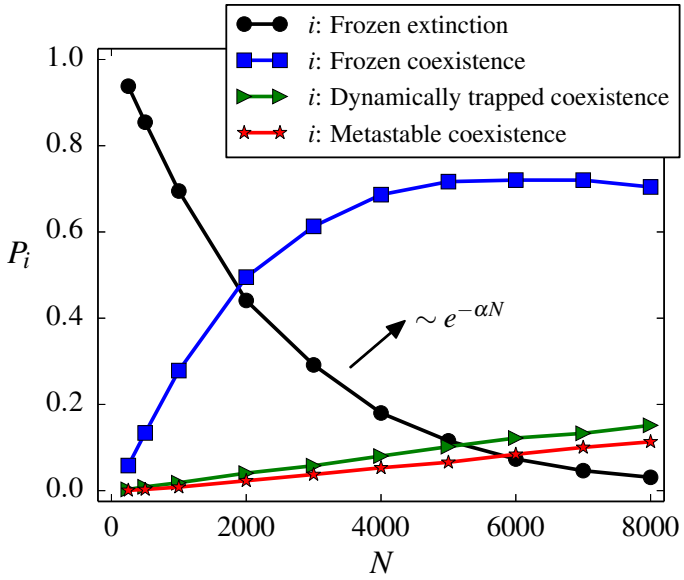

Figure 6.6: Scaling with system size of the fraction of realizations having reached each of the possible asymptotic configurations at time $t = 10^5$, as well as the fraction of those still in a metastable state. A total of 10000 realizations were used, with different networks and different initial conditions.

sizes. Coherent with the results presented above in Fig. 6.6, the coexistence probability becomes closer and closer to one, for any time, as the system size becomes larger and larger. For small systems, on the contrary, the probability of both languages coexisting shows a large decrease around a certain characteristic time, which grows with system size, before asymptotically reaching a plateau. Note, nevertheless, that this plateau is not reached as long as there are metastable realizations able to reach the frozen extinction configuration.

As we can observe in Fig. 6.7, most extinction events take place around a certain characteristic time. For instance, for the system size $N = 1000$, 90% of all extinction events observed in the interval $t \in [0, 10^5]$ take place between $t = 200$ and $t = 2000$. However, for a non-negligible fraction of realizations the extinction of one of the languages happens at significantly longer times, and thus the coexistence probability keeps on slowly decreasing instead of quickly reaching a plateau. In order to further analyze this behavior, we present in Fig. 6.8 the probability distribution of extinction times $p_e(t)$ for the system size $N = 1000$, where, according to the results presented in Fig. 6.6, extinction is predominant.

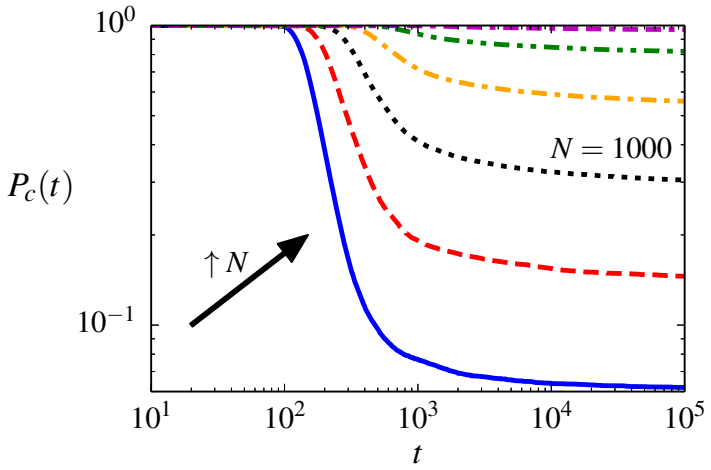

Figure 6.7: Time evolution of the coexistence probability (fraction of realizations not having reached the frozen extinction configuration by time t) for different system sizes, namely $N = 250$, 500, 1000, 2000, 4000, and 8000. A total of 10000 realizations were used, with different networks and different initial conditions.

Note that this distribution is related to the coexistence probability by

$$P_c(t) = 1 - \int_0^t p_e(t')dt' \,. \tag{6.8}$$

In this way, we see that extinction times are broadly distributed and that the decay of their probability for long times seems to be compatible with a power law $p_e(t) \sim t^{-\alpha}$ with exponent $\alpha \sim 0.5$. Being the exponent smaller than one, the mean of the distribution diverges, and thus there is no well-defined characteristic time scale for the extinction events. As a consequence, even if the extinction of one of the languages is predominant for small system sizes, there are, at all time scales, realizations where both languages are still coexisting.

A further characterization of the behavior of the model is given by the time scale at which the system is able to escape from the metastable coexistence states, i.e., the characteristic survival time of these non-trivial dynamical states before the dynamics of the system becomes locked in any frozen or dynamically trapped configuration. In order to study this, let us first introduce the survival probability of the metastable states $P_s(t)$, defined as the fraction of realizations not having reached any frozen or dynamically trapped state by time t. Our results for this probability are presented in Fig. 6.9, on a log–log scale, for different system sizes. Comparing Figs. 6.7 and 6.9 we can observe that, similarly to the coexistence

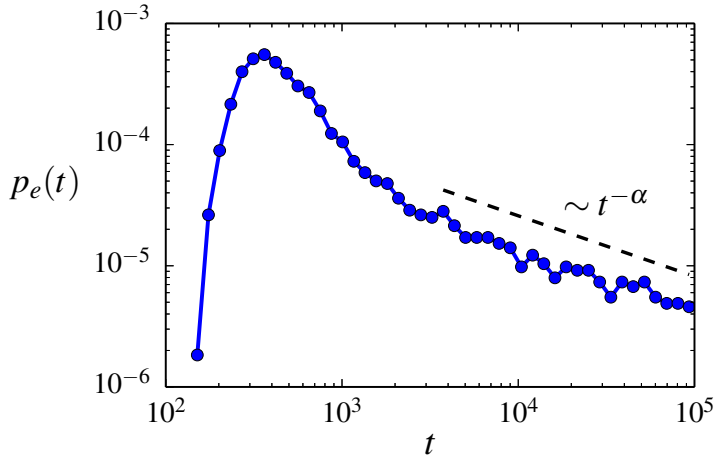

Figure 6.8: Distribution of extinction times for realizations reaching the frozen extinction configuration over the interval $t \in [0, 10^5]$ (69.5% of the 10000 realizations studied) for a system size $N = 1000$. A power-law decay with exponent $\alpha = 0.5$ is shown as a guide to the eye.

probability, surviving realizations are more and more likely, for any point in time, for larger and larger systems. On the contrary, the survival probability of the metastable states does not asymptotically approach any plateau, as it was the case for the coexistence probability. This is coherent with the fact that, by definition, all metastable realizations eventually end up being frozen or dynamically trapped.

Even if the survival probability of the metastable states appears to be fat-tailed in the log–log scale of Fig. 6.9, a closer look at the same results presented on a semilogarithmic scale in Fig. 6.10 shows that any fat-tailed behavior is interrupted by an exponential decay occurring after a long cutoff time. This final exponential decay allows for both the mean and the fluctuations of the distribution of survival times of the metastable states to be well-defined, and thus the mean can play the role of a characteristic duration or survival time of these metastable states τ_s before the system reaches a frozen or dynamically trapped configuration.

The characteristic survival time of the metastable states τ_s can be directly computed from their survival probability $P_s(t)$ as

$$\tau_s = \int_0^\infty P_s(t) dt \,. \tag{6.9}$$

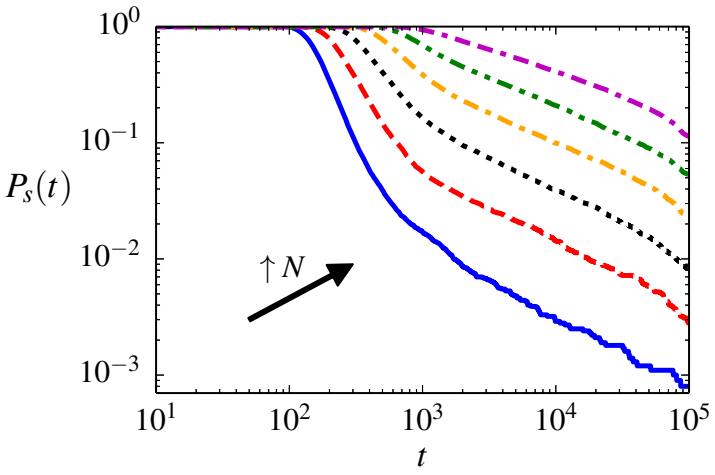

Figure 6.9: Time evolution of the survival probability of the metastable states (fraction of realizations not having reached any frozen or dynamically trapped state by time t) on a log–log scale and for different system sizes, namely $N = 250$, 500, 1000, 2000, 4000, and 8000. A total of 10000 realizations were used, with different networks and different initial conditions.

However, given that a non-negligible number of realizations in our sample stay in a metastable state for the whole period under study —particularly for large system sizes—, we cannot simply discard the queue of the distribution and numerically compute the mean using only the observed survival times. On the contrary, we need to take the queue of the distribution into account, which we can do by fitting the final exponential decay uncovered above in Fig. 6.10. In particular, if we assume that the survival probability of the metastable states takes the functional form

$$P_s(t) = ae^{-b(t-t^*)} \quad \text{for } t > t^* \,, \tag{6.10}$$

from a certain cutoff time t^*, where a, b and t^* are fitting parameters, then we can divide the integral in Eq. 6.9 into two terms,

$$\tau_s = \int_0^{t^*} P_s(t)dt + \int_{t^*}^{\infty} P_s(t)dt = \int_0^{t^*} P_s(t)dt + \int_{t^*}^{\infty} ae^{-b(t-t^*)}dt \,. \tag{6.11}$$

Finally, solving the integral in the last term, we find an expression for the characteristic survival time of the metastable states as a sum of two contributions,

$$\tau_s = \int_0^{t^*} P_s(t)dt + \frac{a}{b} \,, \tag{6.12}$$

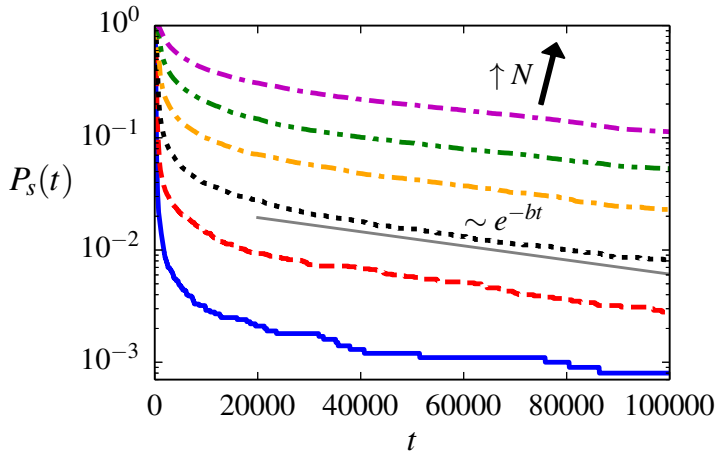

Figure 6.10: Time evolution of the survival probability of the metastable states (fraction of realizations not having reached any frozen or dynamically trapped state by time t) on a semilogarithmic scale and for different system sizes, namely $N = 250$, 500, 1000, 2000, 4000, and 8000. An exponential decay with the slope obtained by fitting the data for $N = 1000$ is also shown as a guide to the eye (thin solid gray line). A total of 10000 realizations were used, with different networks and different initial conditions.

the first of which can be numerically computed as the average of the survival times of the realizations reaching a frozen or dynamically trapped state before t^*. Regarding the second contribution, it can be computed by an exponential fit to the results presented in Fig. 6.10 for $t \geq t^*$.

Results for the scaling with system size of the characteristic survival time of the metastable states are presented in Fig. 6.11, showing a linear relationship between both quantities. Thus, for increasing system sizes, realizations survive for longer and longer times in a metastable state before falling to a frozen or dynamically trapped configuration. Moreover, in the infinite size limit, the system is unable to escape from the metastable states in any finite time.

6.4

Use of the minority language

Once we have identified the different types of configurations associated with the coexistence of both languages, and studied their probabilities and typical

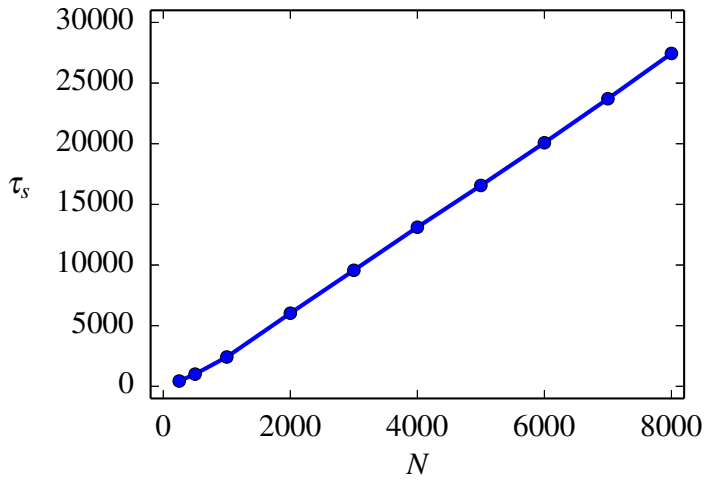

Figure 6.11: Scaling with system size of the characteristic survival time of the metastable states. A total of 10000 realizations were used, with different networks and different initial conditions.

time scales, let us now turn our attention to the extent of this coexistence. In particular, bearing in mind that the situations of coexistence are characterized by one of the languages becoming a clear minority (see Section 6.2), we focus here on two measures quantifying the use of this minority language: the number of speakers who use only this language (minority language monolingual speakers, N^M) and the number of those who use both languages (bilingual speakers, N^{AB}). In order to consider only very long-lived metastable states, apart from frozen and dynamically trapped coexistence configurations, we focus on the last point of the time period under study, $t = 10^5$, and we average only over realizations where both languages are still coexisting (which we note by $\langle\cdot\rangle_c$). Results for the dependence of these two quantities on system size are presented in Fig. 6.12, measured as fractions of the total number of speakers in the main plot and as absolute numbers in the inset.

A first observation is that the state of coexistence is predominantly sustained by bilingual speakers, both their fraction and their absolute number being significantly larger that those corresponding to monolingual speakers of the minority language for any system size. Secondly, while both fractions of minority-language speakers are shown to be decreasing functions of the system size for small systems, they appear to be reaching a plateau for large systems. On the one hand, bearing in mind that averages are computed over coexisting realizations —rare for small systems, predominant for large ones—, this suggests that there is a minimum

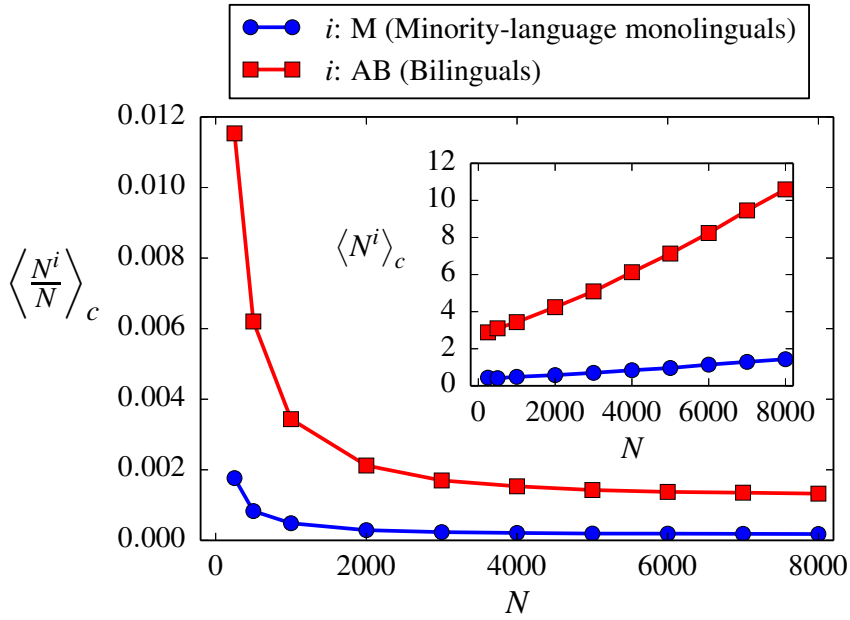

Figure 6.12: Scaling with system size of the fractions of minority-language monolingual and bilingual speakers at the last point of the time period under study, $t = 10^5$, averaged over coexisting realizations. Inset: Scaling with system size of the absolute number of minority-language monolingual and bilingual speakers at the last point of the time period under study, $t = 10^5$, averaged over coexisting realizations.

size of the structures sustaining the use of the minority language. In this way, the smaller the size of the system, the less likely these minimal structures are to appear, but the larger the fraction of the system they represent whenever they actually appear. On the other hand, the asymptotic tendency of both fractions towards a plateau suggests a linear growth with system size of the absolute number of both monolingual and bilingual speakers of the minority language for large systems, which is confirmed in the inset. Finally, the substantially faster growth of the absolute number of bilingual speakers with system size, as compared to minority-language monolinguals, underlines again the importance of bilinguals in sustaining the use of the minority language: bilingualism becomes more and more prevalent among speakers of the minority language for growing systems.

6.5

Comparison with the AB-model

Given the non-standard topology used for our numerical simulations, imposed by the structural constraints of the model —namely, an abundance of triangles—, we present here, for comparison, numerical results for the AB-model in the same networks. Let us first briefly recall the main features of this model, in which language use is considered to be a state of the agents. As outlined in Section 1.3, the AB-model was proposed by Castelló et al. (2006) based on the works of Wang and Minett (2005), and it develops a modification of the original, binary-state Abrams-Strogatz model to account for the case of two non-excluding options by introducing a third, intermediate state. Thus, agents can be in one of the following states: A (monolingual speaker of language A), B (monolingual speaker of language B), or AB (bilingual speaker). Starting from a random initial distribution of states, an agent is randomly chosen at each iteration and its state is updated according to the following probabilities,

$$\begin{aligned} p_{A\to AB} &= \frac{1}{2}\sigma_B\,, & p_{B\to AB} &= \frac{1}{2}\sigma_A\,, \\ p_{AB\to B} &= \frac{1}{2}(1-\sigma_A)\,, & p_{AB\to A} &= \frac{1}{2}(1-\sigma_B)\,, \end{aligned} \tag{6.13}$$

where σ_A, σ_B and σ_{AB} are, respectively, the fractions of neighbors of the chosen agent in state A, B and AB (note that $\sigma_A+\sigma_B+\sigma_{AB}=1$). That is, monolingual speakers of A (B) become bilinguals with a probability proportional to the local fraction of monolingual speakers of B (A), while bilinguals become monolingual speakers of A (B) with a probability proportional to the local fraction of speakers of A (B), which includes both monolingual and bilingual speakers.

Frozen coexistence configurations and dynamically trapped states are not possible in the AB-model, which has, by definition, a single absorbing state: the extinction of one of the languages. Therefore, the order parameter ρ_{AB}, defined now as the density of link interfaces —fraction of links connecting nodes with different states—, is enough to characterize the time evolution of individual realizations, some of which are shown in Fig. 6.13. While this parameter ρ_{AB} is different from the order parameter ρ used above to characterize our model, both of them are measures of the local order of the system. Note that, due to the existence of three different states, all realization start from $\rho_{AB}=2/3$, corresponding to a random initial distribution of states. Similarly to our model, all the realizations go through a substantial ordering process in which one of the languages becomes predominant. In contrast to our model, however, this ordering process takes place around an order of magnitude before ($t\sim 10^2$ as opposed to $t\sim 10^3$)

and it very quickly leads to the complete extinction of one of the languages, all nodes sharing the same state, whether A or B monolingual. Furthermore, only very few realizations are observed to last noticeably longer than the rest of them ($t \sim 600$), suggesting that there are no long-lived metastable coexistence states (compare with Fig. 6.4).

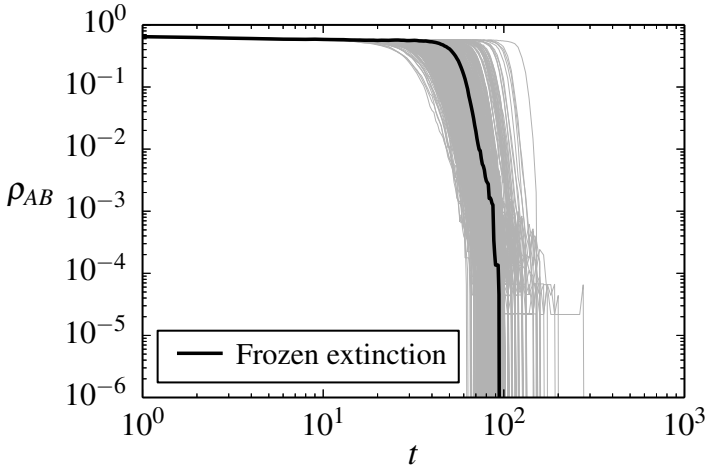

Figure 6.13: Time evolution of the order parameter (interface density) for the AB-model. 200 individual realizations of the process are shown. The system size used is $N = 8000$.

Given that the only asymptotic state of the AB-model is the frozen extinction of one of the languages, the survival of a non-trivial dynamics —not having reached any frozen or dynamically trapped state— and the coexistence of both languages —not having reached the frozen extinction state— are equivalent, and so are their respective probabilities, P_s and P_c. Results for the time evolution of the survival (or coexistence) probability $P_s(t)$ are presented in Fig. 6.14 for different system sizes. As we can observe, after a very short transient (lasting until $t \sim 30$), the likelihood of an active state where both languages coexist quickly falls to zero, with no fat-tailed behavior. Furthermore, this decrease seems to be almost independent of system size. Both features are in agreement with the results reported for the AB-model in random networks without communities (Castelló et al., 2007; Toivonen et al., 2009). They are, however, in sharp contrast with the results corresponding to our model, presented above in Figs. 6.7 and 6.9.

The probability distribution of extinction (or survival) times $p_e(t)$ is shown in Fig. 6.15 for a system size $N = 8000$. As opposed to the results presented in Fig. 6.8 for our model, the extinction times of the AB-model are very closely dis-

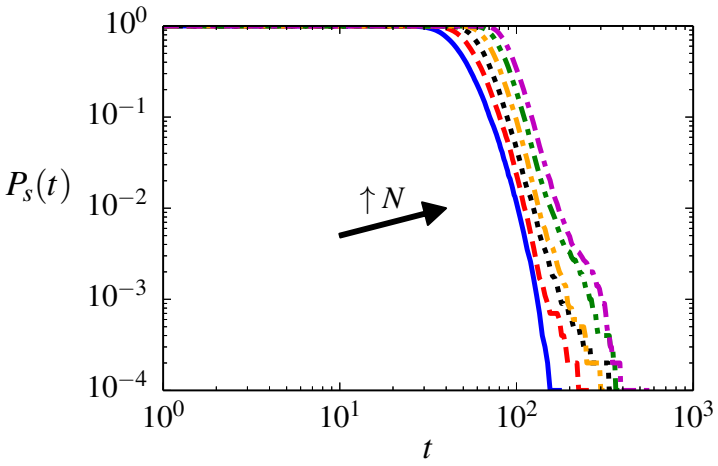

Figure 6.14: Time evolution of the survival probability (fraction of realizations not having reached a frozen state by time t) for the AB-model and for different system sizes, namely $N = 250$, 500, 1000, 2000, 4000, and 8000. A total of 10000 realizations were used, with different networks and different initial conditions.

tributed around the peak, i.e., almost no realization is found to last significantly longer than the rest of them —suggesting the absence of long-lived metastable states—. Therefore, the mean of the distribution is well-defined and it can be used as a characteristic extinction time scale. In contrast with the method used to analyze our model, where a non-negligible number of realizations survived in a non-trivial dynamical state for the whole period of time under study (see Section 6.3), we can here numerically compute the mean of the distribution from our sample of realizations, given that all their survival times are smaller that the studied time period. The dependence of this characteristic extinction time τ_e on system size is also depicted in Fig. 6.15 as an inset. In particular, τ_e is found to be a logarithmic function of the system size, to be compared with the linear relationship found for our model and shown in Fig. 6.11. This result is coherent with the previous observation regarding the small influence of system size on the survival probability.

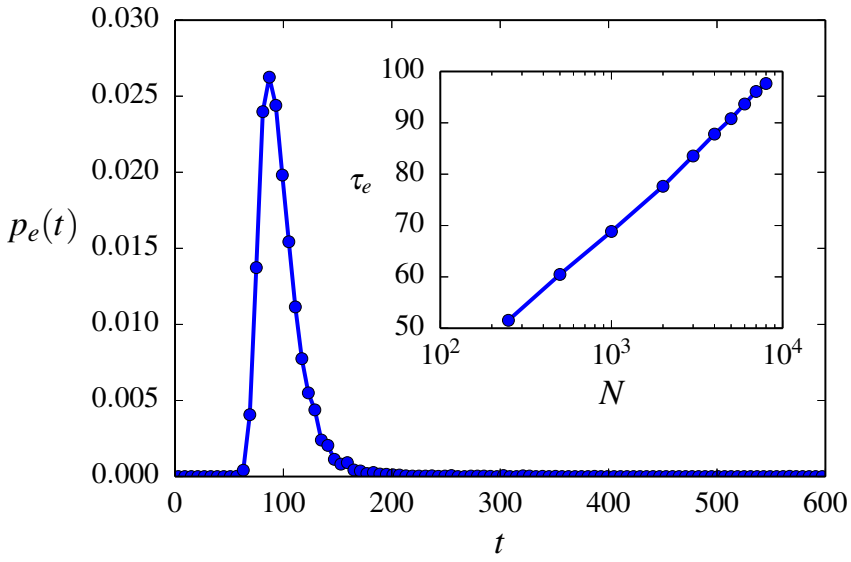

Figure 6.15: Distribution of extinction times for the AB-model and for a system size $N = 8000$. Inset: Scaling with system size of the characteristic extinction time for the AB-model. A total of 10000 realizations were used, with different networks and different initial conditions.

6.6

Concluding remarks

We introduced here a language competition model where both the use and the preference for a given language are included, with different but coupled dynamics. In particular, we proposed to consider the use of a language as a property of the interactions between speakers and the preference or attitude of the speakers towards it as a property of the speakers themselves, and we focused on the case of two socially equivalent languages. In this way, bilingualism is not anymore introduced as an ad hoc, third, mixed state as in previous works, but arises naturally by simply considering speakers who use different languages in different interactions. In the proposed model, the language used in a given interaction results from an interplay between the preferences of both speakers and the languages they use in the rest of their interactions. Furthermore, the preferences of the speakers are influenced by the language used by their social contacts between themselves —triangles in the social network of interactions—.

Thus, we focused on socially inspired network topologies, where triangles are generally abundant.

As opposed to most of the previously proposed models, where the extinction of one of the languages is an inevitable outcome of the dynamics, we found a broad range of possible asymptotic configurations, which can be classified as: frozen extinction states, frozen coexistence states, and dynamically trapped coexistence states. Furthermore, metastable coexistence states with non-trivial dynamics were found to be abundant and with very long survival times. By means of a system size scaling, we showed that the probability of extinction of one of the languages decreases exponentially with system size, therefore becoming negligible for large enough systems. Moreover, we showed that even for small systems extinction times are so broadly distributed that coexisting realizations can be found at all time scales. Regarding the metastable coexistence states, we showed that their characteristic duration or survival time before the system reaches any frozen or dynamically trapped configuration scales linearly with system size. Thus, in the infinite size limit, all realizations will be found to be in a non-trivial dynamical coexistence state for any finite time. Finally, we showed that bilingualism becomes more prevalent among speakers of the minority language the larger the size of the system.

The dynamics of the system being characterized by the fast emergence of a predominant language, we found that, as the use of the minority language decreases, it becomes increasingly confined to the more intimate social spheres or group interactions —triangular relationships—. In particular, the situations of coexistence were found to be based on the existence of "ghetto-like" structures, where predominantly bilingual speakers use the minority language for the interactions among themselves —mostly triangular— while they switch to the majority language for communications with the rest of the population —mostly non-triangular—. In this way, bilingual speakers with a strong preference for the minority language, and using it for their close group interactions, are found to play an essential role in its survival.

APPENDICES TO CHAPTER 6

6.A

Relative time scales for the evolution of nodes and link states

THE model of coupled evolution of node and link states introduced in Section 6.1 includes a parameter p that sets the relationship between the time scales of evolution of the speakers' preferences —node states— and the languages used in conversations —link states—. In particular, at each time step, we choose whether to update the state of a node or the state of a link according to the probabilities p and $(1-p)$, respectively. All the results presented in the main text of the chapter were obtained for the particular case of equal probability of node and link updates, i.e., $p = 0.5$. In this appendix, we explore the influence of this parameter p on some of the quantities studied above, showing that, while there is an influence on how fast the system reaches its asymptotic behavior, the main features of the asymptotic states described in the main text of the chapter are independent of p.

Let us start by considering the influence of p on the time evolution of the probability of coexistence of both languages $P_c(t)$, i.e., on the fraction of realizations not having reached a frozen extinction configuration by time t. We show in Fig. 6.16 this time evolution for a system size $N = 1000$ and for different values of the parameter p. Note that the value $p = 0.5$ in this figure coincides with the system size $N = 1000$ shown above in Fig. 6.7. As we can observe, all curves behave as explained in the main text for small system sizes: all of them experience

a substantial decrease around a certain characteristic time before asymptotically reaching a plateau, whose height appears to be largely unaffected by the value of p. On the contrary, it appears to have a relevant influence on both the characteristic time at which this large decrease takes place and on its duration. In particular, the further away we move from $p = 0.5$ towards $p = 0$ or $p = 1$, the larger the characteristic time of the decrease (see dark red and blue as opposed to light colors). Thus, we see that the arrival of the system to the asymptotic state is delayed whenever there is a difference in the rate of evolution of nodes and links. This is due to the fact that, being their dynamics coupled, if links evolve faster than nodes, then the links have to wait for the evolution of the nodes, and vice versa. Furthermore, larger values of p lead to faster rates of decrease of the probability of coexistence (see the slope of the dark blue curve as opposed to the dark red one), which points at the fact that faster nodes ($p > 0.5$) lead to a faster evolution of the system than faster links ($p < 0.5$).

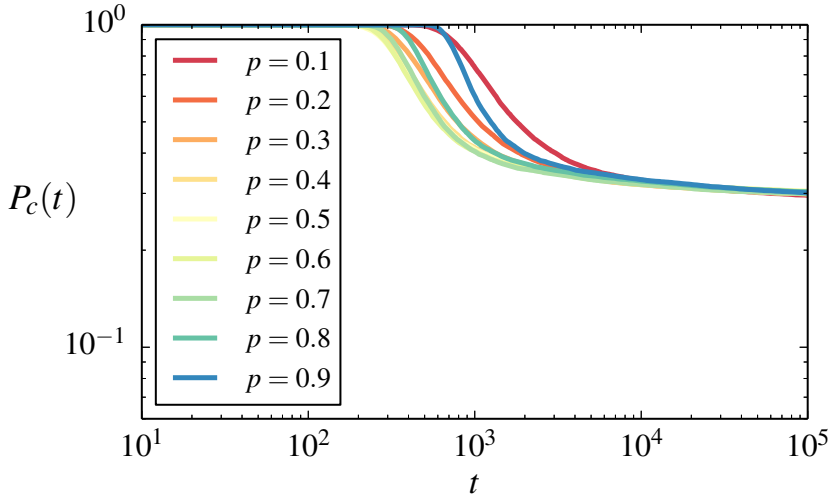

Figure 6.16: Time evolution of the coexistence probability (fraction of realizations not having reached the frozen extinction configuration by time t) for a system size $N = 1000$ and for different values of the parameter p. A total of 10000 realizations were used, with different networks and different initial conditions.

A similar influence of the parameter p can be observed in Fig. 6.17 for the time evolution of the survival probability of the metastable states. Given that all realizations end up escaping from the metastable state and reaching a frozen or dynamically trapped configuration, the asymptotic value of this probability is always zero, independently of the value of p. Again, we observe in panel **(a)** that values of the parameter towards $p = 0$ or $p = 1$ significantly delay the beginning

of the decrease, while larger values of p lead to faster rates of decrease. Regarding the final exponential decay of the probability, we observe in panel **(b)** that the slope of the decay seems to be mostly unaffected by changes in the parameter p.

Finally, let us focus on the influence of the parameter p on the relative likelihood of the different asymptotic states described in the main text of the chapter. In particular, we show in Fig. 6.18 the fraction of realizations having reached each of the possible asymptotic configurations before the end of the studied time period ($t = 10^5$), as well as the fraction of those still in a metastable state, for different system sizes and different values of p (for each color, darker tones identify larger values of p). In general, we observe the same behavior for all values of p, in particular for small system sizes. Note, however, that for large system sizes and both very small and very large values of p, there is a significant number of realizations which, instead of reaching a frozen coexistence configuration, are found to be still in a metastable state at the end of the studied period. This is simply a consequence of the effects described above. In particular, a consequence of the slower evolution of the system for values of p closer to $p = 0$ or $p = 1$.

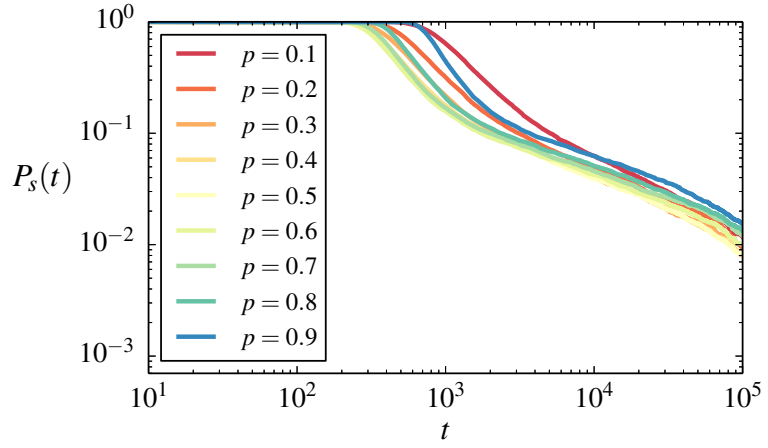

(a) Log–log scale

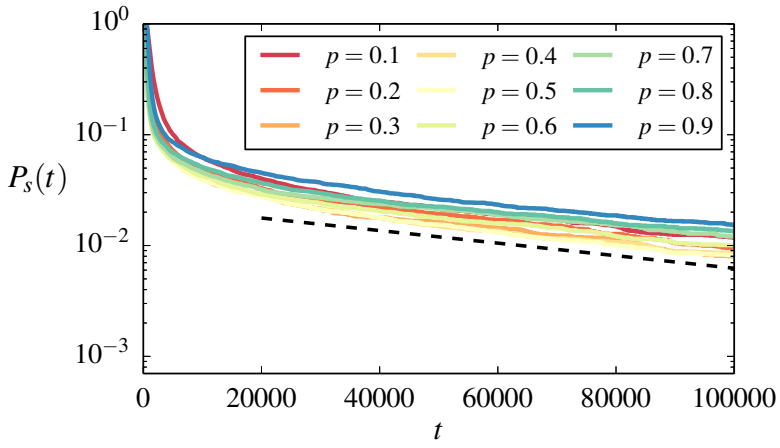

(b) Semilogarithmic scale

Figure 6.17: Time evolution of the survival probability of the metastable states (fraction of realizations not having reached any frozen or dynamically trapped state by time t) on a log–log scale [panel **(a)**] and a semilogarithmic scale [panel **(b)**], for a system size $N = 1000$ and for different values of the parameter p. An exponential decay with the slope obtained by fitting the data for $p = 0.5$ is also shown as a guide to the eye in panel **(b)** (dashed black line). A total of 10000 realizations were used, with different networks and different initial conditions.

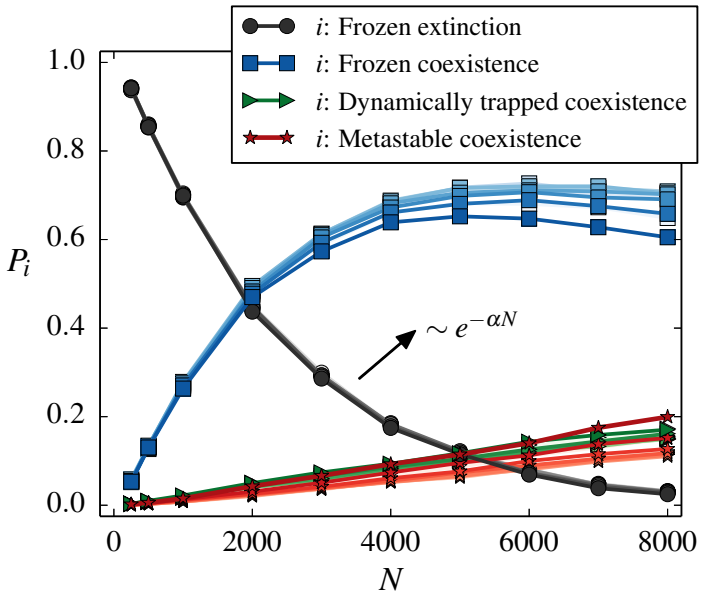

Figure 6.18: Scaling with system size of the fraction of realizations having reached each of the possible asymptotic configurations at the end of the studied time period, $t = 10^5$, as well as the fraction of those still in a metastable state, for different values of the parameter p. Note that, for each color, darker tones identify larger values of p. A total of 10000 realizations were used, with different networks and different initial conditions.

Conclusions

CHAPTER 7

Conclusions and outlook

By means of an agent- or individual-based modeling approach, we have studied the emergence of collective behaviors in social and economic systems. In this way, we have explored different kinds of simple microscopic interaction mechanisms leading to the emergence of complex collective phenomena at the macroscopic level. In particular, we have focused on three main topics: opinion dynamics, herding behavior in financial markets, and language competition.

7.1

Opinion dynamics

In Chapter 2, we studied the influence of the initial distribution of opinions on the asymptotic state of a continuous-opinion, bounded-confidence model based on random pairwise interactions. The results presented underline the importance of this initial distribution of opinions. Indeed, we showed that it is possible to promote or prevent a consensus among a group of agents by imposing an initial distribution of opinions slightly consensual or slightly polarized, respectively. When the agents are given the opportunity to choose a new opinion from a given probability distribution from time to time, however, the influence of the initial condition is mostly replaced by that of the distribution of the noise. Furthermore, we find that the symmetry or lack of symmetry of the initial distribution of opinions does also have an important influence on the outcome of the model, suggesting that the variance of this initial distribution is not enough to predict the asymptotic state, and thus other higher moments should be considered.

Outlook and final remarks

For most of the models presented in the literature, only a random initial condition has been considered. While for some of these models the influence of the initial condition vanishes after a short transient, the analysis presented in the first chapter of this thesis suggests that, for others, the particular asymptotic results obtained might be highly dependent on that initial condition. Thus, the conclusions of such works should be considered as valid only for random initial conditions, until a more detailed exploration of the influence of the initial distribution of states is accomplished. In this context, further work is needed to develop an in-depth classification of models according to their sensitivity to initial conditions.

Regarding the particular model studied in Chapter 2, the Deffuant, Weisbuch et al. model, further work is needed to characterize the influence of higher order moments, beyond the variance, of the initial distribution of opinions. Furthermore, it would be interesting to explore different implementations of the noise. For instance, instead of giving the agents the opportunity to take a random opinion from time to time, which leads sometimes to very large changes, one could think of allowing them to take a new random opinion only in the neighborhood of their current one, or even assuming constant length jumps in the opinion space with a random direction.

7.2

Herding behavior and financial markets

In Chapter 3 we studied the influence of an external source of information upon a financial market model characterized by a competition between herding behavior and idiosyncratic changes of state. By introducing a German index of economic sentiment as an external signal and by comparing the results of the model with the German DAX stock index, we showed that the introduction of an information signal of small strength leads to an improved capacity of the model to reproduce general statistical properties of real financial data, such as the volatility clustering effect, the slow decay of the autocorrelation of the normalized daily volatility for short time lags, and its zero and slightly negative values for long time lags. Furthermore, we were able to identify three different market regimes regarding the assimilation of incoming information, depending on the relative importance of the herding and the idiosyncratic tendencies: an amplification of the incoming information in markets dominated by herding behavior, an undervalu-

ation of incoming information in markets dominated by idiosyncratic behavior, and a regime of precise assimilation of incoming information in-between.

From a practical point of view, it is important to note that the overreaction to incoming information can lead to explosions of fear or confidence triggered from outside the market, and thus not necessarily related to real changes in the fundamental value of the traded asset. We have shown that this amplification of external information is associated with the existence of short periods of enormous price variations, large volatility and, therefore, to a great instability of the market. The results presented in Chapter 3 support the idea that the greater importance of the herding with respect to the idiosyncratic tendency may play an important role in the development of such instabilities in a financial market open to the arrival of external information. In general, the analysis presented in Chapter 3 constitutes an example of how the amplification of incoming information by different social and economic systems can be explained in terms of stochastic resonance phenomena.

In Chapter 4 we focused on the influence of the topology of the social network of interactions between agents in a system characterized, again, by a competition between herding and idiosyncratic behavior. By using an annealed approximation for uncorrelated networks, we were able to uncover the dependence of the asymptotic behavior of the system not only on the mean degree of the underlying topology (the mean-field prediction) but also on more complex averages over the degree distribution. In particular, we showed that different collective behavioral regimes can be achieved by introducing changes in the underlying network of interactions. Furthermore, we showed how the influence of the network on the temporal autocorrelation of the variable characterizing the macroscopic state of the system can be used to infer information about the underlying network —its normalized level of degree heterogeneity— by studying only the aggregate behavior of the system as a whole. The relevance of this latter point is evident for systems where macroscopic, population level variables are easier to measure than their microscopic, individual level counterparts, such as financial markets, where information about the (global) price is much easier to access than information about the market position of each individual trader.

Outlook and final remarks

Regarding the analysis of the influence of an external source of information presented Chapter 3, we did only consider the quality of the response of the market to the arrival of external information. A natural step forward would be to study the delay of the market in following the arrival of news, i.e., to take into account the time lag which leads to the maximum of the cross-correlation function between the input signal and the system output. Our results showing the

existence of different market regimes regarding the assimilation of incoming news open the door for more comprehensive studies taking into account important features of today's information processing by market agents. A most relevant feature of real markets is the existence of different categories of investors, which could be characterized by different levels of sensitivity to incoming information, as empirically found by Lillo et al. (2015). A further aspect to be considered is the asymmetric behavior that traders may have towards positive and negative news, leading, for instance, to explosions of fear but only slow waves of confidence. Note that asymmetry could also be introduced as a different sensitivity to news when prices are rising and when they are falling. Furthermore, we have focused here on the case of a global and passive reception of news. Thus, the modeling of an individual and active search for information, as empirically analyzed by Preis et al. (2010, 2013), Moat et al. (2013), and Curme et al. (2014) is left for future studies.

Given the generality of the approach used in Chapter 4 to study the influence of the underlying network of interactions between agents, it could be easily applied to other stochastic, binary-state models. Even if we compared, for the particular herding model used, our results with those derived from the most simple versions of a mean-field approximation and a mean-field pair-approximation, further research is needed to contrast our method with more nuanced mean-field pair-approximations, such as those based on "link magnetization" (Vazquez and Eguíluz, 2008). In order to keep the presentation of the method as clear and general as possible, we did not use in Chapter 4 the market framework previously introduced in Chapter 3. Therefore, a natural step forward would be to use that one or any other market framework to obtain analytical expressions for the relevant financial variables, such as the autocorrelation of absolute or squared returns, which could then be compared with real financial data.

7.3

Language competition

In Chapter 5 we developed a language competition model with coevolution of the network. In particular, the use of a language is considered as a state of the link between two speakers, its temporal evolution is governed by the majority rule, and links in the local minority can be rewired at random. While topologically static large networks always end up falling into frozen or dynamically trapped configurations where both languages coexist, we showed that, when the rewiring is switched on, the system is able to escape from these configurations and reach an absorbing state that can be either a one-component network where one of the

languages has completely disappeared or a fragmented network with a separate component for each of the two possible languages. The one-component solution is more likely when the plasticity of the network is low or networks are small, while the fragmented solution becomes more and more common as the plasticity of the network increases or networks get larger. For any finite size network, there is a region of the plasticity parameter characterized by the bistability between both possible outcomes. In the very large size limit, however, the bistability region progressively vanishes and thus even very small amounts of rewiring lead to the fragmentation of the network. Thus, we characterized the transition as a finite-size fragmentation transition with a region of bistability. In this way, our results showed that the frozen and dynamically trapped coexistence configurations promoted by the link-based majority rule dynamics are not robust against topological perturbations in the form of a rewiring, since the continuous relinking updates are able to remove the system from the topological traps.

Regarding the language competition model introduced in Chapter 6, where both the use (link state) and the preference (node state) for a given language were included with different but coupled dynamics, a broad range of possible asymptotic configurations were found by numerical simulation of the model on socially-inspired network topologies —based on a mechanism of triadic closure—. We classified these configurations as: frozen extinction states, frozen coexistence states, and dynamically trapped coexistence states. By means of a system size scaling analysis, we showed that the probability of extinction of one of the languages becomes negligible for large enough systems and that, even for small systems, extinction times are so broadly distributed that coexisting realizations can be found at all time scales. Furthermore, metastable coexistence states with non-trivial dynamics were found to be abundant and with survival times which scale linearly with system size. In this way, we showed that, in the infinite size limit, all realizations will be found to be in a non-trivial dynamical coexistence state for any finite time. Interestingly, we found that, as the use of one of the languages decreases, it becomes increasingly confined to the more intimate social spheres or group interactions —triangular relationships—, such that the situations of coexistence were found to be based on the existence of "ghetto-like" structures: groups of predominantly bilingual speakers who use the minority language for the interactions among themselves —mostly triangular— while they switch to the majority language for communications with the rest of the population —mostly non-triangular—. In this way, bilingualism was found to be prevalent among the speakers of the minority language. Thus, our results highlight the importance of the network topology for determining the possibility of coexistence of two competing languages. However, as opposed to previous studies, we find that group interactions —in the form of triangles— can play a more relevant role than simple one to one interactions.

Outlook and final remarks

While examples of language competition are abundant and some of them have been known and studied for a long time, accurate data has traditionally been scarce and limited to aggregate, population level statistics. A further problem is its lack of accurate information about the temporal evolution of language use. This is the kind of data used, for instance, by Abrams and Strogatz (2003), concerning the competition between Quechua and Spanish, between Scottish Gaelic and English, and between Welsh and English. More detailed and up-to-date data has been recently used by Blondel et al. (2008), who analyzed the language used (French or Dutch) by customers of a Belgian mobile phone network, and by Mocanu et al. (2013) and Gonçalves and Sánchez (2014), who studied the use of different languages in Twitter. Unfortunately, these new data sets are still not suitable to test the models developed in this thesis. In the case of phone data, interactions are strictly one-to-one, with no group conversations where speakers can be aware of the language used by their contacts between themselves and modify their preferences accordingly. In the case of Twitter data, the time period available is still too short to capture changes in the network due to language use and the evolution of the speakers' preferences. Furthermore, the broadcasting nature that Twitter inherits from the blog paradigm is likely to influence the speakers' choice of language, which would require a modification of the models presented in this thesis.

Regarding the notion of cognitive cost or effort associated with switching between several languages, it has been suggested in the literature that the cost of switching towards the first language (mother tongue) is lower than the cost of switching towards the second (Meuter and Allport, 1999; Jackson et al., 2001; Abutalebi and Green, 2007; Moritz-Gasser and Duffau, 2009). This asymmetric switching cost could be easily implemented in the models presented here, whether associated to the first language used by a speaker or to its preferred language.

The ideas and methods used here to study language competition processes can also be useful in different contexts. Indeed, the idea of a coevolution of node and link states is very general and could be applied whenever there is a relevant property associated to the interactions between agents or nodes and this property is characterized by a dynamics of its own, which is not completely determined by the states of the agents and their particular dynamics. Examples range from friendship-enmity relationships and trust to the coupled dynamics of trade and economic growth (Garlaschelli et al., 2007). Finally, the importance of triangular structures both in the definition and in the results of the model presented in Chapter 6 calls for a generalization of the concept of network beyond the traditional dyadic interactions, in order to take into account also group interactions of higher order (triadic, tetradic, etc).

Bibliography

Abrams, D. M. and Strogatz, S. H. (2003). Linguistics: Modelling the dynamics of language death. *Nature*, 424(6951):900. [Cited on pages 5, 11, and 190]

Abutalebi, J. and Green, D. (2007). Bilingual language production: The neurocognition of language representation and control. *Journal of Neurolinguistics*, 20(3):242–275. [Cited on pages 15, 133, and 190]

Ahn, Y.-Y., Bagrow, J. P., and Lehmann, S. (2010). Link communities reveal multiscale complexity in networks. *Nature*, 466:761–764. [Cited on page 13]

Al Hammal, O., Chaté, H., Dornic, I., and Muñoz, M. A. (2005). Langevin Description of Critical Phenomena with Two Symmetric Absorbing States. *Physical Review Letters*, 94(23):230601. [Cited on page 82]

Alanyali, M., Moat, H. S., and Preis, T. (2013). Quantifying the relationship between financial news and the stock market. *Scientific Reports*, 3(3578):3578. [Cited on pages 9 and 58]

Albert, R. and Barabási, A.-L. (2002). Statistical mechanics of complex networks. *Reviews of Modern Physics*, 74(1):47–97. [Cited on pages 9 and 81]

Alfarano, S., Lux, T., and Wagner, F. (2005). Estimation of Agent-Based Models: The Case of an Asymmetric Herding Model. *Computational Economics*, 26(1):19–49. [Cited on pages 7, 8, 49, 55, and 61]

Alfarano, S., Lux, T., and Wagner, F. (2008). Time variation of higher moments in a financial market with heterogeneous agents: An analytical approach. *Journal of Economic Dynamics and Control*, 32(1):101–136. [Cited on pages 8, 9, 10, 47, 49, 50, 55, 61, 82, 84, 87, and 101]

Alfarano, S. and Milaković, M. (2009). Network structure and N-dependence in agent-based herding models. *Journal of Economic Dynamics and Control*, 33:78–92. [Cited on pages 7, 10, 49, 61, 82, 84, 88, 90, 91, 94, 95, 96, 97, and 103]

Alfarano, S., Milaković, M., and Raddant, M. (2013). A note on institutional hierarchy and volatility in financial markets. *The European Journal of Finance*, 19(6):449–465. [Cited on pages 10, 49, 82, and 88]

Anderson, R. M., May, R. M., and Anderson, B. (1991). *Infectious Diseases of Humans: Dynamics and Control*. Oxford University Press, Oxford. [Cited on page 81]

Antal, T., Krapivsky, P. L., and Redner, S. (2005). Dynamics of social balance on networks. *Physical Review E*, 72(3):036121. [Cited on page 13]

Antal, T., Krapivsky, P. L., and Redner, S. (2006). Social balance on networks: The dynamics of friendship and enmity. *Physica D: Nonlinear Phenomena*, 224(1–2):130–136. [Cited on page 13]

Appel, R. and Muysken, P. (2006). *Language contact and bilingualism*. Amsterdam University Press. [Cited on page 12]

Arin, K. P., Ciferri, D., and Spagnolo, N. (2008). The price of terror: The effects of terrorism on stock market returns and volatility. *Economics Letters*, 101(3):164–167. [Cited on pages 9 and 58]

Axelrod, R. (2006). Chapter 33 agent-based modeling as a bridge between disciplines. volume 2 of *Handbook of Computational Economics*, pages 1565 – 1584. Elsevier. [Cited on page 4]

Baek, Y., Ha, M., and Jeong, H. (2012). Absorbing states of zero-temperature Glauber dynamics in random networks. *Physical Review E*, 85(3):31123. [Cited on pages 13 and 134]

Baggs, I. and Freedman, H. I. (1990). A mathematical model for the dynamics of interactions between a unilingual and a bilingual population: Persistence versus extinction. *The Journal of Mathematical Sociology*, 16(1):51–75. [Cited on page 12]

Baggs, I. and Freedman, H. I. (1993). Can the speakers of a dominated language survive as unilinguals?: A mathematical model of bilingualism. *Mathematical and Computer Modelling*, 18(6):9–18. [Cited on page 12]

Barabási, A.-L. (1999). Emergence of Scaling in Random Networks. *Science*, 286(5439):509–512. [Cited on pages 4 and 83]

Baronchelli, A., Loreto, V., and Tria, F. (2012). Language dynamics. *Advances in Complex Systems*, 15(3 & 4):1203002. [Cited on page 11]

Barrat, A., Barthelemy, M., and Vespignani, A. (2008). *Dynamical processes on complex networks*. Cambridge University Press. [Cited on pages 9 and 81]

Battiston, F., Cairoli, A., Nicosia, V., Baule, A., and Latora, V. (2016). Interplay between consensus and coherence in a model of interacting opinions. *Physica D: Nonlinear Phenomena*, 323–324:12–19. [Cited on page 4]

Ben-Naim, E., Krapivsky, P. L., and Redner, S. (2003a). Bifurcations and patterns in compromise processes. *Physica D: Nonlinear Phenomena*, 183(3–4):190–204. [Cited on pages 22, 23, 24, and 26]

Ben-Naim, E., Krapivsky, P. L., Vazquez, F., and Redner, S. (2003b). Unity and discord in opinion dynamics. *Physica A: Statistical Mechanics and its Applications*, 330(1–2):99–106. [Cited on page 4]

Benzi, R., Parisi, G., Sutera, A., and Vulpiani, A. (1982). Stochastic resonance in climatic change. *Tellus*, 34(1):10–16. [Cited on page 71]

Benzi, R., Sutera, A., and Vulpiani, A. (1981). The mechanism of stochastic resonance. *Journal of Physics A: Mathematical and General*, 14(11):L453. [Cited on page 71]

Bianconi, G. (2009). Entropy of network ensembles. *Physical Review E*, 79(3):36114. [Cited on pages 10 and 87]

Bianconi, G., Darst, R. K., Iacovacci, J., and Fortunato, S. (2014). Triadic closure as a basic generating mechanism of communities in complex networks. *Physical Review E*, 90(4):42806. [Cited on pages 16 and 157]

Blondel, V., Guillaume, J., Lambiotte, R., and Lefebvre, E. (2008). Fast unfolding of communities in large networks. *Journal of Statistical Mechanics: Theory and Experiment*, 2008(10):P10008. [Cited on page 190]

Boccaletti, S., Latora, V., Moreno, Y., Chavez, M., and Hwang, D.-U. (2006). Complex networks: Structure and dynamics. *Physics Reports*, 424(4–5):175–308. [Cited on page 3]

Boguñá, M., Pastor-Satorras, R., Díaz-Guilera, A., and Arenas, A. (2004). Models of social networks based on social distance attachment. *Physical Review E*, 70:056122. [Cited on page 16]

Boguñá, M., Pastor-Satorras, R., and Vespignani, A. (2003). Absence of Epidemic Threshold in Scale-Free Networks with Degree Correlations. *Physical Review Letters*, 90(2):28701. [Cited on pages 9 and 81]

Boguñá, M., Pastor-Satorras, R., and Vespignani, A. (2004). Cut-offs and finite size effects in scale-free networks. *European Physical Journal B*, 38(2):205–209. [Cited on pages 10, 87, and 104]

Bornholdt, S. (2001). Expectation bubbles in a spin model of markets: Intermittency from frustration across scales. *International Journal of Modern Physics C*, 12(05):667–674. [Cited on page 7]

Bouchaud, J.-P. (2010). The endogenous dynamics of markets: price impact and feedback loops. *arXiv preprint arXiv:1009.2928*. [Cited on page 9]

Brock, W. A. and Hommes, C. (1997). A Rational Route to Randomness. *Econometrica*, 65(5):1059–1096. [Cited on page 7]

Caridi, I., Nemiña, F., Pinasco, J. P., and Schiaffino, P. (2013). Schelling-voter model: An application to language competition. *Chaos, Solitons & Fractals*, 56:216–221. [Cited on page 11]

Carro, A., Toral, R., and San Miguel, M. (2013). The role of noise and initial conditions in the asymptotic solution of a bounded confidence, continuous-opinion model. *Journal of Statistical Physics*, 151(1):131–149. [Cited on page 17]

Carro, A., Toral, R., and San Miguel, M. (2015). Markets, Herding and Response to External Information. *PLoS ONE*, 10(7):e0133287. [Cited on page 17]

Carro, A., Toral, R., and San Miguel, M. (2016a). The noisy voter model on complex networks. *Scientific Reports*, 6:24775. [Cited on page 17]

Carro, A., Toral, R., and San Miguel, M. (2016b). Coupled dynamics of node and link states: A model for language competition. Working paper. [Cited on page 17]

Carro, A., Vazquez, F., Toral, R., and San Miguel, M. (2014). Fragmentation transition in a coevolving network with link-state dynamics. *Physical Review E*, 89(6):62802. [Cited on pages 17, 158, and 159]

Castellano, C., Fortunato, S., and Loreto, V. (2009). Statistical physics of social dynamics. *Reviews of Modern Physics*, 81(2):591–646. [Cited on pages 3, 4, and 81]

Castellano, C., Loreto, V., Barrat, A., Cecconi, F., and Parisi, D. (2005). Comparison of voter and Glauber ordering dynamics on networks. *Physical Review E*, 71(6):66107. [Cited on pages 13 and 134]

Castellano, C. and Pastor-Satorras, R. (2006). Zero temperature Glauber dynamics on complex networks. *Journal of Statistical Mechanics: Theory and Experiment*, 2006(05):P05001. [Cited on pages 13 and 143]

Castellano, C. and Pastor-Satorras, R. (2010). Thresholds for Epidemic Spreading in Networks. *Physical Review Letters*, 105(21):218701. [Cited on page 10]

Castellano, C. and Pastor-Satorras, R. (2012). Competing activation mechanisms in epidemics on networks. *Scientific Reports*, 2. [Cited on page 81]

Castelló, X., Eguíluz, V. M., and San Miguel, M. (2006). Ordering dynamics with two non-excluding options: bilingualism in language competition. *New Journal of Physics*, 8(12):308. [Cited on pages 11, 12, and 171]

Castelló, X., Loureiro-Porto, L., and San Miguel, M. (2013). Agent-based models of language competition. *International Journal of the Sociology of Language*, (221):21–51. [Cited on page 11]

Castelló, X., Toivonen, R., Eguíluz, V. M., Saramäki, J., Kaski, K., and San Miguel, M. (2007). Anomalous lifetime distributions and topological traps in ordering dynamics. *EPL (Europhysics Letters)*, 79(6):66006. [Cited on pages 12 and 172]

Catanzaro, M., Boguñá, M., and Pastor-Satorras, R. (2005). Generation of uncorrelated random scale-free networks. *Physical Review E*, 71(2):27103. [Cited on page 104]

Chakraborti, A., Toke, I., Patriarca, M., and Abergel, F. (2011a). Econophysics review: I. empirical facts. *Quantitative Finance*, 11(7):991–1012. [Cited on page 3]

Chakraborti, A., Toke, I., Patriarca, M., and Abergel, F. (2011b). Econophysics review: Ii. agent-based models. *Quantitative Finance*, 11(7):1013–1041. [Cited on page 3]

Chang, S.-K. (2007). A simple asset pricing model with social interactions and heterogeneous beliefs. *Journal of Economic Dynamics and Control*, 31(4):1300–1325. [Cited on page 7]

Chartrand, G. and Stewart, M. (1969). The connectivity of line-graphs. *Mathematische Annalen*, 182(3):170–174. [Cited on page 14]

Clementi, F., Di Matteo, T., and Gallegati, M. (2006). The power-law tail exponent of income distributions. *Physica A: Statistical Mechanics and its Applications*, 370(1):49–53. [Cited on page 6]

Clifford, P. and Sudbury, A. (1973). A model for spatial conflict. *Biometrika*, 60(3):581–588. [Cited on pages 8, 12, 81, and 82]

Collins, J. J., Chow, C. C., Capela, A. C., and Imhoff, T. T. (1996). Aperiodic stochastic resonance. *Physical Review E*, 54(5):5575–5584. [Cited on page 71]

Collins, J. J., Chow, C. C., and Imhoff, T. T. (1995). Aperiodic stochastic resonance in excitable systems. *Physical Review E*, 52(4):R3321–R3324. [Cited on page 71]

Colomer-de Simón, P., Serrano, M. Á., Beiró, M. G., Alvarez-Hamelin, J. I., and Boguñá, M. (2013). Deciphering the global organization of clustering in real complex networks. *Scientific Reports*, 3. [Cited on pages 16 and 157]

Considine, D., Redner, S., and Takayasu, H. (1989). Comment on "Noise-induced bistability in a Monte Carlo surface-reaction model". *Physical Review Letters*, 63(26):2857. [Cited on pages 8 and 82]

Cont, R. (2001). Empirical properties of asset returns: stylized facts and statistical issues. *Quantitative Finance*, 1(2):223–236. [Cited on pages 6 and 66]

Cont, R. (2005). Long range dependence in financial markets. In Lévy-Véhel, J. and Lutton, E., editors, *Fractals in Engineering*, pages 159–179. Springer London. [Cited on page 66]

Cont, R. and Bouchaud, J.-P. (2000). Herd behavior and aggregate fluctuations in financial markets. *Macroeconomic Dynamics*, 4(02):170–196. [Cited on page 7]

Crawley, M. J. and May, R. M. (1987). Population dynamics and plant community structure: Competition between annuals and perennials. *Journal of Theoretical Biology*, 125(4):475–489. [Cited on page 81]

Curme, C., Preis, T., Stanley, H. E., and Moat, H. S. (2014). Quantifying the semantics of search behavior before stock market moves. *Proceedings of the National Academy of Sciences*, 111(32):11600–11605. [Cited on pages 58 and 188]

Davidsen, J., Ebel, H., and Bornholdt, S. (2002). Emergence of a small world from local interactions: Modeling acquaintance networks. *Physical Review Letters*, 88(12):128701. [Cited on page 16]

Davis, A. (2006). Media effects and the question of the rational audience: lessons from the financial markets. *Media, Culture & Society*, 28(4):603–625. [Cited on page 58]

De Vries, C. G. (1994). Stylized facts of nominal exchange rate returns. In van der Ploeg, F., editor, *The Handbook of International Macroeconomics*, pages 348–389. Blackwell, Oxford. [Cited on page 6]

Deffuant, G., Neau, D., Amblard, F., and Weisbuch, G. (2000). Mixing beliefs among interacting agents. *Advances in Complex Systems*, 3:87–98. [Cited on pages 5, 21, 22, and 23]

Demirel, G., Vazquez, F., Böhme, G. A., and Gross, T. (2014). Moment-closure approximations for discrete adaptive networks. *Physica D: Nonlinear Phenomena*, 267(0):68–80. [Cited on page 14]

Di Matteo, T. (2007). Multi-scaling in finance. *Quantitative Finance*, 7(1):21–36. [Cited on page 6]

Diakonova, M., Eguíluz, V. M., and San Miguel, M. (2015). Noise in coevolving networks. *Physical Review E*, 92(3):32803. [Cited on pages 10, 82, 84, 88, 91, 95, 96, 97, 98, 100, 101, 103, and 127]

Ding, Z., Granger, C. W. J., and Engle, R. F. (1993). A long memory property of stock market returns and a new model. *Journal of Empirical Finance*, 1(1):83–106. [Cited on pages 7 and 66]

Dorogovtsev, S. N., Goltsev, A. V., and Mendes, J. F. F. (2002). Ising model on networks with an arbitrary distribution of connections. *Physical Review E*, 66(1):16104. [Cited on pages 9 and 81]

Dorogovtsev, S. N., Goltsev, A. V., and Mendes, J. F. F. (2008). Critical phenomena in complex networks. *Reviews of Modern Physics*, 80(4):1275–1335. [Cited on page 86]

Dorogovtsev, S. N. and Mendes, J. F. F. (2003). *Evolution of Networks: From Biological Nets to the Internet and WWW (Physics)*. Oxford University Press, Oxford. [Cited on pages 16 and 157]

Drakos, K. (2010). Terrorism activity, investor sentiment, and stock returns. *Review of Financial Economics*, 19(3):128–135. [Cited on page 58]

Durrett, R. (2010). Some features of the spread of epidemics and information on a random graph. *Proceedings of the National Academy of Sciences*, 107(10):4491–4498. [Cited on page 9]

Eguíluz, V. M. and Zimmermann, M. G. (2000). Transmission of Information and Herd Behavior: An Application to Financial Markets. *Physical Review Letters*, 85(26):5659–5662. [Cited on page 8]

Epstein, J. and Axtell, R. (1996). *Growing Artificial Societies: Social Science from the Bottom Up*. The MIT Press. [Cited on page 4]

Erdös, P. and Rényi, A. (1960). On the evolution of random graphs. *Publications of the Mathematical Institute of the Hungarian Academy of Sciences*, 5:17–61. [Cited on page 83]

Evans, T. S. and Lambiotte, R. (2009). Line graphs, link partitions, and overlapping communities. *Physical Review E*, 80(1):16105. [Cited on page 13]

Evans, T. S. and Lambiotte, R. (2010). Line graphs of weighted networks for overlapping communities. *The European Physical Journal B*, 77(2):265–272. [Cited on page 13]

Fama, E. F. (1970). Efficient capital markets: A review of theory and empirical work. *The Journal of Finance*, 25(2):383–417. [Cited on page 7]

Fernández-Gracia, J., Castelló, X., Eguíluz, V. M., and San Miguel, M. (2012). Dynamics of link states in complex networks: The case of a majority rule. *Physical Review E*, 86(6):66113. [Cited on pages 13, 14, 131, 134, 135, 141, 155, 158, and 159]

Fichthorn, K., Gulari, E., and Ziff, R. (1989). Noise-induced bistability in a Monte Carlo surface-reaction model. *Physical Review Letters*, 63(14):1527–1530. [Cited on pages 8 and 82]

Fortunato, S. (2004). Universality of the threshold for complete consensus for the opinion dynamics of deffuant et al. *International Journal of Modern Physics C*, 15(09):1301–1307. [Cited on page 6]

Fortunato, S., Latora, V., Pluchino, A., and Rapisarda, A. (2005). Vector opinion dynamics in a bounded confidence consensus model. *International Journal of Modern Physics C*, 16(10):1535–1551. [Cited on page 5]

Foster, D. V., Foster, J. G., Grassberger, P., and Paczuski, M. (2011). Clustering drives assortativity and community structure in ensembles of networks. *Physical Review E*, 84(6):66117. [Cited on pages 16 and 157]

Gammaitoni, L., Hänggi, P., Jung, P., and Marchesoni, F. (1998). Stochastic resonance. *Reviews of modern physics*, 70(1):223–287. [Cited on page 71]

Garlaschelli, D., Di Matteo, T., Aste, T., Caldarelli, G., and Loffredo, I. M. (2007). Interplay between topology and dynamics in the world trade web. *The European Physical Journal B*, 57(2):159–164. [Cited on page 190]

Gillespie, D. T. (1977). Exact stochastic simulation of coupled chemical reactions. *The Journal of Physical Chemistry*, 81(25):2340–2361. [Cited on page 61]

Gillespie, D. T. (1992). Markov Processes: An Introduction for Physical Scientists. *Academic Press, San Diego CA*. [Cited on page 61]

Gleeson, J. P. (2011). High-Accuracy Approximation of Binary-State Dynamics on Networks. *Physical Review Letters*, 107(6):68701. [Cited on pages 9 and 81]

Gleeson, J. P. (2013). Binary-State Dynamics on Complex Networks: Pair Approximation and Beyond. *Physical Review X*, 3(2):21004. [Cited on pages 9 and 81]

Golub, A., Chliamovitch, G., Dupuis, A., and Chopard, B. (2015). Uncovering Discrete Non-Linear Dependence with Information Theory. *Entropy*, 17(5):2606–2623. [Cited on page 9]

Gonçalves, B. and Sánchez, D. (2014). Crowdsourcing dialect characterization through twitter. *PLoS ONE*, 9(11):1–6. [Cited on page 190]

Granovetter, M. (1978). Threshold Models of Collective Behavior. *American Journal of Sociology*, 83(6):pp. 1420–1443. [Cited on page 60]

Granovsky, B. L. and Madras, N. (1995). The noisy voter model. *Stochastic Processes and their Applications*, 55(1):23–43. [Cited on pages 8, 10, 82, and 84]

Gross, T. and Blasius, B. (2008). Adaptive coevolutionary networks: a review. *Journal of The Royal Society Interface*, 5(20):259–271. [Cited on page 14]

Guerra, B. and Gómez-Gardeñes, J. (2010). Annealed and mean-field formulations of disease dynamics on static and adaptive networks. *Physical Review E*, 82(3):35101. [Cited on page 86]

Gunton, J. D., San Miguel, M., and Sahni, P. S. (1983). The Dynamics of First Order Phase Transitions. In *Phase Transitions and Critical Phenomena*, volume 8, pages 269–466. Academic Press. [Cited on page 81]

Häggström, O. (2002). Zero-temperature dynamics for the ferromagnetic Ising model on random graphs. *Physica A: Statistical Mechanics and its Applications*, 310(3–4):275–284. [Cited on page 13]

Hanousek, J., Kočenda, E., and Kutan, A. M. (2009). The reaction of asset prices to macroeconomic announcements in new {EU} markets: Evidence from intraday data. *Journal of Financial Stability*, 5(2):199–219. [Cited on pages 9 and 58]

Harras, G. and Sornette, D. (2011). How to grow a bubble: A model of myopic adapting agents. *Journal of Economic Behavior & Organization*, 80(1):137–152. [Cited on page 9]

Harras, G., Tessone, C. J., and Sornette, D. (2012). Noise-induced volatility of collective dynamics. *Physical Review E*, 85(1):11150. [Cited on page 58]

Healy, P. M. and Palepu, K. G. (2001). Information asymmetry, corporate disclosure, and the capital markets: A review of the empirical disclosure literature. *Journal of Accounting and Economics*, 31(1–3):405–440. [Cited on page 57]

Hegselmann, R. and Krause, U. (2002). Opinion dynamics and bounded confidence: Models, analysis and simulation. *Journal of Artificial Societies and Social Simulation*, 5:1–24. [Cited on page 5]

Heider, F. (1946). Attitudes and Cognitive Organization. *The Journal of Psychology*, 21(1):107–112. [Cited on page 13]

Heinsalu, E., Patriarca, M., and Léonard, J. L. (2014). The role of bilinguals in language competition. *Advances in Complex Systems*, 17(01):1450003. [Cited on page 12]

Heneghan, C., Chow, C. C., Collins, J. J., Imhoff, T. T., Lowen, S. B., and Teich, M. C. (1996). Information measures quantifying aperiodic stochastic resonance. *Physical Review E*, 54(3):R2228–R2231. [Cited on page 71]

Herrera, J. L., Cosenza, M. G., Tucci, K., and González-Avella, J. C. (2011). General coevolution of topology and dynamics in networks. *EPL (Europhysics Letters)*, 95(5):58006. [Cited on page 14]

Holley, R. A. and Liggett, T. M. (1975). Ergodic Theorems for Weakly Interacting Infinite Systems and the Voter Model. *The Annals of Probability*, 3(4):643–663. [Cited on pages 8, 12, and 82]

Holme, P. and Kim, B. J. (2002). Growing scale-free networks with tunable clustering. *Physical Review E*, 65(2):026107. [Cited on page 16]

Holme, P. and Newman, M. E. J. (2006). Nonequilibrium phase transition in the coevolution of networks and opinions. *Physical Review E*, 74(5):56108. [Cited on page 14]

Hommes, C. (2006). Chapter 23 Heterogeneous Agent Models in Economics and Finance. volume 2 of *Handbook of Computational Economics*, pages 1109–1186. Elsevier. [Cited on page 7]

Hopfield, J. J. (1982). Neural networks and physical systems with emergent collective computational abilities. *Proceedings of the National Academy of Sciences*, 79(8):2554–2558. [Cited on page 81]

Iñiguez, G., Török, J., Yasseri, T., Kaski, K., and Kertész, J. (2014). Modeling social dynamics in a collaborative environment. *EPJ Data Science*, 3(1):1–20. [Cited on page 5]

Iori, G. (2002). A microsimulation of traders activity in the stock market: the role of heterogeneity, agents' interactions and trade frictions. *Journal of Economic Behavior & Organization*, 49(2):269–285. [Cited on page 7]

Isern, N. and Fort, J. (2014). Language extinction and linguistic fronts. *Journal of The Royal Society Interface*, 11(94). [Cited on page 11]

Itô, K. (1951). On stochastic differential equations. *Memoirs of the American Mathematical Society*, 4:1–51. [Cited on page 51]

Jackson, G. M., Swainson, R., Cunnington, R., and Jackson, S. R. (2001). Erp correlates of executive control during repeated language switching. *Bilingualism: Language and cognition*, 4(02):169–178. [Cited on pages 15, 133, 151, 153, and 190]

Jackson, M. O. and Rogers, B. W. (2007). Meeting strangers and friends of friends: How random are social networks? *American Economic Review*, 97(3):890–915. [Cited on page 16]

Jegadeesh, N. and Kim, W. (2006). Value of analyst recommendations: International evidence. *Journal of Financial Markets*, 9(3):274–309. [Cited on pages 9 and 58]

Johansen, A. and Sornette, D. (2002). Endogenous versus Exogenous Crashes in Financial Markets. *arXiv preprint cond-mat/0210509*. [Cited on page 9]

Joulin, A., Lefevre, A., Grunberg, D., and Bouchaud, J.-P. (2008). Stock price jumps: news and volume play a minor role. *arXiv preprint arXiv:0803.1769*. [Cited on page 58]

Kirman, A. (1991). Epidemics of opinion and speculative bubbles in financial markets. In Taylor, M. P., editor, *Money and financial markets*, pages 354–368. Blackwell, Cambridge. [Cited on pages 7, 8, 9, 47, 55, and 82]

Kirman, A. (1992). Whom or what does the representative individual represent? *The Journal of Economic Perspectives*, 6(2):117–136. [Cited on page 7]

Kirman, A. (1993). Ants, rationality and recruitment. *Quarterly Journal of Economics*, 108:137–156. [Cited on pages 7, 8, 9, 10, 47, 48, 49, 82, 84, and 87]

Kirman, A. and Teyssière, G. (2002). Microeconomic Models for Long Memory in the Volatility of Financial Time Series. *Studies in Nonlinear Dynamics & Econometrics*, 5(4):1–23. [Cited on page 55]

Kiymaz, H. (2001). The effects of stock market rumors on stock prices: evidence from an emerging market. *Journal of Multinational Financial Management*, 11(1):105–115. [Cited on pages 9 and 58]

Klemm, K., M Eguíluz, V., Toral, R., and San Miguel, M. (2003). Role of dimensionality in axelrod's model for the dissemination of culture. *Physica A: Statistical Mechanics and its Applications*, 327(1–2):1–5. [Cited on page 10]

Klimek, P., Lambiotte, R., and Thurner, S. (2008). Opinion formation in laggard societies. *EPL (Europhysics Letters)*, 82(2):28008. [Cited on page 4]

Klimek, P. and Thurner, S. (2013). Triadic closure dynamics drives scaling laws in social multiplex networks. *New Journal of Physics*, 15(6):63008. [Cited on pages 16 and 157]

Kononovicius, A. and Gontis, V. (2012). Agent based reasoning for the non-linear stochastic models of long-range memory. *Physica A: Statistical Mechanics and its Applications*, 391(4):1309–1314. [Cited on pages 49, 55, and 61]

Krapivsky, P. L. and Redner, S. (2005). Network growth by copying. *Physical Review E*, 71(3):036118. [Cited on page 16]

Krause, U. (2000). A Discrete Nonlinear and Non-Autonomous Model of Consensus Formation. In Elyadi, S., Ladas, G., Popenda, J., and Rakowski, J., editors, *Communications in Difference Equations*, pages 227–236. Gordon and Breach Pub., Amsterdam. [Cited on page 5]

Krawczyk, M. J., Muchnik, L., Mańka-Krasoń, A., and Kulakowski, K. (2011). Line graphs as social networks. *Physica A: Statistical Mechanics and its Applications*, 390(13):2611–2618. [Cited on pages 14 and 159]

Lafuerza, L. F. and Toral, R. (2013). On the effect of heterogeneity in stochastic interacting-particle systems. *Scientific Reports*, 3. [Cited on pages 10, 85, and 103]

Laguna, M. F., Abramson, G., and Zanette, D. H. (2004). Minorities in a model for opinion formation. *Complexity*, 9(4):31–36. [Cited on page 23]

Lambiotte, R. (2007). How does degree heterogeneity affect an order-disorder transition? *EPL (Europhysics Letters)*, 78(6):68002. [Cited on pages 9, 81, 83, and 97]

Lebowitz, J. L. and Saleur, H. (1986). Percolation in strongly correlated systems. *Physica A: Statistical Mechanics and its Applications*, 138(1):194–205. [Cited on pages 8, 10, 82, and 84]

Leone, M., Vázquez, A., Vespignani, A., and Zecchina, R. (2002). Ferromagnetic ordering in graphs with arbitrary degree distribution. *European Physical Journal B*, 28(2):191–197. [Cited on page 9]

Leskovec, J., Huttenlocher, D., and Kleinberg, J. (2010a). Predicting Positive and Negative Links in Online Social Networks. In *Proceedings of the 19th International Conference on World Wide Web*, WWW '10, pages 641–650, New York, NY, USA. ACM. [Cited on page 13]

Leskovec, J., Huttenlocher, D., and Kleinberg, J. (2010b). Signed Networks in Social Media. In *Proceedings of the SIGCHI Conference on Human Factors in Computing Systems*, CHI '10, pages 1361–1370, New York, NY, USA. ACM. [Cited on page 13]

Lillo, F., Micciché, S., Tumminello, M., Piilo, J., and Mantegna, R. N. (2015). How news affects the trading behaviour of different categories of investors in a financial market. *Quantitative Finance*, 15(2):213–229. [Cited on pages 9, 58, and 188]

Liu, D., Blenn, N., and Mieghem, P. V. (2012). A Social Network Model Exhibiting Tunable Overlapping Community Structure. *Procedia Computer Science*, 9(0):1400–1409. [Cited on page 13]

Lorenz, J. (2007a). Continuous Opinion Dynamics under Bounded Confidence: A Survey. *International Journal of Modern Physics C*, 18(12):1819–1838. [Cited on pages 5 and 6]

Lorenz, J. (2007b). Repeated Averaging and Bounded Confidence-Modeling, Analysis and Simulation of Continuous Opinion Dynamics. *PHD Thesis Universität Bremen*. [Cited on pages 6, 24, 25, 26, 29, and 30]

Lorenz, J. (2010). Heterogeneous bounds of confidence: Meet, discuss and find consensus! *Complexity*, 15(4):43–52. [Cited on pages 24 and 29]

Lorenz, J. and Tonella, G. (2005). Continuous opinion dynamics: Insights through interactive Markov chains. *Proceedings of the Fifth IASTED International Conference on Modelling, Simulation, and Optimization*, pages 61–66. [Cited on pages 22, 24, and 30]

Loreto, V. and Steels, L. (2007). Social dynamics: Emergence of language. *Nature Physics*, 3:758–760. [Cited on page 11]

Lux, T. (2006). Financial power laws: Empirical evidence, models, and mechanism. Technical report, Economics working paper No 2006-12, Christian-Albrechts-Universit{ä}t Kiel, Department of Economics. [Cited on page 7]

Lux, T. and Marchesi, M. (1999). Scaling and criticality in a stochastic multi-agent model of a financial market. *Nature*, 397:498–500. [Cited on pages 7, 8, 49, and 55]

Mandelbrot, B. B. (1963). The variation of certain speculative prices. *The Journal of Business*, 36(4):394–419. [Cited on page 6]

Mandelbrot, B. B. (1997). The variation of certain speculative prices. In *Fractals and Scaling in Finance*, pages 371–418. Springer New York. [Cited on page 66]

Mandrà, S., Fortunato, S., and Castellano, C. (2009). Coevolution of Glauber-like Ising dynamics and topology. *Physical Review E*, 80(5):56105. [Cited on page 14]

Marro, J. and Dickman, R. (1999). *Nonequilibrium phase transitions in lattice models*. Cambridge University Press. [Cited on page 81]

Marvel, S. A., Kleinberg, J., Kleinberg, R. D., and Strogatz, S. H. (2011). Continuous-time model of structural balance. *Proceedings of the National Academy of Sciences*, 108(5):1771–1776. [Cited on page 13]

Mäs, M., Flache, A., and Helbing, D. (2010). Individualization as Driving Force of Clustering Phenomena in Humans. *PLoS Computational Biology*, 6(10):e1000959. [Cited on page 27]

Masuda, N. and Konno, N. (2004). Return times of random walk on generalized random graphs. *Physical Review E*, 69(6):66113. [Cited on pages 10 and 81]

Mańka-Krasoń, A., Mwijage, A., and Kulakowski, K. (2010). Clustering in random line graphs. *Computer Physics Communications*, 181(1):118–121. [Cited on page 14]

Meuter, R. F. I. and Allport, A. (1999). Bilingual language switching in naming: Asymmetrical costs of language selection. *Journal of Memory and Language*, 40(1):25–40. [Cited on pages 15, 133, 151, 153, and 190]

Minett, J. W. and Wang, W. S.-Y. (2008). Modelling endangered languages: The effects of bilingualism and social structure. *Lingua*, 118(1):19–45. [Cited on page 12]

Mira, J. and Paredes, Á. (2005). Interlinguistic similarity and language death dynamics. *EPL (Europhysics Letters)*, 69(6):1031. [Cited on pages 11 and 12]

Moat, H. S., Curme, C., Avakian, A., Kenett, D. Y., Stanley, H. E., and Preis, T. (2013). Quantifying Wikipedia usage patterns before stock market moves. *Scientific Reports*, 3. [Cited on pages 58 and 188]

Mocanu, D., Baronchelli, A., Perra, N., Gonçalves, B., Zhang, Q., and Vespignani, A. (2013). The twitter of babel: Mapping world languages through microblogging platforms. *PLoS ONE*, 8(4):1–9. [Cited on page 190]

Moritz-Gasser, S. and Duffau, H. (2009). Cognitive processes and neural basis of language switching: proposal of a new model. *NeuroReport*, 20. [Cited on pages 15, 133, and 190]

Mufwene, S., editor (2016). *Complexity in language: developmental and evolutionary perspectives*. Cambridge University Press. In press. [Cited on page 11]

Nepusz, T. and Vicsek, T. (2012). Controlling edge dynamics in complex networks. *Nature Physics*, 8:568–573. [Cited on page 13]

Newman, M. E. J. (2003). The Structure and Function of Complex Networks. *SIAM Review*, 45(2):167–256. [Cited on pages 10 and 86]

Newman, M. E. J. (2009). Random Graphs with Clustering. *Physical Review Letters*, 103(5):58701. [Cited on pages 16 and 157]

Newman, M. E. J. (2010). *Networks: an introduction*. Oxford University Press, Oxford. [Cited on pages 3, 9, 16, 81, and 157]

Newman, M. E. J. (2011). Resource letter cs–1: Complex systems. *American Journal of Physics*, 79(8):800–810. [Cited on page 4]

Newman, M. E. J. and Park, J. (2003). Why social networks are different from other types of networks. *Physical Review E*, 68(3):36122. [Cited on pages 9, 16, 81, and 157]

Nicolis, C. and Nicolis, G. (1981). Stochastic aspects of climatic transitions–Additive fluctuations. *Tellus*, 33(3):225–234. [Cited on page 71]

Olejarz, J., Krapivsky, P. L., and Redner, S. (2011a). Zero-temperature freezing in the three-dimensional kinetic Ising model. *Physical Review E*, 83(3):30104. [Cited on page 160]

Olejarz, J., Krapivsky, P. L., and Redner, S. (2011b). Zero-temperature relaxation of three-dimensional Ising ferromagnets. *Physical Review E*, 83(5):51104. [Cited on page 160]

Parshani, R., Carmi, S., and Havlin, S. (2010). Epidemic Threshold for the Susceptible-Infectious-Susceptible Model on Random Networks. *Physical Review Letters*, 104(25):258701. [Cited on page 10]

Pastor-Satorras, R. and Vespignani, A. (2001). Epidemic Spreading in Scale-Free Networks. *Physical Review Letters*, 86(14):3200–3203. [Cited on page 81]

Patriarca, M., Castelló, X., Uriarte, J. R., Eguíluz, V. M., and San Miguel, M. (2012). Modeling two-language competition dynamics. *Advances in Complex Systems*, 15(03n04):1250048. [Cited on page 11]

Patriarca, M. and Leppänen, T. (2004). Modeling language competition. *Physica A: Statistical Mechanics and its Applications*, 338(1–2):296–299. [Cited on page 11]

Pinasco, J. P. and Romanelli, L. (2006). Coexistence of Languages is possible. *Physica A: Statistical Mechanics and its Applications*, 361(1):355–360. [Cited on page 11]

Pineda, M., Toral, R., and Hernández-García, E. (2009). Noisy continuous-opinion dynamics. *Journal of Statistical Mechanics: Theory and Experiment*, 2009(08):P08001. [Cited on pages 6, 21, 26, 31, 36, 38, and 40]

Pineda, M., Toral, R., and Hernández-García, E. (2011). Diffusing opinions in bounded confidence processes. *European Physical Journal D*, 62:109. [Cited on pages 6, 21, and 38]

Pineda, M., Toral, R., and Hernández-García, E. (2013). The noisy hegselmann-krause model for opinion dynamics. *The European Physical Journal B*, 86(12):1–10. [Cited on pages 6 and 21]

Pluchino, A., Latora, V., and Rapisarda, A. (2005). Changing opinions in a changing world: A new perspective in sociophysics. *International Journal of Modern Physics C*, 16(4):515–531. [Cited on page 4]

Porfiri, M., Bollt, E. M., and Stilwell, D. J. (2007). Decline of minorities in stubborn societies. *The European Physical Journal B*, 57(4):481–486. [Cited on page 23]

Preis, T., Moat, H. S., and Stanley, H. E. (2013). Quantifying trading behavior in financial markets using Google Trends. *Scientific Reports*, 3. [Cited on pages 58 and 188]

Preis, T., Reith, D., and Stanley, H. E. (2010). Complex dynamics of our economic life on different scales: insights from search engine query data. *Philosophical Transactions of the Royal Society A: Mathematical, Physical and Engineering Sciences*, 368(1933):5707–5719. [Cited on pages 58 and 188]

Radicchi, F., Vilone, D., Yoon, S., and Meyer-Ortmanns, H. (2007). Social balance as a satisfiability problem of computer science. *Physical Review E*, 75(2):26106. [Cited on page 13]

Rambaldi, M., Pennesi, P., and Lillo, F. (2015). Modeling foreign exchange market activity around macroeconomic news: Hawkes-process approach. *Physical Review E*, 91(1):12819. [Cited on page 9]

Rangel, J. G. (2011). Macroeconomic news, announcements, and stock market jump intensity dynamics. *Journal of Banking & Finance*, 35(5):1263–1276. [Cited on page 58]

Rapoport, A. (1953). Spread of information through a population with socio-structural bias: I. assumption of transitivity. *The bulletin of mathematical biophysics*, 15(4):523–533. [Cited on page 16]

Rooij, A. C. M. and Wilf, H. S. (1965). The interchange graph of a finite graph. *Acta Mathematica Academiae Scientiarum Hungarica*, 16(3-4):263–269. [Cited on pages 14 and 159]

Samuelson, P. A. (1965). Proof that properly anticipated prices fluctuate randomly. *Industrial management review*, 6(2):41–49. [Cited on page 56]

San Miguel, M. and Toral, R. (2000). Stochastic Effects in Physical Systems. In Tirapegui, E., Martínez, J., and Tiemann, R., editors, *Instabilities and Nonequilibrium Structures VI*, volume 5 of *Nonlinear Phenomena and Complex Systems*, pages 35–127. Springer Netherlands. [Cited on pages 53 and 77]

Sayama, H., Pestov, I., Schmidt, J., Bush, B. J., Wong, C., Yamanoi, J., and Gross, T. (2013). Modeling complex systems with adaptive networks. *Computers & Mathematics with Applications*, 65(10):1645–1664. [Cited on page 14]

Schulze, C. and Stauffer, D. (2006). Recent Developments in Computer Simulations of Language Competition. *Computing in Science & Engineering*, 8(3):60–67. [Cited on page 11]

Schulze, C., Stauffer, D., and Wichmann, S. (2008). Birth, Survival and Death of Languages by Monte Carlo Simulation. *Communications in Computational Physics*, 3(2):271–294. [Cited on page 11]

Serrano, M. Á. and Boguñá, M. (2005). Tuning clustering in random networks with arbitrary degree distributions. *Physical Review E*, 72(3):36133. [Cited on pages 16 and 157]

Serrano, M. Á. and Boguñá, M. (2006). Percolation and Epidemic Thresholds in Clustered Networks. *Physical Review Letters*, 97(8):88701. [Cited on page 81]

Serrour, B., Arenas, A., and Gómez, S. (2011). Detecting communities of triangles in complex networks using spectral optimization. *Computer Communications*, 34(5):629–634. [Cited on page 155]

Shapira, Y., Berman, Y., and Ben-Jacob, E. (2014). Modelling the short term herding behaviour of stock markets. *New Journal of Physics*, 16(5):53040. [Cited on page 9]

Solé, R. V., Pastor-Satorras, R., Smith, E., and Kepler, T. B. (2002). A model of large-scale proteome evolution. *Advances in Complex Systems*, 05(01):43–54. [Cited on page 16]

Sonnenschein, B. and Schimansky-Geier, L. (2012). Onset of synchronization in complex networks of noisy oscillators. *Physical Review E*, 85(5):51116. [Cited on pages 10 and 86]

Sood, V., Antal, T., and Redner, S. (2008). Voter models on heterogeneous networks. *Physical Review E*, 77(4):41121. [Cited on page 87]

Sood, V. and Redner, S. (2005). Voter Model on Heterogeneous Graphs. *Physical Review Letters*, 94(17):178701. [Cited on pages 10 and 82]

Sood, V., Redner, S., and Ben-Avraham, D. (2005). First-passage properties of the {E}rdös-{R}{é}nyi random graph. *Journal of Physics A: Mathematical and General*, 38(1):109. [Cited on page 10]

Stauffer, D. (2005). Sociophysics simulations ii: opinion dynamics. *AIP Conference Proceedings*, 779(1):56–68. [Cited on page 5]

Stauffer, D., Castelló, X., Eguíluz, V. M., and San Miguel, M. (2007). Microscopic Abrams–Strogatz model of language competition. *Physica A: Statistical Mechanics and its Applications*, 374(2):835–842. [Cited on page 11]

Stauffer, D., De Oliveira, S. M. M., de Oliveira, P. M. C., and de Sá Martins, J. S. (2006). *Biology, sociology, geology by computational physicists*, volume 1. Elsevier, Amsterdam. [Cited on page 11]

Stauffer, D. and Sornette, D. (1999). Self-organized percolation model for stock market fluctuations. *Physica A: Statistical Mechanics and its Applications*, 271(3–4):496–506. [Cited on page 7]

Suchecki, K., Eguíluz, V. M., and San Miguel, M. (2005a). Conservation laws for the voter model in complex networks. *EPL (Europhysics Letters)*, 69(2):228. [Cited on pages 10, 12, 82, and 84]

Suchecki, K., Eguíluz, V. M., and San Miguel, M. (2005b). Voter model dynamics in complex networks: Role of dimensionality, disorder, and degree distribution. *Physical Review E*, 72(3):36132. [Cited on pages 10, 82, 84, and 97]

Szell, M., Lambiotte, R., and Thurner, S. (2010). Multirelational organization of large-scale social networks in an online world. *Proceedings of the National Academy of Sciences*, 107(31):13636–13641. [Cited on pages 13, 16, and 157]

Szell, M. and Thurner, S. (2010). Measuring social dynamics in a massive multiplayer online game. *Social Networks*, 32(4):313–329. [Cited on pages 16 and 157]

Szell, M. and Thurner, S. (2012). Social dynamics in a large-scale online game. *Advances in Complex Systems*, 15(06):1250064. [Cited on pages 16 and 157]

Tetlock, P. C. (2007). Giving content to investor sentiment: The role of media in the stock market. *The Journal of Finance*, 62(3):1139–1168. [Cited on page 58]

Thurner, S., Farmer, J. D., and Geanakoplos, J. (2012). Leverage causes fat tails and clustered volatility. *Quantitative Finance*, 12(5):695–707. [Cited on page 7]

Toivonen, R., Castelló, X., Eguíluz, V. M., Saramäki, J., Kaski, K., and San Miguel, M. (2009). Broad lifetime distributions for ordering dynamics in complex networks. *Physical Review E*, 79(1):16109. [Cited on pages 12 and 172]

Toral, R. and Tessone, C. J. (2007). Finite size effects in the dynamics of opinion formation. *Communications in Computational Physics*, 2:177–195. [Cited on pages 25, 50, 73, and 138]

Török, J., Iñiguez, G., Yasseri, T., San Miguel, M., Kaski, K., and Kertész, J. (2013). Opinions, conflicts, and consensus: Modeling social dynamics in a collaborative environment. *Physical Review Letters*, 110:088701. [Cited on page 5]

Traag, V. A. and Bruggeman, J. (2009). Community detection in networks with positive and negative links. *Physical Review E*, 80(3):36115. [Cited on page 13]

Van Kampen, N. G. (2007). *Stochastic Processes in Physics and Chemistry*. North-Holland, Amsterdam. [Cited on page 51]

Vázquez, A. (2003). Growing network with local rules: Preferential attachment, clustering hierarchy, and degree correlations. *Physical Review E*, 67(5):056104. [Cited on page 16]

Vazquez, F., Castelló, X., and San Miguel, M. (2010). Agent based models of language competition: macroscopic descriptions and order–disorder transitions. *Journal of Statistical Mechanics: Theory and Experiment*, 2010(04):P04007. [Cited on pages 11 and 12]

Vazquez, F. and Eguíluz, V. M. (2008). Analytical Solution of the Voter Model on Uncorrelated Networks. *New Journal of Physics*, 10(6):63011. [Cited on pages 10, 82, 142, and 188]

Vazquez, F., Eguíluz, V. M., and San Miguel, M. (2008). Generic Absorbing Transition in Coevolution Dynamics. *Physical Review Letters*, 100(10):108702. [Cited on pages 10, 14, 82, 100, 103, 142, and 143]

Vazquez, F., González-Avella, J. C., Eguíluz, V. M., and San Miguel, M. (2007). Time-scale competition leading to fragmentation and recombination transitions in the coevolution of network and states. *Physical Review E*, 76(4):46120. [Cited on page 14]

Viana Lopes, J., Pogorelov, Y. G., dos Santos, J. M. B., and Toral, R. (2004). Exact solution of Ising model on a small-world network. *Physical Review E*, 70(2):26112. [Cited on page 9]

Vilone, D. and Castellano, C. (2004). Solution of voter model dynamics on annealed small-world networks. *Physical Review E*, 69(1):16109. [Cited on page 86]

Vilone, D., Ramasco, J. J., Sánchez, A., and San Miguel, M. (2012). Social and strategic imitation: the way to consensus. *Scientific Reports*, 2. [Cited on pages 9 and 81]

Walras, L. (1954). *Elements of Pure Economics, or the Theory of Social Wealth. Translated by William Jaffé from the original (1874)*. Published for the American Economic Association and the Royal Economic Society. [Cited on page 56]

Wang, W. S.-Y. and Minett, J. W. (2005). The invasion of language: emergence, change and death. *Trends in Ecology & Evolution*, 20(5):263–269. [Cited on pages 12 and 171]

Watts, D. J. (2002). A simple model of global cascades on random networks. *Proceedings of the National Academy of Sciences*, 99(9):5766–5771. [Cited on page 81]

Watts, D. J. and Strogatz, S. H. (1998). Collective dynamics of "small-world" networks. *Nature*, 393:440–442. [Cited on page 4]

Weisbuch, G., Deffuant, G., Amblard, F., and Nadal, J.-P. (2002). Meet, discuss, and segregate! *Complexity*, 7(3):55–63. [Cited on pages 5, 21, 22, and 23]

Weisbuch, G., Deffuant, G., Amblard, F., and Nadal, J.-P. (2003). *Heterogenous Agents, Interactions and Economic Performance*, chapter Interacting Agents and Continuous Opinions Dynamics, pages 225–242. Springer Berlin Heidelberg. [Cited on pages 5 and 23]

Zimmermann, M. G., Eguíluz, V. M., and San Miguel, M. (2001). Cooperation, Adaptation and the Emergence of Leadership. In Kirman, A. and Zimmermann, J.-B., editors, *Economics with Heterogeneous Interacting Agents*, volume 503 of *Lecture Notes in Economics and Mathematical Systems*, pages 73–86. Springer Berlin Heidelberg. [Cited on page 14]

Zimmermann, M. G., Eguíluz, V. M., and San Miguel, M. (2004). Coevolution of dynamical states and interactions in dynamic networks. *Physical Review E*, 69(6):65102. [Cited on page 14]